KERATIN REMODELLING IN STRESS

TAN TONG SAN

NATIONAL UNIVERSITY OF SINGAPORE

2012

KERATIN REMODELLING IN STRESS

TAN TONG SAN

(B. Sc. (Hons.), NUS)

A THESIS SUBMITTED FOR THE DEGREE OF

DOCTOR OF PHILOSOPHY

NUS Graduate School for Integrative Sciences and Engineering

NATIONAL UNIVERSITY OF SINGAPORE

2012

Declaration

I hereby declare that this thesis is my original work and it has been written by me in its entirety. I have duly acknowledged all the sources of information which have been used in the thesis.

This thesis has also not been submitted for any degree in any university previously.

_____

TAN TONG SAN

18 December 2012

ACKNOWLEDGEMENTS

I would like to express my deepest gratitude to my supervisor, Prof. Birgit Lane, for her guidance and mentorship, and for giving me the opportunity, independence and resources to conduct my research. Her depth of knowledge and passion for scientific discovery have been a great source of inspiration and motivation for me throughout these four years of PhD endeavour, and will continue to be in the future. I would also like to thank my thesis advisory committee, Prof. Michael Raghunath and A/Prof. Edward Manser, for their critical feedback along the way. My sincere thanks and appreciation also go to John Common, for his insightful comments and suggestions throughout the course of this project. I would also like to acknowledge Ildiko for initiating the keratin phosphorylation project. Special thanks also go to Cedric, Chida, Darren, Gopi, Nama, John Lim, Delina, Chye Ling, Huijia and Declan, for their help in research techniques.

I am most fortunate to be part of the EBL lab, a stimulating and lively place to work in. Thanks go to Kenneth, Zhou Fan, Paula, Chai Ling, Christine, Yi Zhen, Rosita, Vivien and Giorgiana, fellow students who join me in the pursuit of a doctorate. Appreciation is also extended to Iskandar, Jun Xian, Carol, Anita, Yi Ling, Ting Ting and other lab members for their support and help.

In addition, I would like to thank A*STAR for awarding me this A*STAR Graduate Scholarship, without which I would not be able to come this far.

Finally, I would like to express my heartfelt appreciation to my family, both immediate and extended, for being so understanding and encouraging in this whole process. Their constant support and faith in me have made the difference in my life – and it is to them I dedicate this thesis.

TABLE OF CONTENTS

SUMMARY

Remodelling of keratin cytoskeletal network is essential for cells to respond to environmental cues upon wounding. To understand the stress/wound response, immortalized keratinocytes were used which expressed a keratin mutation mimicking severe EBS Dowling-Meara (a skin fragility disorder), fluorescently tagged for live-cell imaging.

All keratinocytes are "activated" to a stress state through up-regulation of kinases and wound response proteins, but revert to quiescence after confluence. In mutant cells, "activation" is reflected by the presence of keratin aggregates, a hallmark of severe EBS-DM. These keratin aggregates accumulate at the leading edge of the cell; they are highly dynamic and constantly undergo remodelling. It has been proposed that avoiding aggregate formation may improve the disease phenotype. When mutant keratinocytes were grown to confluence in a monolayer, a reduction of peripheral aggregates was observed, accompanied by a decrease in wound response proteins such as β1 integrin and fibronectin. However, upon scratch wounding, these mutant keratinocytes migrated faster and have higher induction of wound response proteins such as K17 than wild-type keratinocytes, highlighting their "pre-stressed" state of activation.

Epidermal growth factor (EGF) is a major signalling molecule in wound healing and thus the EGF signalling pathway was examined for a role in regulating keratin remodelling. EGF-treated wild-type keratinocytes have an increased keratin 14 synthesis and solubility but not mutant keratinocytes. When mutant keratinocytes were cultured in media without EGF, a reduction of peripheral keratin aggregates was observed, accompanied by a change in desmoplakin localization, both of which were

reversed upon re-stimulation with EGF. This EGF-mediated effect appears to be associated with the cytoskeletal linker protein, plectin. Inactivation of ERK1/2 kinases downstream in the pathway, by both inhibitor treatment and siRNA knockdown, resulted in fewer mutant keratinocytes with peripheral aggregates, accompanied by a decrease in plectin levels. Fluorescence live-cell imaging was used to confirm the relationship between ERK1/2 activation, keratin aggregate status and cell migration in mutant keratinocytes. Conversely, plectin knockdown reduced the number of mutant keratinocytes with peripheral aggregates and slowed down cell migration in scratch wound assays. Understanding the link between keratin remodelling and the EGF pathway may identify intervention points for new therapies.

Keratin remodelling is believed to be driven by phosphorylation/dephosphorylation cycles. Examination of the mutation sequence most commonly causing EBS Dowling-Meara suggested a possible interference of the mutation with a nearby phosphorylation site. Phospho-mimetic and phospho-null constructs were therefore made for involved serine and tyrosine residues to investigate this possibility. Phospho-mimetic constructs mimicking phosphorylation at K14 Y129 increased keratin aggregate formation and stress response in osmotic stress assays. A phospho-null construct at K14 Y129 prevents aggregates and slows down cell migration in scratch wound assays. In keratinocytes with both the K14 R125P mutation and a phospho-null K14 Y129 mutation, fewer cells with keratin aggregates were observed than with K14 R125P mutation alone. This implication that the pathogenic effect of the EBS-DM mutations may be working through interference with phosphorylation is a new finding that has not been suspected previously, and may have implications for therapy.

LIST OF TABLES

LIST OF FIGURES

LIST OF APPENDICES

LIST OF ABBREVIATIONS

ABCA12	ATP-binding cassette subgroup 1 membrane 12 transporter
Akt	Protein kinase B
ARVC	Arrhythmic right ventricular cardiomyopathy
ATP2A2	Sarcoplasmic/endoplasmic reticulum calcium ATPase 2
ATP2C1	Calcium-transporting ATPase type 2C member 1
BP180	Bullous pemphigoid antigen 180
BP230	Bullous pemphigoid antigen 230
BPE	Bovine pituitary extract
BSA	Bovine serum albumin
CD151	Tetraspanin
cDNA	Complementary deoxyribonucleic acid
CMV	Cytomegalovirus
Cx	Connexin
DEB	Dystrophic epidermolysis bullosa
DIC	Differential interference contrast
DMEM	Dulbecco's modified Eagle's medium
DMSO	Dimethylsulfoxide
DNA	Deoxyribonucleic acid
DP	Desmoplakin
Dsc	Desmocollin
Dsg	Desmoglein
DUSP	Dual-specificity phosphatase
EB	Epidermolysis bullosa
EBS	Epidermolysis bullosa simplex
EBS-DM	Epidermolysis bullosa simplex, Dowling-Meara type
EBS-MD	Epidermolysis bullosa simplex with muscular dystrophy
ECM	Extracellular matrix
EDTA	Ethylenediaminetetraacetic acid

EGF	Epidermal growth factor
EGFR	Epidermal growth factor receptor
EGFP	Enhanced green fluorescent protein
ERK	Extracellular signal regulated kinase
FA	Focal adhesion
FACS	Fluorescence-activated cell sorting
FAK	Focal adhesion kinase
FBS	Foetal bovine serum
FERM	Protein 4.1, ezrin, radixin, and moesin
FNIII	Type III fibronectin
FRAP	Fluoresence recovery after photobleaching
FRS2	FGF receptor substrate-2
Gab1	Grb2-associated binding protein
GABEB	Generalized atrophic benign epidermolysis bullosa
GLUT	Glucose transporter
Hes-1	Hairy and enhancer of split-1
HPRT	Hypoxanthine-guanine phosphoribosyltransferase
HSP27	Heat shock protein 27
IFAP	Intermediate filament associated protein
IRS1	Insulin receptor substrate-1
JEB	Junctional epidermolysis bullosa
JNK	c-Jun N-terminal kinases
K	Keratin
KS	Kindler syndrome
KSR	Kinase suppressor of Ras signalling
LB	Lysogeny broth
MAPK	Mitogen activated protein kinase
MCS	Multiple cloning site
mInsc	mouse Inscuteable

MMP	Matrix metalloproteinase
M.O.I	Multiplicity of infection
MP1	MEK partner 1
mRNA	Messenger ribonucleic acid
mTOR	Mammalian target of rapamycin
N.A.	Numerical aperture
NP-40	Nonidet P-40
NuMA	Nuclear mitotic apparatus protein
OMIM	Online Mendelian Inheritance in Man
PA-JEB	Junctional epidermolysis bullosa associated with pyloric atresia
PBS	Phosphate buffered saline
PCR	Polymerase chain reaction
PG	Plakoglobin
PKP	Plakophilin
PMSF	Phenylmethanesulfonyl Fluoride
PRL-3	Phosphatase of regenerating liver-3
qRT-PCR	Quantitative real-time polymerase chain reaction
RBP-J	Recombining binding protein suppressor of hairless
RNA	Ribonucleic acid
RPLP0	Ribosomal protein P0
RT-PCR	Reverse transcriptase polymerase chain reaction
SAPK	Stress activated protein kinase
SD	Standard deviation
SDS	Sodium dodecyl sulphate
SDS-PAGE	SDS-polyacrylamide gel electrophoresis
SEM	Standard error mean
siRNA	Small interfering ribonucleic acid
SPINK5	Serine protease inhibitor LEKTI
Src	Sarcoma

SUMO	Small ubiquitin-like modifier
TBE	Tris/borate/EDTA buffer
TGF	Transforming growth factor
TNF	Tumor necrosis factor
ULF	Unit length filament
VEGF	Vascular endothelial growth factor
VEGFR	Vascular endothelial growth factor receptor
WT	Wild-type
ZO	Zonula occludens

CHAPTER 1

INTRODUCTION

1.1   The importance of skin

The skin (integumentary system) is the largest organ system of the body, and forms the exterior surface of the human body. The skin comprises of 15-18% of the total body weight and covers a surface area of approximately 1.5-2.0 m^2 for an adult human being (reviewed in Goldsmith, 1990). Being a sensory organ, the skin harbors many receptors that are capable of sensing pain (nociceptors), pressure (mechanoreceptors) and temperature (thermoreceptors) (reviewed in Schmelz, 2011), thus giving the organisms an awareness of the surroundings. The skin is also a highly regenerative multilayered tissue that is continuously replaced through a process of regeneration (proliferation of basal cells) and desquamation (flaking cells from stratum corneum) that occurs at the same rate. The typical time for epidermal turnover is about 14-30 days, which varies with age, health and body site (Reddy et al., 2000).

1.1.1   Barrier functions of the epidermis

One of the most important functions of the skin is to form an efficient barrier to protect the body from external insults such as microbial (bacteria/fungi/virus), chemical/biochemical (irritants/allergens) and physical (mechanical/ultra-violet radiations) assaults (reviewed in Proksch et al., 2008). For instance, the sebaceous and sweat glands in the skin secrete oil and sweat onto its surfaces to create an acidic environment that is unfavorable for growth of micro-organisms. In addition, hydrolytic enzymes, antimicrobial peptides and macrophages that are residing in the skin can form an immunological barrier against the percutaneous penetration of any irritants or allergens (reviewed in Proksch et al., 2008). Moreover, skin pigmentation (melanin) is photoprotective against the harmful effects of solar radiation, thus

reducing the risk of DNA damage and occurrences of skin cancer (Westerhof et al., 1981; reviewed in Kollias et al., 1991).

1.1.2 Homeostasis of the epidermis

The skin also plays an important role in internal homeostatic maintenance of body temperature and hydration through its ability to regulate heat and water loss respectively. For example, rising body temperatures result in dilation of blood vessels near the skin surface, allowing heat to dissipate, followed by the evaporation of sweat released by the sweat glands which cools the body down (Taylor, 1986). Likewise, the skin barrier prevents the body from excessive water loss and desiccation in a dry environment, thus allowing for adaptation to different terrestrial lives. Most remarkably, the ability of the skin to repair itself after wounding, through a controlled repertoire of phases of cell migration, proliferation and wound contraction, further highlights the vital role of the skin in restoring epidermal barrier function of the body, hence maintaining homeostasis (reviewed in Martin, 1997).

1.1.3 Mechanical resilience of the skin

The skin also exhibits mechanical resilience to physical insults. The ability of the skin to withstand large physical forces and thus protect the underlying organs comes mostly from the elastic, compressible properties of both dermal collagen and elastic fibers (elastin) (Silver et al., 2001). This may then explain why skin can be flexible enough to be stretched to large amounts, for example during pregnancy, and to also allow a large range of body flexture and limb movements.

Some insights into the skin's ability to provide mechanical resilience and barrier function come from understanding the structure of the skin. In the following paragraphs, the compositions of the skin will be discussed in detail.

1.2 Skin composition and functions

1.2.1 The hypodermis

The skin comprises of three distinctive layers: namely, the innermost tissue hypodermis, the dermis and the outermost epidermis. The mesodermally derived hypodermis (subcutis or subcutaneous fat) consists of mainly the loose connective tissues and adipose (fatty) tissues that connect the lower reticular dermis to the underlying skeletal components (McGrath et al., 2004).

1.2.2 The dermis

Overlying the hypodermis is the dermis which consists of connective tissues and is separated into two major compartments: the upper papillary layer which lies just below the dermal-epidermal junction (basement membrane), and the lower reticular layer which is connected to the hypodermis. Epidermal appendages such as hair follicles, sebaceous and sweat glands are embedded in the dermis. The major cell types that are residing in this dermal layer are the fibroblasts, macrophages, mast cells and circulating immune cells. These cells are embedded in a fibrous matrix consisting of collagen and elastin, which provide structural flexibility and tensile strength. The fibroblasts are the ones responsible for the production and metabolism of the collagen fibers (Rudnicka et al., 1994), a major component of the dermis, and elastin (Davis et al., 1999). This ensures control of the dermal composition and configuration.

The blood vessels are found in the dermis, such as the cutaneous plexus (lower part of the reticular layer), and the subpapillary plexus (near the papillary layer), from which fine capillaries loop just below the epidermis. This vascularized dermis provides nutrients to the overlying epidermis, which in itself is devoid of any vascularization.

The dermis contains most of the sensory system of the skin, with Meissner's corpuscles (touch receptors) located just below the epidermis and Pacinian corpuscles (mechanoreceptors that detect pressure) located deeper in the dermis.

There are several important functions that take place within the dermis, such as the regulation of body temperature, activation of immune responses against penetrating antigens, and mechanical resilience through the plasticity and remodelling of the buffering collagen fibers (Demarchez et al., 1992). Thus, the dermis plays an important role in providing mechanical strength and elasticity of the skin.

1.2.3   The basement membrane

The basement membrane is a thin sheet of highly specialized extracellular matrix (ECM) found at the dermal-epidermal junction and is involved in mediating the attachment and orientation of epithelial cells (Edwards and Streuli, 1995). The major components of the basement membrane are type IV collagen, heparin sulfate proteoglycan, fibronectin and laminin (reviewed in Burgeson and Christiano, 1997). The basal cell layer of the epidermis is anchored to the basement membrane by hemidesmosomes or focal contacts (discussed later), whilst the basement membrane is anchored to the underlying dermis by collagen type VII anchoring fibrils (reviewed in Erickson and Couchman, 2000).

Figure 1.1   Architecture of the epidermis
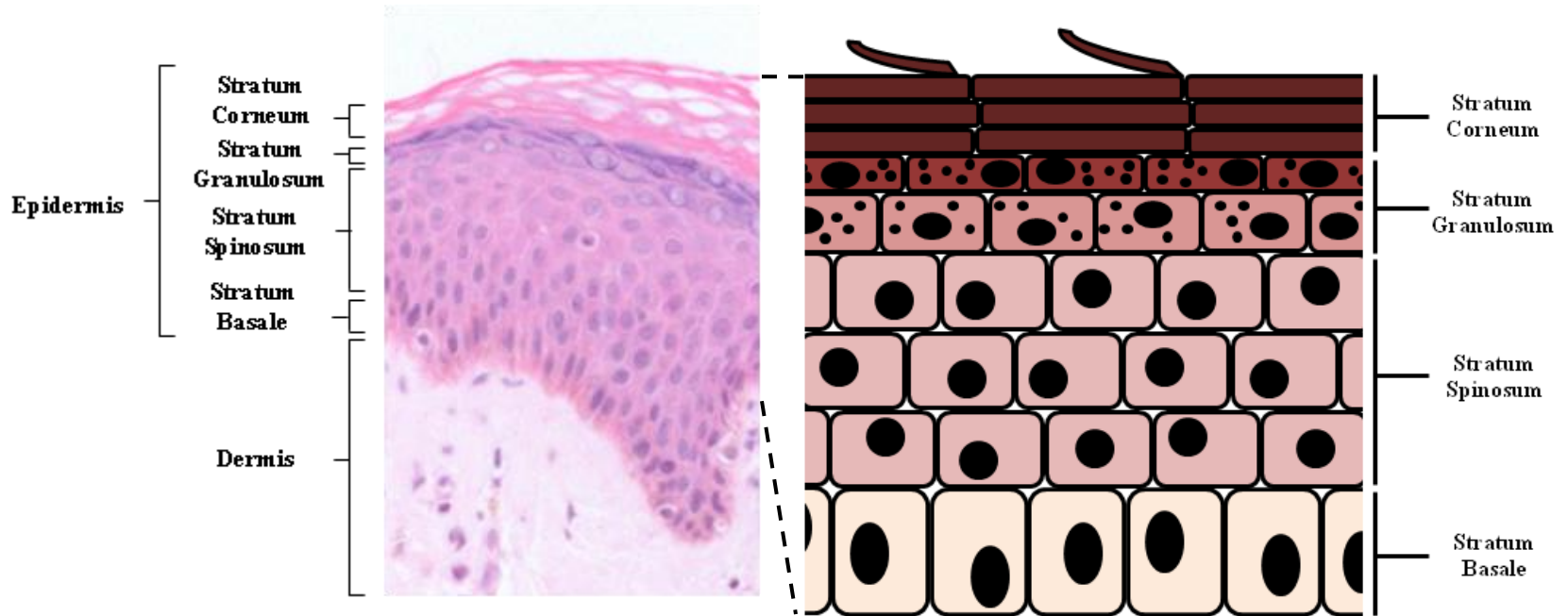
Picture courtesy of Kenneth Tan   Figure redrawn after Brooke et al., 2012.

1.2.4 The epidermis

In early embryogenesis, a single-layered ectoderm gives rise to the mesoderm by cells migrating down to lie between the ectoderm and the endoderm. Later, the ectoderm becomes multilayered and gives rise to the epidermis. At the single layer stage, ectodermal proliferation occurs with the mitotic plane perpendicular to the embryo surface. This process gives rise to two layers, which results in a superficial layer known as the periderm (Weiss and Zelickson, 1975). During development of the postnatal epidermis, basal progenitor cells undergo both symmetric and asymmetric cell divisions to increase surface area and skin thickness respectively (Smart, 1970; Lechler and Fuchs, 2005). In symmetric cell division, mitotic spindles are oriented parallel to the underlying basement membrane, allowing basal keratinocytes to proliferate and expand in the basal layer of the epidermis. The beginning of differentiation is associated with the progenitor cells undergoing asymmetric cell division wherein mitotic spindles are oriented perpendicular to the basement membrane, giving rise to a proliferative basal cell in the basal layer and another daughter cell committed to differentiation in the suprabasal cell layer of the epidermis (reviewed in Ray and Lechler, 2011). During the transition, the keratinocytes undergo both biochemical and morphological changes till they become anucleated, form an impervious cornified envelope and their keratins and cytoplasmic matrix proteins become highly cross-linked and are eventually desquamated from the outermost epidermis. The desquamated keratainocytes are constantly replaced by inner cells differentiating upwards (reviewed in Koster and Roop, 2007). Hence, these continuous processes mediate the self-regenerative properties of the epidermis and are crucial for maintaining epidermal homeostasis (reviewed in Jones and Simons, 2008).

1.2.4.1   Cell types within the epidermis

The epidermis is a non-vascularized, stratified keratinizing squamous epithelium that is composed mostly of keratinocytes. Other cell types that reside in this epithelium are the melanocytes (pigment-producing cells), Langerhans cells (antigen-presenting immune cells) and the neuroendocrine Merkel cells (sensory cells). Melanocytes and Merkel cells typically reside in the basal layer whereas Langerhans cells reside in the suprabasal layer. During development, both melanocytes (Holbrook et al., 1989) and Merkel cells (Szeder et al., 2003) originate from the neural crest whereas Langerhans cells are immune cells derived from the bone marrow (Shelley and Juhlin, 1976; Klareskog et al., 1977; Frelinger et al., 1979; Katz et al., 1979). One conundrum in understanding the origin of Langerhans cells is that although they are of hematopoietic origin, they are derived from precursors that are present in the skin prior to birth and bone marrow development. One possibility is that the Langerhans cells are derived from the yolk sac primitive macrophages that migrate to the skin via blood circulation during mid-embryogenesis (reviewed in Ginhoux and Merad, 2010), because they expressed $Gr1^-CD11b^+MCSF\text{-}R^+F4/80^+CX_3CR1^+$ (Bertrand et al., 2005), a phenotype similar to the putative Langerhans precursors found in embryonic day 18.5 (E18.5) epidermis (reviewed in Ginhoux and Merad, 2010).

The epidermis can be subdivided into four or five different layers depending on body site, namely: stratum basale (basal layer), stratum spinosum (spinous layer), stratum granulosum (granular layer), stratum lucidum (clear layer - only in palms and soles) and the stratum corneum (cornified layer) (see Figure 1.1).

1.2.4.2   The stratum basale

The stratum basale consists of columnar-shaped proliferative keratinocytes that adhere tightly to the basement membrane. These basal keratinocytes express both keratin 5 (K5) and keratin 14 (K14). Some of these basal cells are epidermal stem or progenitor cells, others are transit amplifying cells (reviewed in Blanpain et al., 2007). These epidermal stem cells divide and continuously supply a population of daughter cells that migrate upwards in the epidermis, while at the same time commit to terminal differentiation and cell cycle withdrawal. The stem or progenitor cells of the epidermis maintain epidermal renewal throughout life; there are now believed to be discrete populations of stem cells responsible for different parts of the hair follicle and sweat gland as well as for the interfollicular epidermis (reviewed in Arwert et al., 2012).

1.2.4.3   The stratum spinosum

The stratum spinosum forms part of the suprabasal layer that is generally three to four cell layers thick. Cells residing in this layer are named spinous keratinocytes because in histological preparations, these cells appear to be joined by 'spines'; this appearance is actually caused by a strong uptake of histological stain into the bundles of keratin filaments that attach to desmosome cell-cell junctions. The uppermost spinous cells contain lamellar granules (or lamellar bodies, Odland bodies), which are membrane-bound cytoplasmic organelles that contain a mixture of lipids, proteases, antimicrobial peptides and corneodesmosomal proteins (reviewed in Ishida-Yamamoto and Kishibe, 2011). Ultrastructurally, lamellar granules appear as round granules of 0.2 - 0.5 µm in diameter, with parallel stacks of lipid-enriched disks enclosed by a trilaminar membrane (Menon, 2002). Their appearance marks the various aspects of epidermal differentiation through protein and lipid synthesis. At the

upper spinous layer, the cells begin to flatten and elongate, and migrate to the stratum granulosum. Both keratin 1 (K1) and keratin 10 (K10) are biochemical markers for this spinous layer.

1.2.4.4 The stratum granulosum

The stratum granulosum consists of two to three layers of non-dividing, flattened keratinocytes that produce distinctive electron dense keratohyalin granules. These keratohyalin granules contain both the intermediate filament-associated protein profilaggrin and the protein loricrin (Steven et al., 1990). Lamellar granules are also found in these granular keratinocytes but are clustered at the cell margins and fused with the plasma membrane. In the uppermost granular layer, keratinocytes discharge the ceramide-rich lipid contents of the lamellar granules into the intercellular space, where they form extracellular lipid-enriched layers. This granular zone encompasses the final viable epidermal layers with the uppermost granular layer connecting to the terminally differentiated, non-viable stratum corneum.

1.2.4.5 The stratum corneum

The stratum corneum forms the outermost layer of the epidermis where anucleated cornified keratinocyes (corneocytes) are located. However, in palmoplantar tissues, there is an additional zone known as stratum lucidum seen between the granulosum and stratum corneum. These cells are still nucleated, and are thus referred to transitional cells. Corneocytes in the stratum corneum are interconnected to adjacent cells via the corneodesmosomes. The borders of these corneocytes overlap, interlock and insert into adjacent cells to enhance the stability and strength for the epidermis. It is not surprising that any alterations in cell-cell adhesions may result in disrupted barrier functions. For instance, mutations in *SPINK5* for the gene encoding the serine

protease inhibitor LEKTI, alter the stability of desmosomal proteins, hence leading to Netherton syndrome (Chavanas et al., 2000), which result in defective cell-cell adhesion.

During the final stages of normal differentiation, the keratin filaments of the corneocytes aggregate with filaggrin to form disulphide cross-linked macrofibres (Lynley and Dale, 1983), which caused the cells to collapse into a flattened morphology. The cornified envelope, a tough protein/lipid polymer structure, forms the cell membrane of the terminally differentiated corneocytes by the progressive addition of several cornified envelope proteins (reviewed in Proksch et al., 2008), such as involucrin (Rice and Green, 1977), which is cross-linked by the action of a transglutaminase (Buxman and Wuepper, 1978).

Because a large proportion of the cornified envelope is made up of lipids and cholesterols, mutations affecting the functions of cholesterol efflux transporter (ATP-binding cassette subgroup 1 membrane 12 transporter, ABCA12) can lead to harelequin ichthyosis (Kelsell et al., 2005), resulting in barrier function defects. This suggests that the maintenance of epidermal barrier function is crucial for the integrity of the skin. A list of proteins associated with human skin disorders disrupting barrier function is tabulated in Table 1.1.

Table 1.1

Human diseases of the epidermis

Stratum corneum

Molecular target	Disease	Clinical phenotype (s)	Original finding (s)
ABCA12 (lipid transport)	Harlequin ichthyosis (OMIM # 242500)	Distorted facial features such as eclabion, ectropion	(Kelsell et al., 2005)
Filaggrin	Ichthyosis vulgaris (OMIM # 146700)	Diffuse, fine superficial scaling; Kerotosis pilaris; Marked palmar hyperlinearity	(Smith et al., 2006)
	Atopic dermatitis (OMIM # 605803)	Eczema associated with asthma; Food allergy; Allergic rhinitis	(Palmer et al., 2006)
Corneodesmosin	Hypotrichosis simplex of scalp (OMIM # 146520)	Late childhood onset of alopecia	(Levy-Nissenbaum et al., 2003)
	Generalized peeling of skin syndrome (OMIM # 270300)	Superficial exfoliation with unusal ichthyosiform erythema; Scaling of erythematous patches	(Oji et al., 2010)
SPINK5 (LEKTI)	Netherton syndrome (OMIM # 256500)	Congenital ichthyosis with defective cornificaton; Trichorrexis invaginata; atopic dermatitis and hay fever	(Chavanas et al., 2000)
Transglutaminase 1	Lamellar ichthyosis (OMIM # 242300)	Newborns covered with colloid membrane accompanied with erythroderma; After membrane shedding, the skin developed severe ichthyosis with large hyperkeratotic scales	(Huber et al., 1995)
Loricrin	Vohwinkel's syndrome (Keratoderma hereditaria mutilans) (OMIM # 604117)	Hyperkeratosis of palms and soles with a honeycomb appearance; Pseudoinhum leading to autoamputation; Distinctive starfish-like acral keratoses; Sensorineural hearing loss	(Maestrini et al., 1996)

Figure 1.2   Intercellular junctions of the epidermis
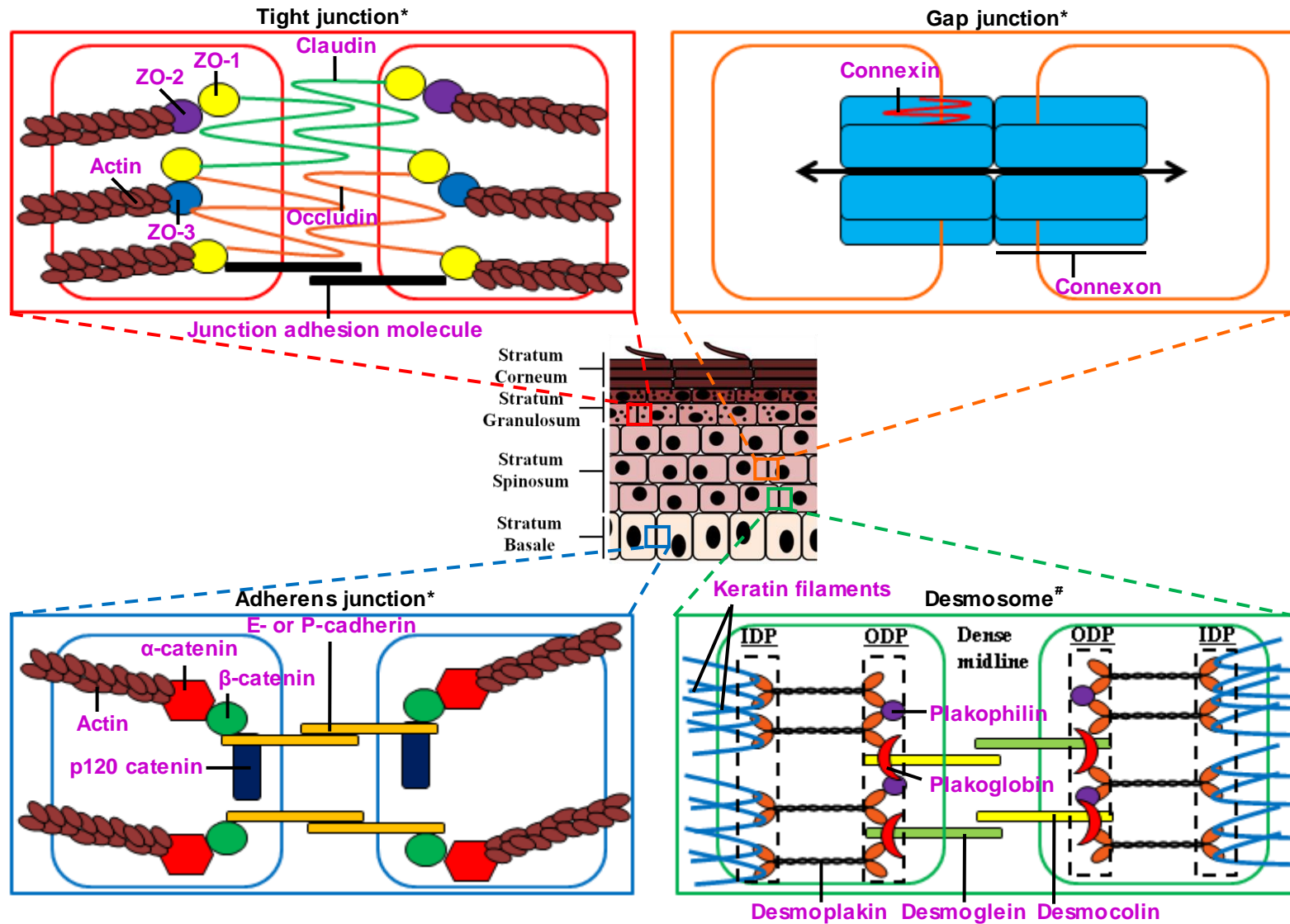
*/# Figures redrawn after Fuchs and Raghavan, 2002 and Simpson et al., 2011.

1.3   Anchoring junctions mediating cell-cell adhesion

Throughout the epidermis, keratinocytes are held together by different cell-cell junctions such as the desmosomes, adherens junctions, gap junctions and the tight junctions (see Figure 1.2). Desmosomes (macula adherens) attach the keratin cytoskeleton of neighboring cells together and confer mechanical resilience (reviewed in Green and Simpson, 2007), whereas adherens junctions (zonula adherens) and tight junctions (zonula occludens) associate with actin microfilaments and seal cells together in an epithelial sheet (reviewed in Madara, 1998; Niessen, 2007). Gap junctions comprise of connexins that allow free exchange of chemical or electrical signals from one cell to another (reviewed in Mese et al., 2007). Taking all these observations together, understanding the properties of each type of junctional proteins can provide some insights in the skin's ability to provide mechanical resilience. In the following paragraphs, the compositions of the anchoring junctions mediating cell-cell adhesion will be discussed in detail.

1.3.1 Desmosomes

Desmosomes (a composition of the Greek words: 'desmos' meaning bond and 'soma' meaning body) are the major adhesion complex found in the epidermis in many stress-bearing tissues such as the skin and the heart. They are responsible for anchoring keratin intermediate filaments to the cell membrane and bridging adjacent keratinocytes, to confer mechanical resilience. The desmosomes have a characteristic ultrastructural appearance, consisting of two principle domains, namely: (1) the extracellular core domain where plasma membrane of two adjacent cells forms a symmetrical junction with a central intercellular space of 30 nm, containing the electron-dense midline region and (2) the plaques of electron dense material running

along the cytoplasm parallel to the junctional region. This cytoplasmic plaque consists of two distinctive regions known as the outer dense plaque (ODP) and the inner dense plaque (IDP) into which intermediate filaments are observed to insert (North et al., 1999). The main desmosomal components comprise of the products of three gene families: the desmosomal cadherins, the *armadillo* family of nuclear and junctional proteins and the plakins (reviewed in Green and Gaudry, 2000). The extracellular core domain is largely composed of the heterophillic associations of the extracellular domains of desmosomal cadherins such as desmocollins and desmogleins (reviewed in Buxton and Magee, 1992; Koch and Franke, 1994). The cytoplasmic plaque comprises of the cytoplasmic tails of desmocollins and desmogleins, together with armadillo proteins (plakoglobin and plakophilin) and plakin proteins (desmoplakin). The localization of these desmosomal proteins within the desmosomal plaque has been mapped using immunogold labeling (North et al., 1999).

1.3.1.1 Desmosomal cadherins

Desmocollins (Dsc) and desmogleins (Dsg) are transmembrane glycoproteins of the desmosomes. In humans, there are seven desmosomal cadherins, three desmocollins (Dsc1-3) (Collins et al., 1991; Mechanic et al., 1991) and four desmogleins (Dsg1-4) (Koch et al., 1990; Amagai et al., 1991; Parker et al., 1991; Schafer et al., 1994; Kljuic et al., 2003). Each of the desmocollin genes encodes a pair of proteins that are generated by alternative splicing, yielding a longer 'a' form and a shorter 'b' form that differ in the length of their cytoplasmic tail (Collins et al., 1991; Parker et al., 1991). Desmosomal cadherins are expressed in a variety of epithelial and cardiac tissue, of which Dsc2 and Dsg2 are expressed in all desmosomal tissues (Schafer et al., 1994; Nuber et al., 1995). Within the epidermis, there is a differential pattern of desmosomal cadherin expressions across the different layers. For instance, Dsc1 and

Dsg1 are preferentially expressed in the suprabasal layers whereas Dsc2 and Dsg2 are preferentially expressed in the basal layers. Dsc3 and Dsg3, on the other hand, are expressed in both the basal and suprabasal layers (see Figure 1.3). Hence, these expression patterns make desmosomal cadherins a useful differentiation marker for stratified epithelia. In support of this, Dsc1 knockout mice exhibited epidermal hyperproliferation with overexpression of keratins 6 and 16 (K6 and K16), indicating abnormal differentiation (Chidgey et al., 2001). However, the process of epidermal stratification does not depend entirely on the presence of desmosomal cadherins because corneal epithelia only express Dsc2 and Dsg2 (Messent et al., 2000). Other regulated gene expression programs such as differentiation-specific keratin expression can also play a role in it (reviewed in Fuchs, 1995).

The importance of desmosomal cadherins in maintaining the integrity of the skin was revealed when it was discovered that autoantibodies against desmosomal cadherins led to skin blistering disorders. For example, the production of autoantibodies against Dsg1 resulted in pemphigus foliaceus (Allen et al., 1993), while autoantibodies against Dsg3 resulted in pemphigus vulgaris (Amagai, 1994). Likewise, Dsg3 knockout mice resulted in a similar phenotype as that of pemphigus vulgaris patients (Koch et al., 1997). Hence, these observations suggest that desmosomal cadherins are important in maintaining tissue integrity.

1.3.1.2 Desmosomal *armadillo* proteins

The cytoplasmic plaque of the desmosomes comprises mainly of the plakophilins 1-3 (PKP1-3), plakoglobin (PG) and desmoplakin (DP). Other proteins identified as associated with desmosomes are desmocalmin (Tsukita, 1985), IFAP 300 (Skalli et al., 1994), pinin (Ouyang and Sugrue, 1996) and periplakin (Ruhrberg et al., 1997). Both

PG and PKP belong to the *armadillo* family of signalling proteins (Peifer et al., 1992). They are characterized by the presence of a central domain containing a variable number of imperfect 42 amino acid repeats (*arm* repeats) (reviewed in Garrod and Chidgey, 2008). All PKPs contain 9 *arm* repeats with a flexible insert between repeats 5 and 6 that introduces a major bend in the overall structure (Choi and Weis, 2005), whereas PG contains 12 *arm* repeats (reviewed in Garrod and Chidgey, 2008). This kind of structure can also be found in β-catenin (McCrea et al., 1991; Butz et al., 1992) and armadillo (Riggleman et al., 1989; Peifer and Wieschaus, 1990), also members of the *armadillo* family of proteins.

Plakophillin (PKP) exists as three distinct isoforms (PKP1-3) that are expressed in a differentiation-specific manner in the epidermis (reviewed in Hatzfeld, 2007). PKP1 shows increased expression in suprabasal cells whereas PKP2 shows highest expression in basal cells. In contrast, PKP3 is expressed equally throughout the epidermal layers (reviewed in Getsios et al., 2004). PKP1 has been shown to localize at the cytoplasmic face of the desmosomal plaque (Kapprell et al., 1988; Heid et al., 1994) where molecular mapping showed that PKP1 lie closer to the plasma membrane as compared to PG or DP (North et al., 1999). A role for PKP1 in mediating tissue integrity of the skin was demonstrated by the discovery of mutations in PKP1 gene that led to ectodermal dysplasia / skin fragility syndrome. Hence, this reveals the importance of PKP1 in both cutaneous cell-cell adhesion and epidermal morphogenesis (McGrath et al., 1997).

Plakoglobin (PG), unlike other members of the *armadillo* family, can interact with the desmosomal cadherins (Cowin et al., 1986). PG interacts with the cytoplasmic domains of the desmosomal cadherins (Dsc and Dsg) that have sequence similarity with other catenin-binding domain of classical cadherins (Mathur et al., 1994;

Troyanovsky et al., 1994). Moreover, PG can also bind to the N-terminal domain of DP, an intermediate filament linker protein (Kowalczyk et al., 1997). These observations demonstrate that PG can link the desmosomal cadherins to the cytoskeleton. Molecular mapping of the desmosome provided the evidence for the localization of the PG interacting with Dsg, Dsc and DP (North et al., 1999). It has been suggested that PG was globular (Kapprell et al., 1987), which could position its internal arm repeats nearer to the plasma membrane than its N- or C- terminals. In consistent with this, it has been shown that the central domain of PG could bind to the N-terminus of the DP (Kowalczyk et al., 1997).

The notion that PG can interact with both desmosomal cadherins and DP suggests that it is important for maintaining tissue integrity. Indeed, deletion in PG led to Naxos disease, which was characterized by arrhythmic right ventricular cardiomyopathy (ARVC), striate palmoplantar keratoderma and woolly hair (McKoy et al., 2000). Likewise, the absence of PG could also lead to lethal congenital epidermolysis bullosa (Pigors et al., 2011), hence emphasizing the crucial role played by PG in maintaining epithelial and cardiomyocyte integrity.

1.3.1.3 Desmosomal plakin proteins

One of the essential components of the desmosome in all tissues is desmoplakin (DP), a member of plakin family. Other members include BP230, plectin and periplakin (Green et al., 1992; Ruhrberg et al., 1997). The common structural features of this family is first described for DP (Green et al., 1990), and all members in this family can bind to intermediate filaments. In addition, members such as plectin have an actin-binding domain that is thought to connect various cytoskeletal systems together (reviewed in Ruhrberg and Watt, 1997).

DP consists of an N-terminal plakin domain, a central coiled-coil rod domain and a C-terminus consisting of three highly homologous plakin repeat domains, namely: A, B and C (Choi et al., 2002). As mentioned earlier, the N-terminus of desmoplakin can bind to the desmosomal outer plaque proteins such as PG and PKP (Kowalczyk et al., 1997) whereas the C-terminus can bind to intermediate filament. The central α-helical rod domain is thought to be involved in dimer formation (Green et al., 1990). Two isoforms of DP exist: DP1 and DP2, where DP2 lacks most of the rod domain due to alternative splicing of exon 23 (Green et al., 1988; O'Keefe et al., 1989). DP1 is expressed in both skin and heart whereas DP2 is mainly expressed in the skin (Angst et al., 1990). Molecular mapping of desmosomes showed that DP could extend across most of the outer plaque and the whole of the inner plaque, suggesting that DP was localized at where it could interact with most of the desmosomal components (North et al., 1999).

The observation that DP can interact with most of the desmosomal components and aid in tethering the intermediate filaments to the neighboring cells suggests that it is crucial for maintaining tissue integrity. Indeed, DP knockout mice are usually embryonic lethal (Gallicano et al., 1998; Gallicano et al., 2001). Using a conditional DP knockout, it was found that the mice exhibited peeling skin and desmosomes lacking inner plaques which were devoid of keratin attachment (Vasioukhin et al., 2001). Moreover, a recessive mutation in DP led to a human disorder characterized by generalized striate keratoderma, woolly hair and dilated left ventricular cardiomyopathy, resulting in the collapse of keratin network and large intercellular spaces (Norgett et al., 2000). On the other hand, DP haploinsufficiency arising from the deletion of the amino-terminus do not result in heart defects but present palmoplantar keratoderma (Armstrong et al., 1999; Whittock et al., 1999).

1.3.1.4 Calcium pumps regulating desmosomal adhesions

Since desmosomal adhesions are dependent on extracellular calcium concentration (Kimura et al., 2007), mutations in the *ATP2A2* and *ATP2C1* genes coding for intracellular calcium pumps are thought to disrupt desmosomal adhesion. Indeed, human conditions such as Darier's disease and Hailey-Hailey disease implicated an important role for calcium in regulating desmosomal adhesions (Sakuntabhai et al., 1999b; Hu et al., 2000) (see Table 1.3).

Taken all these observations together, the presence of desmosomes in tissues experiencing large amounts of mechanical stress, such as the epidermis or the heart, highlights the importance of strong cell-cell adhesion in tissues. This is obvious from the severe phenotypes resulting from mutations or loss of desmosomal components. A list of desmosomal proteins associated with human skin disorders disrupting tissue functions is tabulated in Table 1.2.

Figure 1.3   Differential expressions of the junctional proteins
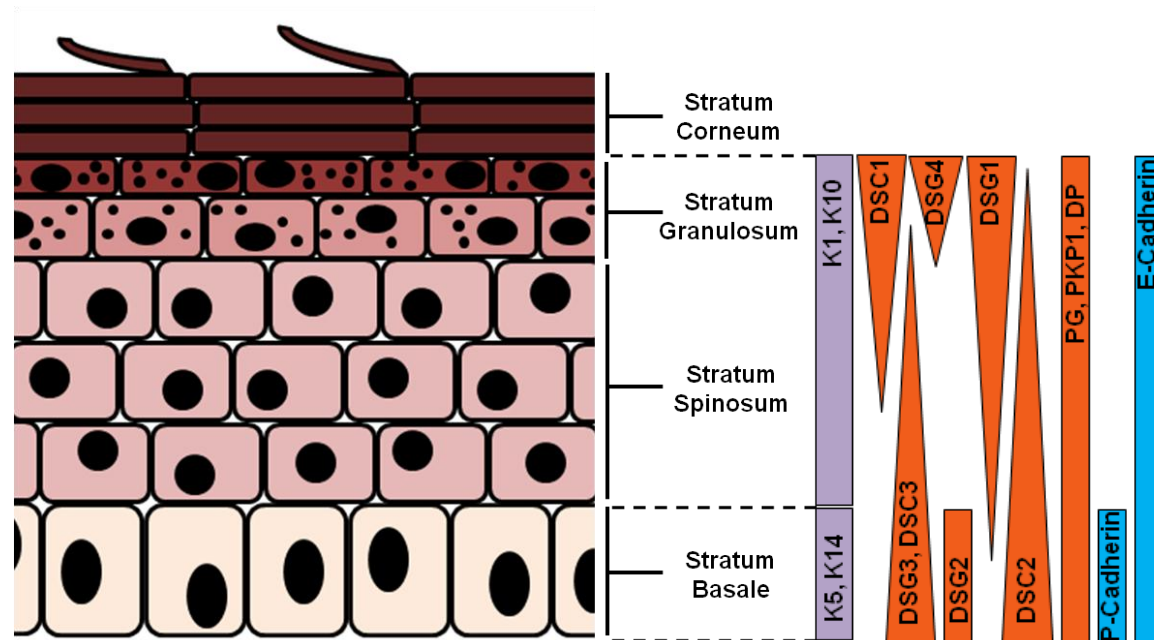
Figure redrawn after Simpson et al., 2011.

Table 1.2

Human diseases of the epidermal junctions

Desmosomes

Molecular target	Disease	Clinical phenotype (s)	Original finding (s)
DSG1	Bullous impetigo Staphylococcal scalded skin syndrome	Epidermal blisters at the granular layer caused by bacterial proteolytic attack (neonatal mice and human keratinocyte cell line)	(Amagai et al., 2000)
	Pemphigus foliaceus	Epidermal blisters at the granular layer caused by autoantibodies; Acantholysis	(Koulu et al., 1984)
DSG3	Pemphigus vulgaris (OMIM # 169610)	Epidermal blisters at the basal-suprabasal layer caused by autoantibodies; Mucosal erosions	(Amagai et al., 1991)
DSG4	Hypotrichosis (OMIM # 607903)	Sparse, fragile hair with bullous "bleb" and curled ingrown hair shafts within hair follicle	(Kljuic et al., 2003)
DSC2	Arrhythmogenic right ventricular cardiomyopathy (ARVC); ARVC with mild palmoplantar keratoderma and woolly hair (OMIM # 610476)	Ventricular arrhythmias with mild interstitial fibrosis and fatty infiltration of myocardium; Mild thickening of palms and soles; Tightly coiled hair	(Heuser et al., 2006; Simpson et al., 2009)
DSC3	Hypotrichosis with skin vesicles (OMIM # 613102)	Sparse, fragile hair with normal hair follicles; Recurrent skin vesicles	(Ayub et al., 2009)
DP/DSG1	Striate palmoplantar keratoderma (DSG1: OMIM # 148700; DP: OMIM # 612908)	Hyperkeratotic bands on the palms and soles	(Armstrong et al., 1999; Rickman et al., 1999; Whittock et al., 1999; Hunt et al., 2001)

DP	Carvajal syndrome (OMIM # 605676)	Longitudinal hyperkeratosis of a striate palmoplantar keratoderma with woolly hair and dilated cardiomyopathy	(Norgett et al., 2000)
	Lethal acantholytic epidermolysis bullosa (OMIM # 609638)	Universal alopecia; neonatal teeth and nail loss; Acantholysis; Early death	(Jonkman et al., 2005)
PKP1	Ectodermal dysplasia/skin fragility syndrome (OMIM # 604536)	Cutaneous fragility and congenital ectodermal dysplasia affecting skin, hair and nails	(McGrath et al., 1997)
PG	Naxos disease (OMIM # 601214)	Woolly hair; Non-epidermolytic palmoplantar keratoderma; Arrhythmogenic right ventricular cardiomyopathy	(McKoy et al., 2000)
	Lethal congenital epidermolysis bullosa	Generalized erythema and epidermolysis with no known cardiomyopathy; Total alopecia; Early death	(Pigors et al., 2011)

Table 1.3

Human diseases of the epidermal junctions

Calcium pumps

Molecular target	Disease	Clinical phenotype (s)	Original finding (s)
ATP2C1 (calcium pump)	Hailey-Hailey disease (OMIM # 169600)	Erythema blistering in the suprabasal layers; Acantholysis	(Hu et al., 2000)
ATP2A2 (calcium pump)	Darier's disease (OMIM # 124200)	Acantholysis; Keratotic papules coalescing into a hyperkeratotic plaque	(Sakuntabhai et al., 1999a; Sakuntabhai et al., 1999b)

1.3.2   Adherens junctions

Adherens junctions are electron dense transmembrane structures that associate with the actin cytoskeleton, which are responsible for cell adhesion, motility and changes in cell shape (Gumbiner, 1996). The transmembrane core of the adherens junctions consists of classical cadherins, namely: epithelial cadherin (E-cadherin) and placental cadherin (P-cadherin).

1.3.2.1   Cadherins

The extracellular domains of E-cadherin form calcium-dependent homophillic adhesive interactions with E-cadherin from adjacent cells. Its cytoplasmic domain, on the other hand, is responsible for clustering of surface cadherins to form a junctional structure (reviewed in Vasioukhin and Fuchs, 2001). The main linkage to the actin cytoskeleton is through α-catenin (Rimm et al., 1995), which apart from its role of mediating E-cadherin-catenin adhesions, is also responsible for regulating actin dynamics and polymerization (reviewed in Vasioukhin and Fuchs, 2001). The regulation of actin dynamics allows for the extension and anchorage of filopodia into neighboring keratinocytes, strengthening cell-cell adhesions. Conditional deletion of E-cadherin in mice resulted in hyperproliferation, abnormal differentiation and impaired barrier formation of the epidermis (Young et al., 2003; Tinkle et al., 2004; Tunggal et al., 2005), while ablation of both E-cadherin and P-cadherin resulted in lethal blistering (Tinkle et al., 2008). Patients harboring CDH3 mutations targeting P-cadherin suffered from hair loss and macular degeneration (Sprecher et al., 2001; Kjaer et al., 2005) (see Table 1.4). Hence, adherens junction components are not only essential for regulating cell-cell adhesion but also modulate epidermal morphogenesis.

Table 1.4

Human diseases of the epidermal junctions

Adherens junctions

Molecular target	Disease	Clinical phenotype (s)	Original finding (s)
P-cadherin (encoded by CDH3)	Hypotrichosis with juvenile macular dystrophy (OMIM # 601553)	Hair loss heralding progressive macular degeneration and early blindness	(Sprecher et al., 2001)
	Ectodermal dysplasia; Ectrodactyly; Macular degeneration (EEM) syndrome (OMIM # 225280)	Hypotrichosis and sparse hair; Syndactyly in hands and feets	(Kjaer et al., 2005)

1.3.3 Gap junctions

Gap junctions are intercellular channels that mediate the direct passage of low molecular weight metabolites (< 1 kDa) and ions between the cytoplasm of adjacent cells (Kelsell et al., 2001). Gap junctions are formed by connexins, which are composed of oligomers of six connexons (Cxs), of which Cx26, Cx43, Cx30, Cx30.3 and Cx31 are expressed in the epidermal keratinocytes. These connexons can form a homotypic or heterotypic channel. Missense mutations in the genes encoding Cx26, Cx30, Cx30.3 or Cx31 can lead to several forms of inherited human disorders such as Vohwinkel's syndrome, Clouston syndrome and Erythrokeratodermia variabilis, causing keratoderma and/or hearing loss (see Table 1.5). Hence, gap junction components are not only essential for regulating cell-cell communication but also modulate epidermal morphogenesis.

Table 1.5

Human diseases of the epidermal junctions

Gap junctions

Molecular target	Disease	Clinical phenotype (s)	Original finding (s)
Cx26	Keratitis ichthyosis deafness syndrome (OMIM # 148210)	Vascularizing keratitis; Progressive erythrokeratoderma; Profound sensorineural hearing loss	(Richard et al., 2002)
	Vohwinkel's syndrome (Keratoderma hereditaria mutilans) (OMIM # 124500)	Papular and honeycomb keratoderma associated with constrictions of digits leading to amputations; Distinctive starfish-like acral keratoses; Moderate sensorineural hearing loss	(Maestrini et al., 1999)
	Bart-Pumphrey syndrome (OMIM # 149200)	Hyperkeratosis of knuckle pads; Diffuse palmoplantar keratoderma with keratotic bands; Sensorineural hearing loss	(Richard et al., 2004)
	Hereditary non-syndromic sensorineural deafness (OMIM # 148350)	Palmoplantar keratoderma; Profound deafness and high-frequency hearing loss	(Kelsell et al., 1997)
Cx30	Clouston syndrome (hidrotic ectodermal dysplasia) (OMIM # 129500)	Palmoplantar hyperkeratosis; Generalized alopecia; Nail dystrophy	(Essenfelder et al., 2004)
Cx30.3, Cx31	Erythrokeratodermia variabilis (OMIM # 133200)	Diffuse scaling and erythema gyratum repens-like migratory lesions	(Richard et al., 1998; Macari et al., 2000)

1.3.4 Tight junctions

Tight junctions are formed by transmembrane and intracellular molecules such as occludin, junction adhesion molecule and claudins (reviewed in Bazzoni and Dejana, 2001). In the granular layer of the epidermis, tight junctions seal epithelial sheets together by forming a belt-like adhesion between the cells, creating an environmental barrier that controls water loss and protects against pathogen invasion (reviewed in Niessen, 2007). Intracellular tight junction components also include scaffolding proteins such as zonula occludens (ZO) proteins, namely: ZO1, ZO2 and ZO3, which cluster the transmembrane molecules and couple to the actin cytoskeleton (reviewed in Niessen, 2007). The role of a transmembrane molecule, claudin, in regulating epidermal permeability was found when mice ablated of claudin-1 died of profound trans-epidermal water loss (Furuse et al., 2002). Moreover, missense mutations in claudin-1 gene led to sclerosing cholangitis associated with ichthyosis (Hadj-Rabia et al., 2004), a gastrointestinal syndrome affecting bile secretion, confirming a role for claudin-1 in regulating paracellular permeability between epithelial cells. Hence, these studies demonstrate that tight junction components are crucial for regulating epidermal permeability.

Figure 1.4   Cell-matrix junctions of the epidermis
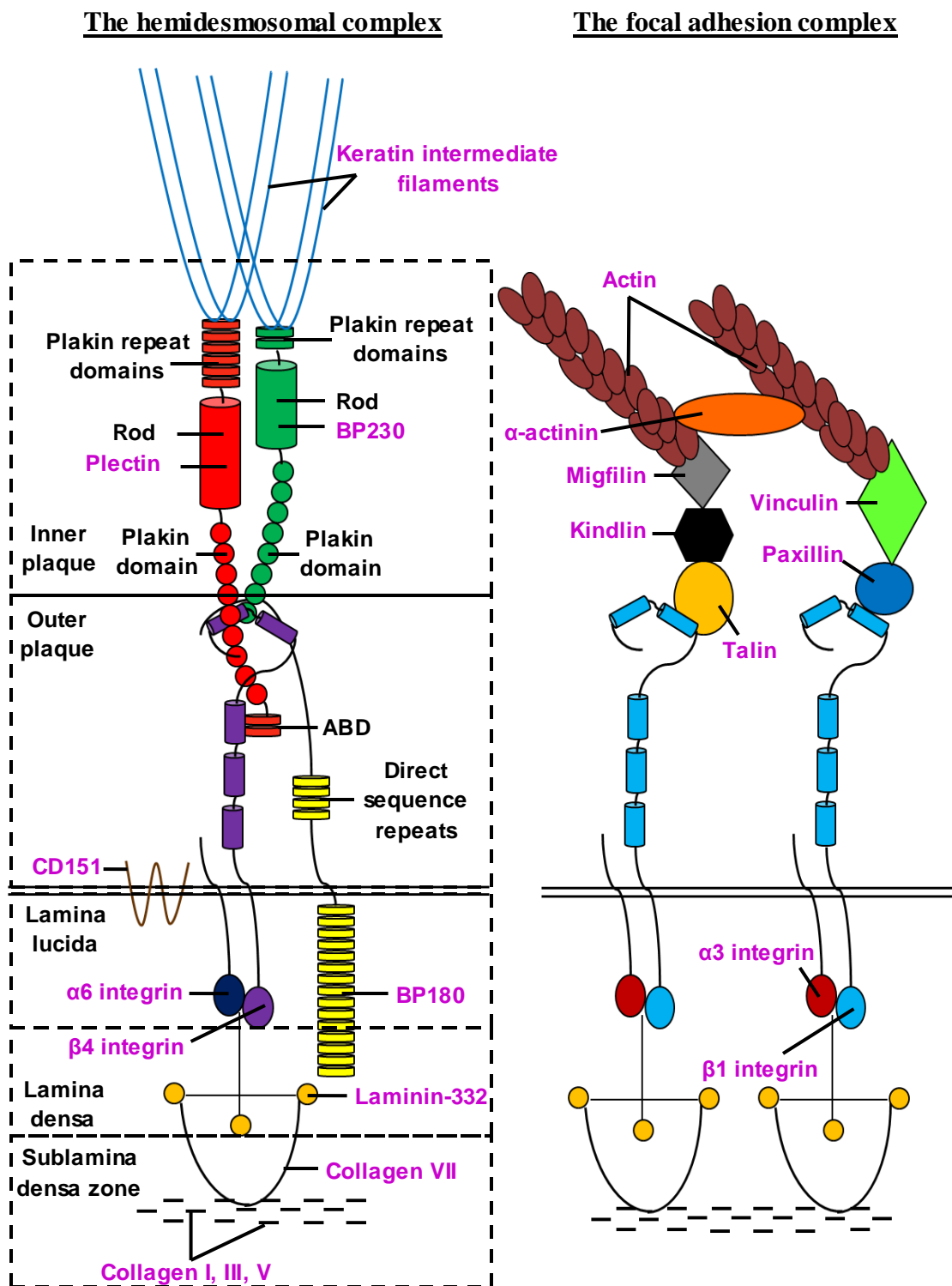
Figures redrawn after Jonkman, 1999 and de Pereda et al., 2009.

1.4   Anchoring junctions mediating cell-matrix adhesion

At the dermal-epidermal junction (basement membrane), keratin intermediate filaments of the basal keratinocytes are anchored to the dermal matrix through the hemidesmosomal proteins, whereas actin microfilaments and microtubule filament systems are anchored through focal adhesions (see Figure 1.4). Hemidesmosomes are multi-protein complexes that mediate epithelial-stroma cohesion in stratified and complex epithelial (reviewed in Borradori and Sonnenberg, 1999). These complexes, which appear as three-layered structures along the plasma membrane of basal cells, are composed of at least five different proteins, namely: the laminin-332 receptor α6β4 integrins, the bullous pemphigoid antigens 180 and 230 (BP180 and BP230), tetraspanin (CD151) and plectin (reviewed in Jones et al., 1998).

Focal adhesions are dynamic structures that not only mediate cell-matrix adhesions, but also play an important role in cell migration, proliferation and survival. Focal adhesions typically undergo assembly and disassembly through the continuous association of proteins such as α3β1 integrins, vinculin, talin, kindlin-1 and α-actinin (reviewed in Watt, 2002). The presence of these complexes provides a means to enhance the stability and also attribute dynamics for the epidermis. The understanding of the properties of these different complexes can provide some insights in the skin's ability to provide mechanical resilience and also adaptability to environmental cues. In the next paragraphs, the compositions of the anchoring junctions mediating cell-matrix adhesion will be discussed in detail.

1.4.1   Hemidesmosomes

There are two distinct types of hemidesmosomes, of which type II hemidesmosomes, found in intestinal epithelial cells or mammary gland epithelial cells, do not have a

clear three-layered structure and are composed solely of α6β4 integrins and plectin (Uematsu et al., 1994). Ultrastructurally, type I hemidesmosomes appear as electron-dense structures comprising of an inner and an outer plaque, accompanied by a sub-basal dense plate. The inner plaque is composed of hemidesmosomal proteins such as plectin and BP230, which serves as an anchorage site for kertain intermediate filaments. The outer plaque, on the other hand, consists of the α6β4 integrins and BP180 (reviewed in Nievers et al., 1999). The basement membrane underlying the hemidesmosomes constitutes a network of interconnecting proteins (reviewed in Timpl, 1996). It consists of laminin-332, collagen type IV, and glycoproteins such as nidogen, perlecan and fibulins that act as stabilizing bridges (reviewed in Yurchenco and O'Rear, 1994). Anchoring filaments, which are composed of BP180 (Masunaga et al., 1997) and laminin-332 (Rousselle et al., 1991), traverse across the sub-basal dense plate and the lamina lucida of the basement membrane, and connect the hemidesmosome to the anchoring fibrils (collagen type IV and VII) in the lamina densa and sub-basal lamina densa respectively. These collagens extend further into the dermis to connect with collagen I from where they loop back into the lamina densa, or insert into anchoring plaques (Keene et al., 1987). This reinforces the attachment of the epidermal basement membrane to the underlying dermal connective tissue.

1.4.1.1 α6β4 integrins

In the outer plaque of the hemidesmosomes, α6β4 integrins serve as a transmembrane receptor for laminin-332 and they together make up the core structure of the hemidesmosome. α6β4 integrins belong to the large family of heterodimeric receptors that mediate the attachments of cells to the extracellular matrix (reviewed in Buck and Horwitz, 1987). Both α and β subunits of the integrins have a large extracellular

portion, a transmembrane segment, and a shorter cytoplasmic domain. α6β4 integrins differ from other integrins in that the cytoplasmic domain of β4 subunit contains over 1000 amino acids in length and contains two pairs of type III fibronectin (FNIII) repeats separated by a connecting segment (Tamura et al., 1990). Transfection of the second FNIII repeat and the adjacent 27 amino acids of the connecting segment are demonstrated to be critical for the correct localization of α6β4 integrins to the hemidesmosomes (Niessen et al., 1997). The cytoplasmic domain of β4 is also crucial for the organization of hemidesmosomes because overexpression of tail-less β4 could block hemidesmosomal formation (Spinardi et al., 1993). Moreover, the extracellular domain of α6β4 integrins is important for cell adhesion. Antibodies against α6β4 prevent hemidesmosomal assembly and induce dermal-epidermal separation *in vitro* (Kurpakus et al., 1990). This is further supported by studies using α6β4 knockout mice where it is observed that there was extensive epithelial detachment devoid of hemidesmosomes (Georges-Labouesse et al., 1996; van der Neut et al., 1996). Indeed, mutations in the genes encoding α6 and β4 integrin subunits led to patients suffering from junctional epidermolysis bullosa associated with pyloric atresia (PA-JEB), resulting in cutaneous aplasia and mucosal erosions (Vidal et al., 1995; Shimizu et al., 1996). Hence, these studies demonstrate that α6β4 integrins are important in maintaining the mechanical integrity of both the basal keratinocytes and the basement membrane.

1.4.1.2 Laminin-332

The α6β4 integrins are receptors for various laminins, but preferentially bind to laminin-332 (Niessen et al., 1994), which is predominately found in the epidermal basement membrane (Rousselle et al., 1991). Laminin-332 belongs to the heterotrimeric proteins of the laminin family, consisting of the α3, β3 and γ2 subunits

(Marinkovich et al., 1992), which can act as a ligand for α6β1 and α3β1 integrins as well as α6β4 integrins. The first repeat of the G domain of α3 subunit of laminin-332 is responsible for the binding sites of these integrins (Rousselle et al., 1995). Laminin-332 also interacts with the NC1 domain of collagen VII, the major component of the anchoring fibrils, linking the α6β4 integrins to the dermal matrix (Rousselle et al., 1997). Cross-linking of laminin-332 with laminin-311 and laminin-321 can result in their self-associations and promote stable epithelial-stromal attachment (Champliaud et al., 1996). The importance of laminin-332 in maintaining anchorage and motility of epithelial cells was demonstrated by the targeted deletion of the α3 subunit of laminin-332 in mice that resulted in junctional blisters and disrupted hemidesmosomes. Moreover, keratinocytes isolated from these mice had a deficit in cell motility (Ryan et al., 1999). Indeed, mutations/deletions in the genes encoding laminin-332 subunits led to patients suffering from lethal (Herlitz) junctional epidermolysis bullosa (JEB), resulting in severe epidermal fragility associated with early death (Kivirikko et al., 1995; Kivirikko et al., 1996).

1.4.1.3 BP180

The other transmembrane component of hemidesmosome is BP180 (also known as BPAG2 or collagen type XVII). BP180 is a type II transmembrane protein with its C-terminus located at the extracellular site of the plasma membrane (Giudice et al., 1992). It contains a series of collagenous repeats in its extracellular domain, which are predicted to form collagen-like triple helix (Hirako et al., 1996). Sequences within the N-terminus of the cytoplasmic tail of BP180 interact with β4 integrin tail (Borradori et al., 1997; Aho and Uitto, 1998) while the NC16A domain of BP180 interacts with the α6 integrin subunit (Hopkinson et al., 1995; Hopkinson et al., 1998). The importance of BP180 in maintaining the stability/assembly of hemidesmosomes was

demonstrated when it was discovered that autoantibodies against BP180 led to bullous pemphigoid, a skin blistering disorder (Stanley et al., 1981). Moreover, inherited mutation or deletion of BP180 led to patients suffering from generalized atrophic benign epidermolysis bullosa (GABEB), resulting in universal alopecia with skin atrophy (Jonkman et al., 1995; McGrath et al., 1995). Deficiencies in BP180 do not seem to affect the normal localization of α6β4 integrins, laminin-332 and BP230 to the basal membrane although the hemidesmosomes are disrupted with a lack of well-defined cytoplasmic plaques. These studies demonstrate that BP180 is important in mediating hemidesmosome assembly and stability.

1.4.1.4 BP230

In the inner plaque of the hemidesmosomes, the major cytoplasmic plaque proteins are the BP230 (Stanley et al., 1988; Sawamura et al., 1991) and plectin (Wiche et al., 1991). BP230 and plectin belong to the plakin family of cytoskeletal linker proteins that anchor intermediate filaments to the plasma membrane (Tanaka et al., 1991). Transfection studies and yeast two-hybrid studies have shown that the N-terminus of BP230 could interact with the N-terminus of the cytoplasmic domain of BP180 (Borradori et al., 1998; Hopkinson and Jones, 2000), which was mediated by the Y-domain of BP230 (Koster et al., 2003). A role for BP230 in attaching keratins to the hemidesmosomal plaque is determined by the C-terminus which contains two copies of plakin repeat domains. This was first demonstrated in BP230 knockout mice that exhibited poorly formed hemidesmosomes devoid of keratin intermediate filament attachment. Moreover, these mice suffered from epidermal blistering, which could be a result of the impaired anchorage of intermediate filament to desmosomes that caused a deficit in mechanical resilience (Guo et al., 1995). In addition, these mice also exhibited spinal nerve degeneration when the gene encoding the neuronal

isoform of BP230 (dystonin) was inactivated (Brown et al., 1995). Indeed, the importance of BP230 in maintaining the stability/assembly of hemidesmosomes was demonstrated when a homozygous nonsense mutation within BP230 gene was found in patients suffering from autosomal recessive epidermolysis bullosa simplex, resulting in skin blistering (Groves et al., 2010). Hence, these studies demonstrate that BP230 is crucial for hemidesmosome assembly and stability.

1.4.1.5 Plectin

Another major plaque protein in the hemidesmosome is plectin. Plectin is a large phosphoprotein expressed in both stratified and simple epithelial, where it acts as the most versatile cytoskeletal linker protein (Steinbock and Wiche, 1999). Plectin, being part of the plakin family, consists of a central α-helical rod domain that is flanked by large globular structures of the N- and C- terminal domains (Wiche et al., 1991). The N-terminus of plectin can associate with the cytoplasmic tail of β4 (Niessen et al., 1997; Rezniczek et al., 1998). This region also has a highly conserved actin-binding domain that is homologous to that of actin-binding proteins such as spectrin and dystrophin (Elliott et al., 1997). The binding site of plectin to intermediate filament is determined by the C-terminus, which contains six copies of plakin repeat domains, and the interaction has been mapped to a stretch of approximately 50 amino acids linking the plakin repeat domains 5 and 6 (Nikolic et al., 1996). The importance of plectin in maintaining hemidesmosomal organization was demonstrated by the observation that plectin knockout mice exhibited epidermal blistering coupled with abnormalities in cardiac and skeletal muscles (Andra et al., 1997), similar to patients suffering from epidermolysis bullosa simplex with muscular dystrophy (EBS-MD) (Gache et al., 1996; McLean et al., 1996; Smith et al., 1996). Hence, these studies

demonstrate that plectin is a critical cytoskeletal linker in mediating hemidesmosome assembly and stability.

1.4.2   Hemidesmosomal assembly

Taken together, a model can be used to describe the sequence of hemidesmosomal assembly based on the interactions between different hemidesmosomal proteins (reviewed in Nievers et al., 1999). Firstly, clustering of the α6β4 integrins with plectin may occur at the inner plaque because both the N- and C- terminus of plectin can directly associate with the first pair of FNIII repeats and the connecting segment of β4 integrin (Rezniczek et al., 1998) and also its cytoplasmic tail (Niessen et al., 1997). Consequently, co-clustering of plectin with the α6β4 integrins results in the association of plectin to keratin intermediate filaments (Nikolic et al., 1996), thus forming type II hemidesmosomes. Subequently, BP180 is recruited to the site of α6β4-plectin clustering because BP180 can directly interact with the cytoplasmic tail of β4 (Borradori et al., 1997; Aho and Uitto, 1998) and also interact with plectin (Gache et al., 1996). Finally, hemidesmosomal assembly is completed by the recruitment of BP230 to the inner plaque, possibly by BP180 (Borradori et al., 1998), and its connection to the keratin intermediate filament (Guo et al., 1995), hence forming type I hemidesmosomes.

In conclusion, hemidesmosomal proteins play an important role in maintaining epidermal morphology and integrity. A summary list of hemidesmosomal proteins associated with human skin disorders disrupting tissue functions is tabulated in Table 1.6.

Table 1.6

Human diseases of the epidermal junctions

Hemidesmosomes

Molecular target	Disease	Clinical phenotype (s)	Original finding (s)
BP180 (ColXVII, BPAG2)	Bullous pemphigoid or Herpes gestationis	Fluid-filled subepidermal blisters caused by autoantibodies	(Morrison et al., 1988; Diaz et al., 1990)
	Generalized atrophic bullous epidermolysis bullosa (GABEB) (OMIM # 226650)	Scalp alopecia with follicular atrophy; Nail atrophy	(Jonkman et al., 1995; McGrath et al., 1995)
BP230 (Dystonin, BPAG1e)	Epidermolysis bullosa simplex (autosomal recessive)	Generalized trauma-induced spontaneous blisters and erosions; Episodic limb numbness	(Groves et al., 2010)
α6β4 integrins	Junctional epidermolysis bullosa with pyloric atresia (PA-JEB) (OMIM # 226730)	Pyloric atresia and cutaneous aplasia; Mucosa erosions	(Vidal et al., 1995; Shimizu et al., 1996)
Plectin	Epidermolysis bullosa simplex with muscular dystrophy (EBS-MD) (OMIM # 226670)	Epidermal blisters heal with atrophic scarring; Nail dystrophy; Muscle weakness that progressively leads to widespread muscular atrophy and ptosis	(McLean et al., 1996; Smith et al., 1996)
Laminin-332: α3, β3 and γ2	Herlitz junctional epidermolysis bullosa (OMIM # 226700)	Extensive blistering of the skin and mucosal surfaces	(Pulkkinen et al., 1994a; Pulkkinen et al., 1994b; Kivirikko et al., 1995)

1.4.3 Focal contacts

Another structure connecting the basal keratinocytes to the dermal matrix is the focal adhesions (FAs). FAs are large complexes of proteins that function as cell-matrix adhesions through connecting the actin microfilaments and microtubule filaments to the underlying extracellular matrix (ECM) such as the dermis (reviewed in Zamir and Geiger, 2001). FAs are dynamic structures that are responsible for signal transduction and cell migration. In migrating cells, FAs frequently undergo assembly and disassembly through the associations and disassociations of many proteins (reviewed in Jockusch et al., 1995).

1.4.3.1 α3β1 integrins

α3β1 integrins are the major transmembrane ECM receptors found in focal contacts (reviewed in Watt, 2002). Integrin clustering occurs at the formation of focal contacts, where focal adhesion kinase (FAK) and tensin are recruited (Miyamoto et al., 1995). Integrin occupancy by ligands such as fibronectin or laminin can further recruit other proteins such as paxillin, vinculin, α-actinin, talin and kindlin to associate with the clustered integrins and initiate signal transduction (Dogic et al., 1998; Sondermann et al., 1999).

1.4.3.2 α-actinin

The first protein to be identified in the adhesion plaque was α-actinin (Lazarides and Burridge, 1975). α-actinin is a rod-shaped antiparallel homodimer that cross-links and bundles actin filament (Meyer and Aebi, 1990). α-actinin can also bind to the cytoplasmic domains of β1 integrin (Otey et al., 1990).

1.4.3.3   Vinculin

The second protein to be identified in the adhesion plaque was vinculin (Geiger, 1979; Burridge and Feramisco, 1980). Vinculin is an anchor protein found within focal adhesions where it is responsible for linking actin microfilaments to the plasma membrane (reviewed in Burridge et al., 1982).

1.4.3.4   Paxillin

Among the adhesion proteins, paxillin is a major component of the focal adhesions. Paxillin contains several distinct structural domains (Turner and Miller, 1994), suggesting that paxillin can act as a scaffold in recruiting structural and regulatory proteins into the focal complex. The N-terminus of paxillin also contains binding sites for vinculin and FAK (Turner and Miller, 1994).

There are two FERM (protein 4.1, ezrin, radixin, and moesin) domain-containing proteins such as talin and kindlin that are responsible for inside-out and outside-in signalling of the integrins (reviewed in Kinashi, 2012).

1.4.3.5   Talin

Talin is an ubiquitous 270 kDa protein that links integrin to actin microfilaments. It consists of a N-terminal globular head that contains the integrin-binding FERM domain, and a rod domain that can associate with the F-actin binding protein vinculin (reviewed in Kinashi, 2012). Talin is important in regulating cell adhesion to the ECM that is essential for cell migration (ie. during embryogenesis, angiogenesis and immune responses), tumour invasion and metastasis (reviewed in Frame and Norman, 2008; Desiniotis and Kyprianou, 2011).

1.4.3.6 Kindlin

Kindlin is part of the kindlin family that contains a FERM and a pleckstrin homology (PH) domain. Like talin, kindlin is also a linker of the integrins to the actin cytoskeleton. The importance of kindlin in regulating integrin signaling was derived from mutations in gene encoding FFH-1 (*KIND1*) leading to patients suffering from Kindler syndrome which was characterized by poikiloderma and trauma-induced blistering (Jobard et al., 2003; Siegel et al., 2003). Kindler syndrome was thus the first FA disorder discovered and the first hereditary skin fragility disorder caused by a defect in actin-ECM attachments, rather than keratin-ECM linkages (Siegel et al., 2003).

Hence, these studies show how focal adhesion complex is important in regulating dynamics and morphogenesis of the epidermis.

Figure 1.5   Key events in the field of epithelial biology with emphasis on intermediate filaments

The epidermal proliferation unit. Ordered structure of the skin where the epidermis is stacked into columns with a clonogenic basal layer. (Mackenzie, 1969)

EGF increases the culture lifetime of epidermal keratinocytes by delaying senescence and keeping them in a proliferative state. (Rheinwald and Green, 1977)

Changes in keratin gene expression during terminal differentiation of the keratinocyte results largely from changes in synthesis. (Fuchs and Green, 1980)

Derivation of the fibrillar substructure of keratin intermediate filament consistent to the 10-nm filament model. (Aebi et al., 1983)

Effects of EGF and TGF-α in colony expansion by increasing cell migration rate. (Barrandon and Green, 1987)

Nuclear lamins undergo reversible mitotic disassembly through phosphorylation of its subunits. (Gerace and Blobel, 1980)

Complete sequencing of epidermal type I keratin subunit and implications of its structure. (Steinert et al., 1983)

Site-specific, phosphorylation-dependent disassembly of the vimentin intermediate filament. (Inagaki et al., 1987)

1969   1975   1977   1979   1980   1982   1983   1985   1987   1990

Epithelial cells isolated directly from the skin can be passaged for many generations when cultured together with the fibroblast feeder layer. (Rheinwald and Green, 1975)

A quantitative description of the *in vitro* assembly/re-assembly of intermediate filaments from BHK-21 cells and established conditions for regulation of intermediate filament assembly. (Zackroff and Goldman, 1979)

First catalog of human cytokeratins established and the nomenclature is still used presently. (Moll et al., 1982)

Keratin type I and II subunits form heterodimers in a 1:1 ratio and exist as parallel chains in axial register. (Hatzfeld and Franke, 1985; Parry et al., 1985; Weber and Geisler, 1985)

Confirmation of keratin heterodimer formation at the dimer stage using site-specific mutagenesis and recombinant proteins. (Hatzfeld and Weber, 1990; Steinert, 1990)

Complete sequencing of epidermal type II keratin. (Steinert et al., 1985)

Mapping of K18 gene to chromosome 12 (Waseem et al., 1990)

41

First report of a hereditary skin fragility disorder, epidermolysis bullosa simplex (EBS), associated with mutations in keratin intermediate filaments. (Bonifas et al., 1991; Coulombe et al., 1991a)

EGF and TGF-α induce the activation and hyperproliferation-associated K6 and K16. (Jiang et al., 1993)

EBS severity correlates with the position of keratin point mutations (phenotype-genotype correlations). (Letai et al., 1993)

Unit length filaments (ULFs) resulting from lateral association of vimentin intermediate filament dimers. (Herrmann et al., 1996)

Compensatory pairing of K15 with K5, in K14 knockout mice, at the basal layer of stratified squamous epithelial. (Lloyd et al., 1995)

Keratins turn over by ubiquitination in a phosphorylation-modulated manner. (Ku and Omary, 2000)

First report of the intermediate filament peptide structure of helix 2B motif with atomic resolution. (Herrmann et al., 2000)

Keratin dynamics (FRAP analysis) in living epithelial cells. (Yoon et al., 2001)

Complete cytolysis and neonatal lethality of K5 knockout mice. (Peters et al., 2001)

1991 1992 1993 1994 1995 1996 1999 2000 2001 2002

Discovery of a point mutation at the helix termination domain of K5, which leads to pathogenesis of EBS. (Lane et al., 1992)

Role of protein phosphatases in regulating the structural organization of intermediate filaments. (Eriksson et al., 1992)

Functional human K14 "knockout" leading to severe EBS. (Chan et al., 1994; Rugg et al., 1994)

The catalog of human hair keratins, I. (Langbein et al., 1999)

The catalog of human hair keratins, II. (Langbein et al., 2001)

Divide-and-conquer crystallographic strategy to unravel the atomic structure of intermediate filaments. (Strelkov et al., 2001)

Role of 14-3-3 binding to keratins during mitosis. (Ku et al., 2002)

Unraveling the roles of conserved segments 1A and 2B of the intermediate filament dimer in filament assembly with atomic resolution. (Strelkov et al., 2002)

42

K8 and K18 mutations are risk factors for developing liver diseases. (Ku et al., 2003)

Wound-induced K17 influences cell growth and size by regulating protein synthesis. (Kim et al., 2006)

Commencement of the human intermediate filament database. (Szeverenyi et al., 2008)

Crystal structure of K5-K14 coiled-coil heterodimer at rod 2B domain and trans-dimer disulfide bond formation for perinuclear organisation of keratin filaments. (Lee et al., 2012)

Roles of K6 and K17 during wound closure in embryonic skin. (Mazzalupo et al., 2003)

New consensus nomenclature for mammalian keratins. (Schweizer et al., 2006)

Consensus meeting on the diagnosis and classification of inherited EB. (Fine et al., 2008)

Keratin glycosylation protects against epithelial injury by promoting phosphorylation and activation of cell survival kinases. (Ku et al., 2010)

2003   2005   2006   2007   2008   2009   2010   2011   2012 onwards

Assymetric cell divisions in the basal layer promote stratification and differentiation of mammalian skin. (Lechler and Fuchs, 2005)

Induction of K17 in basal epidermal keratinocytes upon sulforaphane treatment restores skin integrity in EBS. (Kerns et al., 2007)

Gene targeting strategy that eliminates the entire keratin multiprotein family reveals the roles of keratins in growth and protein biosynthesis. (Vijayaraj et al., 2009)

Assymetric cell divisions in the basal layer promote notch-dependent epidermal differentiation using RNA interference approach. (Williams et al., 2011)

Type II keratins precede type I keratins during early embryonic development. (Lu et al., 2005)

Intercalary subunit exchange along the lengths of intermediate filaments and elongation by end-to-end annealing. (Colakoglu and Brown, 2009)

Keratin hypersumoylation at rod 2B domain alters filament dynamics. (Snider et al., 2011)

43

1.5   Keratin intermediate filaments

1.5.1   Keratin expression in the epidermis

Keratinocyte differentiation plays an important role in the maintanence of epidermal barrier function. Since keratins are the most abundant epidermal proteins that are found in keratinocytes, changes in keratin expressions as the keratinocytes undergo the terminal differentiation program are likely to play a role in epidermal morphogenesis.

Indeed, within the epidermis, there exists a differential pattern of keratin expressions that are tightly regulated across the different layers. For instance, basal keratinocytes at the basal layer express K5 and K14 as their major keratins (Nelson and Sun, 1983), whereas keratinocytes at the spinous and granular layers are found to express K1 and K10 predominantly (Fuchs and Green, 1980). Keratin 2e (now called K2) has been found to localize further up in the granular layer, and its expression is delayed relative to K1 and K10 (Collin et al., 1992). Other site-specific suprabasal keratins include K9, which is confined to palmo-plantar skin (Fuchs and Green, 1980). Why there is a need for different keratin expression in the epidermis is not so well understood, but one reason could be that keratin filaments are differentially orientated in their spatially confined compartments to perform specific functions. Keratin filaments (K5 and K14) are orientated in a parallel manner in basal keratinocytes, wherein these cells can compact together in epidermal folds seen in histological section (see Figure 1.1), allowing them to proliferate in the basal layer. Keratin networks (K1 and K10) are arranged in either parallel arrays or cubic-like structures in the uppermost cornified layers of the epidermis to establish a stiff corneocyte keratin network (Norlen and Al-Amoudi, 2004), and the spacing out of corneocytes seen in histological section (see

Figure 1.1) could therefore confer mechanical resilience to the epidermis. In support of this, *in vitro* formation of the suprabasal cytoskeleton (K1 and K10) is dependent on the pre-existing basal cell intermediate filament (K5 and K14) network (Kartasova et al., 1993; Paramio and Jorcano, 1994), hence stressing the need for different keratin expressions in the epidermis.

1.5.1.1 Stratification process

How these switches in keratin expression occur so precisely as keratinocytes progressively undergo terminal differentiation has not been well understood until recently. A few recent discoveries highlight key events leading to stratification processes. It is shown that in response to canonical Notch/RBP-J (recombining binding protein suppressor of hairless) signalling, basal keratinocytes became committed to undergo terminal differentiation. This occurs through suppression of basal cell gene expression, such as K5 and K14, via Hes-1 (a downstream target of Notch/RBP-J) -independent pathways, and induction of spinous cell differentiation through switching on differentiation-specific genes such as K1 and K10 expression via Hes-1 dependent pathways (Blanpain et al., 2006). In addition, AP2 transcription family factors can promote spinous cell commitment by exerting effects antagonistic to EGFR signalling, which is known to promote proliferation and serve as a suppressor of Notch signalling (Kolev et al., 2008). Moreover, stratification is initiated by asymmetric cell divisions (mitotic spindles perpendicular to basement membrane) to enable vertical expansion of the suprabasal keratinocytes (Lechler and Fuchs, 2005). The control points for mitotic orientation in epidermal development were recently identified in mouse, which involved both the tightly regulated expression of mInsc (mouse Inscuteable) and NuMA (nuclear mitotic apparatus protein), to direct apical-basal spindle orientation during asymmetric cell division

(Poulson and Lechler, 2010). This process was recently reported to be also under the influence of Notch signaling (Williams et al., 2011).

1.5.1.2   Wound healing (re-epithelialization)

In situations of epidermal injury, wounded keratinocytes induce K6 proteins (K6a, b and c), K16 and K17 in suprabasal cells at the expense of K1 and K10 (Weiss et al., 1984; Jiang et al., 1993). At this stage known as the re-epithelialization phase of wound healing, keratinocytes at the wound edge change their morphology from cuboidal to become flattened and extend numerous ruffles known as lamellipodia in a polarized manner. Before they migrate into the wound site, they must disassemble their desmosomes and hemidesmosomes (at least partially), and relocate their integrins onto actin microfilaments to serve as focal adhesions during migration. This ensures that the keratinocytes detach from the basement membrane and enter the wound bed (reviewed in Santoro and Gaudino, 2005). Keratinocytes advance in epithelial sheets (also known as the epithelial tongue) across the wound site, secreting collagenases and proteases such as matrix metalloproteinases (MMPs) to dissolve parts of the damaged ECM at the front of the migrating sheet (Salo et al., 1994). These changes in keratinocyte motility and cell-cell adhesion during re-epithelialization recapitulate several aspects of type II epithelial to mesenchymal transition (EMT) in wound repair (reviewed in Kalluri and Weinberg, 2009), wherein epithelial cells undergoing EMT convert from a sedentary to a migratory phenotype, remodel the ECM surrounding them and secrete MMPs to assist in their migration (reviewed in Leopold et al., 2012). Growth factors and cytokines (Myers et al., 2007), stimulated by integrins and MMPs, cause keratinocytes to proliferate close to wound edges to generate new keratinocytes for replacement of lost cells, which occurs at a much faster rate than in normal tissues (reviewed in Deodhar and Rana, 1997).

Keratinocytes continue migrating across the wound bed till cells from either end meet in the middle, at which contact inhibition prevents them from migrating further. At this point, keratinocytes begin to secrete new basement membrane proteins (Laplante et al., 2001) and reverse their morphology back to cuboidal shapes, re-establishing desmosomes to facilate cell-cell adhesion and hemidesmosomes to anchor to the new basement membrane again. The functional epidermis is then regenerated from epithelial stem cells originating from the basal layer of the interfollicular epidermis (reviewed in Liang and Bickenbach, 2002) and skin appendages such as hair follicle (Cotsarelis et al., 1990; Taylor et al., 2000; Ito et al., 2005) and sweat gland (Lu et al., 2012). These epithelial stem cells are self-renewing, and are able to generate the rapidly proliferating keratinocytes (transit amplifying cells) needed to reconstruct the epidermal barrier (reviewed in Gurtner et al., 2008; Lau et al., 2009). These transit amplifying cells can undergo several cell divisions before differentiating via Notch/p63 cross-talk (Nguyen et al., 2006) to re-form the strata found in the re-epithelialized skin, and restore the epithelial barrier function (reviewed in Raja et al., 2007).

The dramatic changes in keratin expression that are associated with this profound change in keratinocyte behaviour suggest that the functional properties of different keratins may directly regulate growth and regeneration of these epithelia. In the following paragraphs, the structure and functions of keratin proteins in the cytoskeleton will be discussed in detail.

1.5.2 Keratin structure and assembly

Keratins belong to the intermediate filament family of proteins, which all share similar structure, sequence and function, and are expressed in a tissue- and

differentiation-dependent manner. Intermediate filaments, together with actin microfilaments and microtubule filaments, form the major constituents of the cellular cytoskeleton. The name 'intermediate filaments' is derived from their diameter, which is 10-12 nm, being intermediate between that of actin microfilaments (5-8 nm) and the microtubules (25 nm) (reviewed in Omary et al., 2006). Keratins are a major constituent of the epidermal keratinocytes. They typically connect to desmosomes and hemidesmosomes, thereby contributing not only to stability between epithelial cells but also to the stability of the epithelial attachment to the basement membrane, hence conferring mechanical resilience to the skin (reviewed in Fuchs and Karakesisoglou, 2001).

1.5.2.1 Keratin intermediate filament family

Keratin genes form the largest group of the intermediate filament family in the human genome, comprising of 54 distinct functional genes. According to their biochemical properties (isoelectric points and molecular weights), keratins can be classified into two groups, the acidic type I and the basic to neutral type II keratins (Moll et al., 1982). A new consensus nomenclature for mammalian keratin genes and proteins has recently been reported, and is divided into three categories: (1) epithelial keratins, (2) hair keratins and (3) keratin pseudogenes (Schweizer et al., 2006). This nomenclature includes 28 type I (K9, K10, K12-K20, K23-K28, K31-K40) and 26 type II (K1-K8, K71-K86) keratins, which form two clusters of 27 genes each on chromosomes 17q21.2 and 12q13.13 [the gene for type I K18 being located in the type II keratin gene domain as discovered in (Waseem et al., 1990)], thereby extending the catalog of human cytokeratins first set up in 1982 (Moll et al., 1982).

1.5.2.2   Primary structure of keratin

Like all other intermediate filament proteins, keratins contain a central α-helical rod domain of ~ 310 amino acids that is interrupted by non-α-helical linkers and flanked by non-α-helical amino-terminal "head" and carboxy-terminal "tail" domains, giving rise to a highly conserved tripartite structure (reviewed in Herrmann et al., 2009). The central rod domain is composed of sub-domains 1A, 1B, 2A and 2B (Weber et al., 1988) which are separated by linkers L1, L12 and L2, and an additional interruption in segment 2B, the so-called stutter region (North et al., 1994). These regions of sequence discontinuity are highly conserved in all intermediate filament proteins (Weber and Geisler, 1985) and may not form α-helices (reviewed in Steinert et al., 1994) (see Figure 1.6). A role for the stutter region in K14 rod 2B domain is recently suggested wherein the highly conserved cysteine residue at 367 (K14 C367) may be involved in mediating trans-dimer disulfide formation between K5 and K14 heterodimers, hence promoting perinuclear organization of keratin filaments (Lee et al., 2012). Moreover, it is proposed that trans-filament disulfide linkages between pairs of keratin intermediate filament (K5 and K14) may affect its alignment in the reorganisation of nuclear shape in different calcium concentrations mimicking stratification process. It is observed that in low calcium medium, keratinocytes have parallel keratin bundles with elongated nucleus whereas at high calcium concentration, keratin filament bundles tend to wrap around the round shape nuclei, where they cross each other at various angles to form a cube-like architecture (Lee et al., 2012). This suggests that the orientation of keratin intermediate filaments may confer epithelial cells the network stiffness required for the mechanical resilience of the epidermis.

The rod domain is composed of heptad repeats, ie. repeats of seven amino acid residues (a-b-c-d-e-f-g)$_n$, in which positions "a" and "d" are generally occupied by

hydrophobic residues that drive coiled-coil heterodimer formation. Positions "e" and "g" are normally occupied by hydrophilic and charged residues that may provide additional interactions to strengthen the binding (see Figure 1.7). The starting residues of rod 1A domain and the ending residues of rod 2B domain, known as the helix initiation and the helix termination motifs respectively, comprise of ~ 20 amino acid sequence motifs that are highly conserved among the different keratins (see Figure 1.6). These motifs are crucial for initiating keratin intermediate filament assembly and any mutations residing in these motifs will interfere with the early stages of filament elongation (Steinert et al., 1993). Indeed, the helix boundary motifs are known to be mutational "hot spots" in almost all inherited keratin disorders (Muller et al., 2006). On the other hand, variations in the amino acid sequences residing at the "head" and "tail" domains seem to account for the diversity among individual keratin proteins (reviewed in Lane and McLean, 2004). In addition, these end domains can undergo posttranslational modifications that can further modulate the solubility, organization and function of the keratin intermediate filaments (reviewed in Omary et al., 2006).

1.5.2.3   Secondary structure of keratin

Keratins are obligate heterodimers of epidermal type I (Steinert et al., 1983) and type II (Steinert et al., 1985) keratins in a 1:1 molar ratio, which exhibit a parallel, in-register alignment (Parry et al., 1985; Hatzfeld and Weber, 1990; Steinert, 1990). Almost any type I and type II pair will co-polymerize *in vitro* (Hatzfeld and Franke, 1985). However, the resulting filaments are not stable and co-polymerization is not efficient between pairs of keratins that are not normally co-expressed in tissues. Since full-length intermediate filament dimers spontaneously assemble into filaments, this makes intermediate filaments poor candidates for study by crystallization. Hence, up till now, there are still no crystal structure of the full-length intermediate filament

dimer, unlike that of the other cytoskeletal structures such as globular actin (Bubb et al., 2002) or the tubulin dimer (Nogales et al., 1998). In an attempt to overcome the difficulties in studying intermediate filament structure, a divide- and- conquer approach has been used (Strelkov et al., 2001). This method produced and characterized 17 overlapping soluble fragments of intermediate filament protein, and some of these fragments produced useful diffraction data at the resolution between 1.4 and 3 Å. Using these results and molecular modeling, a model of the vimentin homodimer has been constructed (Strelkov et al., 2002). A more recent study revealed the crystal structure of K5-K14 coiled-coil heterodimer in the rod 2B domain, and some distinctive features of K5-K14 rod 2B heterodimer, as compared to vimentin rod 2B homodimer, were observed. Firstly, the hydrogen bonds and most of the salt bridges in the K5-K14 model were unidirectional or asymmetric, which was different from those in vimentin homodimer. Secondly, the K5-K14 model formed more asymmetrical salt bridges with minimal symmetrical hydrophobic interaction clusters and these features could promote a strong inclination for the formation of K5-K14 heterodimers (Lee et al., 2012). Moreover, the crystal structure of the K5-K14 rod 2B heterodimer indicated a strong negative charge potential at the C terminus and a strong positive charge at the N terminus where both K5 and K14 could contribute to the polarized surface potential of the 2B coiled-coil in a complementary manner. This bias in surface-charge distribution was distinct from that of other filament crystal structures previously observed, such as that of the rod 2B domains of lamin A/C (Strelkov et al., 2004) and vimentin (Strelkov et al., 2002), and were thought likely to play a role in the axial alignment of K5-K14 heterodimers in forming larger oligomers (Lee et al., 2012).

1.5.2.4   Keratin intermediate filament formation

Physiologically, the smallest soluble oligomer that can be detected *in vivo* is a tetramer consisting of two anti-parallel heterodimers (Soellner et al., 1985). It was proposed that two adjacent lengths of the coiled-coil dimers aligned in an anti-parallel and a half-staggered arrangement such that their coil 1B subdomains could overlap, forming a protofilament (one tetramer) (Steinert et al., 1993; Bernot et al., 2005). This resultant anti-parallel formation of the tetramer makes keratin filaments apolar in nature. Two of these protofilaments then intertwine to form a protofibril (two tetramers) (Aebi et al., 1983). Four of these protofibrils then rapidly associate laterally into unit-length filaments (eight tetramers) (Herrmann et al., 1996) from where they longitudinally anneal to form short filaments. These filaments then further assemble by end-to-end annealing of filaments which then undergo radial compaction to form ~10 nm diameter intermediate filaments (reviewed in Herrmann et al., 2009) (see Figure 1.8). *In vivo* demonstration of these processes was shown recently whereby exchanges of intermediate filament subunits could occur along the lengths of intermediate filament and this was known as intercalary subunit exchange (Colakoglu and Brown, 2009).

.

Figure 1.6   Keratin structure and its helix motifs
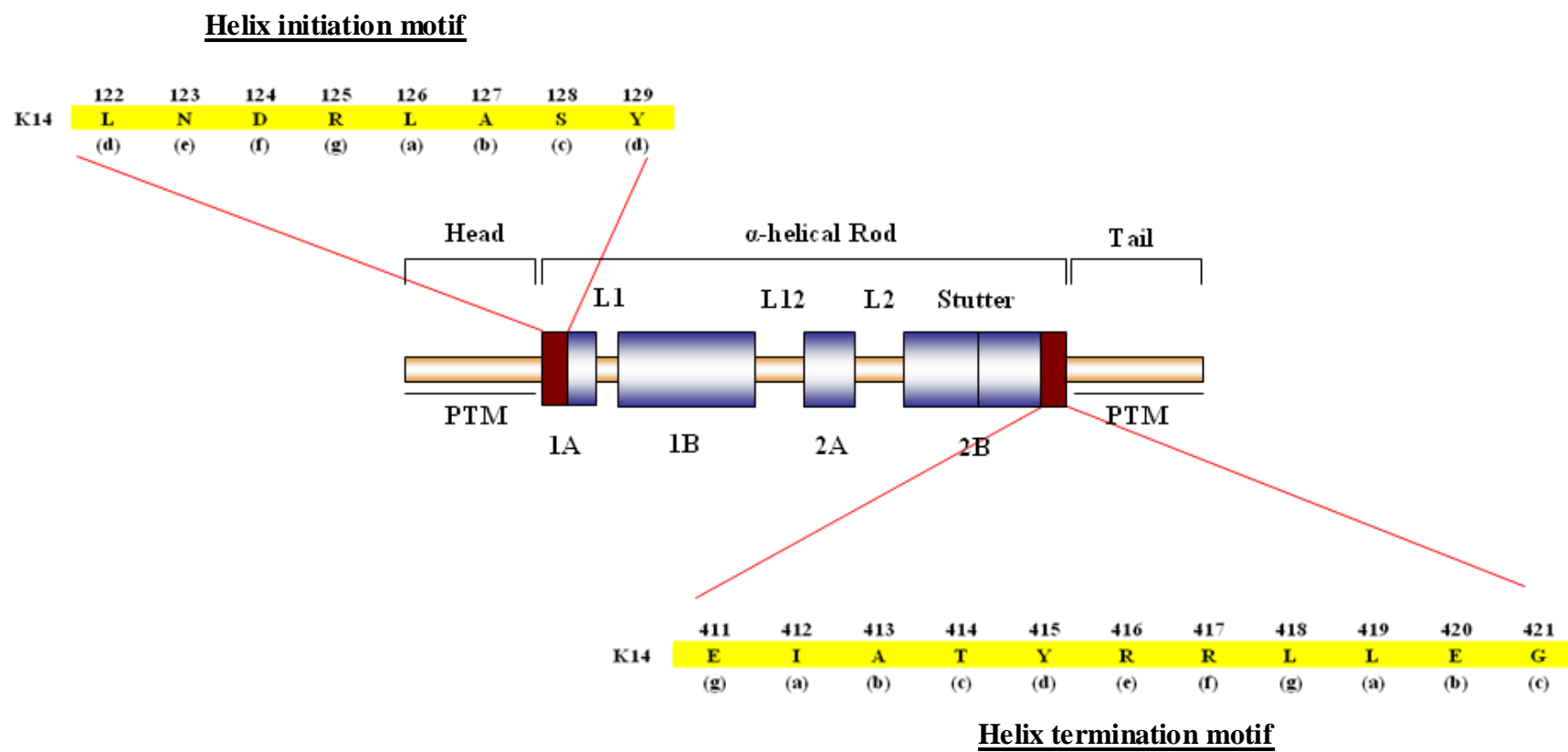
Figure redrawn after Herrmann et al., 2009

Figure 1.7   Pairing of type I (K14) and type II (K5) keratins at the helix motifs

Keratin rod 1A domain

Keratin 14   Keratin 5

Keratin rod 2B domain

Keratin 14   Keratin 5
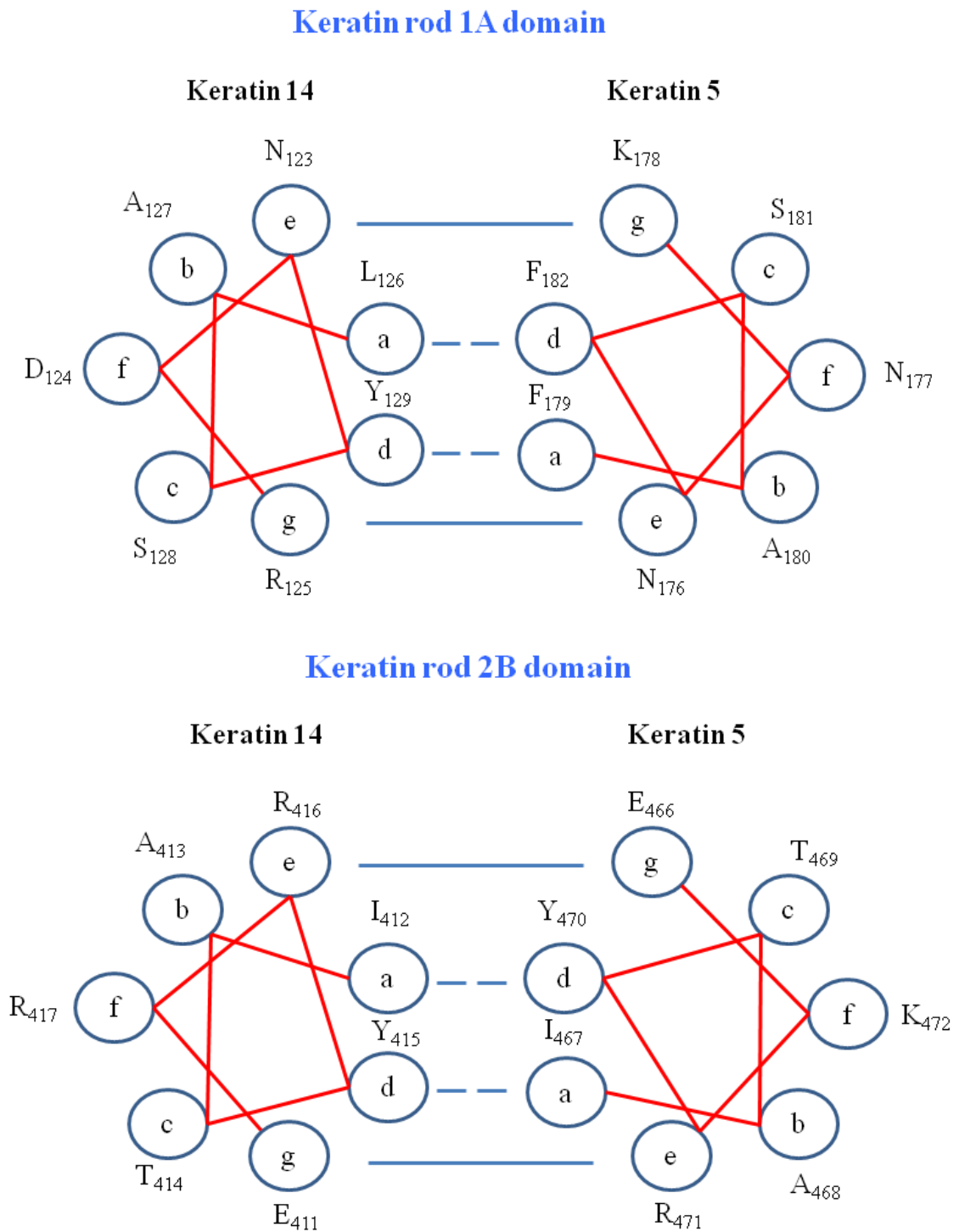
Figure 1.8   Phases of intermediate filament assembly

Parallel dimer in exact register

Anti-parallel tetramer in staggers

X 7

Lateral association of 8 tetramers into unit-length filaments (ULFs)

Longitudinal annealing of ULFs and filaments

Radial compaction of extended filaments
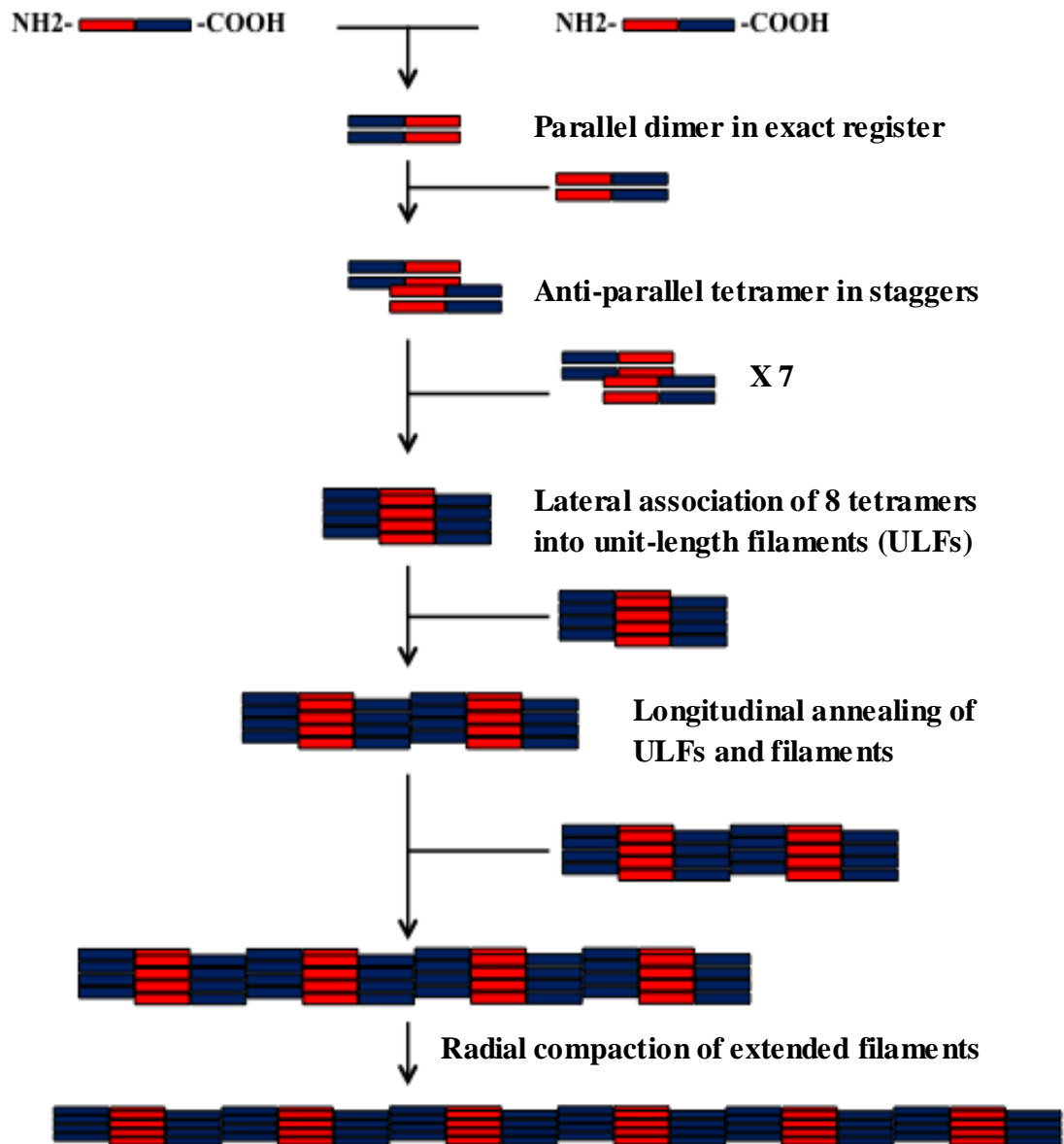
Figure redrawn after Herrmann et al., 2009

1.6 Post-translational modifications of keratin intermediate filament

1.6.1 Phosphorylation

Keratins are subjected to multiple post-translational modifications that have important consequences for their structures and properties (reviewed in Coulombe and Omary, 2002). Post-translational modifications can occur via several modalities including phosphorylation (Gilmartin et al., 1980; Ikai and McGuire, 1983), glycosylation (Tao et al., 2006a), sumoylation (Snider et al., 2011), caspase cleavage (Caulin et al., 1997) and ubiquitylation (Ku and Omary, 2000), of which phosphorylation is the most widely studied (reviewed in Coulombe et al., 2000). For instance, increased levels of phosphorylated keratins were detected in mitotic cells (Celis et al., 1983) or in various stress paradigms (Liao et al., 1997; Toivola et al., 2002), where keratin filaments either disassembled completely into soluble subunits and granular aggregates or collapsed into cage-like thick filament bundles (Lane et al., 1982). Phosphorylation may also affect keratin organization by shifting the equilibrium between the soluble and filamentous state towards the soluble form (Chou and Omary, 1993).

1.6.1.1 Kinases regulating keratin organization

One of the emerging families of kinases that play a role in phosphorylating keratin intermediate filaments is the mitogen activated protein kinases (MAPKs). Several growth factors, including epidermal growth factor (EGF), vascular endothelial growth factor (VEGF), insulin and inflammatory cytokines, activate MAPKs. The best characterized of the MAPK pathways is the MEK/ERK signalling cascade. This signalling casade is activated by protein tyrosine kinase receptors, such as EGF receptor (EGFR) or VEGF receptor (VEGFR). When the growth factors bind to their cognate receptors, the tyrosine receptor dimerizes and concomitantly activates its

intracellular protein tyrosine kinase via auto-phosphorylation. The phosphotyrosine then serve as docking sites for SH2 or PTB domain containing proteins (reviewed in Schlessinger and Lemmon, 2003; Pawson, 2004). These docking proteins include FRS2 (FGF receptor substrate-2), IRS1 (insulin receptor substrate-1), and Gab1 (the Grb2-associated binding protein), which when phosphorylated, recruit multiple Grb2 and Shp2 molecules (reviewed in Lemmon and Schlessinger, 2010). The Grb2 and Shp2 molecules, together with SOS, are brought in close proximity to Ras and activate it. Activated Ras, in turn, triggers a cascade of activation of three protein kinases, Raf1, MEK1/2 and ERK1/2 (Ullrich and Schlessinger, 1990). Activated ERK1/2 can then translocate into the nucleus where it phosphorylates and activates transcription factors such as ATF2, c-Jun, Elk1 and SAP1 (Hill and Treisman, 1995).

Recent studies have revealed the presence of scaffold proteins that can confer spatial and temporal regulation of the MAPK pathway. Originally identified in yeast (Elion, 2001), these scaffold proteins bring multiple components of the MAPK cascade in close proximity to facilitate efficient propagation of the signal (reviewed in Brown and Sacks, 2009). Scaffold proteins that can modulate the assembly and activation of ERK1/2 module have been identified, including KSR (kinase suppressor of Ras signalling) (Kornfeld et al., 1995), MP1 (MEK partner 1) (Schaeffer et al., 1998) and β-arrestin (Luttrell et al., 1999).

Other MAPKs include c-Jun N-terminal kinase (JNK) and p38. JNK was originally identified as the protein kinase stimulated by UV radiation that could phosphorylate and activate the proto-oncogenic transcription factor c-Jun (Hibi et al., 1993). The JNK pathway is mainly activated by cellular stress (UV radiation) and proinflammatory cytokines such as TNFα and IL-1 (reviewed in Davis, 2000), resulting in the activaton of c-Jun and ATF2 (Derijard et al., 1994; Gupta et al., 1995).

These stimuli activate JNKs through several upstream kinases such as MEKK1/MKK4 complex and HPK-1/MLK1/MKK7 signalling module bound by JIP-1 scaffold protein (reviewed in Chang and Karin, 2001; Weston and Davis, 2007).

p38 MAPK was originally identified as a 38 kDa protein that was tyrosine phosphorylated in response to lipopolysaccharide-stimulated macrophages (Han et al., 1994). The p38 MAPK pathway is predominantly activated by environmental stress such as osmotic shock, hypoxia, heat shock and UV radiation (reviewed in Ashwell, 2006), resulting in the activation of ATF2, Fos, Jun and Elk1 (reviewed in Obata et al., 2000). These stimuli activate p38 through several upstream kinases such as MKK3 and MKK6, which are themselves phosphorylated by several upstream kinases, including TAK1 (through TRAF6/TAB1/2), MLK3 and ASK1 (MEKK5) (reviewed in Johnson and Lapadat, 2002; Brancho et al., 2003).

It is suggested that in normal physiological condition, MAPK cascades would occur independently but during pathological situations, there will be significant cross-talks between them (reviewed in Noselli and Perrimon, 2000). Because p38 MAPK and JNK are often activated in stress stimuli, they are collectively known as stress activated protein kinases (SAPK).

A role for MAPKs in keratin phosphorylation was demonstrated when activated p38 MAPK and MK2/3 cooperatively phosphorylated several epithelial keratins such as K8, K18 and K20 in intestinal epithelial cells (Menon et al., 2010). Moreover, p38 MAPK was found to colocalize with keratin granules that were induced during mitosis, in various stress situations and in cells producing mutant keratins, which correlated with phosphorylation of K8 serine 74, a well known p38 target site. In addition, inhibiting kinase activity using p38 MAPK inhibitors reduced the formation

of these granules, suggesting a role for phosphorylation in regulating keratin organization (Woll et al., 2007). Also, when keratinocytes were subjected to hypo-osmotic stress, a sustained stress-activated response (SAPK/JNK pathway) was observed in cells that produced mutant keratins as compared to control cells, concomitant with an increase in phosphorylated K5 (D'Alessandro et al., 2002). These studies show that signalling cascades involving phosphorylation are important in regulating keratin organization.

1.6.1.2 Phosphatases regulating keratin organization

Phosphatases regulate kinase activity by removing phosphate groups and are therefore key players in all phosphorylation driven signalling cascades. Phosphatases also play a role in regulating keratin and other intermediate filament organization. For instance, it was found that structural organization of intermediate filament in interphase cells required protein phosphatase activity (Eriksson et al., 1992). In another study, it was shown that phosphorylated K8 at serine 432 was a physiological substrate for phosphatase PP2A after hypo-osmotic stress and also occured preferentially in mitotically active cells (Tao et al., 2006b). Moreover, phosphatase of regenerating liver-3 (PRL-3), a member of the PRL protein tyrosine phosphatase family, was also shown to mediate the dephosphorylation of K8 at serine residues 74 and 432, and this led to the promotion of cells with increased migration and metastatic potential (Mizuuchi et al., 2009; Khapare et al., 2012). These studies show that signalling cascades involving dephosphorylation are also equally important in regulating keratin organization.

1.6.2 Glycosylation

Keratins are also subjected to glycosylation, which refers to the addition of O-linked single N-acetylglucosamines (O-GlcNAc) to serine and threonine residues. K13 was the first keratin to be modified by glycosylation (King and Hounsell, 1989). It was later shown that keratins such as K8 and K18 (Chou et al., 1992; Chou and Omary, 1993) were being glycosylated, and mutational analysis of these sites suggested a role for glycosylation in filament assembly (Ku and Omary, 1995). A role for keratin glycosylation in protecting epithelial tissue from injury was recently suggested through the promotion of phosphorylation and activation of cell survival kinases (Ku et al., 2010).

1.6.3 Ubiquitylation

The ubiquitin-proteasome pathway starts with the activation of ubiquitin by the ubiquitin-activating enzyme (E1), followed by the transfer of ubiquitin to an ubiquitin-conjugating enzyme (E2). E2 then shuttle the ubiquitin molecule to the substrate-specific ubiquitin ligase (E3), which then delivers the ubiquitin to the substrate destined to be degraded. Polyubiquitin chain formation continues with the conjugation of subsequent ubiquitin moieties to the attached ubiquitin on the substrate and the substrate-ubiquitin conjugate is then degraded by 26S proteasome in an ATP-dependent manner (Hershko and Ciechanover, 1998; Ciechanover et al., 2000). Specifically, the E2s involved in keratin degradation are from the UbcH5/Ub3 families (Jaitovich et al., 2008) whereas the E3s involved in keratin degradation are the RING finger proteins (He et al., 2008; Duan et al., 2009). One of the pathological features of intermediate filament-associated diseases is the accumulation of intracytoplasmic inclusion bodies (aggresomes) that are made up mainly of

intermediate filament proteins and ubiquitin (Lowe et al., 1988). Studies have also shown that there is cross-talk between phosphorylation and ubiquitylation of keratins (Ku and Omary, 2000). For instance, phosphorylation of K8 at Ser 73 was required for ubiquitylation of the keratin protein following shear stress in alveolar epithelial cells (Jaitovich et al., 2008). Signalling kinases such as p38, ERK and src may also play a role in the formation of aggresomes (Wu et al., 2005; Nan et al., 2006), thus strengthening the link between phosphorylation of keratins and ubiquitylation fate for degradation.

1.6.4 Sumoylation

Other than ubiquitylation, sumoylation is also an important regulatory modification for keratin intermediate filament. Sumoylation is a reversible process of adding and removing small ubiquitin-like modifier (SUMO) polypeptides (SUMO-1, -2 or -3) (Bergink and Jentsch, 2009) that targets the internal lysine residues of protein and affects protein localization, interactions with binding partners and degradation (Geiss-Friedlander and Melchior, 2007). A recent study had revealed the role of sumoylation on keratin intermediate filament in response to stress, affecting keratin organization and solubility (Snider et al., 2011). Moreover, the degree of sumoylation could determine keratin dynamics, where modest sumoylation of wild-type K8 could promote solubility whereas hypersumoylation of K8, prominent in chronic liver disease, could result in reduced solubility (Snider et al., 2011).

In summary, these studies have revealed the requirements for rapid assembly and proper organization of intermediate filament subunits into stable filaments in maintaining the cytoskeletal structure of epidermal keratinocytes. Hence, the first discovery of pathogenic mutations in keratin intermediate filaments leading to

patients suffering from the epidermal fragility disorder, epidermolysis bullosa simplex (EBS), further reinforced the idea that keratins play an important role in providing cells with mechanical resilience.

1.7   Keratinopathies (mutations in keratins)

The association between keratin intermediate filament and inherited skin fragility disorders such as EBS was first described in the early 1990s (Bonifas et al., 1991; Coulombe et al., 1991a; Lane et al., 1992). Since then, the number of keratin mutations associated with pathological conditions has increased, with mutations in more than 100 different genes including approximately 20 different keratin genes (for details, see the Human Intermediate Filament Database, www.interfil.org; Szeverenyi et al., 2008). These mutations are mostly autosomal dominant because mutations in one keratin can affect its heterodimer partner in a dominant negative manner during filament assembly and elongation (reviewed in Arin, 2009).

1.7.1   Spectrum of disease phenotypes of keratin mutations

In addition, there exists a wide spectrum of disease phenotypes that are associated with the site (s) at which these mutant keratins are located in the epidermis. For instance, K14 and K5 (expressed in epidermal basal keratinocytes) mutations result in EBS (Bonifas et al., 1991; Coulombe et al., 1991a; Lane et al., 1992) whilst keratin mutations in K10 and K1 (expressed in suprabasal keratinocytes) lead to bullous congenital epidermolytic hyperkeratosis, also known as epidermolytic hyperkeratosis (Cheng et al., 1992; Chipev et al., 1992). K2 (K2e expressed in upper spinous layers) mutations give rise to ichthyosis bullosa of Siemens (Rothnagel et al., 1994), K9 (palmoplantar skin) mutations result in epidermolytic palmoplantar keratoderma (Reis et al., 1994), K4 and K13 (oral mucosa) mutations lead to white-sponge nevus

(Richard et al., 1995; Rugg et al., 1995) and K6 (K6a, b), K16, K17 (plamoplantar skin, oral mucosa and epithelial oesophagus, nail) mutations give rise to pachyonychia congenita (Bowden et al., 1995; McLean et al., 1995) (See Table 1.7 for clinical descriptions).

1.7.1.1   Phenotypic variation between different mutations in the same gene

Of note, there is a phenotypic variation between different mutations in the same gene (reviewed in Lane, 1994; McLean and Lane, 1995). For instance, mutations found at the helix motifs of the keratin intermediate filament usually result in a more severe phenotype than a mutation that is located at the other non-helical domains. These severe phenotypes are usually presumably attributed to a deficit in filament assembly kinetics and organization. Hence, a genotype-phenotype correlation in keratin disorders exists (Letai et al., 1993). In addition, in patients suffering from severe EBS with mutations in K14, the most frequently mutated residue is the arginine at the codon 125 within the helix initiation motif (Szeverenyi et al., 2008). This residue, found within the helix initiation motif, is highly conserved throughout the type I keratins and contain a CpG dinucleotide sequence. CpG nucleotides have a very high rate of mutation due to the de-amination of 5-methylcytosine to thymine. This thymine is not removed by uracil DNA glycosylase during DNA synthesis and thus is subjected to pair with adenine during replication, hence giving rise to a point mutation (reviewed in Corden and McLean, 1996). Point mutations found in the helix initiation motif or the helix termination motif in K5 and K14 have been reported to cause most of the severe EBS Dowling-Meara phenotypes. On the other hand, mutations affecting residues found at the nonhelical head and linker domains in K5/K14 often contribute to milder phenotypes such as EBS-localized or EBS-generalized (Coulombe et al., 2009).

1.7.1.2 Phenotypic variation between different mutations of the same amino acid residue in the same gene

Different mutations of the same amino acid residue in the same gene can also contribute to phenotypic variation. For example, K14 M119T mutation results in EBS-DM (severe phenotype) whereas K14 M119V mutation results in EBS-generalized (mild phenotype) (Cummins et al., 2001). Likewise, K14 A413P mutation results in EBS-localized whereas K14 A413T mutation results in normal phenotype (Murrell et al., 2011; Natsuga et al., 2011). The Natsuga study was supported by *in silico* modelling where proline substitution resulted in deleterious structural defects of K14 protein but not threonine substitution in which slight instability of the structure was observed (Natsuga et al., 2011). It was believed that structurally, threonine and adenine could be considered interchangeable because they could substitute for one another on a frequency that equals their occurence in structured proteins (Henikoff and Henikoff, 1992).

1.7.1.3 Phenotypic variation due to genetic modifiers

In cases where there is an aggravation of disease condition, it was shown that genetic modifiers can play a role in the pathogenesis. Coinheritance of both filaggrin (*FLG*) (p. R2447X) and K16 (*KRT16*) (p. L132P) mutations resulted in a more severe pachyonychia congenita condition than that of K16 mutation (p. L132P) alone (Gruber et al., 2009). Hence, this indicates that *FLG* can serve as a genetic modifier for pachyonychia congenita condition.

1.7.1.4 Phenotypic variation due to functional redundancy for keratins

In addition, there is a functional redundancy for keratins. For instance, functional redundancy was observed in relatively mild phenotype of patients with recessive EBS due to the lost of both K14 alleles. This was probably a result of the compensatory presence of K15 in basal keratinocytes (Jonkman et al., 1996; Batta et al., 2000). Another example was that patients with K1 mutations suffered from palmoplantar keratoderma but not in patients with K10 mutations. This was possibly due to the compensatory presence of another type I keratin, K9, in the palmoplantar skin (DiGiovanna and Bale, 1994). Of note, patients with K9 mutations suffered from palmoplantar keratoderma as well because K10 cannot replace the loss of K9 in palmoplantar skin.

Since basal keratinocytes express K14 and K5 predominately and that K14 and K5 mutations are associated with skin fragility disorder such as EBS (which is within the scope of this thesis), the classification of epidermolysis bullosa (EB) and its subtype EBS will be discussed in detail in the following paragraphs.

1.8 Classification of epidermolysis bullosa (EB)

Epidermolysis bullosa (EB) encompasses a group of heterogenous hereditary diseases that have skin fragility (blister formation) upon mild trauma. The term was first used in 1886 (Koebner, 1886). Over the years, as improvements in the diagnostic and research techniques coupled with insights in the molecular background of EB increased, a novel classification system was developed (Pearson, 1962) and the latest consensus was recently established (Fine et al., 2008).

Presently, EB can be classified into four major subtypes known as EBS, junctional EB (JEB), dystrophic EB (DEB) and Kindler syndrome (KS), distinguished by differences in the ultrastructural level within which blisters occur in the skin, either spontaneously or following minor friction or trauma (Fine et al., 2008). This is often diagnosed using immunofluorescence antigen mapping and/or electron microscopy analysis. For instance, in EBS, the plane of cleavage is intraepidermal (basal or suprabasal). In JEB, the blisters cleave the lamina lucida. In DEB, the blisters form beneath the lamina densa (sub-lamina densa). Skin fragility in KS can give rise to multiple (mixed type) planes of cleavage (see Figure 1.9). A list of EB subtypes is also tabulated in Table 1.8.

Table 1.7

Human keratinopathies of the epidermis

Molecular target	Disease	Clinical phenotype (s)	Original finding (s)
K5, K14	Epidermolysis bullosa simplex (OMIM # 131760)	Skin fragility from cytolysis of basal keratinocytes	(Bonifas et al., 1991; Coulombe et al., 1991a; Lane et al., 1992).
K1, K10	Epidermolytic hyperkeratosis (OMIM # 113800)	Erythematous blistering due to fragility of suprabasal keratinocytes; Later development of hyperkeratosis	(Cheng et al., 1992; Chipev et al., 1992)
K2	Ichthyosis bullosa of Siemens (OMIM # 146800)	Bullous ichthyosis without erythroderma; Epidermolysis limited to upper spinous layers; Later development of dark brown hyperkeratosis	(Rothnagel et al., 1994)
K9	Epidermolytic palmoplantar keratoderma (OMIM # 144200)	Epidermolysis and hyperkerotosis of palm and soles	(Reis et al., 1994)
K4, K13	White-sponge nevus (OMIM # 193900)	Spongy white plaques, often on buccal mucosa; Oral leukokeratosis	(Richard et al., 1995; Rugg et al., 1995)
K6, K16, K17	Pachyonychia congenita (PC-1: OMIM # 167200; PC-2: OMIM # 167210)	Dystrophic nails; Palmoplantar hyperkeratosis; Follicular hyperkeratosis; Oral leukokeratosis	(Bowden et al., 1995; McLean et al., 1995)

Table 1.8

Classification of epidermolysis bullosa (EB)

Molecular target	Disease	Clinical phenotype (s)	Original finding (s)
K5, 14	Epidermolysis bullosa simplex (basal) (OMIM # 131760)	Skin fragility from cytolysis of basal keratinocytes	(Bonifas et al., 1991; Coulombe et al., 1991a; Lane et al., 1992).
PKP1, DP	Epidermolysis bullosa simplex (suprabasal) (PKP1: OMIM # 604536; DP: OMIM # 609638)	Cutaneous fragility and congenital ectodermal dysplasia affecting skin, hair and nails	(McGrath et al., 1997; Jonkman et al., 2005)
Laminin-332: α3, β3 and γ2	Herlitz junctional epidermolysis bullosa (OMIM # 226700)	Extensive blistering of the skin and mucosal surfaces	(Pulkkinen et al., 1994a; Pulkkinen et al., 1994b; Kivirikko et al., 1995)
α6β4 integrins	Junctional epidermolysis bullosa with pyloric atresia (OMIM # 226730)	Pyloric atresia and cutaneous aplasia; Mucosa erosions	(Vidal et al., 1995; Shimizu et al., 1996)
Collagen VII	Dystrophic epidermolysis bullosa (OMIM # 226600)	Severe blistering with atrophic scarring; Nail atrophy; Mucosa erosions	(Christiano et al., 1993)
FFH-1 (*KIND1*)	Kindler syndrome (OMIM # 173650)	Congenital blistering; Photosensitivity; Progressive poikiloderma with dyschromatic macules; Telangiectases and cutaneous atrophy	(Jobard et al., 2003; Siegel et al., 2003)

Figure 1.9   Classification of epidermolysis bullosa (EB)

Normal skin

Suprabasal cells

Basal cells

Lamina lucida
Lamina densa
Anchoring fibrils
Type I and III collagen

EBS (suprabasal)

EBS (basal)

JEB

DEB

KS

+
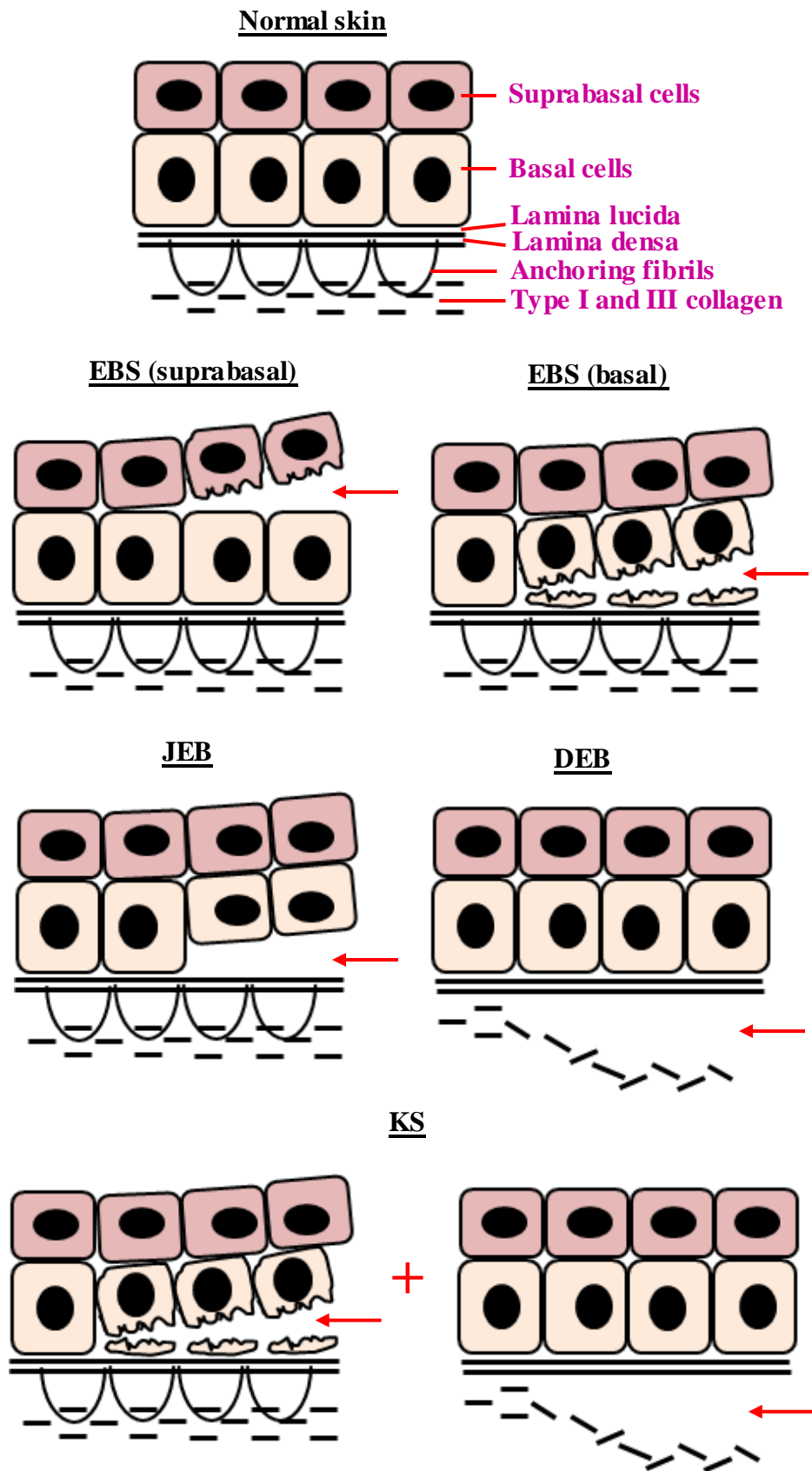
Figure redrawn after Shinkuma et al., 2011.

69

1.9   Classification of epidermolysis bullosa simplex (EBS)

1.9.1   Characterization of EBS phenotypes

EBS is one of the major subtypes of EB and is characterized by an intraepidermal level of blister formation (see Figures 1.9 and 1.10). EBS is the most prevalent type of EB with approximately 1 in 25,000 live births (Horn and Tidman, 2000). According to the latest EB classification, EBS has been subdivided into basal and suprabasal EBS, depending on the ultrastructural level of blistering within the epidermis (Fine et al., 2008). At the structural level, electron microscopy consistently revealed aggregates of electron-dense material in a subset of patients suffering from severe EBS Dowling-Meara (Anton-Lamprecht and Schnyder, 1982). Consequently, immunoelectron microscopy confirmed the presence of keratin intermediate filaments in these electron-dense aggregates (Ishida-Yamamoto et al., 1991) (Figure 1.10). A role for keratins in EBS phenotype was suggested from the expression of mutant keratin cDNAs (both truncations and mutations) in cultured epithelial cells that resulted in a dominant-negative disruption and aggregation of endogenous keratin network (Albers and Fuchs, 1989; Coulombe et al., 1991b). Mutations in the *KRT5* and *KRT14* genes encoding the basal proteins K5 and K14 were subsequently reported in individuals suffering from basal EBS (Bonifas et al., 1991; Coulombe et al., 1991a; Lane et al., 1992). These studies provide the first evidence that epidermal keratins are the site of mutations contributing to basal EBS.

Figure 1.10   Clinical photograph, histological section and ultrastructural details of the skin of EBS-DM patient

Clinical photograph of a EBS-DM patient

Singaporean patient having K14 R125C mutation. Note the severe blistering at the feet. (*Photograph courtesy of Jean Ho, National Skin Center, Singapore*)

Histological section
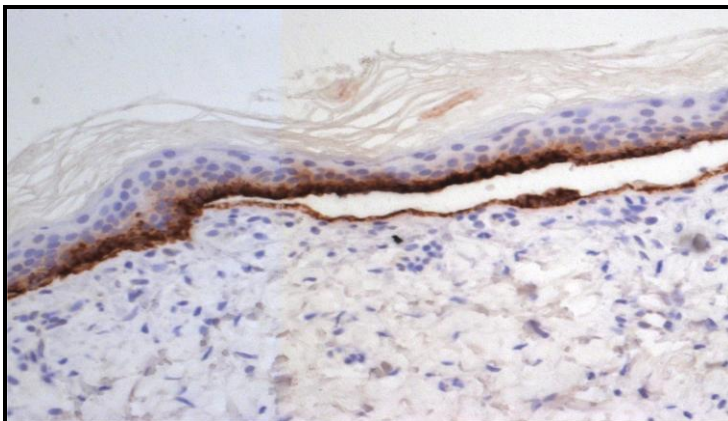
Intraepidermal cleavage of the epidermal basal layer, immunostained with K14 (RCK 107). (*Picture courtesy of Declan Lunny and John Common*)

Ultrastructural section
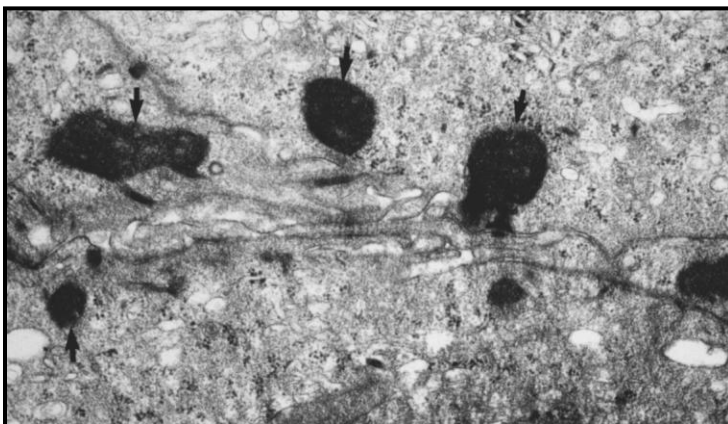
Electron dense clumping of keratin tonofilaments, forming aggregates. (*Picture courtesy of Robin Eady*)

1.9.1.1 Genotype-phenotype correlation of EBS

Missense mutations and small in-frame deletions or insertions are commonly found in the rod domain of K5 and K14 that result in a dominant-negative effect on disrupting keratin cytoskeleton in basal keratinocytes. The phenotype of basal EBS patients varies with the onset and severity of blistering and they can be classified into three main subtypes, namely: EBS-localized (formerly known as Weber Cockayne), which is the mildest form, characterized by mild blistering confined to hands and feets, occurring at 1-2 yrs when the child starts walking; EBS-generalized (previously known as Koebner) with generalized blistering throughout life, occurring upon birth, and EBS-DM (also known as EBS Dowling-Meara), the most severe form, with congenital blistering in a herpetiform (clusters) pattern on erythematous skin, usually involving the oral mucosa and onycholysis. The main distinctive diagnosis for EBS-DM was the presence of keratin clumps (aggregates) in basal keratinocytes (Anton-Lamprecht and Schnyder, 1982). Hence, there exists a genotype-phenotype correlation in EBS based on the positions of keratin mutation and the severity of the skin disorder. A list of other EBS subtypes is also tabulated in Table 1.9.

Table 1.9

Classification of basal epidermolysis bullosa simplex (EBS)

EBS subtypes	Molecular target (s)	Clinical phenotype (s)	Original finding (s)
EBS-localized (OMIM # 131800)	K5, K14	Blistering localized at hands and feet	(Weber, 1926; Cockayne, 1947)
EBS-generalized (OMIM # 131900)	K5, K14	Blistering mainly at hands and feet with generalized skin fragility	(Koebner, 1886)
EBS, Dowling-Meara (EBS-DM) (OMIM # 131760)	K5, K14	Severe, generalized, clusters, hemorrhagic blistering, mucosal and nails affected	(Dowling and Meara, 1954)
EBS, autosomal recessive (EBS-AR) (OMIM # 601001)	K14	Very rare variant. Similar to EBS-generalized though frequency of blistering may be lower	(Batta et al., 2000)
EBS, migratory circinate (EBS-migr) (OMIM # 609352)	K5	Very rare variant. Annulatory migratory multiple erythema circinatum, multiple vesicles on hands and feet, lesions heal with pigmentation	(Gu et al., 2003)
EBS with mottled pigmentation (EBS-MP) (OMIM # 131960)	K5	Mild skin blistering, mottled pigmentation of trunk and limbs, punctate palmoplantar keratoderma, nail dystrophy	(Fischer and Gedde-Dahl, 1979)
EBS, Ogna (EBS-Og) (OMIM # 131950)	Plectin	Widespread skin blistering, Onychogryphosis	(Olaisen and Gedde-Dahl, 1973; Koss-Harnes et al., 2002)
EBS with pyloric atresia (EBS-PA) (OMIM # 612138)	Plectin	Pyloric atresia and cutaneous aplasia; Skin blistering on trunk and limbs	(Nakamura et al., 2005)
EBS with muscular dystrophy (EBS-MD) (OMIM # 226670)	Plectin	Epidermal blisters heal with atrophic scarring; Nail dystrophy; Muscle weakness that progressively leads to widespread muscular atrophy and ptosis	(McLean et al., 1996; Smith et al., 1996)

1.10 Other functions of keratin intermediate filament

1.10.1 A role for keratins in regulating cell size and protein synthesis

Cell growth requires the strict orchestration during development and in response to various injuries. Two recent studies demonstrate a keratin-mediated modulation of epidermal cell size (Kim et al., 2006; Galarneau et al., 2007). K17, an intermediate filament protein rapidly induced in wounded stratified epithelia, is reported to regulate keratinocyte size by upregulating protein synthesis through association with 14-3-3σ. This could allow the nuclear translocation of 14-3-3σ to initiate protein translation, which takes place through activation of the Akt and mTOR signalling pathways (Kim et al., 2006). In addition, K8 and K18 could also regulate hepatic cell size and protein synthesis through regulating Akt kinase activity (Galarneau et al., 2007). Additional support of a role for keratins in regulating cellular metabolism came from the generation of transgenic mice devoid of the entire keratin intermediate filament family, which (although lethal) revealed a role for keratin in cells localizing glucose transporters (GLUT1 and 3) via activation of mTOR signalling pathways (Vijayaraj et al., 2009).

1.10.2 A role for keratins in regulating stress kinase activity

Keratins may also protect tissues from injury by serving as a phosphate "sponge" to absorb stress-induced kinase activity such as p38 and JNK (Ku and Omary, 2006).

To summarize, these studies emphasize that there is now an emerging shift in paradigm, that intermediate filaments are not only structural proteins but also play an essential role as signalling organizers and buffers of cellular stress (Eriksson et al., 2009).

1.11 Aims and outline of thesis

The observations that keratin aggregates (which co-exist with proper filament formation) arised solely from EBS-DM mutations (K14 R125C/K14 R125H) but not EBS-generalized type of mutation (K14 L384P) (Letai et al., 1993) were particularly intriguing because this would mean that the severity of disease might be attributed to the impairment of proper elongation of keratin filaments (since EBS-DM mutations are known to predominantly reside in the helix initiation or helix termination motifs of the keratin) and this could affect the physiological condition of the keratinocytes. To address this issue, keratinocytes were derived from the skin of patients suffering from EBS-localized and EBS-DM conditions, immortalized and maintained in cell cultures (Morley et al., 2003). These led to reports showing that EBS-DM keratinocytes had an intrinsic upregulation of stress kinases and they showed sustained stress responses to osmotic stress (D'Alessandro et al., 2002) and faster migration during scratch wound assays (Morley et al., 2003). These reports were in line with their intrinsic down-regulation of dual-specificity phosphatases (DUSPs) (Liovic et al., 2008) and junction proteins (Liovic et al., 2009) respectively. Moreover, ERK1/2 activation in EBS-DM keratinocytes provided resistance for these mutant cells against apoptosis during mechanical stress (Russell et al., 2010). Hence, these studies demonstrate that there exists a change in the physiological condition of EBS-DM keratinocytes. Though much work has been done to characterize these cells, the detailed molecular mechanism underlying keratin remodelling in stress (in terms of keratinocyte activation status, keratin dynamics and modifications) in these EBS-DM keratinocytes is still not well understood.

Therefore, experiments are designed to address the following questions:

1. Why do EBS-DM cells show faster re-epithelialization in culture than wild-type cells? – Chapter 3

Hypothesis: EBS-DM cells are in a constitutively stressed or activated state reminiscent to a wound condition.

Hypothesis testing: Analyze for markers of wound activated state such as wound-associated keratin, integrin, extracellular matrix protein and matrix metalloproteinase in various cell culture conditions such as subconfluence, confluence (monolayer) and scratch wound assays that will mimic an *in vitro* assay system of the experimental keratinocyte activation cycle.

2. What influences keratin remodelling and how does it play a role in cell migration? – Chapter 4

Hypothesis: EGF influences keratin remodelling to affect cell migration

Hypothesis testing: Analyze for indicators of keratin remodelling such as keratin solubility, keratin aggregate formation and changes in keratin dynamics using kinase inhibitors or siRNAs to intervene with the EGF/ERK1/2 signaling pathway.

3. Why do EBS-DM cells form peripheral keratin aggregates? – Chapter 5

Hypothesis: Phosphorylated K14 residues at the rod 1A domain influences keratin aggregate formation.

Hypothesis testing: Generate phospho-null and phospho-mimetic constructs of the serine and tyrosine residues involved at the K14 rod 1A domain and analyze their phenotypes through osmotic stress and scratch wound assays.

CHAPTER 2

MATERIALS AND METHODS

2.1   Materials

Table 2.1.1   Chemicals and reagents used in this thesis

Company	Chemicals and reagents
Calbiochem (Darmstadt, Germany)	EGFR inhibitor, AG1478
Promega (Madison, USA)	MEK1/2 inhibitor, U0126
Invitrogen (Carlsbad, USA)	Agarose
A.G. Scientific, Inc. (San Diego, USA)	NP-40
GE Healthcare (Piscataway, USA)	Urea Amersham Hyperflim Amersham ECL^{TM} Prime reagents
Sigma-Aldrich (St. Louis, USA)	Sodium orthovanadate Bovine Serum Albumin (BSA) Dimethylsulfoxide (DMSO) Sodium fluoride β-glycerolphosphate Tween 20 Sodium chloride Ethylenediaminetetraacetic acid (EDTA) Sodium deoxycholate Paraformaldehyde Epidermal growth factor (EGF) Ponceau S solution
Roche Applied Science (Indianapolis, USA)	Complete mini EDTA-free Protease inhibitor
Calbiochem (Darmstadt, Germany)	Phenylmethanesulfonyl Fluoride (PMSF)
Applied Biosystems	Power SYBR$^{®}$ green PCR master mix
1st base	Tris buffer (pH 8.0) Tris-buffered saline (TBS)
VWR International Ltd (Radnor, USA)	Triton X-100
Thermo Fisher Scientific Inc. (Waltham, USA)	Lonza GelStar* nucleic acid gel stain Lab-Tek II #1.5 chambered coverslips (2-well/4-well).
WillCo-wells (Amsterdam, The Netherlands)	WillCo-dish® Glass Bottom Dishes

Table 2.1.2   Antibodies used in this thesis

Company	Antibody
Cell signaling Technology Inc. (Danvers, MA, USA)	Mouse monoclonal anti-phospho-ERK1/2 (Thr202/Tyr204) Mouse monoclonal anti-phospho-p38 (Thr180/Tyr182) Mouse monoclonal anti-phospho-JNK (Thr183/Tyr185) Rabbit polyclonal anti-ERK1/2 Rabbit polyclonal anti-p38 Rabbit polyclonal anti-JNK Rabbit polyclonal anti-GAPDH
BD Biosciences (San Jose, CA, USA)	Mouse monoclonal anti-plectin (clone 31) Mouse monoclonal anti-fibronectin (clone 10)
Sigma-Aldrich (St. Louis, USA)	Mouse monoclonal anti-FLAG (clone M2) Mouse monoclonal anti-actin (clone AC-15)
Jackson ImmunoResearch Laboratories (West Grove, USA)	Rhodamine red-X-conjugated donkey anti-mouse secondary antibodies Rhodamine red-X-conjugated donkey anti-rabbit secondary antibodies FITC-conjugated donkey anti-mouse secondary antibodies
Dako Cytomation (Glostrup, Denmark)	Horseradish peroxidase (HRP)–conjugated swine anti-rabbit secondary antibody Horseradish peroxidase (HRP)–conjugated rabbit anti-mouse secondary antibody
Novacastra (Wetzlar, Germany)	Mouse monoclonal anti-$\beta1$ (CD29) Mouse monoclonal anti-K5 (XM-26) Mouse monoclonal anti-K17 (E3) (Troyanovsky et al., 1989)
Molecular probes (Life Technologies; Carlsbad, USA)	Alexa Fluor® 647 Phalloidin
Antibodies generated by our laboratory or gifts from other laboratories	Mouse monoclonal anti-K14 (LL001) (Purkis et al., 1990) Rabbit polyclonal anti-K5 (BL-18) (Purkis et al., 1990) Rabbit polyclonal anti-phospho-K5 (LJ4) (Liao et al., 1997) Mouse monoclonal anti-desmoplakin (11-5F) (David Garrod, Manchester)

2.1.3 Plasmids

pXJ40 FLAG-ERK2 mammalian expression vector encoding rat ERK2 protein was fused to an N-terminal FLAG epitode tag that was driven by the cytomegalovirus (CMV) enhancer/promoter. This plasmid, together with the pXJ40 FLAG expression vector (Manser et al., 1997), was kindly provided by Dr. Edward Manser, Institute of Medical Biology, Singapore. The pEGFP K14 WT and pEGFP K14 R125P mammalian expression vectors, encoding for either human K14 wild-type protein or K14 mutant protein respectively, were fused to an N-terminal EGFP epitode tag that was driven by the CMV promoter. These two plasmids were previously made and described in (Liovic et al., 2009). pLVX-EF1α-AcGFP1-C1 lentiviral expression vector was kindly provided by Dr. Lim Sai Kiang, Institute of Medical biology, Singapore. pHR-CMV 8.2 delta packaging vector and pCMV VSV-G envelope vector were kind gifts from Nick Leslie, University of Dundee.

2.1.4 Cell lines and cell culture

Both NEB-1 and KEB-7 keratinocytes were patient-derived cell lines that were immortalized through HPV16. NEB-1 keratinocytes express wild-type keratins while KEB-7 keratinocytes express the severe EBS-DM mutation R125P in the K14 rod 1A domain (Morley et al., 2003). Isogenic pathomimetic cell lines, NEB-1 EGFP-K14 WT and NEB-1 EGFP-K14 R125P, were generated as previously described in (Liovic et al., 2009). Cell lines were cultured in 75% DMEM (Dulbecco's modified Eagle's medium) plus 25% Ham's F12 medium, containing 1% L-glutamine, 1% penicillin/streptomycin and 10% fetal bovine serum (FBS), with additional growth factors such as hydrocortisone (0.4 μg/ml), transferrin (5 μg/ml), lyothyronine (2 x 10^{-11} M), adenine (1.9 x 10^{-4} M), insulin (5 μg/ml) and epidermal growth factor (EGF)

(10 ng/ml). EGF was omitted from culture media for cells to be cultured in the absence of EGF. N/TERT-1 was an hTERT-immortalized human keratinocyte cell line that maintained the ability to differentiate (Dickson et al., 2000). N/TERT-1 cells were cultured at low density in serum-free media (KSFM, Invitrogen), supplemented with 0.3 mM Ca^{2+}, 0.2 ng/ml EGF, 25 µg/ml BPE, 1% L-glutamine and 1% penicillin/streptomycin. To sustain confluent cultures, medium was changed to a 1:1 mixture of KSFM and DF-K medium (DF-K medium consisted of equal volumes of DMEM high glucuose and Ham's F-12 supplemented with 0.3 mM Ca^{2+}, 0.2 ng/ml EGF, 25 µg/ml bovine pituitary extract (BPE), 1% L-glutamine and 1% penicillin/streptomycin). HEK293T cells were cultured in DMEM supplemented with 10% FBS and 1% penicillin/streptomycin. These cell lines were fibroblast feeder cell independent and were cultured at 37°C in 5% CO_2. Cells were regularly passaged at 80-90% confluence, except for N/TERT-1 cells (30-40% confluence). This procedure began by aspirating the existing culture media from the tissue culture flask, washed with phosphate buffer saline (PBS) once, and then incubated in the presence of trypsin/versene with 0.125% EDTA. After incubation at 37°C for 7 min, the detached cells were neutralized with 5 ml of media and transferred into an empty 15 ml falcon tube. Cells were pelleted by centrifuging at 1000 rpm for 5 min, and the pellets were resuspended in 1 ml culture media, and seeded at 1:10 in new tissue culture flasks.

2.1.5 Cryopreservation of cell lines

Subconfluent cell cultures were trypsinised, pelleted and resuspended in freezing media containing 70% DMEM, 20% FBS and 10% dimethylsulphoxide (DMSO). The cell suspensions were then aliquoted at 1 x 10^6 cells/ml in cryovials, placed into Mr.

Frosty freezing container (Nalgene, NUNC), and kept at -80°C overnight before transferring to liquid nitrogen tank for longer storage.

2.1.6 Thawing of cell lines

Frozen cryotubes were taken out from liquid nitrogen tank, rapidly thawed in a 37°C water bath and transferred into 5 ml of pre-warmed culture media. The cell suspension was pelleted by centrifugation, resuspended in culture media and seeded into tissue culture flask to allow for overnight adhesion of cells to the vessel surface.

2.2 Drug/EGF treatment methodology

Cells were seeded onto either 6-well plates with 22 mm² glass coverslips or 100 mm petri dish for 3 days to reach 80% confluence before the drug treatment regime. The inhibitors, U0126 (10-100 μM) (Promega) and AG1478 (10 μM) (Calbiochem) were dissolved in dimethylsulphoxide (DMSO). Final concentrations of DMSO added to cells were ≤ 1% and this amount was observed to have no effect on cell viability in these experiments. U0126 (10-100 μM) were added into the media and cells were then incubated for 1 hr before fixation or lysis. For EGF treatment study, cells were cultured in media without EGF for 48 hrs and subjected to EGF (10-100 ng/ml) treatment for 48 hrs before being harvested for RNA and immunoblot analysis. Alternatively, cells were cultured in media without EGF (-EGF) for two passages before seeding them onto either 6-well plates with 22 mm² glass coverslips or 100 mm petri dish. Cells were then first serum starved (in the absence of FBS) for 6 hrs before incubation in media supplemented with EGF (100 ng/ml) for 2 hrs. After 2 hrs, drug inhibitors such as U0126 (10 μM) or AG1478 (10 μM) were then added into the media in the presence of EGF (100 ng/ml) and cells were incubated for another hour before lysis or fixation.

2.3 Molecular biology methodology

2.3.1 Site-directed mutagenesis

Site-directed mutagenesis was performed using the QuikChange Site-directed Mutagenesis kit (Agilent Technologies, CA, USA) according to manufacturer's instructions. pEGFP-K14 WT plasmid DNA was used as a template at 100 ng/µl for introducing specific mutations (underlined red) through PCR-based method by using the following mutagenic primers to generate the respective constructs: **K14 S128A** (Forward: 5'-CAA TGA CCG CCT GGC CGC CTA CCT GGA CAA GG-3'; Reverse: 5'-CCT TGT CCA GGT AGG CGG CCA GGC GGT CAT TG-3'); **K14 S128D** (Forward: 5'-CAA TGA CCG CCT GGC CGA CTA CCT GGA CAA GG-3'; Reverse: 5'-CCT TGT CCA GGT AGT CGG CCA GGC GGT CAT TG-3'); **K14 Y129F** (Forward: 5'-GCC TGG CCT CCT TCC TGG ACA AGG TG-3'; Reverse: 5'-CAC CTT GTC CAG GAA GGA GGC CAG GC-3') and **K14 Y129E** (Forward: 5'-GAC CGC CTG GCC TCC GAA CTG GAC AAG GTG CGT G-3'; Reverse: 5'-CAC GCA CCT TGT CCA GTT CGG AGG CCA GGC GGT C-3') respectively. Likewise, pEGFP-K14 R125P plasmid DNA was also used as a template at 100 ng/µl for introducing specific mutations (underlined red) by using the following mutagenic primers to generate **K14 R125P_Y129F** as follows: (Forward: 5'-GCC TGG CCT CCT TCC TGG ACA AGG TG-3'; Reverse: 5'-CAC CTT GTC CAG GAA GGA GGC CAG GC-3'). For introducing deletions (~~strikethrough red~~), pEGFP-K14 WT plasmid DNA was used as a template at 100 ng/µl by using the following mutagenic primers to generate **K14 S128del** as follows: (Forward: 5'-CAA TGA CCG CCT GGC CT~~CCT~~A CCT GGA CAA GG-3'; Reverse: 5'- CCT TGT CCA GGT ~~AGG~~ AGG CCA GGC GGT CAT TG-3'); and pEGFP-K5 WT plasmid DNA was used as a template at 100 ng/µl by using the following mutagenic primers to generate **K5**

S181del as follows: (Forward: 5'-CTC AAC AAT AAG TTT GCC ~~TCC~~ TTC ATC GAC AAG GTG CGG-3'; Reverse: 5'- CCG CAC CTT GTC GAT GAA ~~GGA~~ GGC AAA CTT ATT GTT GAG-3'). The mixture of 1 x QuikChange reaction buffer, template DNA, forward and reverse mutagenic primers, dNTPs, H$_2$O and *PfuTurbo* DNA polymerase were then incubated in the thermal cycler with the following cycling parameters: Step 1: 95ºC for 1 min (initial denaturation), Step 2: 95ºC for 50 s (denaturation), Step 3: 65ºC for 50 s (annealing), step 4: 68ºC for either 8 min (EGFP-K14) or 10 min (EGFP-K5) (extension). Steps 2-4 were then repeated for either 18 cycles (single amino acid changes) or 19 cycles (deletions), and at the end of it Step 5 was operated at 68ºC for 7 min (final extension). The resulting PCR product was mixed with Dpn I restriction enzyme and incubated at 37ºC for 3 hrs to digest the parental methylated and hemimethylated DNA. The intact site-mutated plasmid DNA was then transformed using XL-1 blue supercompetent cells. The mixture of plasmid DNA and supercompetent cells were heat-shocked at 42°C for 30 s, and incubated with SOC media at 37°C shaker for 1 hr. The mixture was then spread onto LB agar plate containing 240 μg/ml kanamycin and incubated at 37°C overnight for growing single colonies. Positive clones were verified and all the mutant constructs were confirmed by sequencing.

2.3.2 Cloning

2.3.2.1 Restriction digestion of DNA

The pEGFP-C1 plasmid DNA was first linearised using the restriction enzyme XbaI, and the K14 (WT, R125P, S128del, Y129F, Y129E and R125P_Y129F) DNA sequences were next sub-cloned from the pEGFP-C1 plasmid into the pLV-EF1α-AcGFP1-C1 lentiviral plasmid through PCR-based method. A unique BstBI restriction enzyme recognition site was introduced in the design of the forward primer (in bold) (5'-TCC ATC CA**T TCG AA**T ACT ACC TGC AGC CGC CAG-3') and was used together with the reverse primer (5'-GGT TCA GGG GGA GGT GTG GG-3'). The mixture of 1 x PCR reaction buffer, template DNA, forward and reverse primers, Q buffer, dNTPs, H_2O and *Taq* DNA polymerase were then incubated in the thermal cycler with the following cycling parameters: Step 1: 94ºC for 2 min (initial denaturation), Step 2: 94ºC for 30 s (denaturation), Step 3: 60ºC for 30 s (annealing), Step 4: 72ºC for 1 min 30 s (extension). Steps 2-4 were then repeated for 35 cycles, and at the end of it Step 5 was operated at 72ºC for 10 min (final extension). Both pLV-EF1α-AcGFP1-C1 lentiviral vector and the respective PCR products were digested by BstBI and BamHI restriction enzymes in the presence of restriction enzyme buffer at 37ºC overnight.
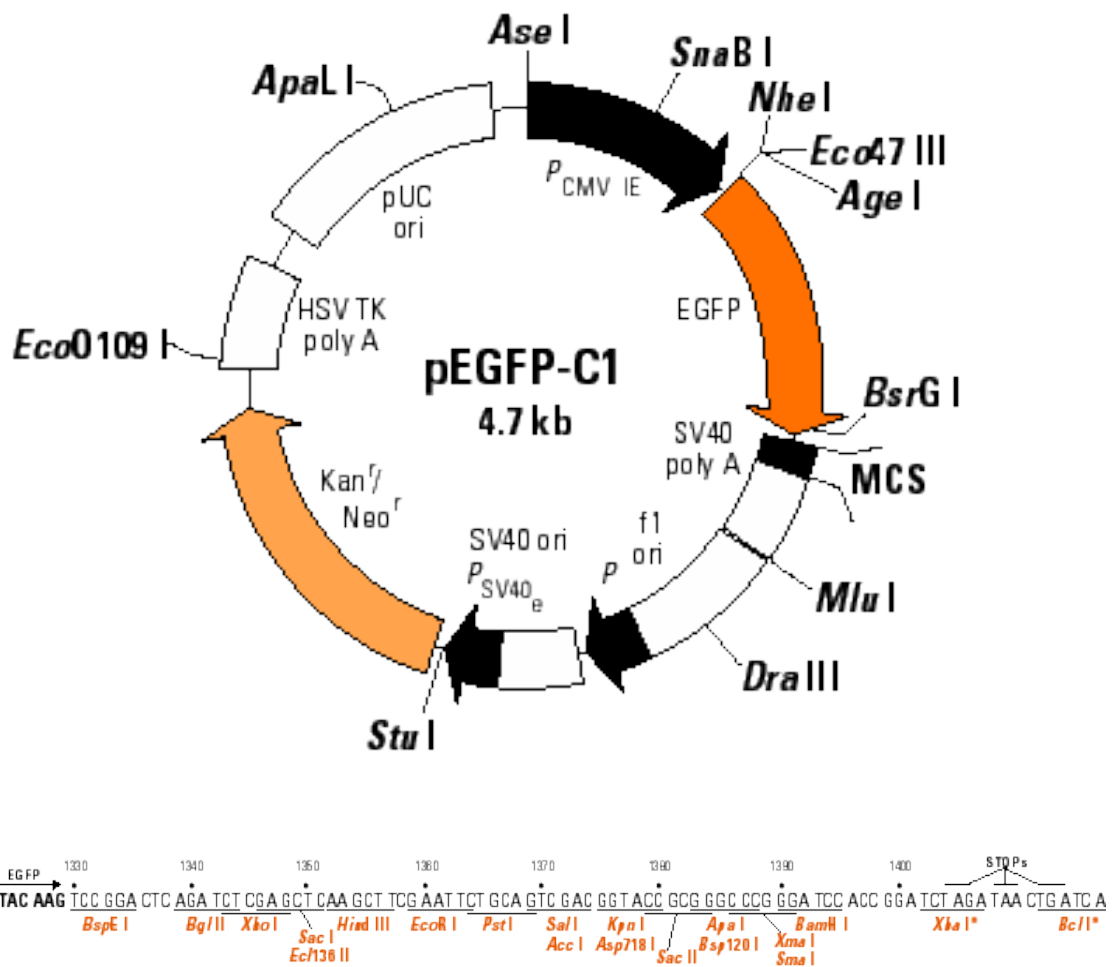
Figure 2.1 Map of mammalian expression vector pEGFP-C1

Genes of interest (K14 WT/R125P) were ligated into the multicloning sites (MCS) of pEGFP-C1 plasmid (from www.clontech.com) and fused with EGFP.
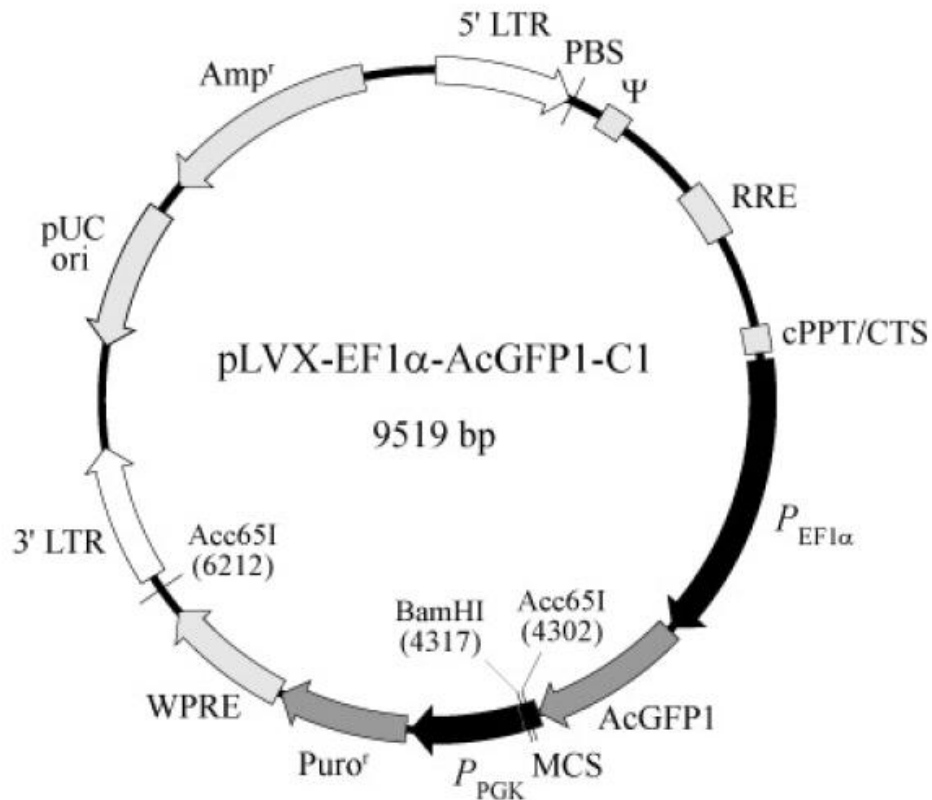
Figure 2.2 Map of mammalian expression vector pLVX-EF1α-AcGFP1-C1

Genes of interest (K14 WT/R125P/S128del/Y129F/Y129E/R125P_Y129F) were cloned from pEGFP-C1 plasmid and ligated into the multicloning sites (MCS) of pLVX-EF1α-AcGFP1-C1 plasmid (from www.clontech.com) and fused with AcGFP1.

2.3.2.2　DNA agarose gel electrophoresis

A 1% (w/v) agarose gel was cast by weighing 1 g of agarose into 100 ml of 1 x TBE buffer and microwaved till the agarose melted. Lonza GelStar* nucleic acid gel stain was added to the melted agarose, poured into the gel casting apparatus and allowed to solidify. 6x DNA loading dye was added to DNA samples to a final 1x concentration and loaded onto the wells of the gel which was submerged in 1x TBE buffer and electrophoresed at 70 V for 2 hrs. The separated DNA bands were visualized using the Fujiflim LAS4000 illuminator and photographed for record purpose.

2.3.2.3　DNA gel extraction

DNA gel extraction was performed using the QIAquick Gel Extraction Kit. Briefly, DNA band was excised from the gel using a clean scalpel under blue light and weighed in eppendorf tubes. 3 volumes of QG buffer were added to the gel slice and the mixture was incubated at 50ºC for 10 min until the agarose gel was completely melted. 1 gel volume of isopropanol was added to the tubes and mixed before transferring into the QIAquick spin column. The column was centrifuged at 13,000 rpm for 1 min to allow binding of the DNA to the column. 750 µl of PE buffer was added to wash the filter column once and the DNA was eluted into 30 µl of RNAse-free water.

2.3.2.4　Dephosphorylation of plasmid DNA

To facilitate efficient ligation of vector DNA (lentiviral plasmid) to insert DNA (PCR product), vector DNA was dephosphorylated by incubating with the shrimp alkaline phosphatase at 37ºC for 30 min and then heat inactivated for 15 min.

2.3.2.5   Ligation of DNA

Ligation of both vector and insert DNA was performed at a ratio of 1:5 respectively in the presence of T4 DNA ligase buffer and T4 DNA ligase. The mixture was incubated at room temperature for 1 hr for ligation to take place.

2.3.3   Transformation of chemically competent cells

5 µl of ligated DNA product was mixed into one vial of One Shot® TOP10 chemically competent *E.coli* cells and incubated on ice for 30 min. The mixture of ligated DNA product and competent cells was heat-shocked at 42°C for 30 s, and incubated with SOC media at 37°C shaker for 1 hr. The mixture was then spread onto LB agar plate containing 100 μg/ml ampicillin and incubated at 37°C overnight for growing single colonies.

2.3.4   PCR analysis of transformants

Bacterial colonies were screened for positive ligation events as follows: A single bacterial colony was inoculated to 6 µl of sterile H_2O to serve as a PCR template. PCR reactions were carried out in 10 µl volumes comprising of 1 x Green GoTaq® Flexi buffer, template DNA, forward and reverse primers, dNTPs, $MgCl_2$, H_2O and GoTaq® DNA polymerase. The PCR cycling parameters were as follows: Step 1: 95ºC for 6 min (initial denaturation), Step 2: 95ºC for 30 s (denaturation), Step 3: 52ºC for 30 s (annealing), Step 4: 72ºC for 4 min (extension). Steps 2-4 were then repeated for 30 cycles, and at the end of it Step 5 was operated at 72ºC for 5 min (final extension). PCR products were resolved on 1% agarose gels at 70 V for 2 hrs to check for correct insert size.

2.3.5 Amplification and isolation of plasmid DNA from bacteria (Mini-prep)

Bacterial colonies containing positive ligation events were inoculated into 3 ml LB broth with 100 µg/ml ampicillin and leave it to incubate at 37ºC with shaking for 8 hrs. Plasmid DNA isolation from bacteria was performed using the QIAprep® Spin Miniprep Kit. Briefly, 2 ml of overnight bacterial culture was retrieved and centrifuged at 13,000 rpm. The supernatant was removed and the bacterial pellet was resuspended in 250 µl of P1 buffer containing RNase A and LyseBlue reagent. 250 µl of P2 lysis buffer was added and the tube was inverted gently and left for 5 min. 350 µl of chilled N3 buffer was then added immediately for neutralization and the cell debris was pelleted by centrifugation at 13,000 rpm. The supernatant was collected and decanted into the QIAprep spin column. The column was centrifuged at 13,000 rpm for 1 min to allow DNA to settle onto the column and bounded to it by PB buffer. 750 µl of PE buffer was added to wash the filter column once and the plasmid DNA was eluted by 30 µl of RNAse-free water.

2.3.6. DNA sequencing

DNA sequencing was carried out using BigDye® Terminator v3.1 Cycle sequencing kit by mixing the DNA template, forward or reverse primer, H_2O and Terminator Ready Reaction Mix in a total of 10 µl reaction volumes. The PCR cycling parameters were as follows: Step 1: 96ºC for 1 min, Step 2: 96ºC for 10 s, Step 3: 50ºC for 5 s, Step 4: 60ºC for 4 min. Steps 2-4 were then repeated for 25 cycles, and at the end of it hold at 4ºC. Samples were submitted to the DNA sequencing facility at Institute of Molecular and Cell Biology for purification and subjected to capillary electrophoresis on the ABI PRISM 3730xl DNA Analyzer.

2.3.7. Bacterial DNA maxi-prep using Endofree® Plasmid Maxi Kit

Large-scale amplification of plasmid DNA and its isolation from bacteria was performed using the Endofree® Plasmid Maxi Kit. Briefly, 1 ml of bacterial culture broth was added into 100 ml of lysogeny broth (LB) containing 100 µg/ml ampicillin and incubated at 37ºC with shaking for 16 hours. 90 ml of overnight bacterial culture was retrieved and centrifuged at 6,000 g for 15 min at 4 ºC. The supernatant was removed and the bacterial pellet was resuspended in 10 ml of P1 buffer containing RNase A and LyseBlue reagent. 10 ml of P2 lysis buffer was added and the tube was inverted gently and left for 5 min. 10 ml of chilled P3 buffer was then added immediately for neutralization and the cell debris was decanted into the QIAfilter Maxi Cartridge. The cell lysate was filtered through the cartridge and collected onto a 50 ml falcon tube. 2.5 ml of ER buffer was added to the filtered lysate, mixed by inverting and incubate on ice for 30 min. The filtered lysate was then decanted into the QIAGEN-tip and then washed twice with 30 ml QC buffer. Plasmid DNA was eluted with 15 ml QN buffer and precipitated with 10.5 ml isopropanol. The plasmid DNA pellet was collected by centrifugation at 4,000 rpm for 1 hr, washed with 70% ethanol for 1 hr at 4,000 rpm, air-dried and finally dissolved in endotoxin free TE buffer.

2.3.8 Preparation of bacteria stocks

Bacterial stocks of successful transformation events were prepared in 50% glycerol. The LB-glycerol suspension was thoroughly mixed and then placed in -80ºC freezer for long term storage.

2.3.9   Transient transfection

For transient transfection studies, NEB-1 cell line was plated at 80% confluency on 22 mm² coverslips in a 6-well plate and transfected with the pEGFP-K14 WT and mutant constructs using the Effectene^{TM} reagents (Qiagen, Germany) according to manufacturer's protocol. Briefly, 0.4 µg of DNA were added into an eppendorf tube with 100 µl of DNA condensation (EC) buffer, and 3.2 µl of Enhancer. Mixture was vortexed and incubated at room temperature for 5 min. 10 µl Effectene^{TM} transfection reagent was then added into the mixture followed by vortexing and incubated at room temperature for 10 min to allow transfection complex to form. Meanwhile, culture media was aspirated from the flask and replenished with new media. After 10 min, the transfection mixture was then added dropwise onto the cells and cells were harvested for respective assays at least 24 hrs post transfection. The expression of pEGFP-K14 WT and mutant constructs were then analyzed after 36 hrs post-transfection using immunofluoresence.

2.3.10   Viral packaging and collection

To establish stable cell lines expressing EGFP-K14 constructs, high-titre lentiviruses were ultilized. Non-replicative lentiviruses were produced by triple transfection of HEK293T cells in 15 cm dishes with 1.5 µg pLVX-EF1α-AcGFP1-C1 lentiviral expression vector, 1 µg pHR-CMV 8.2 delta packaging vector and 1 µg pCMV VSV-G envelope vector using Effectene transfection reagent (Qiagen, Germany). The viral supernatant was collected after 48 hrs and 72 hrs post transfection before filtering through 22 µm filter system to remove cell debris. The supernatant was then ultracentrifuged at 16,000 g for 2 hrs at 4ºC. The resultant pellet was resuspended in DMEM and frozen at -80ºC in aliquots.

2.3.11   Viral titration of N/TERT-1 cells and quantification

40, 000 N/TERT-1 cells were seeded onto each well of the 24-well plate for 16 hrs before they were infected by the various viral-packaged constructs in the presence of 24 μg/ml of polybrene in titrations of 10^{-2}, 10^{-3}, $10^{-3}/2$ dilutions (of each construct) and incubated for 72 hrs. The cells in each well were then trypsinized, collected onto fluorescence-activated cell sorting (FACS) tubes and centrifuged for 5 min at 1000 rpm. The pellet was then washed once in PBS, centrifuged and resuspended in PBS for FACS analysis. The viral titer for each construct was then derived from the percentage of GFP-positive cells in a population of 40, 000 infected cells at the specific dilution and determined as the number of viral particles per ml. The multiplicity of infection (M.O.I) was then calculated by determining the number of cells to be infected divided by the viral titer (number of viral particles per ml) and the volume of viral supernatant to be added in experiments could be derived.

2.3.12   Viral infection of N/TERT-1 cells to generate stable cell lines

To generate stable cell lines, various viral-packaged constructs (M.O.I =1.0) were added together with 24 μg/ml of polybrene to infect 1 million N/TERT-1 cells in suspension and pre-incubated at 37ºC for 1 hr before seeding them onto 100 mm dishes. GFP-positive cells were then selected by FACs sorting after one week of transduction and remained in culture for further experiments. The levels of expression of transfected AcGFP-K14 wild type and mutant constructs and their ratio with the endogenous wild-type K14 were then assessed by immunoblotting with LL001 monoclonal antibody against K14 (Purkis et al., 1990). Cells having a 1:1 ratio of transfected AcGFP-keratin wild type or mutant protein to endogenous wild type keratin were then cultured and expanded.

2.3.13   Transient infection of N/TERT-1 cells

For transient viral infection, viral-packaged constructs (AcGFP-K14 R125P, AcGFP-K14 R125P_Y129F) of various multiplicity of infection values (M.O.I = 0.5, 1.0, 2.0) were added together with 24 µg/ml of polybrene to infect 100, 000 N/TERT-1 cells in suspension and pre-incubated at 37ºC for 1 hr before seeding them onto 22 mm² coverslips in a 6-well plate. The cells were then incubated at 37ºC for 72 hrs before fixation.

2.4   Gene expression analysis

2.4.1   RNA extraction

Total RNA was extracted from the cells using the RNeasy Mini Kit (Qiagen, Germany). Briefly, cells were kept on ice, washed in ice-cold PBS, scrapped and collected in 1 ml of PBS onto respective tubes. Cells were pelleted by centrifugation at 5,000 rpm at 4ºC and the pellet was lysed in 350 µl of RLT buffer with β-mercaptoethanol. Lysate was homogenized using the QIAshredder spin column and RNA was precipitated with 70% ethanol. The precipitated RNA was decanted into RNeasy spin column and centrifuged at 13,000 rpm for 1 min. The column was washed with 700 µl RW1 buffer and DNase digestion was carried out on the column using the RNase free DNase set to avoid genomic DNA contamination. Column was then washed with 500 µl RPE buffer twice before the RNA was eluted by 30 µl of RNAse-free water. The RNA quantity and concentration were determined using Nanodrop ND-1000.

2.4.2 cDNA synthesis

cDNA (complementary DNA) synthesis was performed with 1 μg of total RNA, using the Transcriptor First Strand cDNA Synthesis kit (Roche Applied Science). Briefly, total RNA was first denatured with oligo(dT)$_{15}$ primer for 10 min before mixing with the 1x reaction buffer, protector RNase inhibitor, dNTPs, H_2O and reverse transcriptase. Reverse transcription was then carried out at 50ºC for 60 min.

2.4.3 Quantitative real-time PCR (qPCR)

Real-time quantitative PCR was carried out using the ABI-PRISM 7500 Sequence Detection System (Applied Biosystems). 3 μl of 10 x diluted reversed transcribed cDNA samples were added to 5 μl of Power SYBR Green PCR Master Mix (Applied Biosystems) and 2 μl of primers mix (forward and reverse primers). Reactions were conducted in triplicate within 384-well reaction plates (Applied Biosystems) at a final volume of 10 μl on the ABI-PRISM 7500 machine. The list of forward and reverse primers was listed in Table 2.2. The cycling parameters were as follows: Step 1: 95ºC for 10 min, Step 2: 95ºC for 15 s and Step 3: 60ºC for 60 s. Steps 2-3 were repeated for 40 cycles. A dissociation curve was added as an additional parameter to check primer amplification integrity with the following steps: 95ºC for 15 s, 60ºC for 15 s and 95ºC for 15 s. Data was analyzed using the Sequence Detection System 7500 software (Applied Biosystems). Relative quantification was calculated by the $\Delta\Delta C_t$ method normalized to either hypoxanthine-guanine phosphoribosyltransferase (*HPRT*) or ribosomal protein P0 (*RPLP0*) housekeeping genes.

2.4.4   Over-expression studies

For over-expression studies, isogenic pathomimetic cell lines were plated at 80% confluence in 100 mm dishes and transfected with a rat FLAG-tagged ERK2 cDNA using 2 μg DNA and 60 μl Effectene^{TM} reagent. The expression of FLAG-ERK2 was then analyzed from a time scale of 24-48 hrs post-transfection using western blotting.

2.4.5   RNA interference (siRNA)

For knockdown studies, isogenic cell lines were plated at 80% confluence in 100 mm dishes and transfected with DharmaFECT^{TM} 1 siRNA transfection reagent (Dharmacon) according to the manufacturer's instructions. Cells were transfected with either ON-TARGETplus siRNA (Dharmacon) targeting MAPK3 (ERK1), catalog no: J-003592-08-0020, ON-TARGETplus SMARTpool siRNA (Dharmacon) targeting MAPK1 (ERK2), catalog no: L-003555-00-0005 or ON-TARGETplus siRNA (Dharmacon) targeting plectin (PLEC), catalog no: J-003945-09-0020 (see Table 2.3). The mixture of ERK1-ERK2 siRNAs, PLEC siRNAs or control siRNA against GAPD (Dharmacon), catalog no: D-001830-01-20, was used in experiments at 100 nM concentrations. After 24 hrs, fresh medium was replaced and cells were harvested for RNA or immunoblot analysis 48-72 hrs post-transfection.

Table 2.2   Primer sequences for qPCR using SYBR Green Master Mix

Genes	Forward primer	Reverse primer
β1 integrin	5'-TTA TTG GCC TTG CAT TAC TGC T-3'	5'-CCA CAG TTG TTA CGG CAC TCT-3'
ERK1 (MAPK3)	5'-ACA TTG TGC AGG ACC TGA TGG AGA-3'	5'-TAA GGT CGC AGG TGG TGT TGA TGA-3'
ERK2 (MAPK1)	5'-CCA CCC ATA TCT GGA GCA GT-3'	5'-CAG TCC TCT GAG CCC TTG TC-3'
Fibronectin	5'-CAC AGC TTC TCC AAG CAT CA-3'	5'-TGG CTG CAT ATG CTT TCC TA-3'
HPRT	5'-CCT GGC GTC GTG ATT AGT GAT-3'	5'-AGA CGT TCA GTC CTG TCC ATA A-3'
KRT17	5'-GGT GGG TGG TGA GAT CAA TGT-3'	5'-CGC GGT TCA GTT CCT CTG TC-3'
MMP9	5'-TAC CAC CTC GAA CTT TGA CAG CGA-3'	5'-GCC ATT CAC GTC GTC CTT ATG CAA-3'
Plectin	5'-ACC CTC TGA GCT TTG CAT GT-3'	5'-CCC ACG TCA GGT TA GTG TT-3'
KRT14	5'-CTT GGG TGG TGG CTT TGG-3'	5'-GTC CAC TGT GGC TGT GAG AA-3'
KRT5	5'-CAC TGT CAA CCA GAG TCT CCT GAC T-3'	5'-CGG TCC TCA CCC TCT GGA T-3'
RPLP0	5'-CAG ATT GGC TAC CCA ACT GTT-3'	5'-GGG AAG GTG TAA TCC GTC TCC-3'

Table 2.3   siRNAs for knockdown studies

ON-TARGETplus siRNA	Target sequences
Human ERK1 (MAPK3)	5'-CCU GCG ACC UUA AGA UUU G-3'
Human ERK2 (MAPK1)	5'-UCG AGU AGC UAU CAA GAA A-3'
	5'-CAC CAA CCA UCG AGC AAA U-3'
	5'-GGU GUG CUC UGC UUA UGA U-3'
	5'-ACA CCA ACC UCU CGU ACA U-3'
Human Plectin (PLEC)	5'-GAA GAG ACA CAG AUC GAC A-3'

2.5   Protein expression analysis

2.5.1   Cell lysis and protein quantification

1 million cells were seeded onto 100 mm petri dish and grown to 80% confluence. Cells were kept on ice, washed in ice-cold PBS, scrapped and collected in 1 ml of PBS onto respective tubes. The cell suspensions were then centrifuged at 5,000 rpm for 5 min. The supernatant was removed and the cell pellet was re-suspended in 100 µl of lysis buffer containing: 20 mM Tris-HCl (pH 7.6), 140 mM NaCl, 5 mM EDTA, 1% (v/v) NP-40, 0.5% (w/v) sodium deoxycholate supplemented with Complete, Mini (EDTA-free) protease inhibitor cocktail tablet (Roche) per 10 ml lysis buffer, 1 mM sodium orthovanadate (Na_3VO_4) and 1 mM phenylmethylsulphonyl fluoride (PMSF), 5 mM sodium fluoride, 50 mM β-glycerolphosphate, of which all were added fresh, immediately prior to use. The cells were then lysed on ice for 15 min. Cell lysates were then centrifuged at 16, 000 g for 15 min at 4 ºC. Supernatant was then homogenized by passing through a QIAshredder column tube (QIAGEN) with centrifugation at 16, 000 g for 2 min at 4 ºC. The homogenized supernatant was collected and stored at -80 ºC. For the pellet, it was re-suspended in pelleting buffer [Tris-HCL (pH 8.0). 10 mM $MgCl_2$, 5 mM EDTA, 1 mM Na_3VO_4 and 1 mM PMSF] containing 250 U benzonase nuclease (Novagen) and was incubated for 30 min at room temperature. After repelleting, the final pellets were washed in PBS containing 1 mM PMSF and 1 mM Na_3VO_4 and then re-suspended in 4X LDS buffer (Invitrogen), in a volume equivalent to the supernatant. Protein concentration of the supernatant was then determined by BCA assay (Thermo Scientific Pierce) and standardized using bovine serum albumin.

2.5.2 Sodium dodecylsulphate polyacrylamide gel electrophoresis (SDS-PAGE)

For sodium dodecylsulphate (SDS) polyacrylamide gel electrophoresis, $20 - 40$ µg of each sample's supernatant or pellet was mixed with 4X LDS sample buffer (Invitrogen), boiled for 10 min at 70 ºC, and separated on 4-12 % Bis-Tris SDS polyacrylamide precast gels (invitrogen) for 50 min at 200V constant. In cases where higher molecular weight proteins (plectin, fibronectin or desmoplakin) are to be blotted, $20 - 40$ µg of each sample was mixed with 4X LDS buffer (Invitrogen), heated for 10 min at 70 ºC and separated on 3-8 % Tris-Acetate SDS polyacrylamide precast gels (invitrogen) for 60 min at 150V constant.

2.5.3 Protein detection and chemiluminesence

For immunoblotting, protein transfer was carried out using the iBlot dry blotting machine system onto nitrocellulose membranes (Invitrogen) for 7 min. Non-specific binding to the membrane was blocked by incubation in TBS-T containing 5% milk, for 1 hr with gentle agitation. Blots were then incubated overnight at 4 ºC with the primary antibodies in 5 ml TBS-T containing 5% BSA with gentle agitation. The membranes were then washed twice with TBS-T, and bound primary antibodies were then incubated for 1 hr with secondary antibodies. The membranes were then washed four times before visualized by enhanced chemiluminescence (ECL) using the Fujiflim LAS4000 illuminator.

2.5.4 Immunocytochemistry

100, 000 cells were seeded onto 22 mm² glass coverslips in 6-well plate and grown to 80% confluence (either non-treated or prior to drug treatment regime) before being fixed with 4% parafarmaldehyde in PBS, pH 7.4 at room temperature for 7 min. After

fixation, cells were treated in blocking buffer (3% normal goat serum in PBS) and permeabilized with 0.1% Triton X-100 in PBS at room temperature for 20 min. On the other hand, for methanol fixation, cells were fixed with methanol at -20ºC for 10 min and blocked with 10% FBS for 20 min. Cells were washed twice with PBS and then incubated overnight with primary antibodies. Cells were then washed 3 x 5 min in PBS and the primary antibodies were detected using the respective secondary antibodies by incubating 45 min in the dark. Cells were then washed 3 x 5 min in PBS and incubated in 4-6-diamidino-2-phenyllindole (DAPI) (1:2500) (Sigma) dissolved in PBS. Cells were subsequently washed 3 x 5 min in PBS and mounted on coverslips using Hydromount with 2.5% DABCO to reduce photobleaching. Slides were air-dried and viewed with an inverted Deltavision epifluorescence microscope (Applied Precision, USA). Images were visualized with either an Olympus UApo/340 20x (N.A. 0.75) objective lens; Olympus UApo/340 40x (N.A. 1.35) or an Olympus PlanApo 60x (N.A. 1.42) oil immersion objective lens with a Photometric CCD camera (CoolSNAP HQ2) using the SEDAT filter set. Images were then processed using the SoftWorRx application (Applied Precision, USA).

2.6   Time-lapse microscopy imaging and image processing

2.6.1   Differential interference contrast (DIC) live-cell migration

For DIC live-cell imaging, 100 – 300 cells were grown on a 4-well Lab-Tek II #1.5 chambered coverslips. Single cell was selected with the 'mark and visit' tool of SoftWoRx from each cell line. To generate movies of randomly migrating live cells, repetitive images were collected every 5 min for a total of 5 hrs using an Olympus UApo/340 20x (N.A. 0.75) objective lens. A minimum of ten individual fields was recorded for each cell line. DIC image stacks of single cell migration were analyzed

and processed using several macros written with ImageJ. One macro was written to apply top-hat and variance filters on the DIC time-lapse sequence while the other was written to segment the single cell body and analyzed the filtered sequence. During this stage, auto-threshold was manually adjusted for the best possible segmentation. Total distance travelled by each cell for 5 hrs was then extracted using another macro and their corresponding migration paths were plotted.

2.6.2 Fluorescence live-cell imaging

For fluorescence live-cell imaging, 10, 000 cells were grown on a 35 mm WillCo-dish® glass-bottomed dish (WillCo-wells, Amsterdam). Images (1024x1024 dpi, 1x1 binning) of cells expressing the fluorescence constructs were collected every 15 sec for a period of 30 min using an Olympus UPlanApo/IX70 100x (N.A. 1.35) oil immersion objective lens. These sequences of images were then converted into movies and subsequently analyzed using SoftWoRx software (Applied Precision, USA). Image series, presented as inverse fluorescence micrographs, were taken from time-lapse recordings and shown as data in the results section. Both DIC and fluorescence live-cell imaging were carried out using an inverted Deltavision epifluorescence microscope (Applied Precision, USA), equipped with a fully motorized Z stage (Applied Precision, USA) and linked to Photometrics CCD camera (CoolSNAP HQ2) using the SEDAT filter set. Samples were maintained at 37ºC in a 5% CO_2 environment.

2.6.3 Phase contrast live-cell imaging of scratch wounds using IncuCyte^{TM}

20, 000 cells were seeded onto each well of an Essen ImageLock 96-well plate and grown to confluence before being subjected to wounding with a 96-well WoundMaker Tool, which gently removed cells from the confluent monolayer using a 96 array of PTFE pin tips. Cells were then washed twice with media and the plate was placed inside the IncuCyte. For EGF treatment study, cells were treated with either DMSO, AG1478 (10 μM) or U0126 (10 μM) in fresh media before imaging. Alternatively, cells grown to sub-confluence were transfected with DharmaFECT^{TM} 1 siRNA transfection reagent (Dharmacon) according to the manufacturer's instructions. Cells were transfected with ON-TARGETplus siRNA (Dharmacon) targeting plectin (PLEC), catalog no: J-003945-09-0020. The mixture of PLEC siRNAs or control siRNA against GAPD (Dharmacon), catalog no: D-001830-01-20, was used in experiments at 100 nM concentrations. After 24 hrs, fresh medium was replaced and after 48 hrs post-transfection, cells were then subjected to wounding with a 96-well WoundMaker Tool. Wound images were acquired immediately and at 1 hr intervals for 14-28 hrs. Scratch wound data was analyzed and processed using several macros written with ImageJ. One macro applies the built-in ImageJ Sobel edge filter to locate the edges of the wound while the other applies auto-threshold methods to find the wound area and calculate the recovery of the wound. Red line marks the denuded area from which cells were removed at the start of the wound (0 hr); green line marks the remaining uncovered area after 14-28 hrs. Areas between red (or green) lines were derived from a macro written with ImageJ. Area covered was obtained by the subtraction of the initial wound area and the remaining uncovered area, and the data for area covered / initial wound area were presented for each treatment.

2.6.4   Confocal live-cell imaging using MEK1/2 inhibitor treatment

10, 000 cells were grown on a 35 mm WillCo-dish® glass-bottomed dish (WillCo-wells, Amsterdam). Time-lapse analyses were then performed with a Zeiss LSM510 inverted confocal microscope. For each movie, images were taken every minute for 1 hr using an EC Plan-Neofluar 40x/1.30 oil immersion objective lens. This was performed by using the filter, BP-505-530 and the beam splitters: MBS: HFT 405/488/561, DBS1: NFT 565, DBS2: NFT 490 respectively. Argon LASER was used at 488 nm wavelength at 19.8% power and the pinhole was set to 124 µm. The scan mode was: Plane, line series, with an average limited to Line 2 so as to limit the LASER exposure to the cells to minimize cell death or photobleaching. Drug treatment was initiated after 1 hr of acquisition by removing the original medium and replacing it with fresh medium containing the MEK inhibitor U0126 at 100 µM. Such treatment was maintained for another hour before washing out by replacing it with fresh medium. For image processing and migration analysis, false color coding images were obtained by first converting the images extracted from the movies to TIFF files, then importing them into ImageJ software and converting them to 8-bit images. Next, for each movie ("control", "treatment" and "washout" movies), an artificial color was given to the images corresponding to the time points: 0 min, 30 min and 60 min (green, blue and red color, respectively). The three images were then merged together and presented as shown.

2.7   Functional studies

2.7.1   Osmotic stress assay

1 million cells were seeded onto 100 mm petri dish and cultured to 80% confluence. The subconfluent culture was left intact or being subjected to hypo-osmotic shock upon immersion in 150 mM urea for 5 min at 37 ºC as described in (D'Alessandro et al., 2002). Cells were then allowed to recover in fresh media for varying periods of time before being harvested for immunoblot analysis.

2.7.2   Confluence assay

100, 000 cells were seeded onto 22 mm² glass coverslips in 6-well plate or 1 million cells were seeded onto 100 mm petri dish and they were grown to subconfluence (80%), confluence (monolayer) (100%), 1 day post confluence (100% + 1) or 2 days post confluence (100% + 2) before being fixed for immunostaining or harvested for immunoblot analysis respectively.

2.7.3   Multiple scratch wound assays

100, 000 cells were seeded onto 35 mm petri dish and grown to 2 days post confluence. Upon confluent, the monolayer was left intact or subjected to wounding using 3 yellow tips mounted onto a multi-channel pipette to generate multiple scratch wounds vertically and horizontally across the 35 mm petri dish. Cells were then washed twice in media and left to recover for either 18 hrs or 24 hrs post-wounding before being harvested for immunoblot analysis.

2.8   Statistical analysis

2.8.1   Differential interference contrast (DIC) live-cell migration

For single cell migration study, the distribution of cell migration for each cell line was represented in the form of histograms using the histogram data analysis tool add-in in Microsoft® Excel. The total distance travelled by each cell for 5 hrs was determined and the results were represented as mean distance travelled by each cell for $n = 55$ (NEB-1) and $n = 45$ (KEB-7) respectively.

2.8.2   Confluence assay

For confluence assay, $500 - 800$ cells at different confluence states were counted using ImageJ analysis software. The total number of cells and the number of cells with aggregates were counted and represented as % of cells with aggregates.

2.8.3   Drug/EGF treatment

For the EGF treatment study, $700 - 900$ cells from each treatment group were counted for 4 independent experiments using ImageJ analysis software. The total number of cells and the number of cells with aggregates were counted and represented as % of cells with aggregates.

2.8.4   Phase contrast live-cell imaging of scratch wounds using IncuCyte[TM]

For scratch wound assays, both the initial wound area (denoted by red line) and the area of wound region covered (denoted by the green line) for each treatments were derived and presented as ratio of area covered/initial wound area for $n = 3$.

2.8.5 Co-localization study

For quantification of co-localization studies, data were obtained from 20 cells immunostained with either P-ERK1/2 (Thr202/Tyr204) or ERK1/2 and they were represented as Pearson Coefficient of Correlation values using the SoftWoRx software (Applied Precision, USA).

2.8.6 MEK1/2 inhibitor treatment

For the U0126 inhibitor treatment studies, 400-1000 cells from each treatment group were counted for n = 8 independent experiments using imageJ analysis software. The number of cells with aggregates were counted and represented as number of cells with aggregates relative to control.

2.8.7 Viral titration of N/TERT-1 cells with AcGFP-K14 R125P and AcGFP-K14 R125P_Y129F constructs

For the infection study, 500 – 3000 cells from each multiplicity of infection (M.O.I) treatment group of 0.5, 1.0 and 2.0 respectively were counted for 3 independent experiments using ImageJ analysis software. The total number of cells, the number of GFP-positive cells and the number of cells with aggregates were counted and represented as % infection efficiency and % of cells with aggregates.

2.8.8 General statistical analysis

All data were presented as mean $\pm$ SD, except for single cell migration which was presented as mean $\pm$ S.E.M. Data analysis was performed by one-way analysis of variance (ANOVA) followed by post hoc Tukey's test for multiple comparisons of at least three groups or unpaired Student's t-test between two groups using Prism 5.0 (Graphpad Software Inc.). p values of < 0.05 were considered statistically significant.

CHAPTER 3

KERATINS AND KERATINOCYTE

ACTIVATION CYCLE

3.1   Introduction

Normal homeostasis of the epidermis is maintained by a tightly controlled keratinocyte differentiation program that provides the barrier function of the body. However, in response to injury, this self-renewal program is interrupted and the keratinocytes become "activated", which occurs not only on wounding but also in *in vitro* culture conditions (reviewed in Grinnell, 1990; Grinnell, 1992). During this wound healing process, the junction and adhesion molecules of the keratinocytes undergo significant changes (reviewed in Martin, 1997). For instance, the keratinocytes partially disintegrated their hemidesmosomes and began to express vitronectin, fibronectin receptors and $\alpha5\beta1$ integrins, which allowed them to migrate over the provisional wound matrix (Cavani et al., 1993; Haapasalmi et al., 1996; Singer and Clark, 1999). Fibronectin is a major component of this provisional wound matrix (reviewed in Clark, 1990), which accumulates in wound fluid such as in the suction blisters (Wysocki and Grinnell, 1990).

One of the markers of activated keratinocytes is the suprabasal expression of K6, K16 and K17 proteins at the expense of K1 and K10 (Weiss et al., 1984), hence deviating from the usual differentiation program. It is thought that these wound-induced keratins provide plasticity and flexibility of the cytoskeleton of the migrating keratinocytes (Coulombe, 1997), hence promoting the reorganization of keratin filaments during the onset of re-epithelialization (Paladini et al., 1996).

As the keratinocytes migrate, they form new focal adhesion complexes and undergo intracellular actinomyosin filaments contraction as they push forward towards the wound bed (Mitchison and Cramer, 1996). Due to the switching of integrin receptors ($\beta4$ to $\beta1$) and assembly of associated actin filament networks, there is a lag of several

hours before epidermal migration begins (Grinnell, 1992). Initiation of keratinocyte migration occurred 16-24 hours after injury (Winter, 1962), and its early phase was not affected by mitosis (Matoltsy, 1955). However, keratinocytes located behind the migrating sheet could undergo a transient burst of proliferation a few hours after the onset of migration, providing more cells to sustain re-epithelialization (Garlick and Taichman, 1994).

Wound-edge keratinocytes also up-regulate several matrix metalloproteinases (MMP) such as MMP-2 and MMP-9 (gelatinases), which can cleave basal lamina collagen (type IV) and anchoring fibril collagen (type VII) (Salo et al., 1994), thus aiding in tissue remodelling.

Once the activation cycle is completed, keratinocytes become deactivated and revert to normal differentiation, giving rise to the quiescent stratified epidermis. This process is termed the keratinocyte activation cycle (Freedberg et al., 2001).

EBS Dowling-Meara (EBS-DM) keratinocytes have an intrinsic upregulation of activated stress kinases and they show sustained stress responses to osmotic stress (D'Alessandro et al., 2002) and faster migration during scratch wound assays (Morley et al., 2003). Why these EBS-DM keratinocytes have a faster wound response is not completely understood, although this could have something to do with their keratinocyte activation state.

In this chapter, it is hypothesized that EBS-DM cells are in a constitutively stressed or activated state reminiscent to a wound condition. Experiments are designed to address the following: (1) the differences between wild-type and EBS-DM cells at sub-confluence in terms of (a) their stress activated protein kinase (SAPK) activation, (b) their difference in migration speeds (single and collective cell migration) and (c)

wound response protein expression (K17, β1 integrin, fibronectin and MMP-9); (2) changes in wound response protein levels in EBS-DM cells as they transit to quiescent state (100 % confluence or more) and (3) changes in wound response protein levels upon reverting from confluence to an activation state when subjected to multiple scratch wounding. It is found that EBS-DM cells are intrinsically "primed" to be in the constitutively activated state, which might be a consequence of the pathogenesis of recurrent blister formation in EBS-DM patients.

3.2   Results

3.2.1   Characterization of EBS-DM cell lines

As the first step to identify the physiological differences between wild-type cells and EBS-DM cells, wild-type keratinocytes isolated from the skin of a normal individual, immortalized and named as NEB-1 (wild-type K14) (Morley et al., 2003), mutant keratinocytes isolated from the skin of a EBS-DM patient (harbouring EBS-DM mutation K14 R125P), immortalized and named as KEB-7 (Morley et al., 2003) and NEB-1 keratinocytes stably expressing EGFP-tagged K14 WT and K14 R125P (Liovic et al., 2009) were used in this study.

It was confirmed that KEB-7 keratinocytes show spontaneous appearance of keratin aggregates at the periphery, and that this occurs in the presence of intact filament formation [Figure 3.1 (I) (i) (B)], compared to wild-type NEB-1 keratinocytes in [Figure 3.1 (I) (i) (A)]. Characterization of NEB-1 keratinocytes stably expressing EGFP-K14 R125P showed a phenotype reminiscent to that of KEB-7 cells from their densely packed keratin bundles at the perinuclear region and keratin aggregates

segregated at the cell periphery [Figure 3.1 (I) (ii) (B)]. This was distinct from cells stably expressing EGFP-K14 WT, which did not show any peripheral keratin aggregates [Figure 3.1 (I) (ii) (A)]. Moreover, the presence of normal filament formation was not completely impaired in the EGFP-K14 R125P keratinocytes [Figure 3.1 (I) (ii) (B)], which was similar to that of KEB-7 cells [Figure 3.1 (I) (i) (B)], and showed a co-existent of normal filaments with peripheral keratin aggregates. It is also observed that there are variations in the level of K14 expression in tissue culture, as is commonly seen in many cell lines, and this could be due to the time lapse since the last cell division or due to an unidentified microenvironmental factor that affect keratin synthesis in culture.

To evaluate the protein levels of endogenous and exogenous K14 of the different cell lines, immunoblot analysis was performed on cell lysates from NEB-1, KEB-7, EGFP-K14 WT and EGFP-K14 R125P cell lines at subconfluence [Figure 3.1 (II)]. It was shown that KEB-7 cells have significantly higher (* $p < 0.05$) levels of K14 proteins (2.02 ± 0.99 folds) than NEB-1 cells (1.00 ± 0.00), although the ratio of wild-type K14 and mutant K14-R125P proteins of the KEB-7 cells within this band could not be determined [Figure 3.1 (III) (i)]. Equal amounts of endogenous K14 (1.00 ± 0.00) and exogenous K14 (1.03 ± 0.21 folds) protein levels were observed in EGFP-K14 WT cells [Figure 3.1 (III) (ii)], whereas the amount of exogenous K14 proteins (1.59 ± 0.50 folds) were significantly higher (* $p < 0.05$) than that of the endogenous K14 proteins (1.00 ± 0.00) in EGFP-K14 R125P cells [Figure 3.1 (III (ii)], an observation similar to that reported in (Beriault et al., 2012) using the same cell lines. These results showed that NEB-1 K14 R125P cells predominantly expressed the exogenous mutant K14 proteins, with the endogenous wild-type K14 proteins contributing to 40% of the total [Figure 3.1 (III (ii)]. This may be because the CMV-

driven transfected K14 construct is not responding to local feedback signals when the K14 level in the cell becomes too high, whereas the normal K14 promoter driving the endogenous K14 is responsive to such signals. Thus, synthesis of the endogenous K14 can be regulated and shut down whilst the transfected K14 cannot. These observations also suggest that EBS-DM cell lines have an abnormal K14 expression profile, because the levels of K5 proteins are the same in all four cell lines [Figure 3.1 (III) (iii)], and this could be a response to the accumulating mutant keratins (in the form of aggregates) at the leading edge.

(I)

(i)

NEB-1   **KEB-7 (K14 R125P)**

K14 (LL001)

(ii)

NEB-1

EGFP-K14 WT   **EGFP-K14 R125P**

EGFP-K14

(II)

	NEB-1	KEB-7	EGFP-K14 WT	EGFP-K14 R125P
EGFP-K14 (LL001)				
Endogenous K14 (LL001)				
K5 (XM-26)				
Actin				

(III)

(i)

(ii)

EGFP-K14 WT   EGFP-K14 R125P
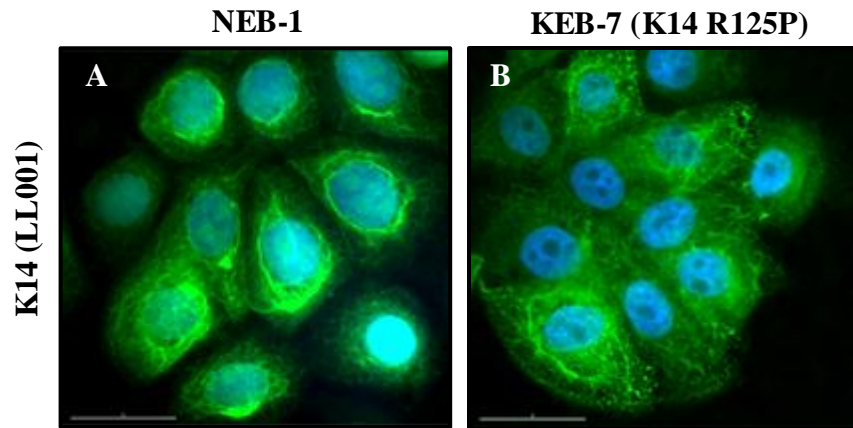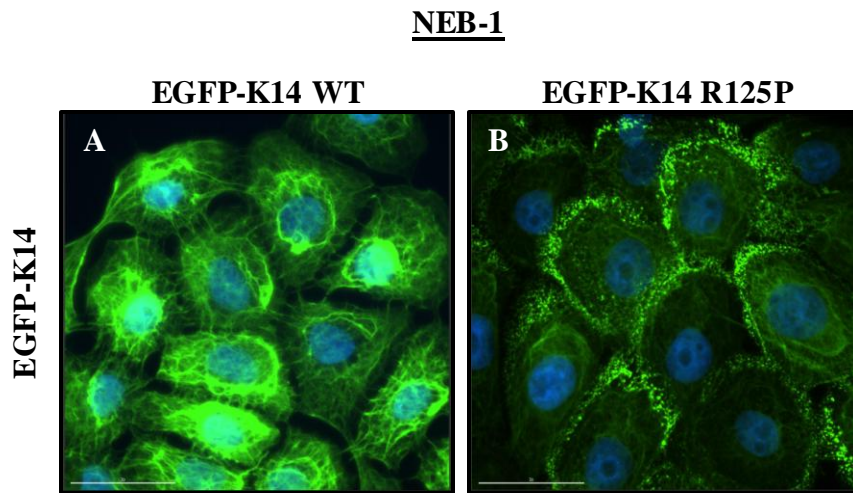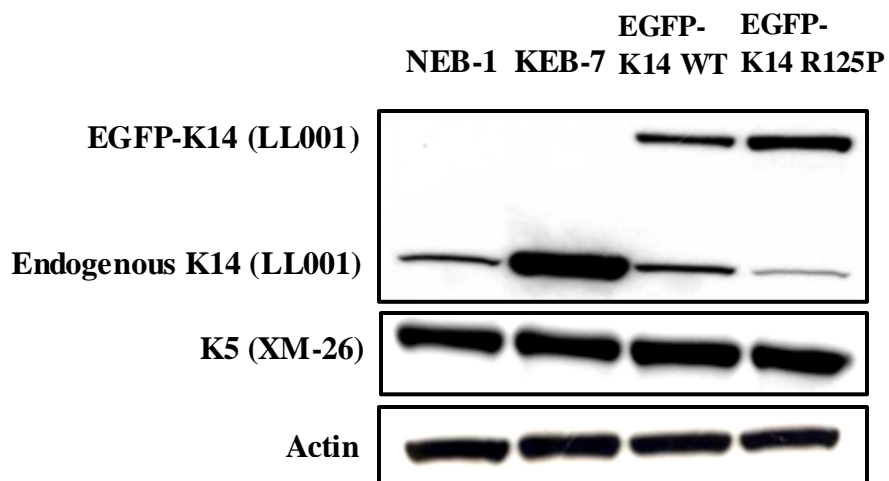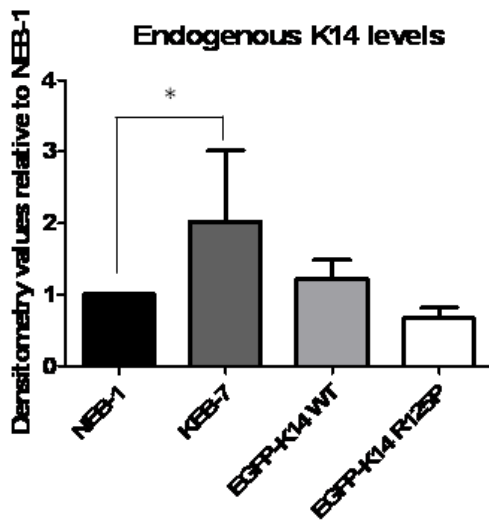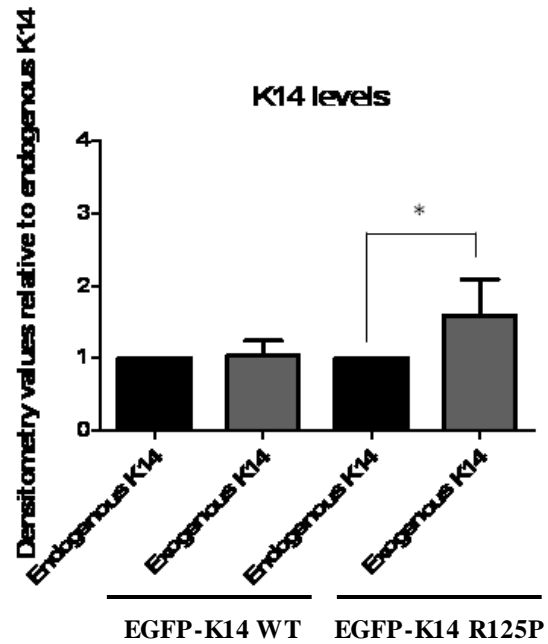
(iii)
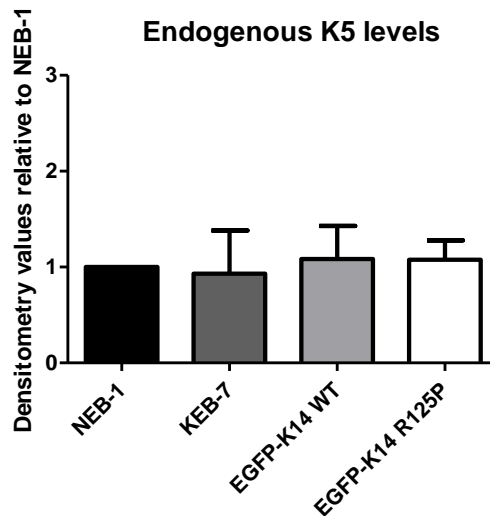
Figure 3.1 Characterization of EBS-DM cell lines. (I) Spontaneous formation of keratin aggregates co-existing with filaments in EBS-DM cells. (i) Immunostaining of (A) NEB-1 and (B) KEB-7 keratinocytes with anti-K14 (LL001). Scale bar, 30 μm. (ii) Stable expression of (A) EGFP-K14 WT and (B) EGFP-K14 R125P in NEB-1 keratinocytes. Scale bar, 30 μm. (II) EBS-DM (KEB-7) cells expressed higher levels of K14 than wild-type (NEB-1) cells. Insoluble fractions of cell extracts were prepared from these cell lines at subconfluence. Immunoblot analysis of these cell lysates shown using antibodies to K14 (LL001) and K5 (XM-26). Actin used as loading control. (III) Densitometry values of (i) endogenous K14 levels, (ii) exogenous K14 relative to endogenous K14 levels and (iii) K5 protein levels of the respective cell lines at subconfluence, normalized to actin loading control and data presented as relative to NEB-1 group or endogenous K14 group and as mean ± S.D for n= 3. Statistical significance was assessed by one-way analysis of variance, followed by Tukey's test, * $p < 0.05$ vs NEB-1 group or endogenous K14 group. 114

3.2.2 Keratin aggregates localized at the leading edge are highly dynamic

To demarcate the region where the keratin aggregates were segregated, mutant keratinocytes expressing EGFP-K14 R125P was immunostained with phalloidin, which could bind F-actin subunits specifically. It was observed that keratin aggregates were organized in a polarized manner [Figure 3.2 (i) (A)], at sites of lamellipodial protrusions where directed cell migration normally occurred [Figure 3.2 (i) (B)]. Time-lapse imaging of EGFP-K14 R125P cell line showed that the small, highly dynamic peripheral keratin aggregates originated from the base of the lamellipodium, coalesced to form larger keratin granules, disassembled and incorporated into the pre-existing keratin network in a retrograde transport fashion [Figure 3.2 (ii)]. This observation was consistent to another study that utilized EYFP-K14 R125C, where the authors demonstrated that the keratin aggregates localized at the periphery were transported in an actin-meditated manner and incorporated into perinuclear keratin filaments (Werner et al., 2004). Hence, these results showed that keratin aggregates at lamellipodial protrusions were highly dynamic. This would allow for the rapid remodelling of both keratin and actin subunits during directed cell migration.

(i)

EGFP-K14   **Actin (Phalloidin)**

(ii)

EGFP-K14 R125P
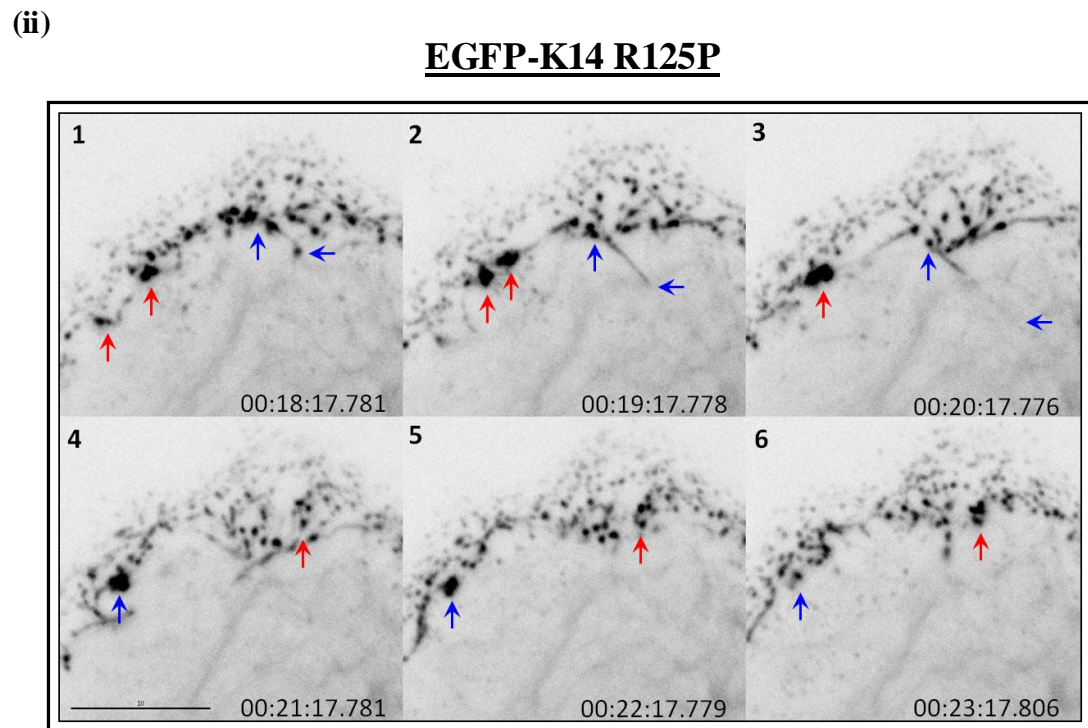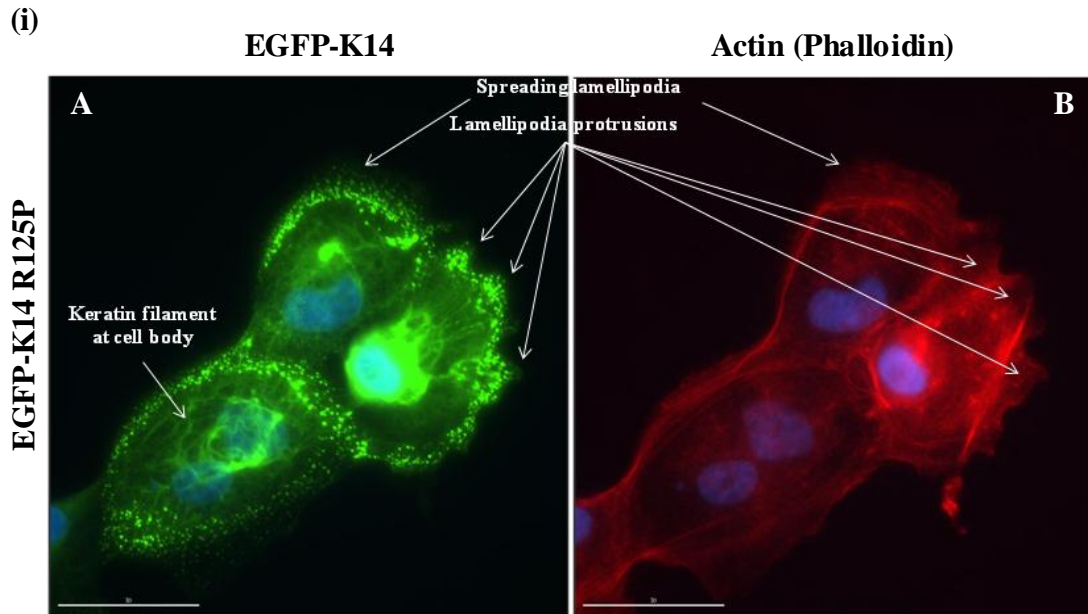
Figure 3.2 Keratin aggregates localized at the leading edge are highly dynamic. Continuous remodelling of keratin aggregates at sites of lamellipodial protrusions. (i) (A) Localization of keratin aggregates at sites of (B) F-actin (phalloidin) formation in EGFP-K14 R125P cells. Scale bar, 30 μm. (ii) Time-lapse imaging of EGFP-K14 R125P cell at intervals of 15 sec for 30 min. The montage showed movements of keratin aggregates at intervals of 1 min during acquisition from 18th to 23th min. Small peripheral keratin aggregates observe to coalesce (red arrows), disassemble and incorporate into the pre-existing keratin network (blue arrows). Scale bar, 10 μm.

3.2.3 Intrinsic and sustained stress activation in isogenic EBS-DM cells during osmotic stress

It was previously shown that EBS-DM (KEB-7) keratinocytes have an intrinsic upregulation of stress activated kinases and they showed sustained stress responses to osmotic stress (D'Alessandro et al., 2002). These results were reproducible when the isogenic pathomimetic cell line (EGFP-K14 R125P) was exposed to the same osmotic stress regime and then examined for stress kinase activation [Figure 3.3 (i)]. It was observed that upon 30-60 min recovery from 5 min of 150 mM urea treatment, phosphorylated K5 was upregulated in both cell lines, suggesting that there was a remodelling of keratin intermediate filaments under stress [Figure 3.3 (i)]. A concomitant increase in both JNK1/2 and p38 phosphorylation [Phospho-JNK (P-JNK1/2) /phospho-p38 (P-p38)] were also observed in this recovery time course, confirming that both JNK1/2 and p38 activation were involved in this stress regime [Figure 3.3 (i)].

One consistent observation was the intrinsic and sustained levels of stress-activated protein kinases (SAPKs: P-p38 and P-JNK1/2) in the mutant cells during the osmotic stress treatment regime as compared to the wild-type cells [Figure 3.3 (ii)]. For instance, the mutant cells have higher basal levels of P-p38 and P-JNK1/2 than wild-type cells, suggesting intrinsic stress activation [Figure 3.3 (ii)]. Moreover, the mutant cells have higher levels of p38 and JNK1/2 activation than wild-type cells throughout the time course after recovery from osmotic stress, indicating sustained stress activation [Figure 3.3 (ii)]. This could be associated with altered filament kinetics of mutant keratin protein leading to a misfolded protein response (Russell et al., 2010). Keratinocytes derived from patients suffering from EBS-localized mutation (mild phenotype with no keratin aggregates) also have an intrinsic activation of SAPKs

(D'Alessandro et al., 2002). This state also leads to mutant keratinocytes downregulating their dual-specificity phosphatases which will further shift the equilibrium of SAPKs being constitutively activated in these cell lines (Liovic et al., 2008).
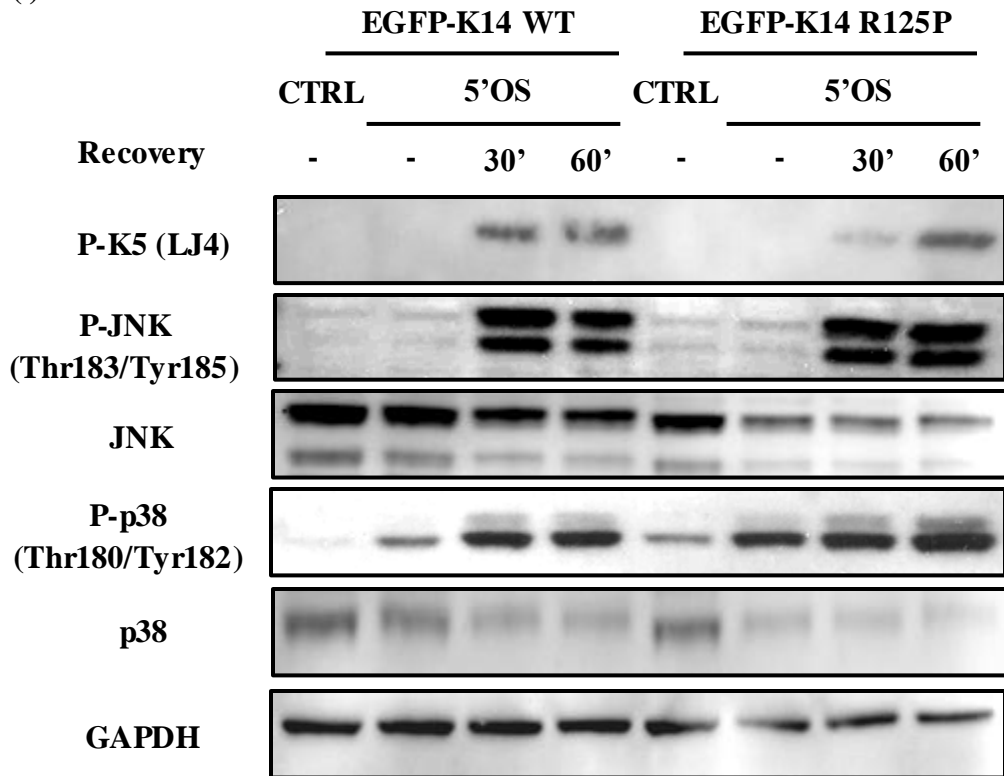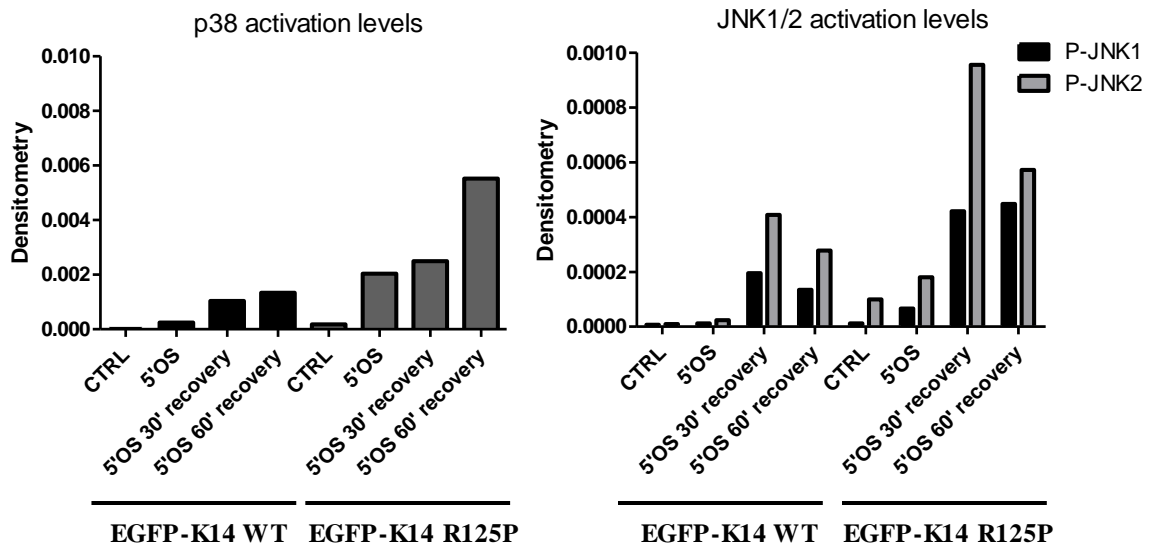
Figure 3.3 Intrinsic and sustained stress activation in isogenic EBS-DM cells during osmotic stress. EBS-DM cells have intrinsic and sustained upregulation of stress-activated protein kinases (P-p38 and P-JNK). (i) EGFP-K14 WT and EGFP-K14 R125P cells were exposed to 5 min of 150 mM urea treatment, and left to recover for 30 min and 1 hr respectively. Soluble fractions of cell extracts were prepared from these cells. Immunoblot analysis of these cell lysates shown using antibodies to P-K5, P-JNK (Thr183/Tyr185), JNK, P-p38 (Thr180/Tyr182) and p38. GAPDH used as loading control. (ii) Densitometry values of P-p38 and P-JNK protein levels for the respective cell lines at different conditions, normalized to total p38 or total JNK and GAPDH loading control.

3.2.4 EBS-DM mutation predisposes keratinocytes to have directional persistence in single cell migration

To determine whether the EBS-DM mutation has any effect on the directional migration of keratinocytes, single cell motility of each cell line was investigated by using live-cell DIC (differential interference contrast) imaging to monitor the random migration of keratinocytes (Sehgal et al., 2006; Hamill et al., 2009). Tracked plots of randomly migrating single cell suggested that the KEB-7 cells show more directional persistence and migrated further away from the central origin [Figure. 3.4 (i) (B)], whereas majority of the NEB-1 cells migrated around the central origin in a non-directional manner [Figure. 3.4 (i) (A)]. The total distances travelled over 5 hrs by each cell from each cell line were represented as a distribution in the form of histograms: NEB-1 (49-638 µm) and KEB-7 (68-996 µm) respectively [Figure 3.4 (ii) (A-B)]. The mean distance travelled by KEB-7 cells (444.0 ± 31.48 µm) was significantly higher (*** $p < 0.001$) than that of NEB-1 cells (276.1 ± 18.05 µm) [Figure 3.4 (iii)], thus demonstrating an intrinsic faster migration rate over a period of 5 hrs.

3.2.5 Keratinocytes harboring EBS-DM mutation close up wounds faster in scratch wound assays

Epidermal keratinocytes do not normally migrate as single cells but as sheets of interconnected cells, so it is possible that the migration response of single cells is exaggerated and/or the stress state is abnormally high. Therefore, *in vitro* scratch wound assays were used to examine the collective migration of keratinocytes, monitored by live-cell phase contrast imaging of the cell monolayer after wounding. It was confirmed that KEB-7 shows faster migration than NEB-1 at 26 hrs post-wounding [Figure 3.5 (i)], and that EGFP-K14 R125P cells close up wound faster than that of EGFP-K14 WT cells at 14 hrs post-wounding [Figure 3.5 (ii)]. These

results were consistent with previous studies (Morley et al., 2003; Liovic et al., 2009) and further demonstrated that the presence of keratin aggregates, which is correlated with intrinsic stress in these EBS-DM keratinocytes, is associated with faster migration in both single and collective cell migration assays.
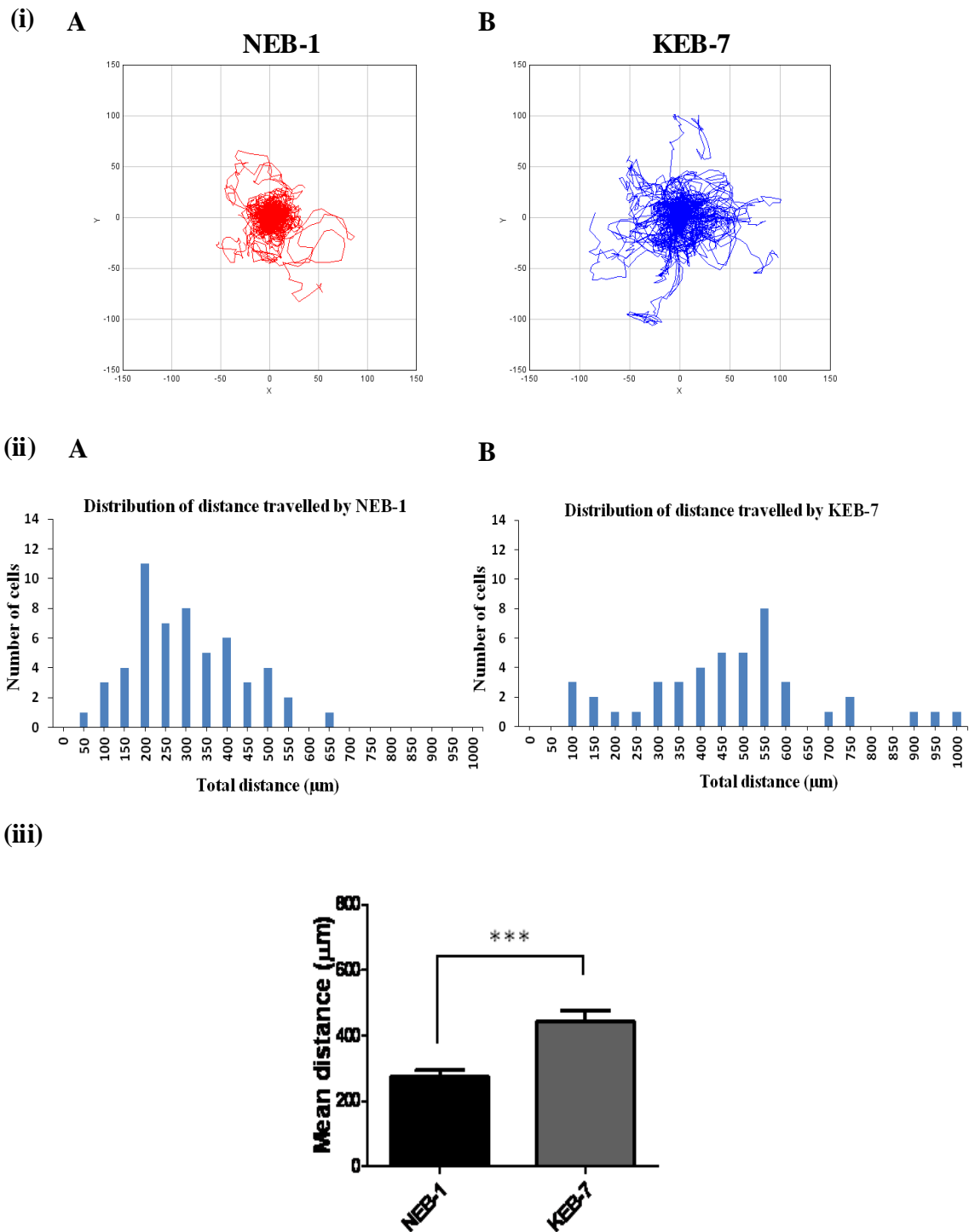
Figure 3.4 EBS-DM mutation predisposes keratinocytes to have directional persistence in single cell migration. EBS-DM cells have higher motility rates in single cell migration. (i) Live-cell DIC images of single cell from each cell line were obtained every 5 min for a total of 5 hours. DIC images of single cell were then filtered, segmented and adjusted to auto-threshold by macros written with ImageJ. Each track represented a cell over a period of 5 hours for n = 55 (NEB-1) and n = 45 (KEB-7). (ii) Total distance travelled by each cell for 5 hrs was extracted and represented in the form of histograms. (iii) Data presented as mean distance travelled and as mean ± S.E.M. Statistical significance was assessed by unpaired t-test, *** $p < 0.001$ vs. NEB-1 group.

122

(i)
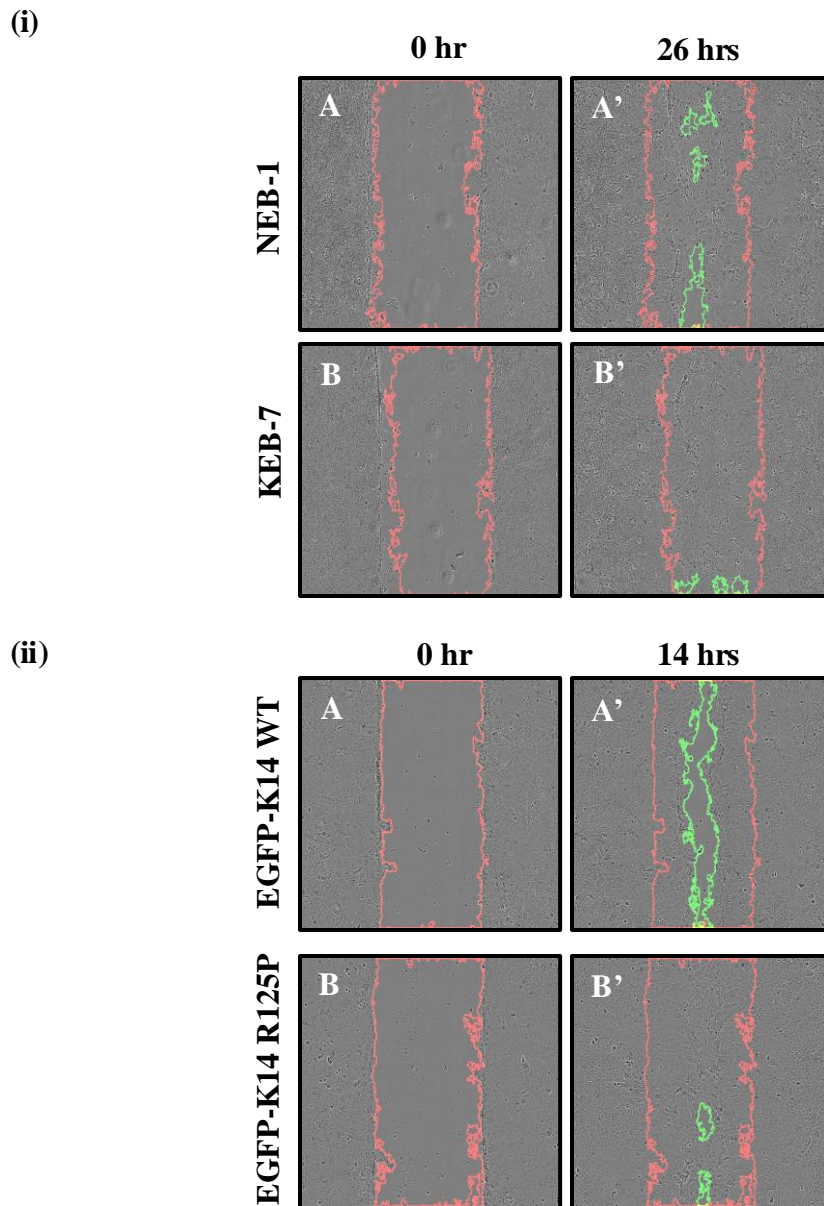
Figure 3.5 Keratinocytes harbouring EBS-DM mutation close up wounds faster in scratch wound assays. EBS-DM cells have faster migration speeds in collective cell migration. (i-ii) Cells grown to confluence in an Essen ImageLock 96-well plate were subjected to wounding with a 96-well WoundMaker Tool. Images acquired immediately and at 1 hr intervals for 14 or 26 hrs using the IncuCyte imaging system. Data were processed by ImageJ software. Red line marks the denuded area from which cells were removed at the start of the wound (0 hr); green line marks the remaining uncovered area after 14 or 26 hrs wound closure time (14 or 26 hrs).

3.2.6 EBS-DM cells express more wound response proteins at both the mRNA transcript and protein levels

The observations that EBS-DM cells have intrinsic stress activation and that they migrated faster than wild-type cells lead to the hypothesis that they are in an "activated" state of the keratinocyte activation cycle. To test this hypothesis, the levels of proteins associated with a wound response (reviewed in Santoro and Gaudino, 2005) were examined in the four cell lines at sub-confluence. An upregulation of K17 (wound-induced keratin) expression was observed in the EBS-DM cells as compared to wild-type cells, at both the mRNA transcript [Figure 3.6 (I) (i)] and protein levels [Figure 3.6 (II) (i)]. Other wound-associated genes observed to be up-regulated in the EBS-DM cells as compared to wild-type cells included the β1 integrin (wound-associated integrin), fibronectin (wound-associated extracellular matrix, ECM protein), and MMP-9 (wound-associated matrix metalloproteinase), a gelatinase induced during wound healing and a marker for migratory phenotype [Figure 3.6 (I) (ii-iv), Figure 3.6 (II) (ii) and (iii)]. These differences in expression levels of wound response proteins between EBS-DM and wild-type cells suggest that EBS-DM cells are more activated than the wild-type cells, and these increased levels of wound response proteins such as β1 integrin and MMP-9 may be the factors predisposing EBS-DM cells to migrate further and faster in cell migration assays.

(I)

(i) <u>**Wound-induced keratin**</u>
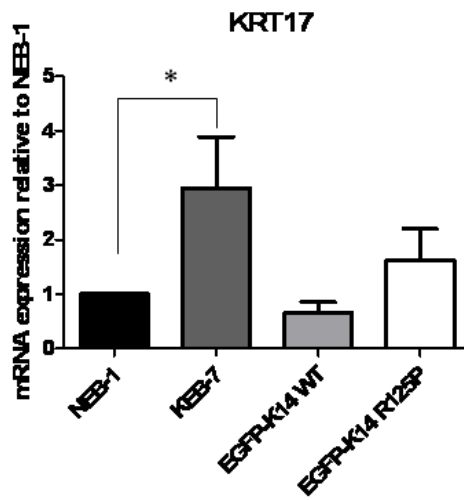
(ii) <u>**Wound-associated integrin**</u>
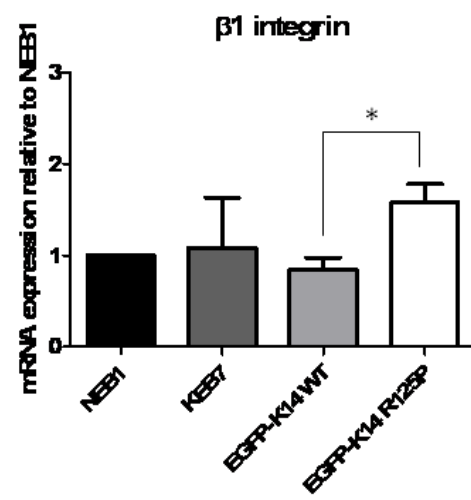
(iii) <u>**Wound-associated ECM protein**</u>
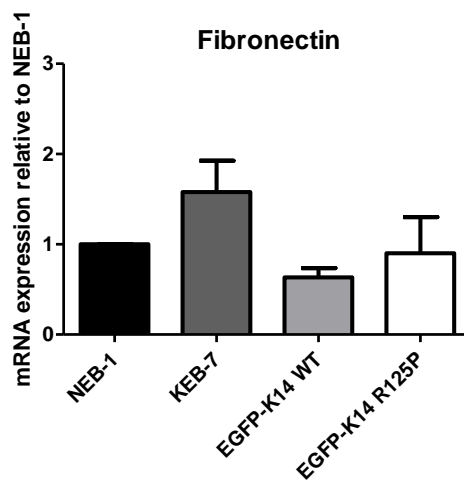
(iv) <u>**Wound-associated MMPs**</u>
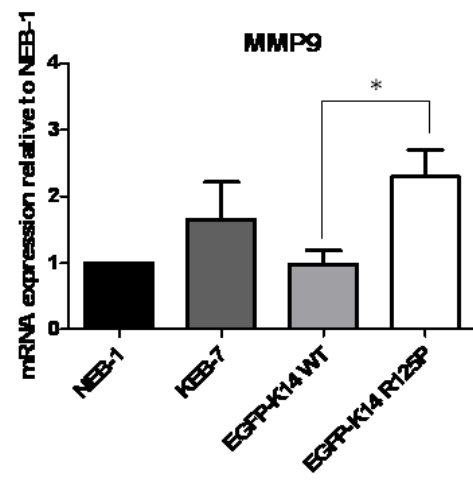
(II)

(i)
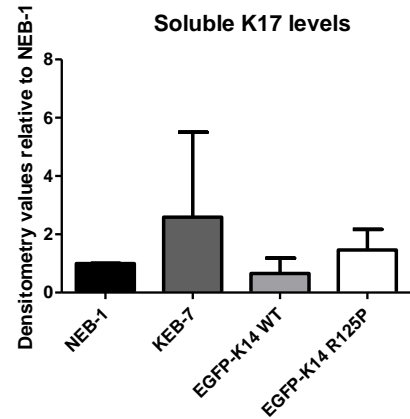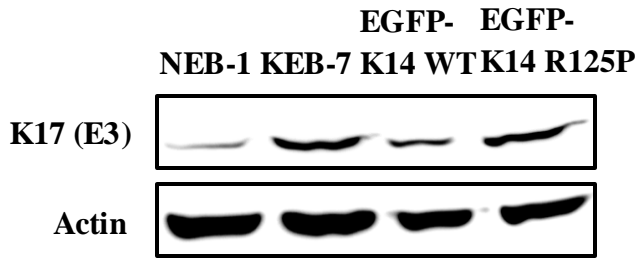
(ii)
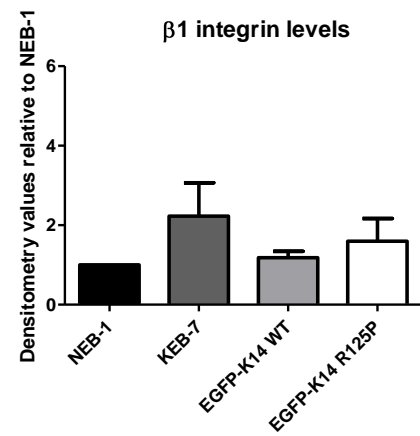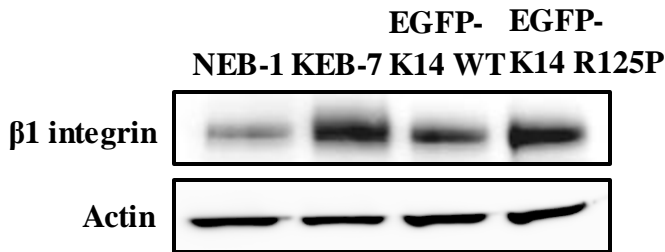
(iii)
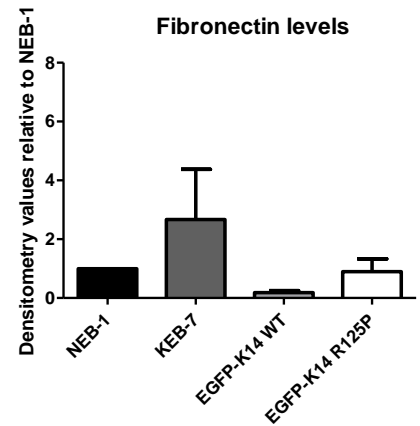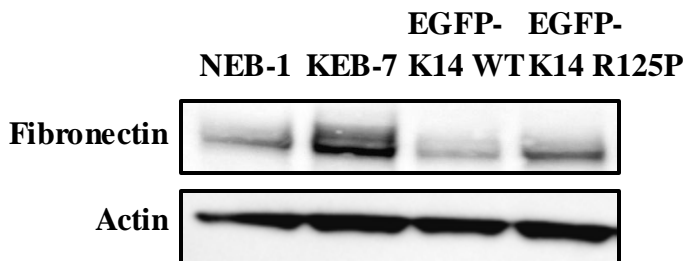
Figure 3.6 EBS-DM cell lines expressed high levels of wound response proteins at both the mRNA transcript and protein levels. EBS-DM cells were more "activated" than wild-type cells. (I) RNA isolated from NEB-1, KEB-7, EGFP-K14 WT and EGFP-K14 R125P cell lines at sub-confluence. cDNAs were prepared and analyzed by real-time PCR for quantification using specific primers to (i) K17, (ii) β1 integrin, (iii) fibronectin, (iv) MMP-9, normalized to RPLP0. Data presented as mRNA expression relative to NEB-1 and as mean ± S.D for n = 3 of each group. Statistical significance was assessed by one-way analysis of variance, followed by Tukey's test, * $p < 0.05$ vs. NEB-1 or EGFP-K14 WT group. (II) Soluble fractions of cell extracts were prepared from each cell line at sub-confluence. Immunoblot analysis of these cell lysates shown using antibodies to (i) K17 (E3), (ii) β1 integrin (CD29) and (iii) fibronectin (clone 10). Actin used as loading control. Densitometry values of (i) soluble K17 levels, (ii) β1 integrin levels and (iii) fibronectin levels of the respective cell lines at subconfluence, normalized to actin loading control. Data presented as relative to NEB-1 group and as mean ± S.D for n= 2 sets of experiments. 126

3.2.7   Loss of keratin aggregates as EBS-DM cells become confluent

Experiments were then undertaken to assess whether driving the mutant cells into confluence would influence the number of keratin aggregates. Subconfluent (80% confluence) keratinocytes were first cultured to 100% confluence (into a monolayer) and further grown to 1 and 2 days post-confluence (i.e. quiescence, or approaching quiescence) before fixing them or harvesting them for immunoblot analysis. It was observed that as these mutant keratinocytes were grown from full confluence to 1 and 2 days post-confluence, EGFP-K14 R125P cells began to lose their peripheral keratin aggregates [Figure 3.7 (i) and (ii)]. These changes in appearance could be due to a change in activation status as they transited from activated to quiescent state.

3.2.8 Loss of keratin aggregates is accompanied by a change in desmoplakin localization

It was observed that mutant keratinocytes grown beyond confluence have a change in desmoplakin localization [Figure 3.8 (A') and (B')], wherein cytoplasmic desmoplakin (seen in subconfluent cells with aggregates) became increasingly localized to cell-cell adhesion sites in the confluent EGFP-K14 R125P cells [Figure 3.8 (A'') and (B''), insert], thus suggesting that the presence of keratin aggregates was influenced by the state of the desmosomal adhesion between adjacent mutant keratinocytes. This inverse correlation between less extensive desmoplakin localization to the desmosomes and the presence of more misfolded keratin aggregates in cells with EBS-DM mutation suggests that desmoplakin may directly affect the stability of mutant K14-containing filaments. If this is so, then reduction of desmosomes may promote a more migratory phenotype and increase keratin aggregate formation, whereas more extensive desmosome assembly could limit cell migration and reduce keratin aggregates.

(i)

EGFP-K14

80%   100%

A   B

EGFP-K14 R125P

C   D

100% + 1 day   100% + 2 days

(ii)

EGFP-K14 R125P

Confluence state

% cells with aggregates relative to 80% confluence
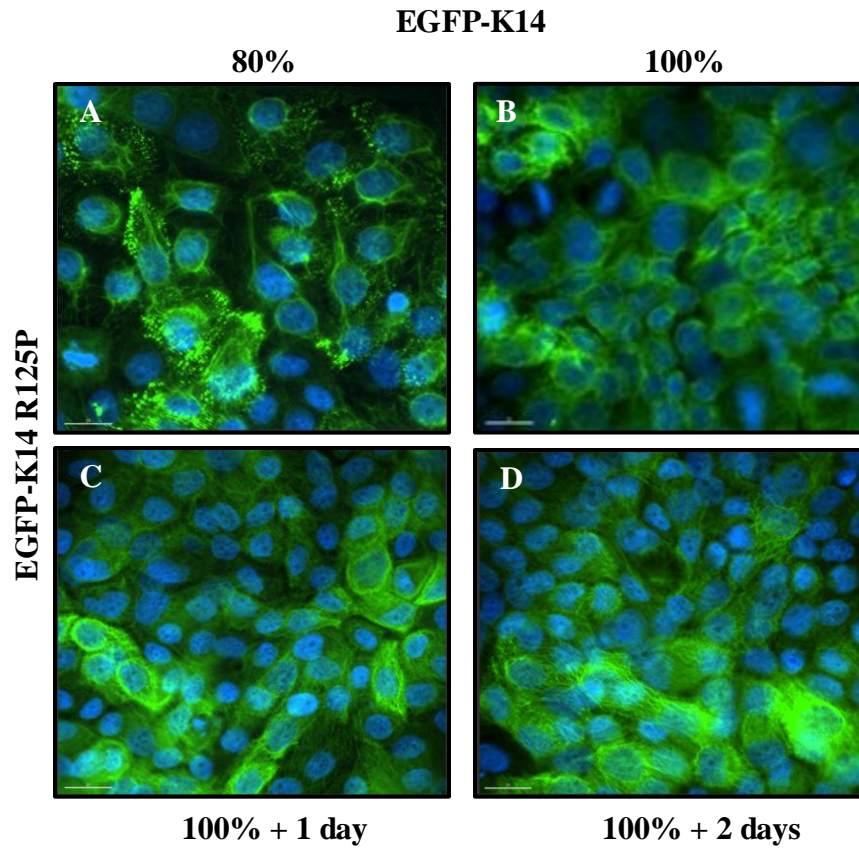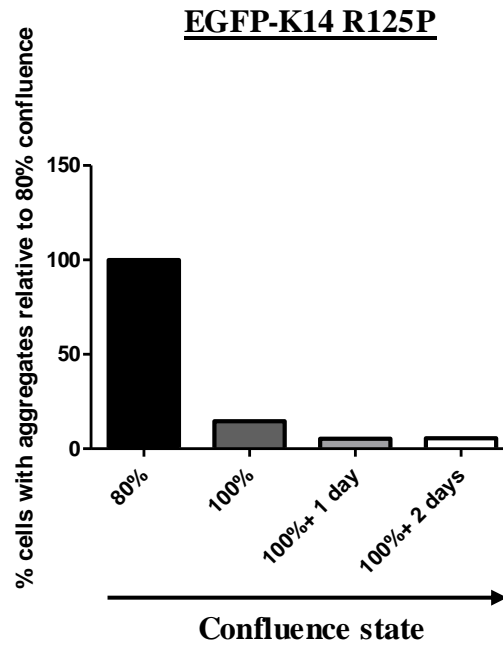
Figure 3.7 Loss of keratin aggregates as EBS-DM cells become confluent. Loss of peripheral aggregates as EBS-DM cells approach the quiescent state. (i) Immunofluorescence images showing EGFP-K14 R125P cells at different confluence states from (A) 80%, (B) 100%, (C) post confluence for 1 day (100% + 1) and (D) 2 days (100% + 2). Scale bar, 20 μm. (ii) Quantification of the number of cells with keratin aggregates at different confluence states using ImageJ. Data presented as % of cells with aggregates relative to 80% confluence group for n = 500-800 cells counted.

EGFP-K14 R125P

EGFP-K14   Desmoplakin (11-5F)
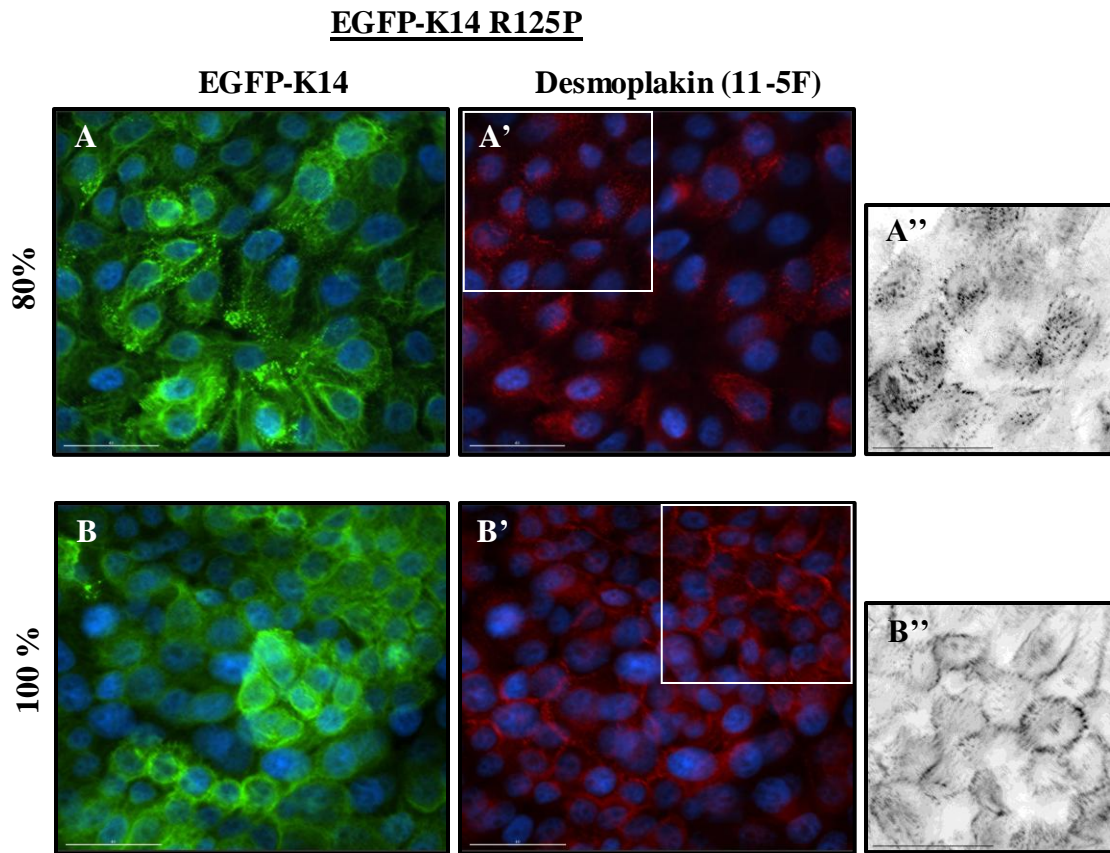
Figure 3.8 Loss of keratin aggregates is accompanied by a change in desmoplakin localization. Desmoplakin localization in EBS-DM cells changed from cytoplasmic to cell-cell adhesion borders as confluence increased. (A-B) Immunofluorescence images showing EGFP-K14 R125P cells at 80% and 100% confluence. (A'-B') Immunostaining of EGFP-K14 R125P cells with anti-desmoplakin I/II (11-5F), and (A''-B'') a 2x magnified image of desmoplakin localization shown in the insert. Scale bar, 40 μm.

3.2.9 Loss of peripheral aggregates is associated with changes in β1 integrin and fibronectin levels

Because a change in appearance (reduction of keratin aggregates) of the mutant keratinocytes was observed by growing them beyond confluence (approaching quiescent state), experiments were conducted by immunoblot analysis to determine whether increasing quiescence could induce a change in their activation state. In all the four cell lines, it was observed that there was a decrease in the levels of wound response proteins such as β1 integrin and fibronectin as confluence increased [Figure 3.9 (i) and (ii)]. Hence, driving the mutant keratinocytes into a quiescent state (increasing confluence) could neutralize their activation status and loss of keratin aggregates could be an indicator of a shift in activation state.

3.2.10 EBS-DM cells induce more soluble K17 proteins upon wounding

For biochemical analysis of the scratch wound-induced activation changes, a multiple scratch protocol was devised [Figure 3.10 (I) (A) and (A')]. Multiple scratch wounds were generated on the confluent monolayer of both EGFP-K14 WT and EGFP-K14 R125P cells to drive the cells into an activated state. The levels of wound response proteins at 18 hrs or 24 hrs post-scratch were then analysed using immunoblot analysis. It was observed that there was an increase in β1 integrin levels in both cell lines upon wounding, supporting the migratory phenotype of keratinocytes during wound closure [Figure 3.10 (II) (i) and (ii)]. It was further demonstrated that EGFP-K14 R125P keratinocytes induced more soluble K17 proteins (0.23 ± 0.19) than wild-type keratinocytes (0.15 ± 0.14) at 18 hrs post-scratch, and that the levels of soluble K17 proteins in the EBS-DM cells were higher than the wild-type cells at all time

points after wounding [Figure 3.10 (II) (i) and (ii)]. Hence, these results confirmed that EBS-DM cells are more activated than wild-type cells.

In summary, the findings in this chapter demonstrate that EBS-DM keratinocytes are more activated than wild-type keratinocytes in terms of its constitutive activated SAPK activation, up-regulation of wound-associated proteins such as K17 and β1 integrin and faster migration. Confluence leads to a reduction of keratin aggregates in EBS-DM keratinocytes, accompanied by a decrease in activation state and wounding results in a faster reactivation of wound response as compared to controls.

(i)
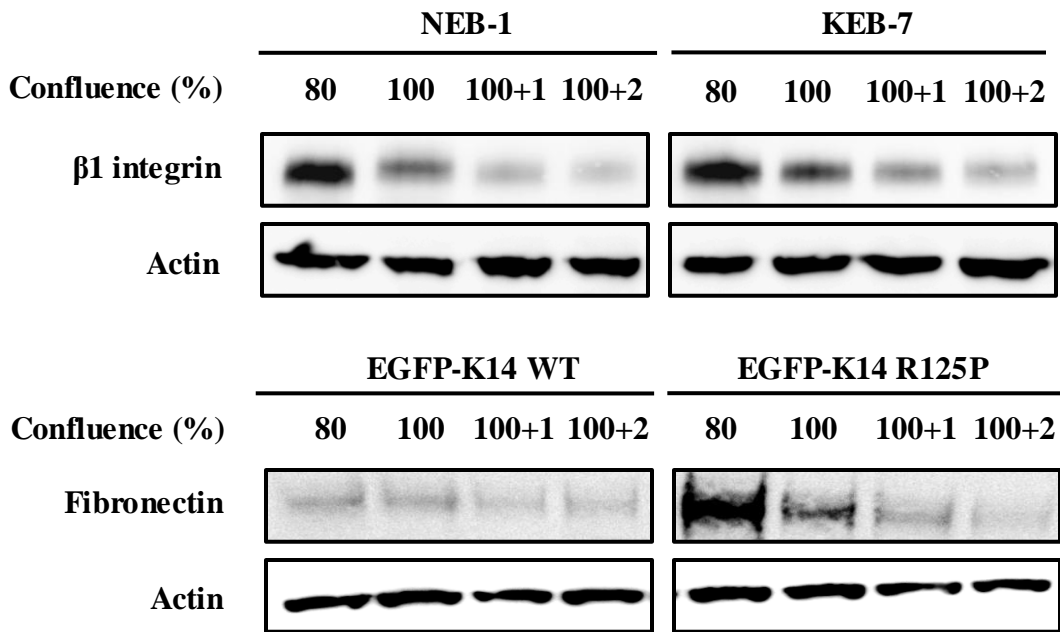
(ii)
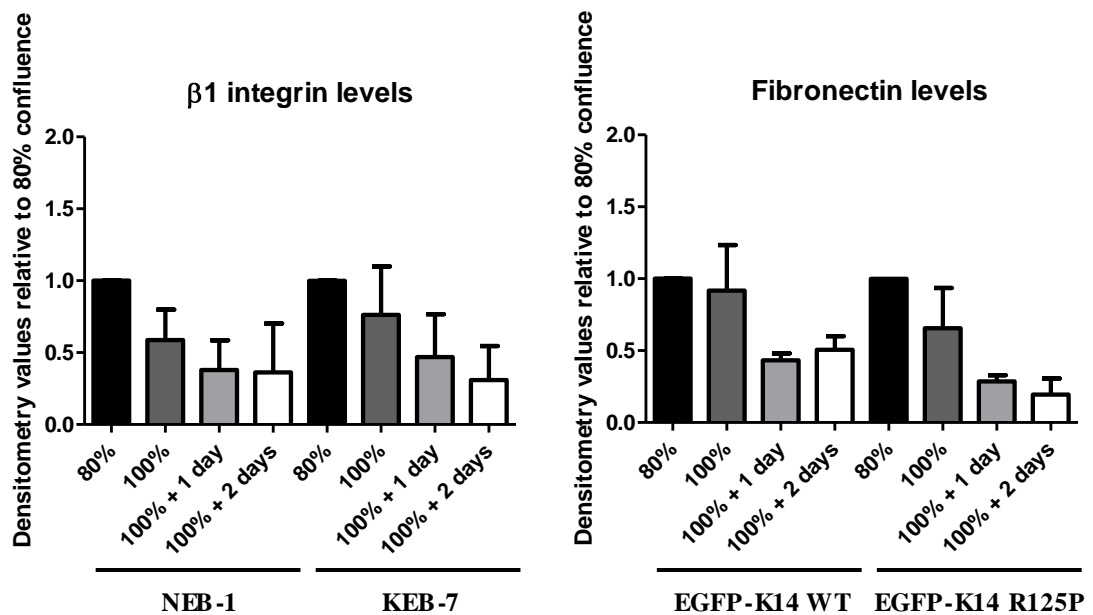
Figure 3.9 Loss of peripheral aggregates is associated with changes in β1 integrin and fibronectin levels. Loss of keratin aggregates is associated with a decrease in activation state. (i) Soluble fractions of cell extracts were prepared from each cell line at different confluence states from 80%, 100%, post-confluence for 1 day (100% + 1) and 2 days (100% + 2). Immunoblot analysis of these cell lysates shown using antibodies to β1 integrin (CD29) and fibronectin (clone 10). Actin used as loading control. (ii) Densitometry values of β1 integrin and fibronectin protein levels of the respective cell lines in different confluence states, normalized to actin loading control. Data presented as relative to 80% confluence group and as mean ± S.D for n= 2 sets of experiments.

(I)

Confluent monolayer

Multiple scratch wound

(II)

(i)

Post-Scratch (hrs)	EGFP-K14 WT			EGFP-K14 R125P			
	-	18	24	-	18	24	
β1 integrin							Soluble fractions
Actin							
K17 (E3)							
Actin							
K5 (XM-26)							
Actin							
K17 (E3)							Insoluble fractions
Actin							
K5 (XM-26)							
Actin							

133
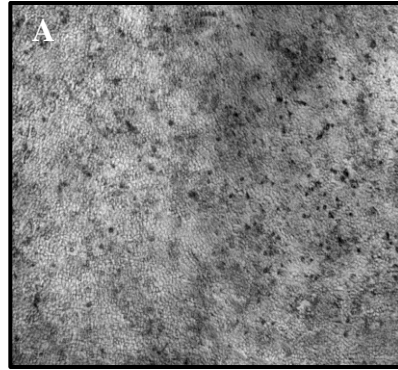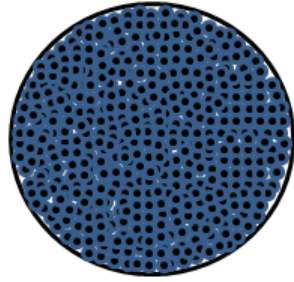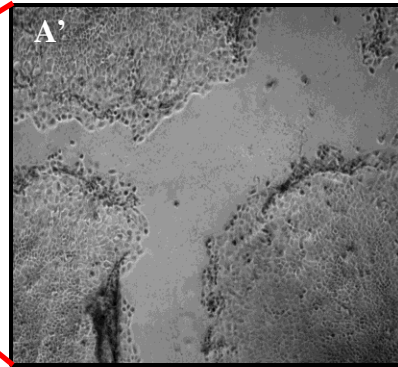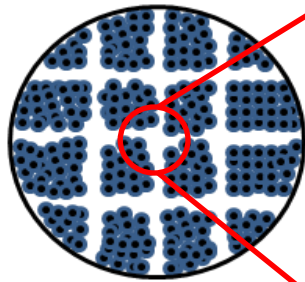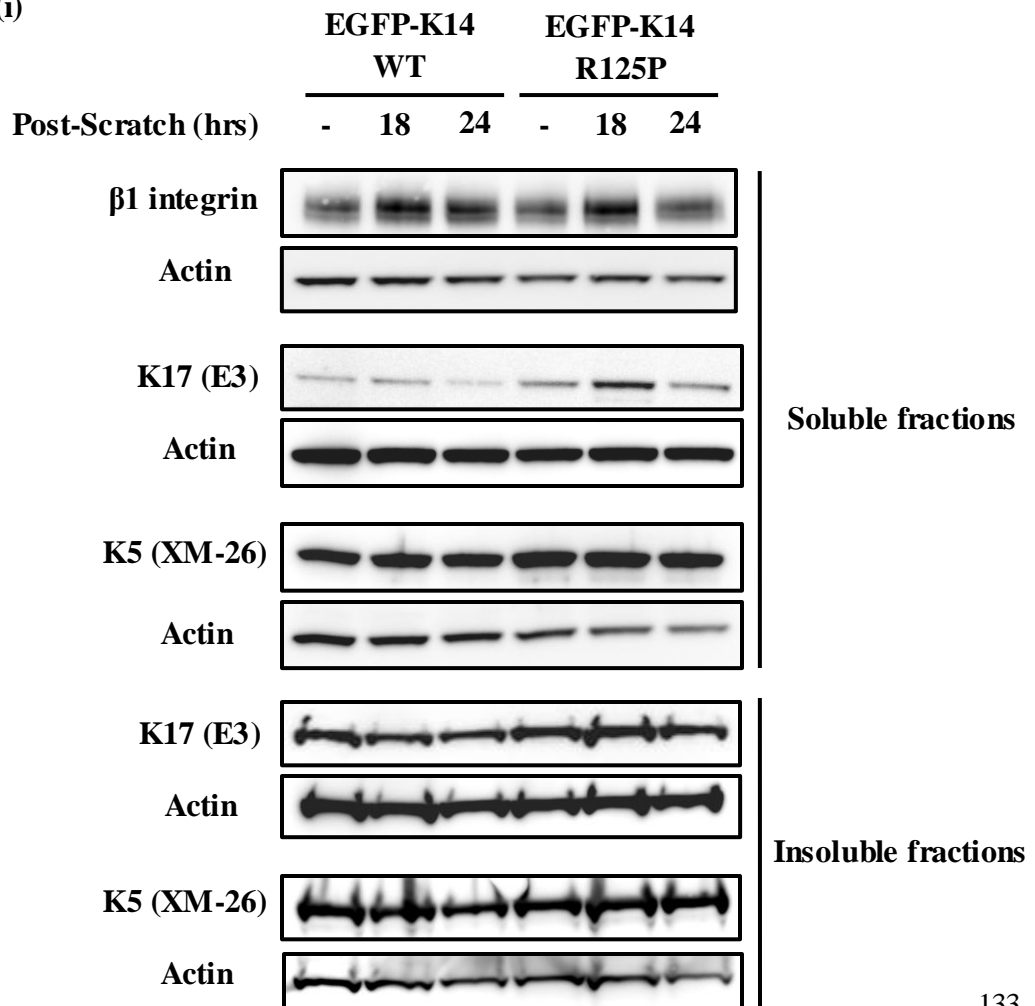
(ii)
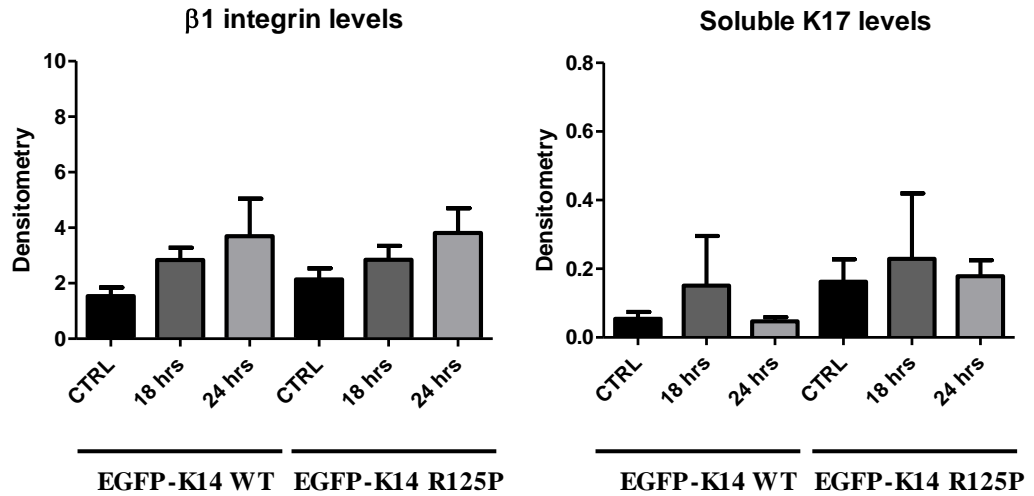
Figure 3.10 EBS-DM cells induce more soluble K17 proteins upon wounding.
EBS-DM cells have a greater wound response than wild-type cells. (I) Formation of multiple scratch wounds (A') from a monolayer of cells (A). (II) (i) Soluble and insoluble fractions of cell extracts were prepared from each cell line that were unscratched, post-scratched for 18 hrs and 24 hrs respectively. Immunoblot analysis of these cell lysates shown using antibodies to β1 integrin (CD29), K17 (E3) and K5 (XM-26). Actin used as loading control. (ii) Densitometry values of β1 integrin and soluble K17 protein levels of the respective cell lines in different conditions, normalized to actin loading control and presented as mean ± S.D for n= 2 sets of experiments.

3.3   Discussion

The work described in this chapter is based on the use of an *in vitro* model of the epithelial wound response. (1) An experimental keratinocyte activation cycle was established in an *in vitro* assay system, by growing cells to confluence and then scratch wounding them. The transition of the cultured keratinocytes could then be studied from subconfluent (activated) to confluence (quiescent) and then re-activating the cells by scratch wounding to stimulate the wound response processes. (2) The transition from normal state (wild-type cells) to activated state (EBS-DM cells) is associated with up-regulation of wound response proteins such as K17, MMP-9, β1 integrin and fibronectin, as has been described for wounds *in vivo*, validating this model. (3) EBS-DM cells were confirmed to be in a more activated state than wild-type cells, even without the application of additional stress, as indicated by their higher levels of several stress-associated proteins. (4) The tight correlation between the appearance of keratin aggregates (rapid remodelling of keratin precursors at the leading edge) and the activation state of the keratinocytes suggests that the presence of aggregates could be an indicator of activation state.

The observations of peripheral keratin aggregates in the mutant keratinocytes (KEB-7 and EGFP-K14 R125P), but not in the wild-type keratinocytes (NEB-1 and EGFP-K14 WT), were consistent with previous studies in either EBS-DM patient-derived keratinocytes or over-expression of mutant constructs in cell culture system (Letai et al., 1993; Werner et al., 2004). An abnormal K14 expression profile was observed in EBS-DM cells as compared to wild-type cells, although it is not known whether this imbalance of keratin levels is a general feature of keratin mutation. Time-lapse imaging showed that the peripheral keratin aggregates were highly dynamic, undergoing rapid remodelling at sites of lamellipodial protrusions. The present data

also showed the inherent stress activation in EGFP-K14 R125P cells, as seen by constitutive upregulation of activated stress kinases (P-JNK and P-p38), in agreement with earlier work (D'Alessandro et al., 2002). It was reported that during wound healing, p38 activation was observed in the leading keratinocytes (Harper et al., 2005). Since EBS-DM cells show constitutive stress activation, their responses in single and collective cell migration assays were further examined. It was demonstrated that the EBS-DM mutation pre-disposed the cells to migrate further and faster in single and collective cell migration respectively, suggesting that the inherent stress is connected to the increased motility of these mutant keratinocytes.

Keratinocytes that are "activated", or in a wound-healing state, expressed several wound response markers. For instance, K6, K16 and K17 are important wound-induced keratins that when ablated, resulted in compromised wound healing (Mazzalupo et al., 2003) and delayed re-epithelialization (Wojcik et al., 2000). Migrating keratinocytes also undergo a switch in integrins (β4 to β1) at wound sites (reviewed in Santoro and Gaudino, 2005), which facilitates migration over the fibrin-fibronectin rich provisional wound matrix (O'Keefe et al., 1985; Nickoloff et al., 1988). Other keratinocyte-upregulated components such as MMP-2 and MMP-9 are also known to facilitate wound healing (Salo et al., 1994).

To determine whether these EBS-DM mutant keratinocytes were in an "activated" state equating to wound healing, levels of these wound-induced proteins were examined in both the wild-type and EBS-DM cell lines. It was found that wound-induced proteins such as K17, MMP-9, β1 integrin and fibronectin were intrinsically upregulated in EBS-DM cells as compared to wild-type cells, supporting the proposition that EBS-DM cells are in a constitutively activated state, effectively "primed" for wound healing.

Cells grown to confluence in culture (epithelial cell monolayer) are known to mimic a quiescent state of the keratinocyte activation cycle (reviewed in Santoro and Gaudino, 2005). In the present study, EBS-DM cells were grown to high confluence in culture to bring them out of their activation state. It was observed that as confluence increased, there was a reduction of peripheral keratin aggregates seen in the mutant cells, accompanied by a change in desmoplakin localization from a cytoplasmic distribution of desmoplakin to its localization at cell-cell borders.

Desmoplakin is known to interact directly with keratin intermediate filaments through part of its C-terminal domain (Kouklis et al., 1994). Previous studies have shown that desmosomes are able to adopt two alternative adhesive states, one calcium-dependent (weakly adhesive) and the other calcium-independent (hyper-adhesive) (Kimura et al., 2007), which could be modulated by PKC (Wallis et al., 2000). The calcium independent state was distinguished by strong desmoplakin staining at cell-cell borders in confluent cultures, to which its hyper-adhesiveness was attributed (Kimura et al., 2007), whereas desmosomes at the wound edge were characterized by a calcium-dependent state, with weak desmoplakin staining at cell-cell borders, possibly due to internalisation of desmosomes (Garrod et al., 2005).

The importance of desmoplakin in tethering keratin intermediate filaments to cell-cell junctions was revealed by the phenotype of desmoplakin conditional knockout mice, which exhibited peeling skin and desmosomes that lacked inner plaques and were devoid of keratin attachment (Vasioukhin et al., 2001). In the present study, the reduction of keratin aggregates upon increasing confluence could be explained by a cessation of keratin remodelling at the leading edge, as cells no longer need to migrate and keratin filaments become attached to stabilized desmosomes at cell-cell borders. Members of our group have observed a connection between desmosomal adhesive

state and keratin aggregate formation (unpublished data) and the work presented here also suggests that restoring desmoplakin localization might be crucial in attenuating the activation status of EBS-DM cells.

Next, it was established that the activation states of EBS-DM cells decreased upon increasing confluence, as seen by a decline in β1 integrin and fibronectin protein levels. Finally, the activated state of these confluent keratinocytes could be restored by scratch wounding, where a higher induction of soluble K17 in EBS-DM cells at 18 hrs post-wounding was observed as compared to wild-type cells, thus confirming the constitutive stress activation of EBS-DM cells.

Recent findings have shown that ERK1/2 activation in EBS-DM keratinocytes could protect these mutant cells against apoptosis during mechanical stress (Russell et al., 2010). This suggests that cells effectively "primed" for wound healing are more able to adapt to stress, and that altered filament kinetics may play a role in this. Identification of the mechanisms underlying the regulation of keratin filament kinetics could give us some insights to the pathogenesis of skin fragilty disorder or even aggresome formation (Mallory body) in cholestatic liver diseases (Fickert et al., 2003).

In conclusion, the results in this chapter demonstrated that EBS-DM cells are constitutively activated, and the presence of keratin aggregates (rapid remodelling of keratin precursors at the leading edge) could be an indicator for the activation state. A schematic diagram summarising the results of Chapter 3 is depicted in Figure 3.11.
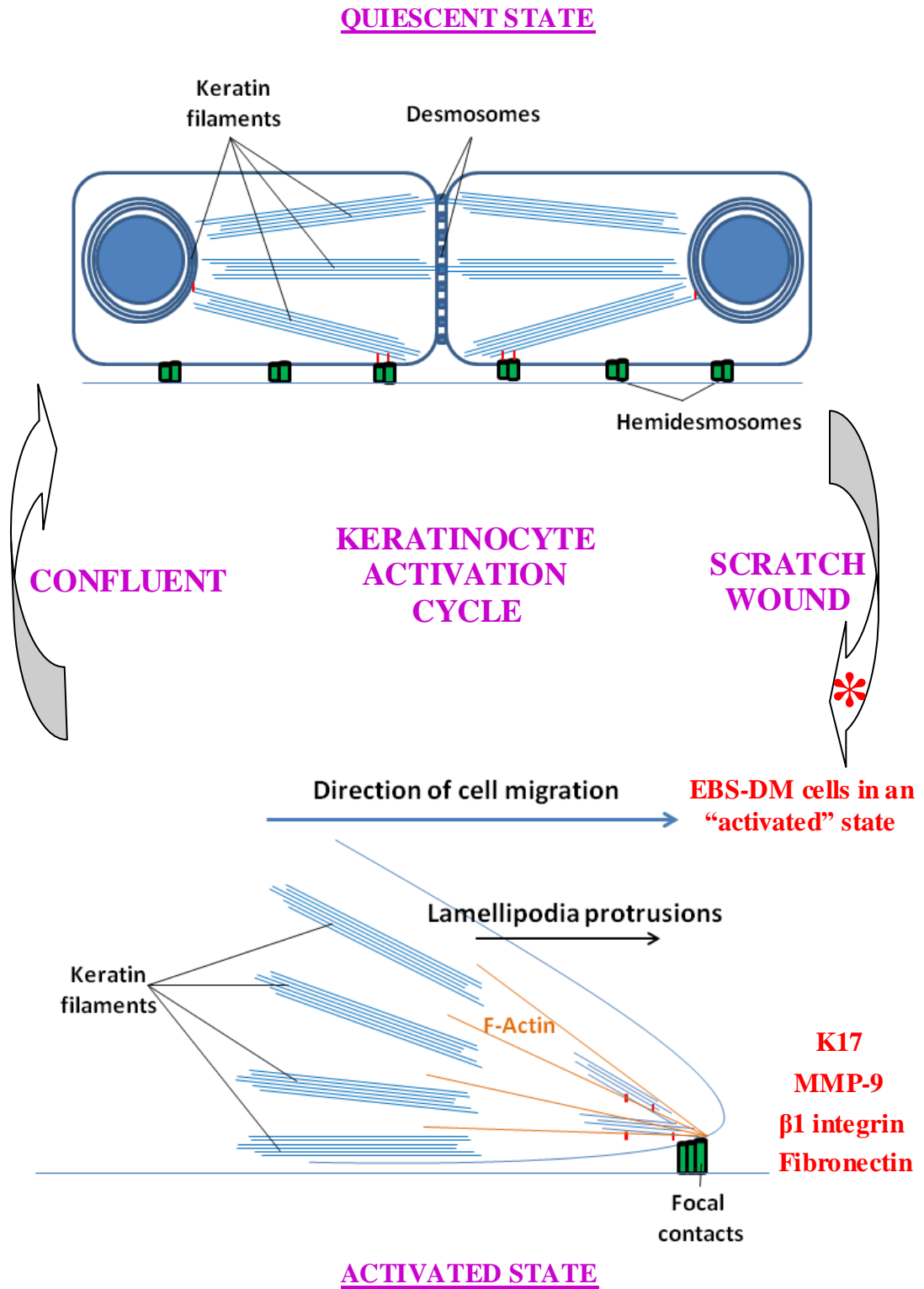
Figure 3.11 Schematic diagram summarising the results of Chapter 3.

CHAPTER 4

EGF INVOLVEMENT IN REGULATING

KERATIN EXPRESSION AND DYNAMICS

4.1 Introduction

The keratinocyte activation cycle is regulated by extracellular signal cues such as the tumor necrosis factor α (TNF-α), epidermal growth factor (EGF), transforming growth factor α and β (TGF-α and TGF-β) and interferon γ (IFN-γ) (Freedberg et al., 2001). EGF and TGF-α, members of the EGF family and ligands for EGF receptor (EGFR), are considered the key mitogens and chemotactic factors that drive wound closure (reviewed in Kirfel and Herzog, 2004). It has been shown that both EGF and TGF-α can play an important role in colony expansion through the induction of epithelial cell migration (Barrandon and Green, 1987). This induction of cell migration is attributed to the rapid formation of lamellipodia and filopodia (Chinkers et al., 1979), mediated by the activation of small guanosine triphosphatase (GTPase) Rac by EGF (Nobes and Hall, 1995).

During re-epithelialization of wounds, epidermal keratinocytes revert to a migratory phenotype and move over a fibronectin-rich provisional wound matrix (Midwood et al., 2004). Forward locomotion is mediated by the formation of lamellipodia that extend into the wound (reviewed in Lauffenburger and Horwitz, 1996; Welch et al., 1997), and this may involve a coordination between the three interconnected filament systems, namely intermediate filaments, actin microfilaments and microtubules (reviewed in Mikhailov and Gundersen, 1998; Waterman-Storer and Salmon, 1999; Chang and Goldman, 2004). In addition, intermediate filament-associated proteins such as BPAG-1 and plectin from the plakin family (Leung et al., 2002) also have a role to play in cell migration during wound healing. It was shown that BPAG-1 knockout mice have defects in wound healing (Guo et al., 1995) while plectin^{-/-} fibroblasts have difficulty in reorganizing their actin cytoskeleton, resulting in reduced cell migration (Andra et al., 1998). Together, these studies show that there is

an interplay between filaments and filament-associated proteins contributing to cell migration.

Keratin intermediate filaments play a major role in the structural stability of epithelial tissues by forming a cytoskeletal scaffold and providing mechanical resistance to stress (reviewed in Owens and Lane, 2003). Keratin intermediate filaments typically connect to both desmosomes and hemidesmosomes and thereby not only contribute to stability between epithelial cells but also to the stability of the epithelial attachment to the basement membrane (reviewed in Kowalczyk et al., 1999; Nievers et al., 1999). Besides its structural role, accumulating experimental evidence has shown that the keratin cytoskeletal network is highly dynamic, with constant turnover in cells (Windoffer and Leube, 1999; Yoon et al., 2001; Windoffer et al., 2004). Time-lapse imaging of cultured cells expressing fluorescent-tagged keratins revealed the dynamics of keratin particles being transported along microtubules (Yoon et al., 2001; Liovic et al., 2003) or actin stress fibers (Woll et al., 2005; Kolsch et al., 2009). A recent model to account for the assembly and disassembly of keratins, independent of biosynthesis, has been proposed by Leube and colleagues and is suggested to explain how the rigid keratin cytoskeletal network can be remodelled rapidly without network disruption (reviewed in Windoffer et al., 2011). For instance, during cell migration, keratin precursors were observed to nucleate at the lamellipodial regions, possibly associated with focal adhesions (Windoffer et al., 2006), and then to elongate and move towards the cell interior in an actin-mediated retrograde manner, before becoming incorporated into the peripheral keratin network (Woll et al., 2005). Although much of this work was done by imaging live cells and measuring morphological changes in keratin structures, the molecular mechanism regulating

keratin remodelling in wound-induced stress response is not well understood, and Leube's model remains hypothetical to date (reviewed in Windoffer et al., 2011).

Keratin aggregates in EBS-DM cells form in lamellipodia [Figure 3.2] and lamellipodia are produced in response to EGF-induced Rac activation (Nobes and Hall, 1995) during cell migration. In this chapter, it is hypothesized that EGF influences keratin remodelling to affect cell migration during wound response. Experiments are carried out using the EBS-DM (EGFP-K14 R125P) cells (previously established in Chapter 3 to be in a constitutively activated state) as a model to dissect the signalling pathways involved. The results obtained show that EGF can affect keratin synthesis and solubility by increasing soluble K14 levels and also regulate keratinocyte migration in scratch wound assays. It is demonstrated that when EGFP-K14 R125P cells are cultured in media without EGF, a reduction of keratin aggregates is observed, which can be restored upon re-stimulation with EGF. This EGF-mediated effect appears to be associated with the cytoskeletal linker protein, plectin. Inactivation of ERK1/2 kinase downstream of EGF signalling results in fewer mutant keratinocytes with peripheral aggregates, accompanied by a decrease in plectin levels. In the mutant keratinocytes, ERK1/2 knockdown with siRNA also results in a decrease of both peripheral aggregates and plectin levels. Fluorescence live-cell imaging is used to confirm the relationship between ERK1/2 activation, keratin aggregate status and cell migration in mutant keratinocytes. Conversely, plectin knockdown could reduce the number of mutant keratinocytes with peripheral aggregates and slow down mutant cell migration in scratch wound assays. In summary, these results suggest that EGF signalling plays a role in regulating keratin remodelling in wound-induced stress activated cells during migration, through modulating plectin levels.

4.2   Results

4.2.1   EBS-DM cells have more soluble K5 and K14 proteins than wild-type cells

It has been shown that remodelling of the keratin intermediate filament network is mediated by post-translational modifications such as keratin phosphorylation, which might favour the unpolymerised state of keratins by increasing their solubility (Toivola et al., 2002; Omary et al., 2006).

In Chapter 3, it was observed that there was an abnormal K14 expression profile in KEB-7 (EBS-DM) cells when compared to NEB-1 (wild-type) cells. Experiments were therefore carried out to determine whether the abnormal K14 expression profile was consistently observed when compared to another wild-type cell line (N/TERT-1 cells) and whether there is any difference in keratin solubility. Soluble/supernatant and insoluble/pellet fractions were prepared from N/TERT-1 (wild-type) cells and KEB-7 (EBS-DM) cells at subconfluence. Immunoblot analysis of cell lysate fractions showed that at the basal level, KEB-7 (EBS-DM) cells expressed more K14 (2.98 ± 0.79 folds) ($* p < 0.05$) and K5 (2.61 ± 0.47 folds) ($** p < 0.01$) proteins than N/TERT-1 (wild-type) cells (1.00 ± 0.00) in the soluble fraction (non-filamentous, disassembled) but not in the insoluble fraction (pelletable, filamentous) [Figure 4.1 (i-ii)]. These results confirmed the abnormal K14 expression profile in EBS-DM cells. It is possible that the presence of severe keratin mutation results in increased synthesis or it could be that the location of the R125P mutation alters K14 phosphorylation (a hypothesis tested in Chapter 5), hence attributing to its increased solubility.

(i)

	N/TERT-1 KEB-7	N/TERT-1 KEB-7
K14 (LL001)		
Actin		
K5 (XM-26)		
Actin		
	Soluble fraction	**Insoluble fraction**
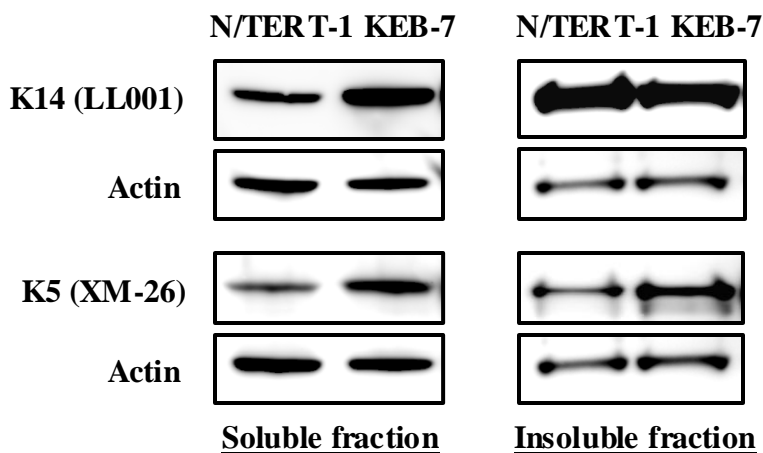
(ii)
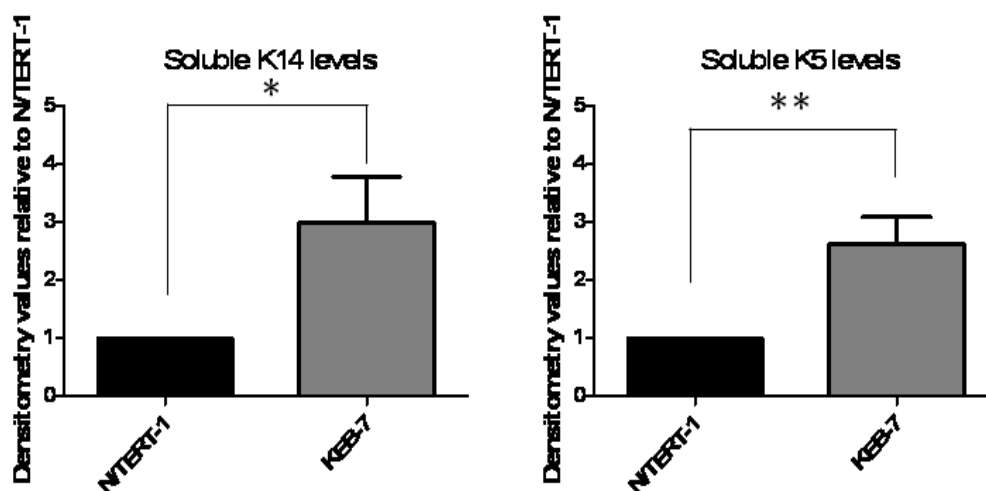
Figure 4.1 EBS-DM cells have more soluble K5 and K14 proteins than wild-type cells. (i) Soluble and insoluble fractions of cell extracts were prepared from these cell lines at subconfluence. Immunoblot analysis of these cell lysates shown using antibodies to K14 (LL001) and K5 (XM-26). Actin used as loading control. (ii) Densitometry results showing the intensity of soluble K14 or K5 levels for each cell line, normalized to its actin loading control and data presented as relative to N/TERT-1 group and as mean ± S.D for n = 3 of each treatment. Statistical significance was assessed by unpaired t-test, * $p < 0.05$, ** $p < 0.01$ vs. N/TERT-1 group.

4.2.2 EGF treatment increases K14 synthesis and solubility in wild-type but not EBS-DM cells

EGF is known to be an essential mitogenic and chemotactic factor for keratinocytes during wound healing (reviewed in Kirfel and Herzog, 2004), and to induce keratinocyte migration (Barrandon and Green, 1987). EGF is also known to induce keratin gene expression (Jiang et al., 1993; Tomic-Canic et al., 1998) which is mediated by downstream signalling pathways involving transcription factors such as c-Fos and c-Jun components of AP-1 that activate keratin promoter (Ma et al., 1997; Sinha et al., 2000). In an effort to understand the mechanisms regulating keratin remodelling in response to stress, the EGF signalling pathway was therefore explored to assess its effects on the keratin cytoskeleton.

To address whether EGF could regulate keratin remodelling, the effects of EGF on keratin synthesis and solubility were examined in both cell lines. N/TERT-1 cells cultured in serum-free media without EGF for 48 hrs were subjected to EGF (10 ng/ml, 100 ng/ml) treatments for 48 hrs. It was found that there was a significant increase (* $p < 0.05$) in K14 mRNA transcript in N/TERT-1 cells upon treatment with EGF (10 ng/ml) (1.36 ± 0.22 folds) and EGF (100 ng/ml) (1.44 ± 0.20 folds) as compared to untreated control (1.00 ± 0.00), whereas there was no significant change in K5 mRNA transcript in N/TERT-1 cells upon treatment with EGF (100 ng/ml) (0.99 ± 0.16 folds) as compared to untreated control (1.00 ± 0.00) [Figure 4.2 (I) (i) (A-C)], indicating increased K14 synthesis in response to EGF.

To determine the changes in keratin protein solubility upon EGF treatment, soluble/supernatant and insoluble/pellet fractions were prepared from N/TERT-1 cells. It was found that the soluble fraction of K14 (non-filamentous, disassembled) in

N/TERT-1 cells increased significantly (* $p < 0.05$) upon treatment with EGF (100 ng/ml) (2.36 ± 0.63 folds), as compared to untreated control (1.00 ± 0.00), whereas there was no significant change in the insoluble fraction of K14 (pelletable, filamentous), indicating increased solubility of K14 in response to EGF [Figure 4.2 (I) (ii) and (iii)]. There was also no significant change in the soluble K5 expression of N/TERT-1 cells upon EGF (100 ng/ml) treatment (1.23 ± 0.88 folds) as compared to untreated control (1.00 ± 0.00) [Figure 4.2 (I) (ii) and (iii)].

EBS-DM cells (KEB-7) were cultured without EGF for 48 hrs prior to the same EGF treatment regimes. It was found that there was no significant change in K14 mRNA transcript in KEB-7 cells upon treatment with EGF (100 ng/ml) (1.14 ± 0.18 folds) as compared to untreated control (1.00 ± 0.00), as well as no significant change in K5 mRNA transcript in KEB-7 cells upon treatment with EGF (100 ng/ml) (1.12 ± 0.28 folds) as compared to untreated control (1.00 ± 0.00) [Figure 4.2 (II) (i) (A-C)].

To determine the changes in keratin protein solubility upon EGF treatment, soluble/supernatant and insoluble/pellet fractions were prepared from KEB-7 cells. It was found that there was a slight increase in the soluble K14 expression (non-filamentous, disassembled) upon EGF (100 ng/ml) treatment (1.42 ± 0.30 folds), though it was not significant as compared to untreated control (1.00 ± 0.00) [Figure 4.2 (II) (ii) and (iii)]. Similarly, there was also a slight increase in the soluble K5 expression upon EGF (100 ng/ml) treatment (1.33 ± 0.36 folds), but it was also not significant as compared to untreated control (1.00 ± 0.00) [Figure 4.2 (II) (ii) and (iii)]. These results suggest that changes in keratin expression in EBS-DM cells are relatively subtle to EGF treatment, possibly because of a constitutively activated EGF signalling in these mutant cells, a hypothesis that is tested below [see 4.2.6].

(I)

(i) (A)

N/TERT-1 KRT14 expression

(B)

N/TERT-1 KRT5 expression
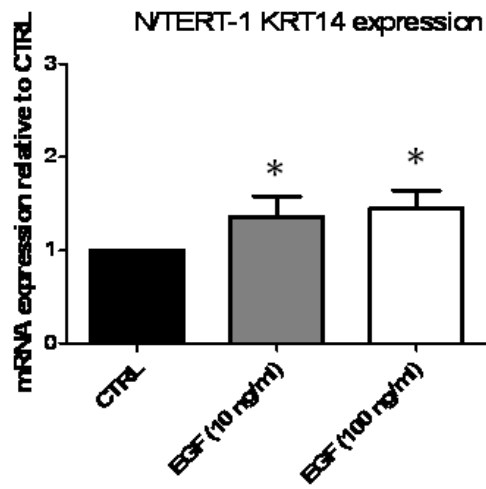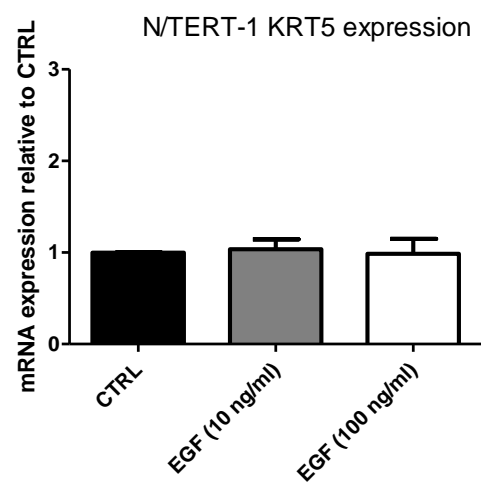
(C)
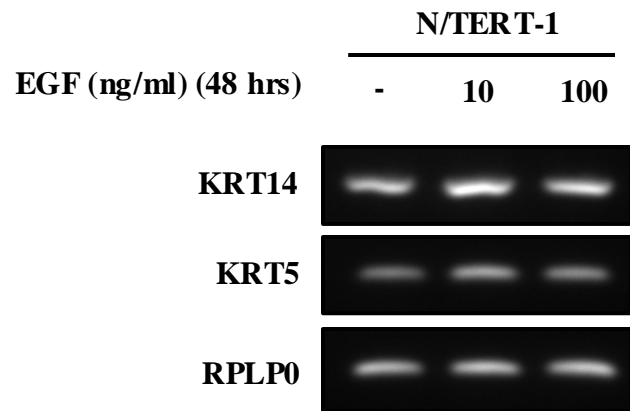
(ii)
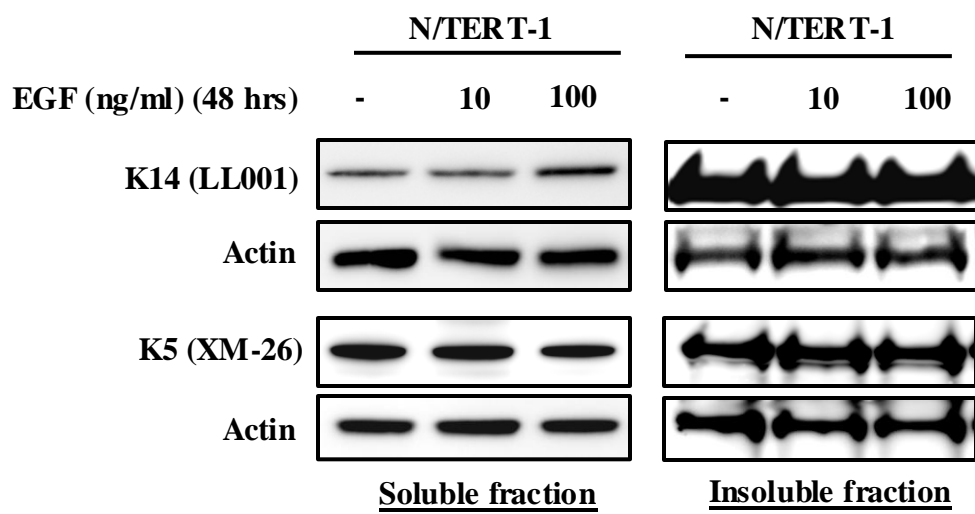
(iii)
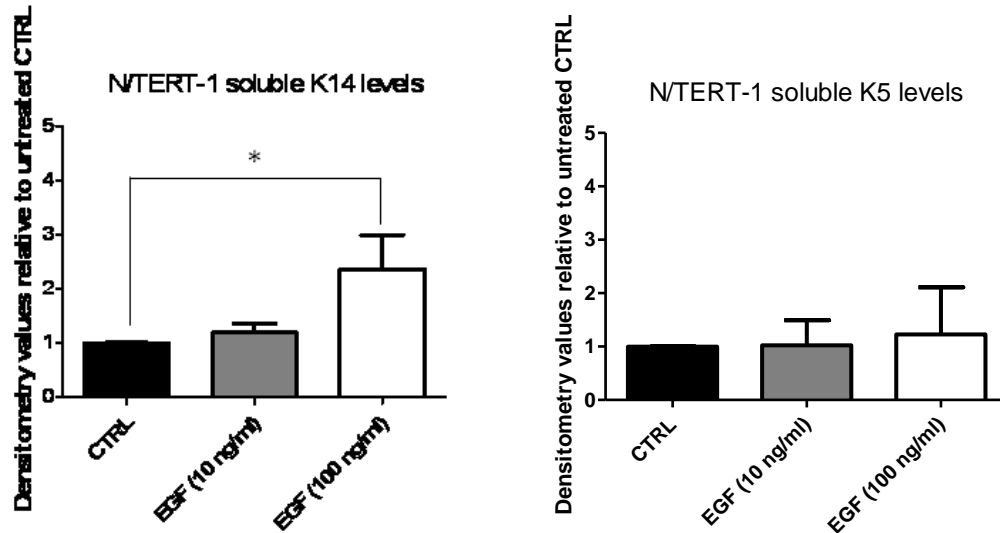
Figure 4.2 (I) EGF treatment increases K14 synthesis and solubility in wild-type cells.
N/TERT-1 cells cultured in serum-free media without EGF for 48 hrs were subjected to
EGF treatments (10 ng/ml and 100 ng/ml) for 48 hrs. (i) RNA was isolated from each
treatment group. cDNAs were prepared and analyzed by real-time PCR for quantification
using specific primers to (A) KRT14, (B) KRT5, normalized to RPLP0. Data presented as
mRNA expression relative to untreated control (CTRL), and as mean ± S.D for n = 3 of
each treatment. Statistical significance was assessed by one-way analysis of variance,
followed by Tukey's test, * $p < 0.05$ vs. CTRL group. (C) Amplified cDNA products from
real-time PCR showing the levels of KRT14 and KRT5 mRNA expression upon EGF
treatment (ii) Soluble and insoluble fractions of cell extracts were prepared from each
treatment group. Immunoblot analysis of these cell lysates shown using antibodies to K14
(LL001) and K5 (XM-26). Actin used as loading control. (iii) Densitometry results
showing the intensity of soluble K14 or K5 levels for each EGF treatment group,
normalized to its actin loading control and data presented as relative to untreated CTRL
group and as mean ± S.D for n = 3 of each treatment. Statistical significance was assessed
by one-way analysis of variance, followed by Tukey's test, * $p < 0.05$ vs. CTRL group.

(II)

(i)(A)

KEB-7 KRT14 expression

(B)

KEB-7 KRT5 expression
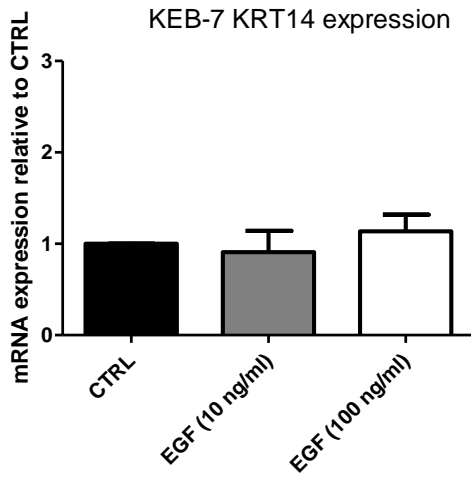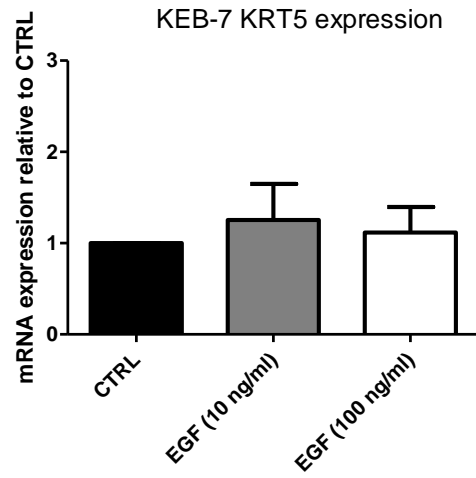
(C)
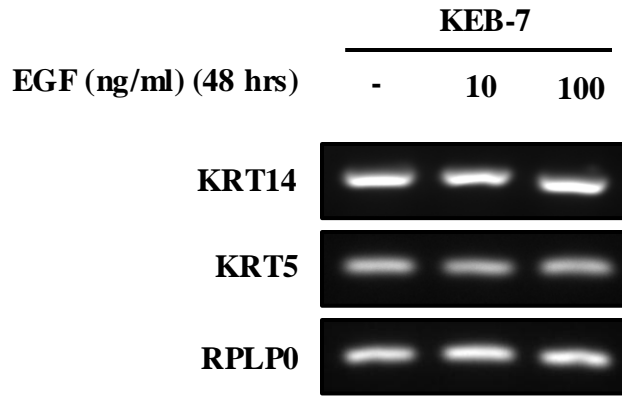
(ii)
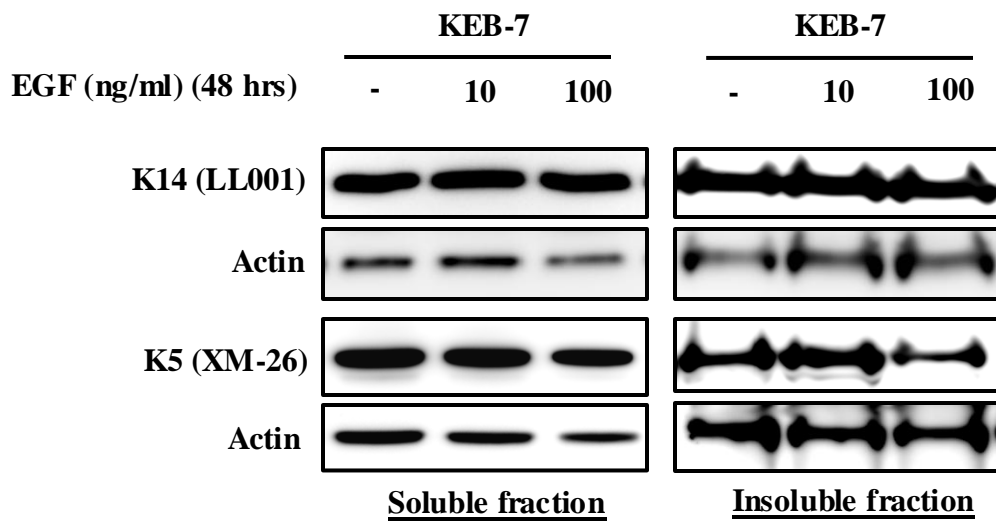
(iii)
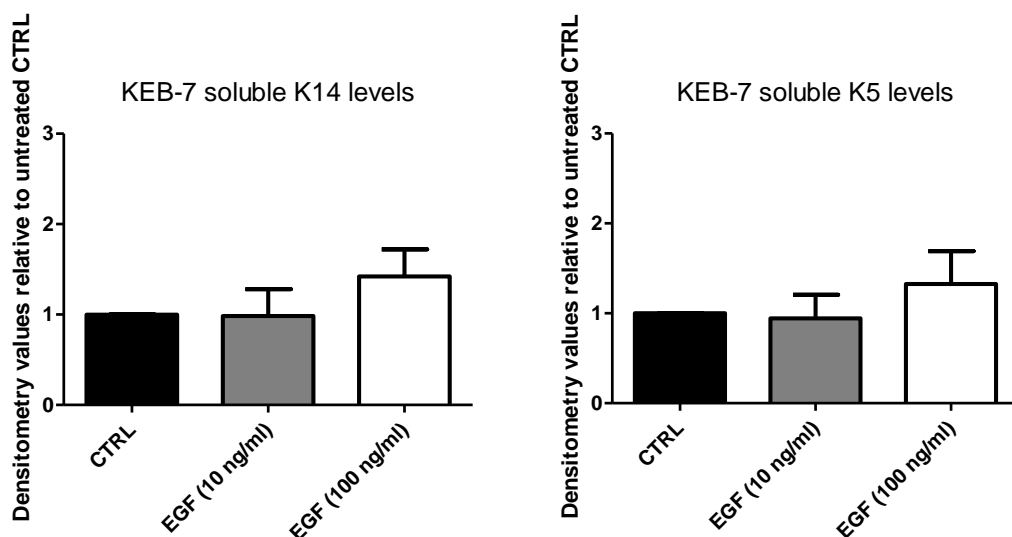
Figure 4.2 (II) No significant change in keratin synthesis and solubility in EBS-DM cells in response to EGF treatments. KEB-7 cells cultured in media without EGF for 48 hrs were subjected to EGF treatments (10 ng/ml and 100 ng/ml) for 48 hrs. (i) RNA was isolated from each treatment group. cDNAs were prepared and analyzed by real-time PCR for quantification using specific primers to (A) KRT14, (B) KRT5, normalized to RPLP0. Data presented as mRNA expression relative to untreated control (CTRL), and as mean $\pm$ S.D for n = 3 of each treatment. Statistical significance was assessed by one-way analysis of variance, followed by Tukey's test. (C) Amplified cDNA products from real-time PCR showing the levels of KRT14 and KRT5 mRNA expression upon EGF treatment. (ii) Soluble and insoluble fractions of cell extracts were prepared from each cell line. Immunoblot analysis of these cell lines shown using antibodies to K14 (LL001) and K5 (XM-26). Actin used as loading control. (iii) Densitometry results showing the intensity of soluble K14 or K5 levels for each EGF treatment group, normalized to its actin loading control and data presented as relative to untreated CTRL group and as mean $\pm$ S.D for n = 3 of each treatment. Statistical significance was assessed by one-way analysis of variance, followed by Tukey's test.

4.2.3   EGF regulates keratinocyte migration through its downstream signalling pathways

Since remodelling of the keratin cytoskeleton is active during cell migration and EGF is known to stimulate migration, the effect of EGF on cells with defective keratins was investigated. It was observed that collective migration of keratinocytes, measured by the area recovered in a scratch wound assay, could be slowed down drastically in the presence of AG1478, a known EGFR inhibitor, in both EGFP-K14 WT (0.12 ± 0.05) ($^{+++} p < 0.001$) and EGFP-K14 R125P (0.06 ± 0.03) ($^{\#\#\#} p < 0.001$) cells [Figure 4.3 (iii) and (iv)] as compared to DMSO-treated controls [Figure 4.3 (i) and (iv)]. In addition, the effects of a downstream signalling kinase in the EGF pathway, ERK1/2, was examined by incubating the cells with U0126 [(MEK inhibitor known to prevent MEK1/2 from phosphorylating its downstream target, ERK1/2 (Favata et al., 1998)] prior to scratch wounding. The data showed that U0126 treatment could also slow down cell migration significantly in both EGFP-K14 WT (0.46 ± 0.12) ($^{++} p < 0.001$) and EGFP-K14 R125P (0.63 ± 0.14) ($^{\#\#} p < 0.01$) cells [Figure 4.3 (ii) and (iv)] as compared to DMSO-treated controls [Figure 4.3 (i) and (iv)].
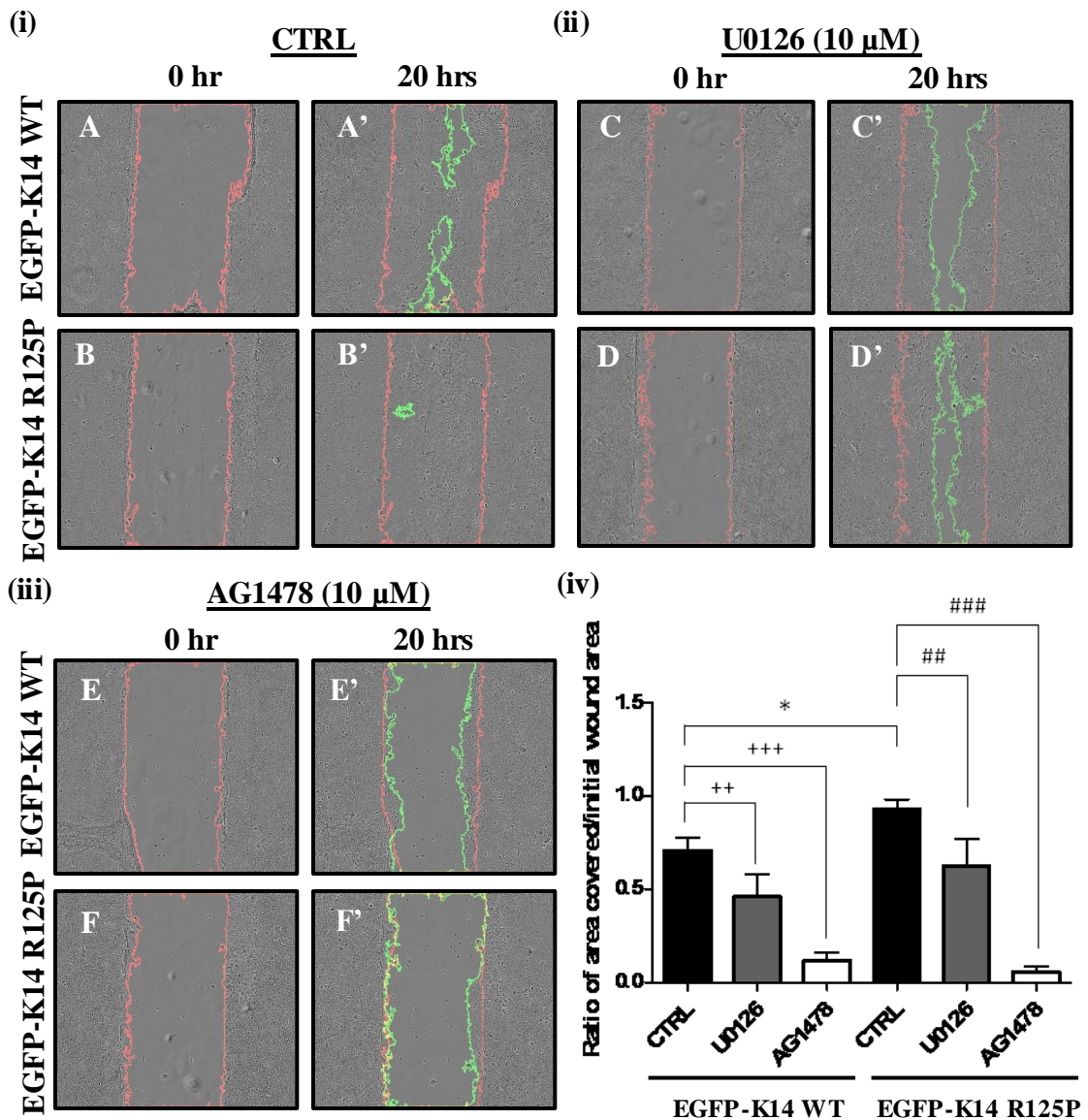
Figure 4.3 EGF regulates keratinocyte migration through its downstream signalling pathways. (i-iii) Cells grown to confluence in an Essen ImageLock 96-well plate were subjected to wounding with a 96-well WoundMaker Tool and treated with either DMSO, AG1478 (10 μM) or U0126 (10 μM) in fresh media. Images were acquired immediately and at 1 hr intervals for 20 hrs using the IncuCyte imaging system. Data were then processed by ImageJ software. Red line marks the denuded area from which cells were removed at the start of the wound (0 hr); green line marks the remaining uncovered area after 20 hrs wound closure time (20 hrs). (iv) Areas between red (or green) lines were derived from a macro written with ImageJ and quantified. Data presented as ratio of area covered/initial wound area and as mean $\pm$ S.D for n = 3 of each group. Statistical significance was assessed by one-way analysis of variance, followed by Tukey's test, * $p < 0.05$ vs. EGFP-K14 WT CTRL group; [++] $p < 0.01$, [+++] $p < 0.001$ vs. EGFP-K14 WT CTRL group; and [##] $p < 0.01$, [###] $p < 0.001$ vs. EGFP-K14 R125P CTRL group.

4.2.4 EGF influences keratin aggregate formation

To investigate whether EGF plays a role in mediating keratin remodelling in wound-induced stress activated cells, EBS-DM (EGFP-K14 R125P) cells were cultured in media without EGF for two passages and subconfluent cultures were assessed for the number of cells with aggregates [Figure 4.4 (I) (i)]. In the absence of EGF, cells proliferated in tight colonies [Figure 4.4 (I) (i) (A)] whereas colony boundaries were more diffuse in those cells constantly cultured with EGF [Figure 4.4 (I) (i) (B)]. It was observed that there was fewer cells having aggregates in the −EGF group [Figure 4.4 (I) (i) (A)] as compared to those constantly cultured with EGF [Figure 4.4 (I) (i) (B)]. Moreover, desmoplakin staining showed that cells cultured in −EGF group have well-developed desmosomes with neighboring cells (cell-cell borders) [Figure 4.4 (I) (ii) (A)] as compared to cells constantly cultured with EGF (where desmoplakin was more cytoplasmic) [Figure 4.4 (I) (ii) (B)].

In order to remove the effects of serum on keratin aggregate formation in the EGFP-K14 R125P cells, experiments on subconfluent cells were carried out by first serum-starving the cells for 6 hrs before EGF treatment [Figure 4.4 (II) (i) (A)]. In addition, a 'rescue' experiment was performed where cells in the −EGF control (CTRL) group were re-stimulated with EGF (100 ng/ml) for a short-term exposure of 3 hrs. The results showed that there was an increase in the number of cells with peripheral aggregates after 3 hrs of EGF stimulation [Figure 4.4 (II) (i) (B)]. It was shown that cells in the CTRL + EGF group also yielded a significant (* $p < 0.05$) increase in the number of cells with aggregates (12.3 ± 4.2) as compared to control group (7.37 ± 2.6) [Figure 4.4 (II) (ii)]. Moreover, it was observed that there was a significant ($^{\#} p < 0.05$) reduction in the number of cells with aggregates in the CTRL + EGF + AG1478

group, (7.8 ± 1.4) as compared to CTRL + EGF group (12.3 ± 4.2) [Figure 4.4 (II) (ii)].

These studies support a role for the EGF signalling pathway in regulating keratin aggregate formation, possibly because EGF induces keratin synthesis to a level where the mutant K14 protein cannot become incorporated, or retained, in filaments in the EBS-DM cells.

EGFP-K14 R125P

- EGF   + EGF

(ii)
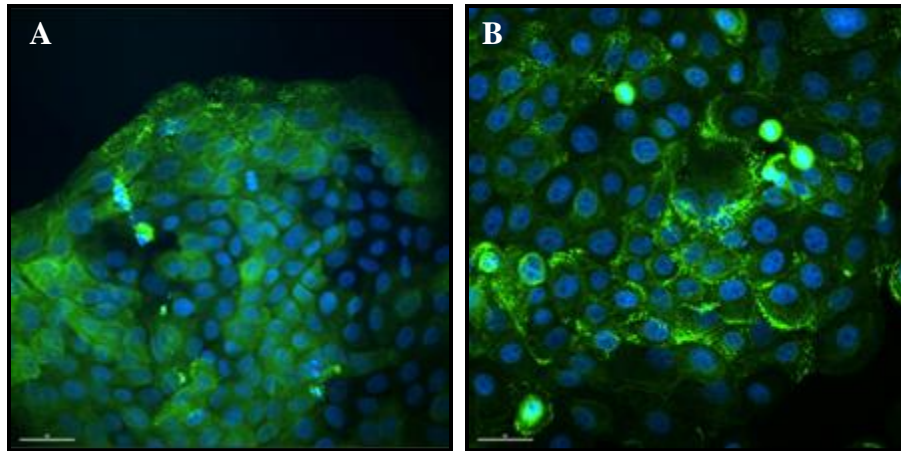
EGFP-K14 R125P

- EGF   + EGF
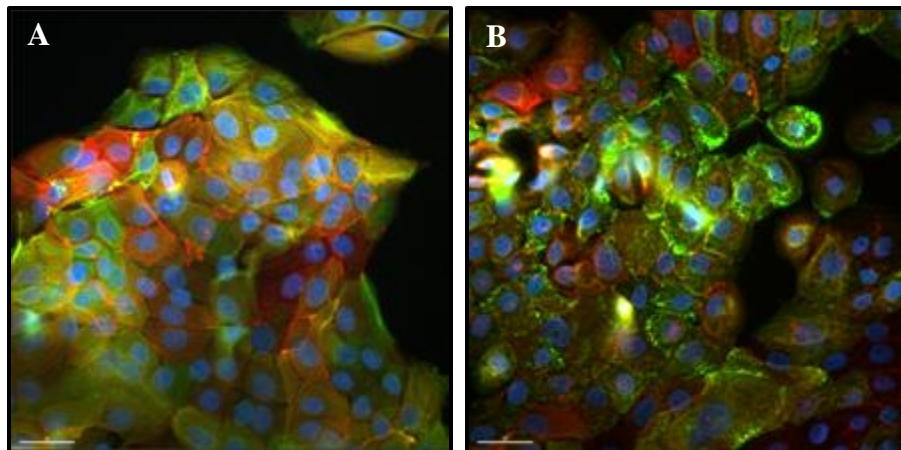
Figure 4.4 (I) EGF influences keratin aggregate formation. Loss of keratin aggregates was associated with a decrease in EGF exposure. (i) Immunofluorescence images showing the effects of EGF removal on keratin aggregates formation. EGFP-K14 R125P cells cultured in (A) media without EGF for two passages or (B) constantly cultured with EGF before fixation. Scale bar, 40 μm. (ii) Immunofluorescence images showing the effects of EGF removal on keratin aggregate formation and desmoplakin localization. EGFP-K14 R125P mutant cells cultured in (A) media without EGF for two passages or (B) constantly cultured with EGF were immunostained with antibodies to desmoplakin (11-5F). Scale bar, 40 μm.

(II)

(i)

EGFP-K14 R125P

-EGF (CTRL)   CTRL + EGF (100ng/ml)
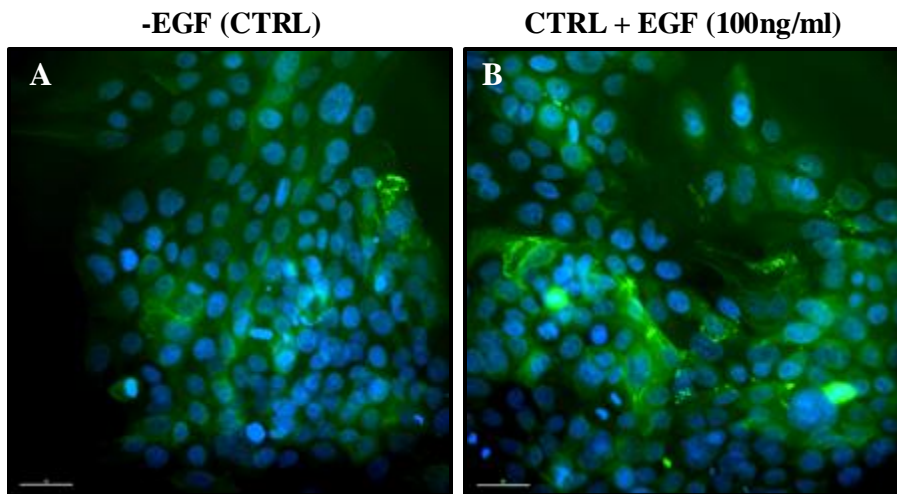
(ii)
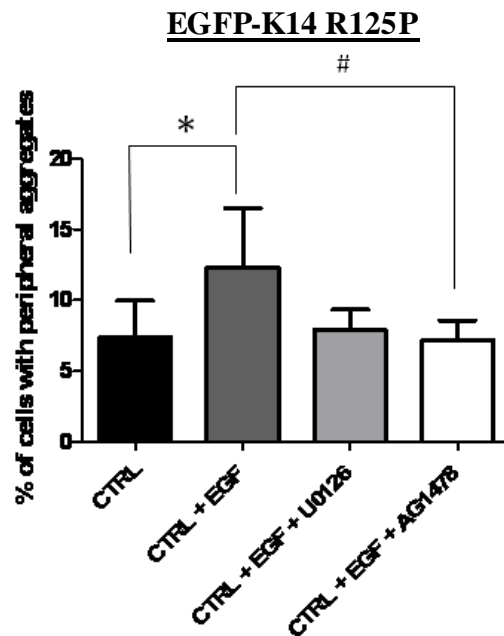
Figure 4.4 (II) EGF influences keratin aggregate formation through its downstream signalling pathways. (i) Immunofluorescence images showing the effects of EGF removal on keratin aggregates formation. (A) EGFP-K14 R125P cells were cultured in media without EGF (CTRL) and serum starved for 6 hrs before (B) re-stimulated with EGF (100 ng/ml) for 3 hrs. Scale bar, 40 μm. (ii) EGFP-K14 R125P cells were cultured in media without EGF (CTRL), serum starved for 6 hrs, re-stimulated with EGF for 3 hrs prior to treatment with inhibitors U0126 (MEK1/2 inhibitor) and AG1478 (EGFR inhibitor) for 1 hr. Quantification of the number of EGFP-K14 R125P keratinocytes showing keratin aggregates after EGF removal (CTRL), EGF re-stimulation for 3 hrs and treatment with inhibitors U0126 (MEK1/2 inhibitor) and AG1478 (EGFR inhibitor) for 1 hr. Numbers of cells with aggregates were counted using ImageJ. Data presented as % of cells with aggregates as mean $\pm$ S.D for n = 4 sets of 700-900 cells counted. Statistical significance was assessed by one-way analysis of variance, followed by Tukey's test, * $p < 0.05$, vs. CTRL group or [#] $p < 0.05$ vs. CTRL + EGF group.

4.2.5 EGF also modulates plectin levels

Because of the changes in keratin aggregate appearance, the effect of EGF stimulation was examined in further detail. The phosphorylation status of downstream signalling kinase ERK1/2 in these treatment groups was examined by immunoblot analysis [Figure 4.5]. As expected, there was an increase in ERK1/2 phosphorylation [phospho-ERK1/2 (P-ERK1/2)] upon EGF stimulation, which could be abolished by both U0126 (10 μM) and AG1478 (10 μM) treatments [Figure 4.5].

As well as its effects on keratin and desmoplakin, differential effects of EGF signalling pathway activation on keratin mutant cells were seen for the hemidesmosomal-associated protein, plectin, but not adherens junction protein, E-cadherin or *armadillo* protein, plakoglobin [Figure 4.5]. The cytoskeleton linker protein plectin is one of the major keratin-associated proteins in keratinocytes forming part of the hemidesmosomes. Treatment with EGF increased plectin levels in the 3 hrs treatment regime [Figure 4.5]. However, only the EGFP-K14 R125P cells showed plectin downregulation upon inhibitor treatment, but not the EGFP-K14 WT cells, suggesting that plectin levels are especially sensitive to EGF signalling in the mutant EGFP-K14 R125P cells. Thus, an increase in EGF leads to both an increase in plectin levels and an increase in keratin aggregate formation in the EBS-DM cells, and both are reversed by an EGF signalling inhibition in the mutant cells [compare Figures 4.4 (II) (ii) and 4.5]. These results suggest that EGF may influence keratin dynamics by modulating plectin levels, a hypothesis that is tested below [see 4.2.12].

	EGFP-K14 WT					EGFP-K14 R125P				
	+EGF	-EGF				+EGF	-EGF			
EGF (100 ng/ml) 3 hrs	-	-	+	+	+	-	-	+	+	+
U0126 (10 μM)	-	-	-	+	-	-	-	-	+	-
AG1478 (10 μM)	-	-	-	-	+	-	-	-	-	+

(1 hr for U0126 and AG1478 treatment)

Rows: Plectin, E-Cadherin, Plakoglobin, P-ERK1/2 (Thr202/Tyr204), ERK1/2, Actin
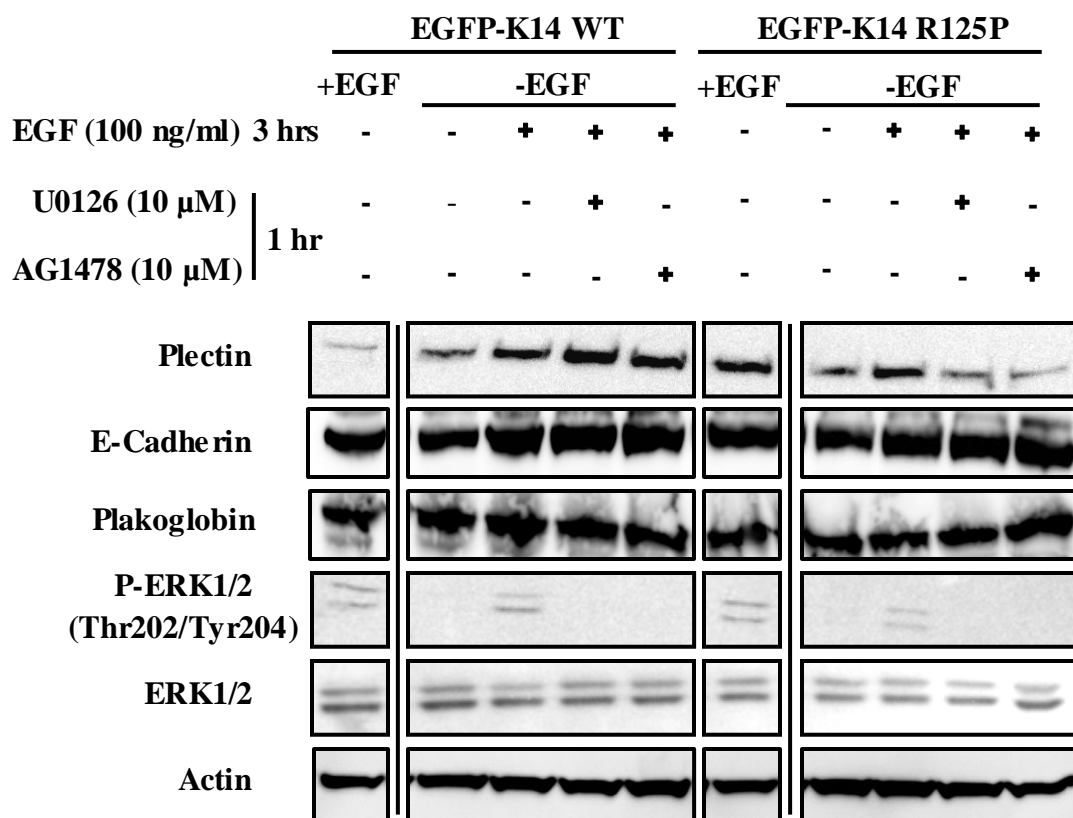
Figure 4.5 EGF also modulates plectin levels. EGFP-K14 WT and EGFP-R125P cell lines were cultured in media without EGF and serum starved for 6 hrs before the treatment regimes. They were re-stimulated with EGF for 3 hrs prior to treatment with inhibitors U0126 (MEK1/2 inhibitor) and AG1478 (EGFR inhibitor) for 1 hr. Soluble fractions of cell extracts were prepared from the cells. Immunoblot analysis of these cell lysates shown using antibodies to plectin (clone 31), E-cadherin (clone 36), plakoglobin (clone 15), P-ERK1/2 (Thr202/Tyr204) and ERK1/2 respectively. Actin used as loading control.

4.2.6 Misregulated ERK1/2 activation in EBS-DM cell lines

The level of activated ERK1/2 was examined in all the four cell lines at subconfluence. Both KEB-7 and EGFP-K14 R125P (cells expressing EBS-DM mutation) show higher levels of P-ERK1/2 than NEB-1 and EGFP-K14 WT (both K14 wild-type) cell lines respectively [Figure 4.6 (i)]. Moreover, when both EGFP-K14 WT and EGFP-K14 R125P cells were serum-starved and immunoblotted with P-ERK1/2 antibody, intrinsic activation of ERK1/2 was observed in the EBS-DM cells which were not seen in the wild-type cells [Figure 4.6 (ii)]. Re-stimulation with EGF (100 ng/ml) restored ERK1/2 phosphorylation in both the cell lines. Thus, cells harboring the K14 R125P mutation show constitutive ERK1/2 activation.

Activation of ERK1/2 was further examined in both EGFP-K14 WT and EGFP-K14 R125P keratinocytes by over-expressing FLAG-ERK2 for 24-48 hrs and then probing by immunoblotting. ERK1/2 activation upon FLAG-ERK2 over-expression was sustained from 24-36 hrs in both cells [Figure 4.6 (iii)]. However, at 48 hrs post-transfection, P-ERK1/2 levels in EGFP-K14 WT keratinocytes had declined, whilst the signal was still sustained in EGFP-K14 R125P cells, even when its FLAG expression had diminished [Figure 4.6 (iii)]. This indicates a high level of constitutive ERK1/2 activation in EGFP-K14 R125P cells, possibly connected with their low level of phosphatase activity (Liovic et al., 2008).
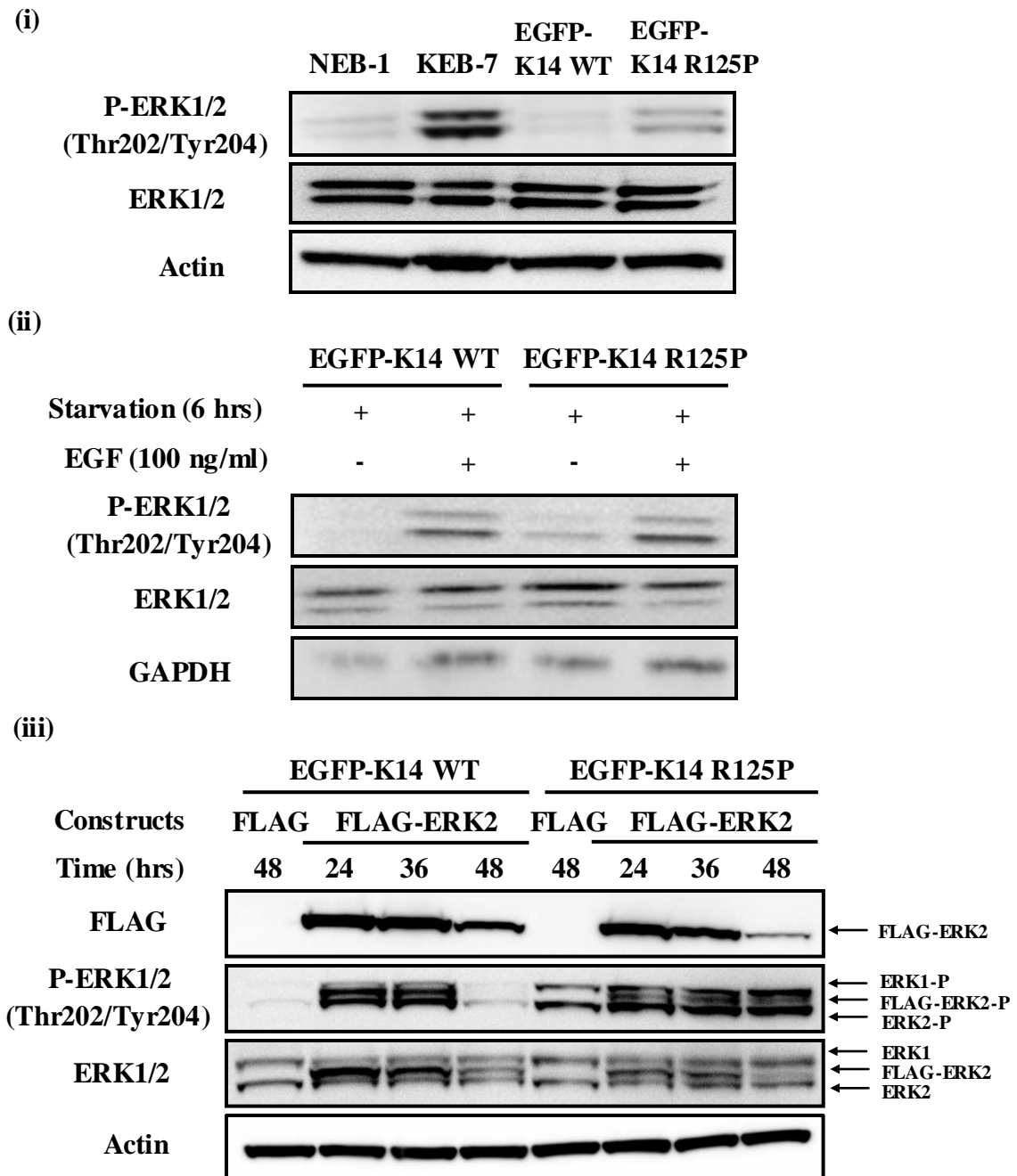
Figure 4.6 Misregulated ERK1/2 activation in EBS-DM cell lines. Intrinsic and sustained activation of ERK1/2 in EBS-DM cells. (i) Soluble fractions of cell extracts were prepared from each cell line at sub-confluence. Immunoblot analysis of these cell lysates shown using antibodies to P-ERK1/2 (Thr202/Tyr204) and ERK1/2. Actin used as loading control. (ii) Both EGFP-K14 WT and EGFP-K14 R125P cells were serum-starved for 6 hrs before re-stimulation with EGF (100 ng/ml) for 3 hrs. Soluble fractions of cell extracts were prepared. Immunoblot analysis of these cell lysates shown using antibodies to P-ERK1/2 (Thr202/Tyr204) and ERK1/2. GAPDH used as loading control. (iii) EGFP-K14 WT and EGFP-R125P cells were transiently transfected with either FLAG CTRL or FLAG-ERK2 expression plasmid for 24-48 hrs. Soluble fractions of cell extracts were prepared from each cell line. Immunoblot analysis of these cell lysates shown using antibodies to FLAG, P-ERK1/2 (Thr202/Tyr204) and ERK1/2. Actin used as loading control.

161

4.2.7   Co-localization of P-ERK1/2 and the peripheral keratin aggregates

Immunofluorescence analysis with antibodies to P-ERK1/2 showed co-localization of activated ERK1/2 with the peripheral keratin aggregates in the mutant keratinocytes [Figure 4.7 (i) A''']. Co-localization results showed a significant increase (*** $p <$ 0.001) in Pearson's coefficient of correlation values of P-ERK1/2 (0.78 ± 0.08) as compared to ERK1/2 (0.26 ± 0.10) staining respectively [Figure 4.7 (ii) and (iii)], which demonstrated that the activated forms of ERK1/2 co-localized with mutant keratin aggregates.

4.2.8   ERK1/2 inhibition reduces peripheral keratin aggregates

Because P-ERK1/2 co-localized with peripheral keratin aggregates of the EGFP-K14 R125P cells, the effect of the MEK1/2 inhibitor, U0126 on these mutant keratinocytes was examined. Cells were exposed to DMSO or U0126 (10-100 µM) treatments for 1 hr before fixation [Figure 4.8 (i) (A-D)]. Immunofluoresence images showed a dose-dependent reduction in the number of cells with aggregates from U0126 (10 µM) (0.81 ± 0.09 folds) (** $p <$ 0.01) to U0126 (100 µM) (0.56 ± 0.08 folds) (*** $p <$ 0.001) as compared to DMSO-treated control (1.00 ± 0.00) [Figure 4.8 (ii)]. These observations were further confirmed by staining cells with P-ERK1/2 antibody after 1 hr treatment with U0126 (100 µM). Immunofluoresence images showed that co-localization of P-ERK1/2 with the peripheral aggregates was abolished upon U0126 treatment as compared to DMSO-treated control [Figure 4.8 (iii) (A'') and (B'')]. It was also observed that ERK1/2 inhibition resulted in more of the mutant keratin localizing into filaments [Figure 4.8 (iii) (B)].

(i)

EGFP-K14

Merged

EGFP-K14 R125P

A A' A''

P-ERK1/2

B B' B''

ERK1/2

(ii) **(iii)**

Analysis Output

P-ERK1/2 ERK1/2

A''' B'''

Figure 4.7 Co-localization of P-ERK1/2 and peripheral keratin aggregates. Interaction between P-ERK1/2 and keratin aggregates. (i) Immunofluorescence images showing the localization of both (A') P-ERK1/2 (Thr202/Tyr204) and (B') ERK1/2 in EGFP-K14 R125P cells, merged with images of (A-B) EGFP-K14 R125P respectively. (A''-B'') Image areas used as co-localization analysis shown. Scale bar, 30 μm. (ii) (A'''-B''') Pearson coefficient of correlation was 0.8081 (P-ERK1/2) and 0.3827 (ERK1/2) respectively. (iii) Co-localization quantification of 20 EGFP-K14 R125P cells at the aggregate region stained with either P-ERK1/2 (Thr202/Tyr204) or ERK1/2. Data presented as Pearson coefficient of correlation value and as mean ± S.D. Statistical significance was assessed by unpaired t-test, *** $p < 0.001$ vs. ERK1/2 stained group.

(i)

(ii)

(iii)

<u>EGFP-K14 R125P</u>

Figure 4.8 ERK1/2 inhibition reduces peripheral keratin aggregates. ERK1/2 was involved in regulating keratin aggregate formation. (i) Immunofluorescence images showing the effects of MEK1/2 inhibition on the formation of peripheral keratin aggregates. EGFP-K14 R125P mutant cells subjected to either (A) DMSO (CTRL) or (B-D) U0126 (MEK1/2 inhibitor) (10, 50, 100 µM) treatment for 1 hr. Scale bar, 40 µm. (ii) Quantification of the number of EGFP-K14 R125P keratinocytes with peripheral aggregates after either DMSO or U0126 (MEK1/2 inhibitor) (10, 50 and 100 µM) treatments for 1 hr. Number of cells with peripheral keratin aggregates were counted in each of the treatment groups using ImageJ. Data presented as relative control (number of cells with aggregates) as mean ± S.D for n = 8 sets of 400-1000 cells counted. Statistical significance was assessed by one-way analysis of variance, followed by Tukey's test, ** $p < 0.01$, *** $p < 0.001$ vs. DMSO (CTRL) group. (iii) Immunofluoresence images showing EGFP-K14 R125P mutant cells subjected to either DMSO or U0126 (MEK1/2 inhibitor) (100 µM) treatments for 1 hr. Cells were then stained with P-ERK1/2 and their merged images shown. Scale bar, 30 µm.

4.2.9 ERK1/2 inhibition only reduces plectin levels in EBS-DM cells

Immunoblot analysis of protein levels after 1 hr treatment with U0126 (10-100 μM) showed complete loss of phosphorylated ERK1/2 in both EGFP-K14 WT and EGFP-K14 R125P cells [Figure 4.9]. Since plectin in the EGFP-K14 R125P cells was affected during the EGF treatment regime described previously, plectin levels upon U0126 treatment was examined to understand its role in regulating keratin aggregate formation. Basal level of plectin of the untreated EGFP-K14 R125P cells was already significantly higher than that of the EGFP-K14 WT cells [Figure 4.9]. In addition, a dose-dependent decrease in the levels of plectin was only observed in the EGFP-K14 R125P cells upon increasing concentrations of U0126 treatment, but this was not seen in the EGFP-K14 WT cells [Figure 4.9], further supporting the possibility that plectin levels are associated with the formation of keratin aggregates and this effect is downstream of ERK1/2 activity. Hence, these experiments indicated that the formation of keratin aggregates might be modulated by the activity of ERK1/2 kinase and plectin levels.
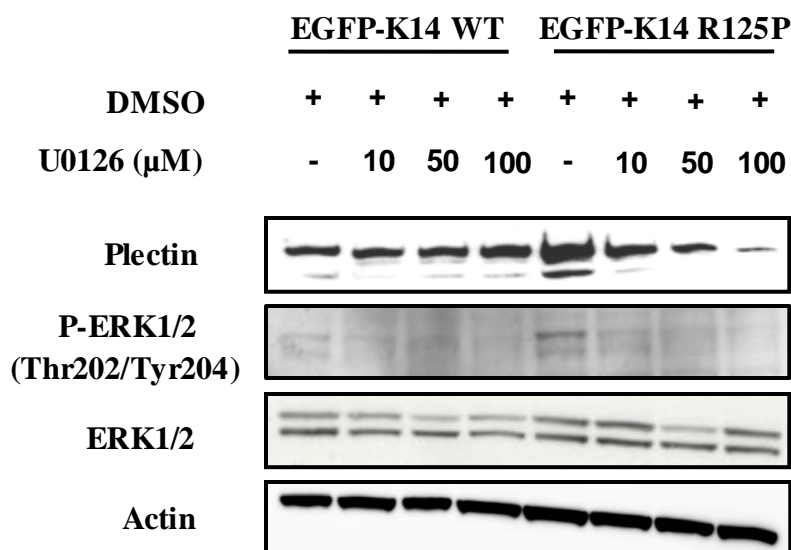
Figure 4.9 ERK1/2 inhibition only reduces plectin levels in EBS-DM cells. EGFP-K14 WT and EGFP-K14 R125P cells subjected to either DMSO (CTRL) or U0126 (MEK1/2 inhibitor) (10, 50, 100 μM) treatments for 1 hr. Soluble fractions of cell extracts were prepared from these cells. Immunoblot analysis of these cell lysates were shown using antibodies to plectin (clone 31), P-ERK1/2 (Thr202/Tyr204) and ERK1/2. Actin used as loading control.

4.2.10 ERK1/2 knockdown reduces peripheral keratin aggregates

To eliminate the possibility of non-specific effects of U0126 treatment, siRNA knockdown experiments were performed in EGFP-K14 R125P cells, specifically targeting the genes *ERK1* and *ERK2*. At 48 hrs and 72 hrs post-transfection of the siRNA, there was a significant decline (*** $p < 0.001$; ### $p < 0.001$) in both ERK1 and ERK2 expression at the mRNA transcript [Figure 4.10 (i)] and protein [Figure 4.10 (ii)] levels. The results consistently showed fewer mutant cells with keratin aggregates in ERK1/ERK2 siRNA transfected cells as compared to control siRNA transfected cells at 72 hrs post-transfection [Figure 4.10 (iii)], further supporting a direct regulation of keratin aggregate formation by ERK1/2 activity. At 72 hrs post-transfection, ERK1/ERK2 knockdown was the most effective and a decrease in the number of mutant cells with aggregates was observed. At this time, a slight decrease in plectin levels was also apparent [Figure 4.10 (ii)]. This lends support to the possibility of plectin involved in regulating keratin aggregate formation through ERK1/2 activity.

(i) EGFP-K14 R125P

(ii) EGFP-K14 R125P

siRNAs	CTRL	ERK1/ERK2	
Time (hrs)	72	48	72

Plectin

P-ERK1/2
(Thr202/Tyr204)

ERK1/2

Actin

(iii)

CTRL siRNA (72 hrs)   ERK1/ERK2 siRNA (72 hrs)
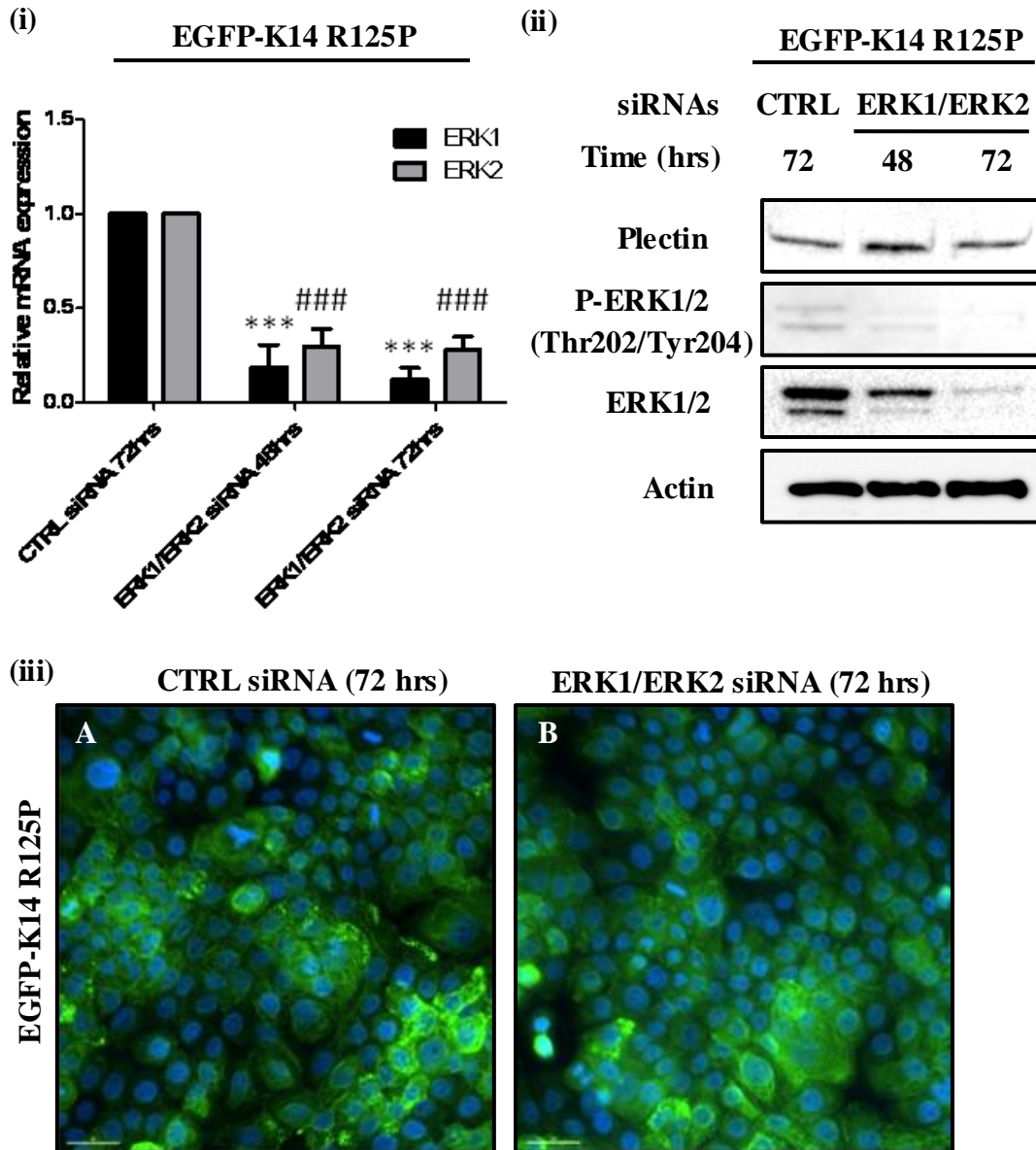
EGFP-K14 R125P

Figure 4.10 ERK1/2 knockdown reduces peripheral keratin aggregates.
Direct involvement of ERK1/2 activation in regulating keratin aggregate formation. (i)
RNA isolated from EGFP-K14 R125P cells that were transiently transfected with either
CTRL siRNA for 72 hrs or ERK1/ERK2 siRNA for 48 hrs and 72 hrs respectively.
cDNA were prepared and analyzed by real-time PCR for quantification using specific
primers to ERK1 and ERK2, normalized to HPRT. Data presented as relative mRNA
expression to CTRL siRNA and as mean ± S.D for n = 3 of each group. Statistical
significance was assessed by one-way analysis of variance, followed by Tukey's test,
*** $p < 0.001$ vs. ERK1 CTRL siRNA group; ### $p < 0.001$ vs. ERK2 CTRL siRNA
group. (ii) Soluble fractions of cell extracts were prepared from EGFP-K14 R125P cell
line that was transiently transfected with either CTRL siRNA for 72 hrs or ERK1/ERK2
siRNA for 48 hrs and 72 hrs respectively. Immunoblot analysis of these cell lysates
shown using antibodies to plectin (clone 31), P-ERK1/2 (Thr202/Tyr204) and ERK1/2.
Actin used as loading control. (iii) Immunofluoresence images showing EGFP-K14
R125P cells transiently transfected with either CTRL siRNA or ERK1/ERK2 siRNA
treatment for 72 hrs. Scale bar, 40 μm.

169

4.2.11 ERK1/2 regulates keratin dynamics and cell migration

The link between ERK1/2 activity and keratin aggregate formation was further supported by time-lapse live-cell imaging of subconfluent EGFP-K14 R125P cells during exposure to U0126 treatment, imaged over 1 hr [Figure 4.11]. In basal conditions, keratin aggregates were localized at the leading edge of each cell during migration. Upon U0126 (100 μM) treatment, the cells were observed to initially retract, and showed a decrease in keratin dynamics, and aggregate formation appeared to cease very quickly. After washout of U0126 and replenishment with fresh medium, keratin aggregates reappeared in the peripheral cytoplasm and cells began to migrate again [Figure 4.11]. These experiments further demonstrated that P-ERK1/2 localization at the leading edge was involved in regulating keratin dynamics.

EGFP-K14 R125P
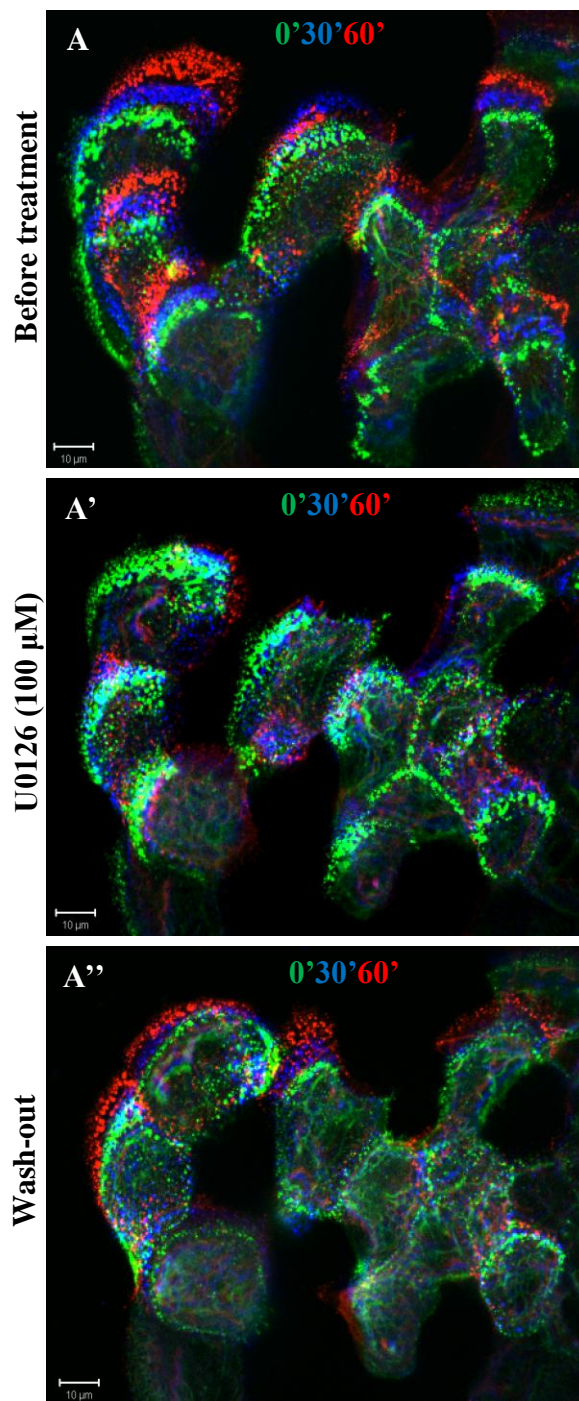
Figure 4.11 ERK1/2 regulates keratin dynamics and cell migration. ERK1/2 activation affects keratin dynamics and cell migration. Time-lapse imaging of EGFP-K14 R125P cells under the effect of U0126 (MEK1/2 inhibitor) (100 μM). (A) Cells at the basal level were recorded at intervals of 1 min for 1 hr, (A') treated with U0126 for 1 hr, (A'') followed by a wash out of U0126, replenished with fresh media and further imaged for 1 hr. Images were processed using imageJ and different color codings were used to demarcate the distance travelled by the keratinocytes at 0 (green), 30 min (blue) and 60 min (red) after each treatment respectively. Scale bar, 10 μm.

4.2.12 Plectin knockdown reduces peripheral keratin aggregates

To establish whether plectin directly regulated keratin aggregate formation, siRNA knockdown experiments were performed in both EGFP-K14 WT and EGFP-K14 R125P cells, specifically targeting the plectin gene, *PLEC*. At 48 hrs and 72 hrs post-transfection of the PLEC siRNA, there was a significant decrease in plectin expression of the EGFP-K14 WT (* $p < 0.05$) and EGFP-K14 R125P (** $p < 0.01$) cells at the mRNA transcript as compared to CTRL siRNA transfected cells [Figure 4.12 (i)]. This led to the down-regulation of plectin levels in both cell lines after 48 hrs and 72 hrs post-transfection [Figure 4.12 (ii)]. Significantly fewer mutant cells with keratin aggregates were observed in PLEC siRNA transfected cells as compared to control siRNA transfected cells at 72 hrs post-transfection [Figure 4.12 (iii)], confirming an involvement of plectin in the likelihood of keratin aggregate formation in the EBS-DM cells.

4.2.13 Plectin knockdown in EBS-DM cells slows down wound closure

The role of plectin in regulating cell migration of both wild-type and EBS-DM cells were then examined in scratch wound assays. At 72 hrs post-transfection, plectin knockdown was the most effective and a decrease in the number of mutant cells with aggregates was observed. At this time, wound closure was slowed down significantly (*** $p < 0.001$) in PLEC siRNA transfected mutant cells (0.50 ± 0.10) as compared to control siRNA transfected mutant cells (0.78 ± 0.10) [Figure 4.13 (i) and (ii)], thus suggesting that plectin could also affect cell migration, possibly through modulating keratin dynamics in the mutant cells. However, a reverse result was observed in the wild-type cells, wherein PLEC siRNA transfected wild-type cells (0.74 ± 0.15) resulted in faster wound closure as compared to control siRNA transfected wild-type

cells (0.58 ± 0.15) [Figure 4.13 (i) and (ii)], an observation that was consistent to that reported in (Osmanagic-Myers et al., 2006). This intriguing observation suggests that plectin expression in the EBS-DM cells may be different from that of the wild-type cells and that it may affect cell behaviour in terms of cell migration in this context. More work will be needed to understand these differences.

In summary, the results presented in this chapter demonstrate that EGF signalling not only affects keratin synthesis and solubility but also affects keratin remodelling, as aggregate formation in EBS-DM cells, through its downstream ERK1/2 signalling pathways, and that this may be effected through modulation of plectin levels.

(i)

(ii)

siRNAs	EGFP-K14 WT			EGFP-K14 R125P		
	CTRL	PLEC		CTRL	PLEC	
Time (hrs)	72	48	72	72	48	72
Plectin						
Actin						

(iii)

**CTRL siRNA (72 hrs)**   **PLEC siRNA (72 hrs)**
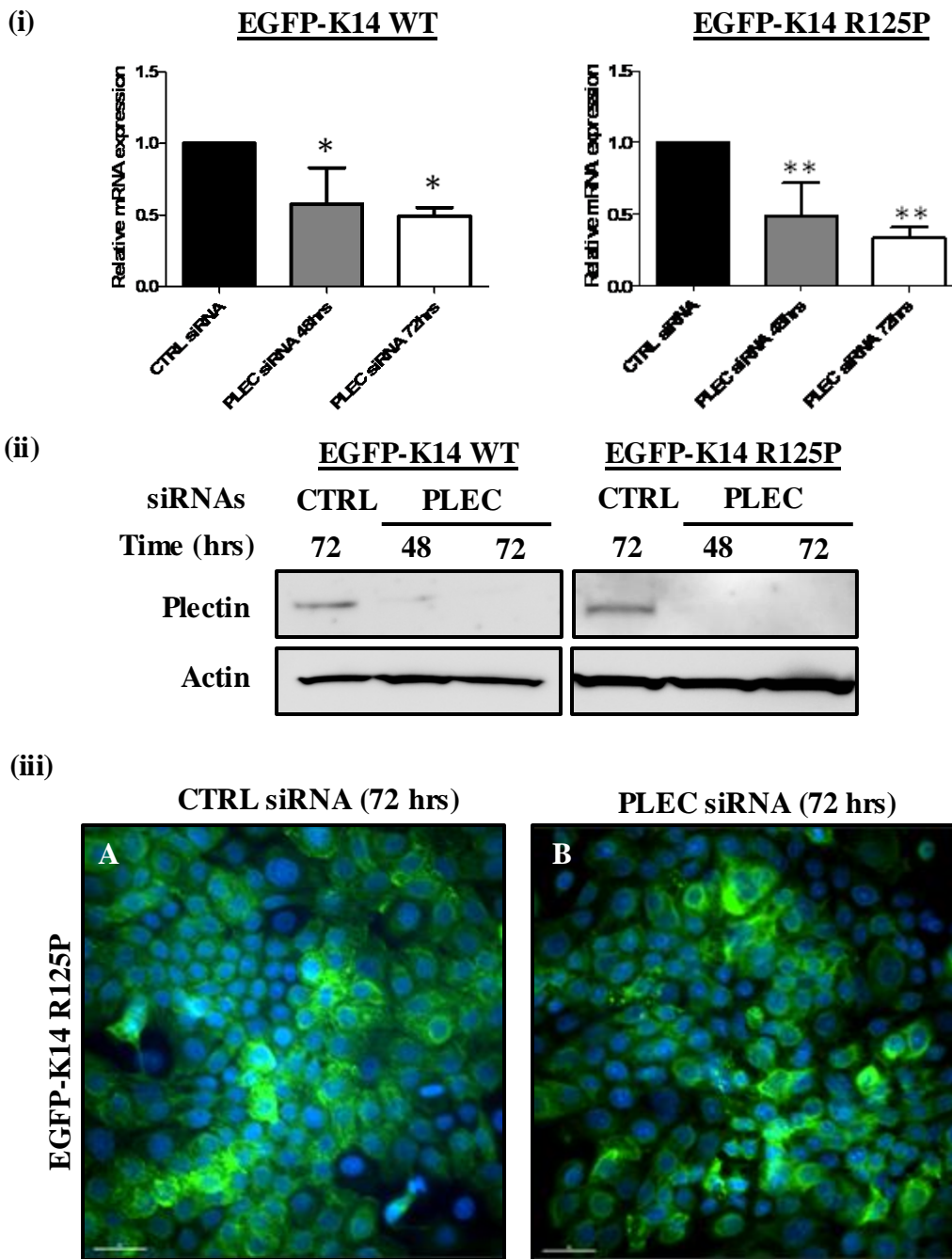
EGFP-K14 R125P

Figure 4.12 Plectin knockdown reduces peripheral keratin aggregates. Direct involvement of plectin in regulating keratin aggregate formation. (i) RNA isolated from both EGFP-K14 WT and EGFP-K14 R125P cells that were transiently transfected with either CTRL siRNA for 72 hrs or PLEC siRNA for 48 hrs and 72 hrs respectively. cDNAs were prepared and analyzed by real-time PCR for quantification using specific primers to plectin, normalized to HPRT. Data presented as relative mRNA expression to CTRL siRNA and as mean ± S.D for n = 3 of each group. Statistical significance was assessed by one-way analysis of variance, followed by Tukey's test, * $p < 0.05$; ** $p < 0.01$ vs. CTRL siRNA group. (ii) Soluble fractions of cell extracts were prepared from both EGFP-K14 WT and EGFP-K14 R125P cell line that was transiently transfected with either CTRL siRNA for 72 hrs or PLEC siRNA for 48 hrs and 72 hrs respectively. Immunoblot analysis of these cell lysates shown using antibodies to plectin (clone 31). Actin used as loading control. (iii) Immunofluoresence images showing EGFP-K14 R125P mutant cells transiently transfected with either CTRL siRNA or PLEC siRNA treatment for 72 hrs. Scale bar, 40 μm.

174

(i)
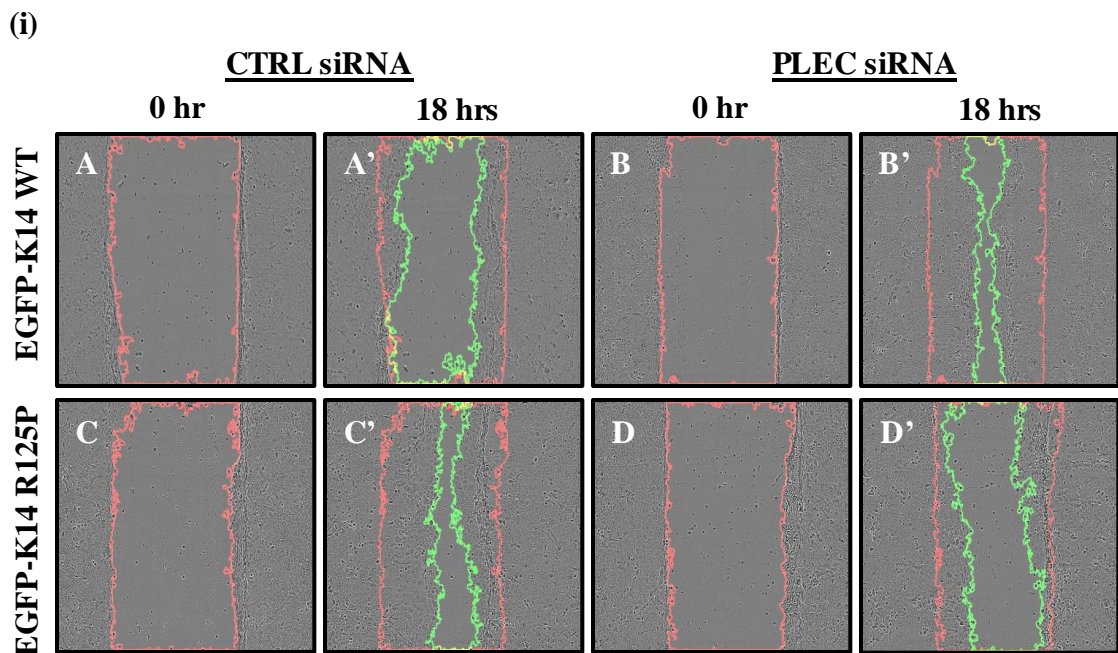
(ii)
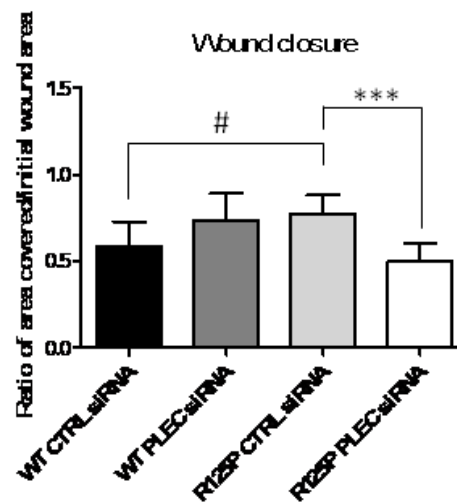
Figure 4.13 Plectin knockdown in EBS-DM cells slows down wound closure. Direct involvement of plectin in regulating cell migration. (i) EGFP-K14 WT and EGFP-K14 R125P cells were transiently transfected with either CTRL siRNA or PLEC siRNA and grown to confluence in an Essen ImageLock 96-well plate. After 48 hrs post-transfection, the cells were subjected to wounding with a 96-well WoundMaker Tool. Images were acquired immediately and at 1 hr intervals for 18 hrs using the IncuCyte imaging system. Data were then processed by ImageJ software. Red line marks the denuded area from which cells were removed at the start of the wound (0 hr); green line marks the remaining uncovered area after 18 hrs wound closure time (18 hrs). (ii) Areas between red (or green) lines were derived from a macro written with ImageJ. Data presented as ratio of area covered/initial wound area and as mean $\pm$ S.D for n = 3 of each group. Statistical significance was assessed by one-way analysis of variance, followed by Tukey's test, [#] $p <$ 0.05 vs. WT CTRL siRNA group, *** $p < 0.001$ vs. R125P CTRL siRNA group.

4.3   Discussion

The results reported in this chapter demonstrate several important aspects of regulation of keratin remodelling, namely that (1) EGF can regulate keratin expression and remodelling in keratinocytes, (2) EGF signalling through ERK1/2 can modulate the activated state of EBS-DM cells and (3) plectin probably plays a role in keratin remodelling during cell migration.

Keratin remodelling involves an interchange between the soluble subunits and the insoluble filamentous protein, and is mediated by regulation of post-translational modifications such as phosphorylation (Chou and Omary, 1993). In the present study, it is shown that there is an imbalance in soluble keratin (K14 and K5) levels in KEB-7 cells when compared to wild-type cells, suggesting that there is increased keratin synthesis or remodelling in the mutant cells.

EGF is known to induce keratin synthesis and expression (Wang et al., 2006; Yoneda et al., 2011). In the present study, it is further shown that EGF can increase keratin synthesis and solubility, indicated by an increase in both K14 mRNA expression and soluble K14 proteins, in the wild-type but not EBS-DM cells. The subtle changes in keratin expression in EBS-DM cells upon EGF treatments may possibly be explained by a constitutively activated ERK1/2 signalling in these mutant cells, which may account for its higher basal keratin expression. Together, these results suggest a role for EGF in keratin synthesis and remodelling in keratinocytes, and also highlight a misregulated EGF signalling in EBS-DM cells.

During migration, cells constantly remodel their cytoskeleton in response to extracellular cues. This is especially important in wound healing, where basal keratinocytes undergo a dramatic reorganization of the cytoskeleton during the

transition from stationary cuboidal tissue residents to flattened, polarized migrating cells as they migrate across the wound bed (Ortonne et al., 1981). EGF has long been known to be a key mitogen and motogen of keratinocytes in driving wound closure (Hudson and McCawley, 1998) and this EGF-mediated cell motility is attributed to activation of downstream ERK1/2 kinase that can contribute to alterations in the actin cytoskeleton through Rac-induced lamellipodia formation (Klemke et al., 1997; Vial et al., 2003).

In this study, EGFR and MEK1/2 inhibitors were used in scratch wound assays to show that EGF and ERK1/2 activation were required for facilitating wound closure in the keratinocyte cell lines used in these experiments. It was observed that EGFR inhibition was more potent in slowing down cell migration than MEK1/2 inhibition in both cell lines, suggesting that other pathways parallel to EGF-ERK1/2 signalling, such as PKC or Akt pathways, might also be involved in regulating cell migration.

A direct role of EGF in mediating keratin remodelling was demonstrated in stress activated EBS-DM cells, whereby it was observed that fewer cells expressed the classic keratin aggregates that are the hallmark of severe EBS when the cells were cultured in media without EGF as compared to cells constantly cultured in EGF.

Besides its effect on keratin solubility and cell migration, EGF also probably affects other cytoskeleton components. A previous study reported that desmoplakin localization can be affected by EGF (Yin et al., 2005). In the present study, it was observed that there was a change in localization of desmoplakin proteins, from cytoplasmic to membrane-bound (junction-associated) in the mutant keratinocytes in response to EGF removal. Desmoplakin is an important component of desmosomes that provides anchoring sites for keratin intermediate filaments through its C-terminal

domain, to facilitate cell-cell adhesion (reviewed in Getsios et al., 2004). Interference with desmosomal adhesion leads to reduced tissue integrity and tissue blistering (Anhalt et al., 1990). Indeed, a recent study has shown that EBS-DM cells exhibited a down-regulation of junction proteins as compared to wild-type cells, suggesting that keratin mutations led to a reduction in cell-cell adhesion, which could contribute to defective tissue integrity and skin blistering (Liovic et al., 2009).

The present study showed that by increasing cell-cell adhesion upon EGF removal, keratin dynamics were slowed down and resulted in a reduction in the number of mutant cells with keratin aggregates. A 'rescue' experiment was performed by re-stimulating the cells with EGF and it was observed that there was an increase in the number of cells with peripheral aggregates, which correlated with increased ERK1/2 activation. These results suggested that EGF signalling could induce an increase in the activation state of EBS-DM cells and increase the likelihood of the mutant cells forming keratin aggregates. This is the converse of the decrease in aggregates seen as cells become confluent whilst approaching a quiescent state (Chapter 3).

During wound healing, hemidesmosomes are reorganised in response to chemotactic factors such as EGF, allowing cells to migrate (Mainiero et al., 1996). Plectin, being localized at hemidesmosomes (reviewed in Wiche, 1998), could be affected by the influence of EGF. In this study, it was observed that the levels of plectin were increased in response to EGF stimulation, and that the plectin levels were decreased by EGFR and ERK1/2 inhibition in mutant cells (but not wild-type cells), and this correlated with a decrease in peripheral keratin aggregates. Hence, these observations suggest that plectin is involved in keratin remodelling under the influence of EGF.

It was also found in this study that ERK1/2 kinase in EBS-DM cells (EGFP-K14 R125P) are constitutively activated, both intrinsically and sustained, as compared to wild-type cells. To study the possible role of ERK1/2 kinase in regulating keratin remodelling, co-localization studies were undertaken and it was observed that activated ERK1/2 kinase in the mutant cells co-localized with peripheral keratin aggregates at sites of lamellipodial protrusion. The sustained activation of ERK1/2 at lamellipodial protrusion and its minimial nuclear localization in mutant keratinocytes would suggest that there was a lack of nuclear anchoring proteins such as DUSPs that could mediate dephosphorylation of ERK1/2 in the nucleus (Caunt et al., 2008a; Caunt et al., 2008b). Indeed, one observation made from EBS-DM cell lines was the differential regulation of DUSPs where the authors showed that MKP-1, MKP-2 and hVH3 (DUSP-5) were significantly downregulated in KEB-7 cells as compared to NEB-1 cells at basal conditions (Liovic et al., 2008). This suggests that the up-regulation of ERK1/2 activity could be a consequence of lower DUSPs activity in the mutant cells. Moreover, the possibility of a scaffold protein modulating the localization of activated ERK1/2 in close proximity to peripheral keratin aggregates is apparent because recent studies have shown that scaffold protein such as KSR could control whether ERK1/2 phosphorylate cytosolic or nuclear substrates by regulating its dimerisation state (Casar et al., 2008). More work will be needed to understand this better.

Previous studies have also reported that keratinocytes exposed to various stress stimuli show abnormally elevated ERK1/2 activation and keratin phosphorylation. For instance, it was shown that in response to osmotic stress, KEB-7 showed higher and persistent levels of activated ERK1/2 that correlated with increased phosphorylated keratin 5 (Morley et al., 2003). Moreover, studies have reported that phosphorylation

of K8-S432 is mediated by EGF through ERK1/2 signalling (Ku and Omary, 1997), and this ERK1/2-mediated phosphorylation could contribute to K8 reorganisation and epithelial tumour cell migration (Busch et al., 2012). Another study also revealed that the increased ERK1/2 signalling in response to mechanical stretching could provide EBS-DM keratinocytes resistance to stretch-induced apoptosis (Russell et al., 2010). These studies show how keratinocytes can adapt to stress stimuli by remodelling their keratin cytoskeleton via phosphorylation.

In this study, the results further substantiated the role of ERK1/2 as a regulator of keratin remodelling in wound-induced stress activated cells. By inhibiting ERK1/2 activity, it was observed that there was a reduction in the number of cells with peripheral keratin aggregates. In addition, ERK1/2 inhibition resulted in keratinocytes having more bundled keratin filaments at the perinuclear regions as compared to untreated control.

One observation was that the basal plectin level was already higher in the mutant cells as compared to wild-type cells. Moreover, this plectin level seemed to be particularly sensitive to ERK1/2 inhibition in the mutant cells but not wild-type cells. One could speculate that because the mutant keratinocytes with peripheral keratin aggregates would undergo continual actin and keratin remodelling till they formed elongated filaments, they would have to synthesize more plectin proteins in order to stabilize the intermediate filament network. Since ERK1/2 inhibition resulted in the reduction of both actin and keratin dynamics in the mutant cell line, plectin cross-linkers that could not incorporate into the filament network would be degraded and thus reduce its level. This is in contrast to wild-type keratinocytes that could incorporate proper actin and keratin filament network with plectin cross-linkers and hence were possibly unaffected by ERK1/2 inhibition. A previous work has also described an altered

plectin stability in EBS-DM cells when KEB-7 cells were subjected to cyclic mechanical stretch. It was found that plectin was relocated from cell junctions and associated with the fragmented keratin rings that formed upon mechanical stress, a phenomenon that was not observed in the wild-type cells (Russell et al., 2004).

To substantiate these results, it was shown in this study that ERK1/2 knockdown resulted in a reduction of number of cells with keratin aggregates and a decrease in plectin levels, thus confirming a direct role of ERK1/2 in regulating keratin aggregate formation and plectin levels. This observation was also confirmed by performing time-lapse imaging of U0126 treated EGFP-K14 R125P cells, where a decrease in keratin dynamics was accompanied with slower cell migration that could be restored upon removing the U0126 inhibitor. This demonstrates that ERK1/2 could regulate keratin dynamics during cell migration.

Recent study has also revealed the role of plectin in its ability to organize and stabilize the intermediate filament system in plectin$^{-/-}$ keratinocytes (Osmanagic-Myers et al., 2006). The keratin network of these keratinocytes is less rigid and has irregularly loosened bundles of intermediate filaments. In view of this observation, the role of plectin in regulating keratin aggregate formation was examined in this study. It was demonstrated that plectin knockdown mutant keratinocytes have a reduction in the number of cells with keratin aggregates, accompanied by a reduced cell migration in scratch wound assays, a result consistent to the findings of plectin$^{-/-}$ fibroblasts (Andra et al., 1998) but different from that of plectin$^{-/-}$ keratinocytes (Osmanagic-Myers et al., 2006). On the contrary, plectin knockdown wild-type keratinocytes were able to migrate faster in scratch wound assay similar to that reported in (Osmanagic-Myers et al., 2006). These differences in results could possibly be attributed to the presence of different plectin isoforms, as expressed in

181

EBS-DM keratinocytes compared to normal keratinocytes. This particular switch in plectin isoforms might be important to cause a change in keratinocyte activation state so as to be "primed" for wound response. Further experiments will be needed to verify this idea.

In conclusion, the results in this chapter show that EGF signalling could play a role in regulating keratin remodelling in constitutively activated EBS-DM cells during cell migration, through modulating plectin levels. A schematic diagram summarising the results of Chapter 4 is depicted in Figure 4.14.
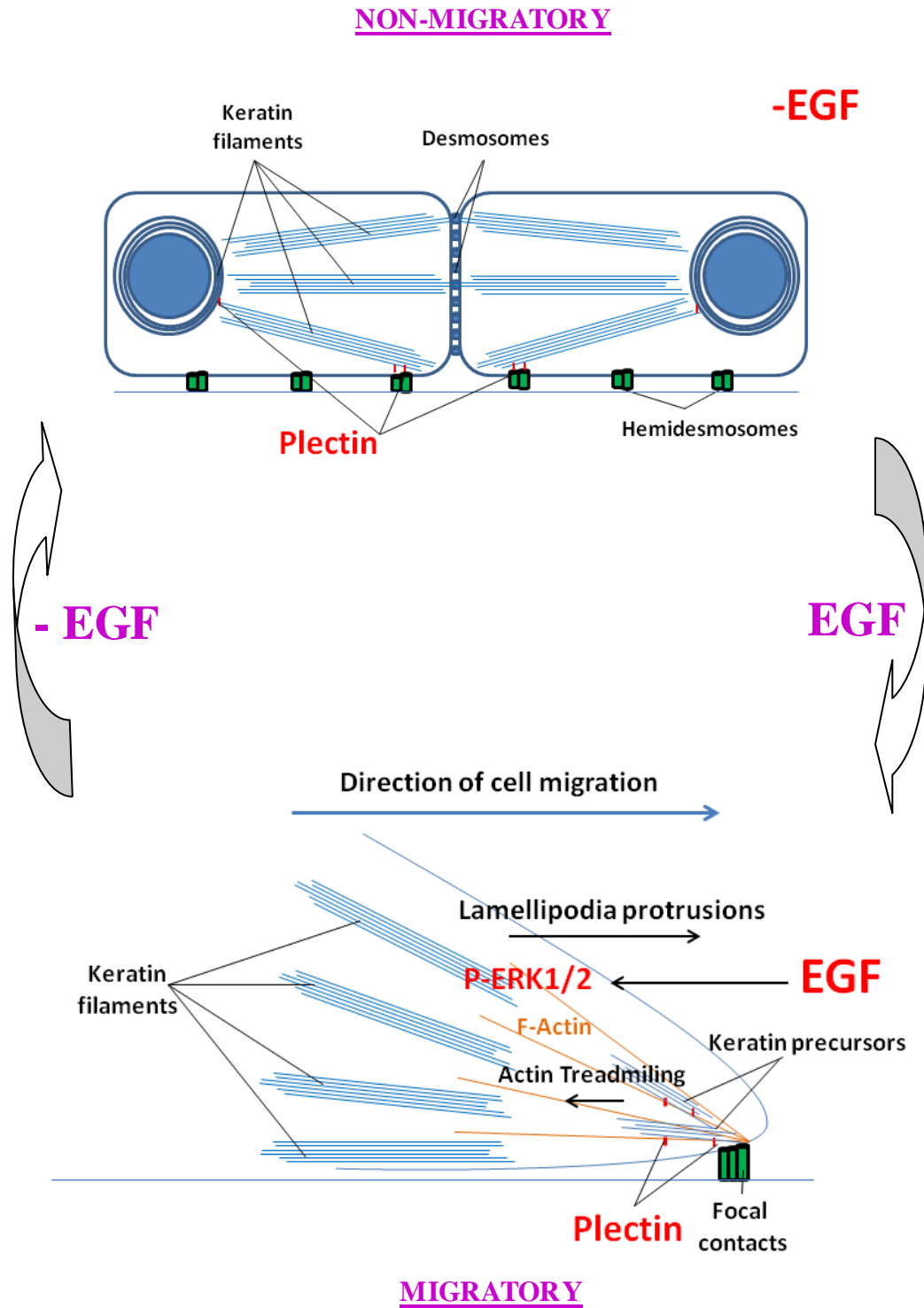
Figure 4.14 Schematic diagram summarising the results of Chapter 4.

CHAPTER 5

KERATIN PHOSPHORYLATION IN EBS

PATHOLOGY

5.1   Introduction

Structural modifications of keratin intermediate filaments, which ranges from physiological assembly and disassembly of keratin subunits, to detrimental keratin aggregation in many forms of stress and disease, are deemed to be important for cellular response to environmental cues (reviewed in Magin et al., 2004; Pekny and Lane, 2007; Godsel et al., 2008). These changes in keratin filament network is mostly mediated by phosphorylation, as seen in keratin reorganization upon sheer stress (Ridge et al., 2005), during cell division (Celis et al., 1985) and phosphatase inhibitor treatments (Paramio, 1999). The sites and extent of post-translational modifications that keratins can undergo are largely defined by their structural characteristics. For instance, the tripartite structure of keratins is comprised of a central α-helical coiled-coil domain flanked by the non-α-helical "head" and "tail" domains. It is well established that the "head" and "tail" domains are consensus sites for post-translational modifications such as glycosylation and phosphorylation, and have important mechanistic link to disease manifestations (reviewed in Omary et al., 2006). For example, mice that over-expressed human K8 S74A, which cannot be phosphorylated by SAPK at Ser74, had an increased predisposition to Fas-mediated liver injury than wild-type mice. This was further supported by mice over-expressing K8 G62C that showed a dramatic decrease in K8 Ser74 phosphorylation and a similar injury phenotype to the K8 S74A mutant (Ku and Omary, 2006). These studies demonstrated that the highly conserved S74-containing phosphoepitope (LLpSPL) of K8 could serve to sequester SAPK activity, thus acting as a "phosphate sponge" to protect tissues from injury (Ku and Omary, 2006). A similar function was also found for the phosphosite of K20 S13, which served as a unique marker for intestinal tissue injury (Zhou et al., 2006). In addition, transgenic mice expressing K18 S53A mutant

further revealed that this phosphosite was crucial in protecting hepatocytes from liver injury (Ku et al., 1998b). Moreover, mice that over-expressed human K18 S34A, which prevented Ser34 phoshorylation and 14-3-3 binding, resulted in abnormal mitotic bodies after partial hepatectomy and persistent 14-3-3 nuclear localization (Ku et al., 1998a; Ku et al., 2002). A role for keratin reorganisation was also found in a phosphosite of K8 S432, which was mediated by MAPK after EGF stimulation and cdc2 kinases during mitotic arrest respectively (Ku and Omary, 1997). Hence, these studies demonstrate that phosphorylation at the "head" and "tail" domains have importance in disease manifestions and that they play a role in keratin remodelling.

However, to date, there is limited experimental evidence of post-translational modifications occuring in the keratin rod domain, other than caspase-mediated cleavage of type I keratins occuring at the rod domain during apoptosis (Caulin et al., 1997; Ku et al., 1997; Ku and Omary, 2001) and a recent study showing sumoylation at rod 2B domain (Snider et al., 2011). The rod domain is comprised of heptad repeats, ie. repeats of seven amino acid residues (a-b-c-d-e-f-g)$_n$, in which positions "a" and "d" are generally occupied by hydrophobic residues that drive coiled-coil heterodimer formation. Positions "e" and "g" are normally occupied by hydrophilic and charged residues that may provide additional interactions to strengthen the binding. The starting residues of rod 1A domain and the ending residues of rod 2B domain, known as the helix initiation and the helix termination motifs respectively, comprise of ~ 20 amino acid sequence motifs that are highly conserved among the different keratins. These motifs are crucial for initiating keratin intermediate filament assembly and thus any mutations residing in these motifs will interfere with the early stages of filament elongation (Steinert et al., 1993).

In this chapter, it is hypothesized that phosphorylation can occur at the rod 1A domain because other post-translational modification such as sumoylation of lysine residues were found in the rod 2B domain (Snider et al., 2011). This hypothesis is tested using cell culture models and demonstrated that the tyrosine residue, but not the serine residue, located in K14 rod 1A domain could possibly be phosphorylated and gives rise to cells having peripheral aggregates, reminiscent to the appearance of EBS-DM cells. It is also shown that this phosphorylated tyrosine residue is responsible for increased stress response and contributes to cell migration, thus suggesting its role in the pathogenesis of EBS.

5.2   Results

5.2.1   Schematic diagram showing the position of possible keratin phosphorylation sites in the K14 rod 1A domain

Keratins are obligate heterodimers of epidermal type I (Steinert et al., 1983) and type II (Steinert et al., 1985) keratins in a 1:1 molar ratio, which exhibit a parallel, in-register alignment (Parry et al., 1985; Hatzfeld and Weber, 1990; Steinert, 1990). The pairing of type I (K14) and type II keratin (K5) is initiated by the rod 1A domain (helix initiation motif) and terminated at the rod 2B domain (helix termination motif). In the rod 1A domain of K14, the highly conserved arginine residue at 125 [in bold in Figure 5.1] is the "mutational hot spot" for being the most frequently mutated amino acid, giving rise to a wide spectrum of skin disorders ranging from epidermolysis bullosa simplex to epidermolytic hyperkeratosis (Szeverenyi et al., 2008). As can be seen from the helical model of K14 rod 1A domain, K14 R125 (positively charged residue) reside in the "g" position of the heptad repeat that is responsible for

electrostatic interactions between the asparagine residue of K5 at 176 (K5 N176) at the "e" position of the heptad repeat [Figure 5.1]. Residing beside K14 R125 residue is a serine residue at 128 (K14 S128) and a tyrosine residue at 129 (K14 Y129). K14 Y129 occupies in the "d" position of the heptad repeat that drives coiled-coil formation of the heterodimer between the phenylalanine residue of K5 at 179 (K5 F179) at the "a" position of the heptad repeat [Figure 5.1]. Hence, any alterations of these residues could disrupt heterodimer formation and lead to skin fragility disorders.

5.2.2 Muliple sequence alignment of human keratins (K12-K17) and its orthologs

To determine whether the serine and tyrosine residues residing in the helix initiation motif are conserved in the type I keratin family, a multiple sequence alignment of selected keratins (K12-K17) was performed. The clustalw results showed that the tyrosine residue was remarkably conserved in all the human keratins (K12-K17) and across its orthologs (*Mus musculus* and *Rattus norvegicus*) whereas even though the serine residue was also highly conserved in all the human keratins (K12-K17), it was not conserved across its orthologs as exemplified by K14 and K16 [Figure 5.2, multiple alignment using clustalw at www.interfil.org/toolClustal.php]. Reports pertaining to keratin mutations affecting the serine or tyrosine residues of the helix initiation motif were identified from the Human Intermediate Filament Database (www.interfil.org) and it was observed that these mutations were found to be associated with diseases such as epidermolytic palmoplantar keratoderma, epidermolytic hyperkeratosis, epidermolysis bullosa simplex and pachyonychia congenital types 1 and 2 [Table 5.1]. Interestingly, it was found out that K14 Y129D (a possible phospho-mimicking residue) gave rise to severe EBS-DM condition (Chan et al., 1996) whereas K14 Y129C (a possible non-phosphorylatable residue) gave rise

to a milder phenotype, intermediate between EBS-generalized and EBS-DM conditions (Rugg et al., 2007), suggesting that the disease phenotype was not due to the lost of the highly conserved hydrophobic tyrosine residue per se (since both mutations replace the tyrosine residue) but rather the charged status of K14 Y129 may be involved in determining the degree of heterodimer disruption and hence affect the severity of the skin fragility disorder. Since these two serine and tyrosine residues are potential phosphorylation sites for either serine/theronine or tyrosine kinases to act on, it is hypothesized that phosphorylation can occur at the rod 1A domain, typically at the helix initiation motif.

Figure 5.1 Schematic diagram showing the position of possible keratin phosphorylation sites at the K14 rod 1A domain.

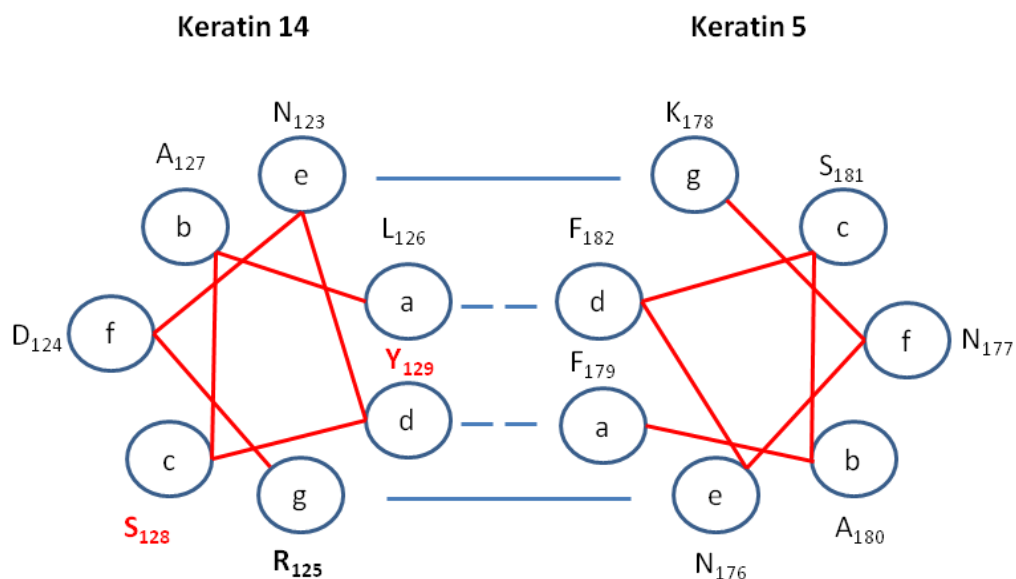**Figure 5.2   Multiple sequence alignment of human keratins (K12-K17) and its orthologs**

```
                                             defgabcdefg
Human|K12           LGILSGNDGGLLSGSEKETMQNLNDRLASYLDKVRALEEANTELENKIREWYETRGTGTA
R_norvegicus|K12    LCIFSGNDGGLLSGSEKETMQNLNDRLASYLGKVRALEEANAELENKIREWYETRRTGDS
M_musculus|K12      LCIFSGNDGGLLSGSEKETMQNLNDRLASYLGKVRSLEEANAELENKIREWYETRRTRDA

Human|K13           --DFGACDGGLLTGNEKITMQNLNDRLASYLEKVRALEEANADLEVKIRDWHLKQ---SP
R_norvegicus|K13    --DFGSVDGGLLSGNEKITMQNLNDRLASYLEKVRALEAANADLEVKIRDWHLKQ---SP
M_musculus|K13      --DFGGVDGGLLSGNEKITMQNLNDRLASYLDKVRALEAANADLEVKIRDWHLKQ---SP

Human|K14           -------GDGLLVGSEKVTMQNLNDRLASYLDKVRALEEANADLEVKIRDWYQRQ---RP
R_norvegicus|K14    SGFGGGLGDGLLVGSEKVTMQNLNDRLATYLDKVRALEEANSDLEVKIRDWYQRQ---RP
M_musculus|K14      GGLGGGIGDGLLVGSEKVTMQNLNDRLATYLDKVRALEEANTELEVKIRDWYQRQ---RP

Human|K15           --GFGGGDGGLLSGNEKITMQNLNDRLASYLDKVRALEEANADLEVKIHDWYQKQ---TP
R_norvegicus|K15    --DFGGGDGGLLSGNEKVTMQNLNDRLASYLDKVRALEEANTELEVKIRDWYQKQ---SP
M_musculus|K15      --DFGGGDGGLLSGNEKVTMQNLNDRLASYLDKVRALEQANTELEVKIRDWYQKQ---SP

Human|K16           --GGFAGGDGLLVGSEKVTMQNLNDRLASYLDKVRALEEANADLEVKIRDWYQRQ---RP
R_norvegicus|K16    --FGGGLGDGLLVGSEKVTMQNLNDRLATYLDKVRALEEANSDLEVKIRDWYQRQ---RP
M_musculus|K16      --LGGGIGDGLLVGSEKVTMQNLNDRLATYLDKVRALEEANRDLEVKIRDWYQRQ---RP

Human|K17           -------VDGLLAGGEKATMQNLNDRLASYLDKVRALEEANTELEVKIRDWYQRQ---AP
R_norvegicus|K17    -------VDGLLAGGEKATMQNLNDRLASYLDKVRALEEANTELEVKIRDWYQKQ---AP
M_musculus|K17      -------VDGLLAGGEKATMQNLNDRLASYLDKVRALEEANTELEVKIRDWYQKQ---AP
                      .*** *.** **********:** ***:** ** :** **::*:  :     .
```

Figure 5.2   Multiple sequence alignment of human keratins (K12-K17) and its orthologs using clustalw at www.interfil.org/toolClustal.php

Table 5.1   Patient keratin mutation (s) affecting the serine or tyrosine residues of the helix initiation motif

Type I keratin	Serine mutation (s) / Disease phenotype / Original report		Tyrosine mutation (s) / Disease phenotype / Original report	
K9	No report yet		**Y167del ins WL**/ Epidermolytic palmoplantar keratoderma / (He et al., 2004)	
K10	No report yet		**Y160D** / Epidermolytic hyperkeratosis / (Chipev et al., 1994)	**Y160S** / Epidermolytic hyperkeratosis / (Arin et al., 1999)
K14	**S128del** / EBS-DM / (Wood et al., 2003; Bolling et al., 2011)	**S128P** / EBS-DM / (Jerabkova et al., 2010)	**Y129D** / EBS-DM / (Chan et al., 1996)	**Y129C** / Severity intermediate between EBS-generalized and EBS-DM / (Rugg et al., 2007)
K16	**S130del** / Pachyonychia congenital type 1 / (Smith et al., 1999; Wilson et al., 2011)		No report yet	
K17	**S97del** / Pachyonychia congenital type 2 / (Terrinoni et al., 2001)		**Y98D** / Pachyonychia congenital type 2 / (Smith et al., 1997)	

Table 5.1   Reports pertaining to keratin mutations affecting the serine or tyrosine residues of the helix initiation motif were identified from the Human Intermediate Filament Database (www.interfil.org).

5.2.3 Spontaneous formation of keratin aggregates in K14 Y129 but not K14 S128 phospho-mimetic cells

To test the hypothesis, several EGFP-tagged constructs that were phospho-null (K14 S128A and K14 Y129F) and phospho-mimetic (K14 S128D and K14 Y129E) were generated using site-directed mutagenesis [Figure 5.3 (i)]. By transiently expressing these EGFP-tagged constructs in NEB-1 cells, it was observed that the phospho-mimetic construct EGFP-K14 Y129E gave rise to cells that have peripheral aggregates, whereas EGFP-K14 S128D gave rise to cells with only filamentous keratin networks, a phenotype similar to phospho-null constructs EGFP-K14 S128A and EGFP-K14 Y129F [Figure 5.3 (ii)]. These observations suggested that altering the charge of K14 Y129 residue (negatively charged K14 Y129E mimicking phosphorylation) could affect keratin remodelling during filament elongation (similar to EGFP-K14 R125P cells described in Chapter 4) but not negatively charged K14 S128 residue (K14 S128D), hence supporting a role for phosphorylation at the rod 1A domain, particularly targeting the K14 Y129 residue.

However, the conventional view of keratin structure suggests that in normal physiological condition the K14 Y129 residue at position "d" of the heptad repeats would be buried in the hydrophobic core of the heterodimer, thus making it less accessible to kinase action. It was of interest to find out if shifting this tyrosine residue away from its position "d" to a position "c" at the outermost positions of the coiled coil, making it readily accessible to kinase action, would affect keratin remodelling. The results showed that by expressing EGFP-K14 S128del in NEB-1 cells, which could shift the K14 Y129 residue from the "d" to a "c" position [Figure 5.3 (iii)], cells with peripheral aggregates were observed [Figure 5.3 (ii)], suggesting that K14 Y129, now being accessible, could possibly be phosphorylated to give rise to

this phenotype. One might argue that the deletion of K14 S128 residue could distort the entire keratin protein sequence and thus gave rise to keratin aggregates. Helical wheel modelling of the residues repositioned by deleting K14 S128 revealed that both the hydrophobic and electrostatic interactions would be restored by K14 L130 (hydrophobic) occupying the "d" position and K14 D131 (negatively charged) occupying the "g" position [Figure 5.3 (iii)]. Hence, deleting K14 S128 residue should not affect the helical structure to a significant extent. This prediction was supported by a control experiment in which EGFP-K5 S181del was expressed in NEB-1 cells: this construct shifts the K5 F182 residue to the "c" position [Figure 5.3 (iv)]. This gave rise to cells with filamentous keratin networks [Figure 5.3 (ii)]. Helical wheel modelling again predicted that reshuffling the residues by deleting K5 S181 would retain both the hydrophobic and electrostatic interactions by placing K5 I183 (hydrophobic) in the "d" position and K5 D184 (negatively charged) in the "e" position [Figure 5.3 (iv)]. Hence, the deletion of K5 S181 did not affect the helical structure to a significant extent, as it did not generate a dominant negative or disruptive phenotypes and the recombinant K5 is still able to incorporate into filaments.

These data demonstrated that deletion of an amino acid at these 'c' positions in the helix initiation motif does not per se disrupt the keratin network, due to the compensation by adjacent hydrophobic and charged residues that maintained appropriate electrostatic interactions. Thus, the severe pathogenic effect of the K14 mutations S128del and Y129D are unlikely to be due to misfolding of the helix, but to the altered phosphorylation status of the mutant protein. It was also interesting to note that patients harbouring serine deletions at the helix initiation motif of K14 or

K16/K17 suffered from EBS-DM or pachyonychia congenital type I/II respectively [Table 5.1].

One obstacle to the hypothesis of phosphorylation acting on the rod domains has always been the prediction that the coiled-coil rod domains woud be inaccessible to kinase action. However, this obstacle may be lessened by recent suggestion that the helix 1A region of keratins may not be as tightly folded as was previously thought (Parry et al., 2002; Smith et al., 2002; Strelkov et al., 2002). It was suggested that in the intermediate filament dimer, the head domain may fold back across helix 1A and the dimer may alternate between a two-stranded coiled-coil rope and two separate α-helical strands, with linker L1 acting as a flexible hinge (Parry et al., 2002; Strelkov et al., 2002). It was postulated that this arrangement could be destabilized under appropriate conditions such as phosphorylation or in the presence of cations, which could cause the head domain to detach from the surface of the dimer, thereby unwinding the α-helical strands of the two-stranded coiled-coil segment 1A, and the separation was facilitated by the extended linker L1 (Smith et al., 2002).

NEB-1
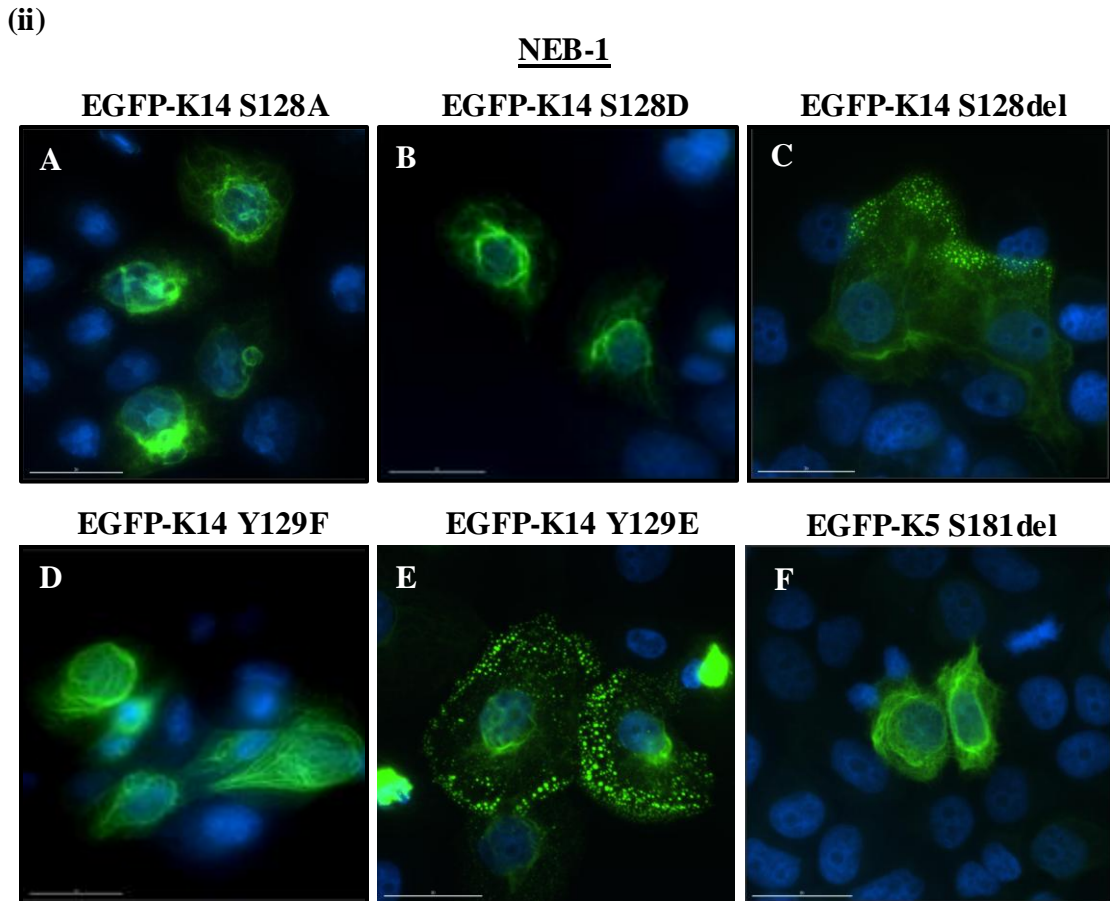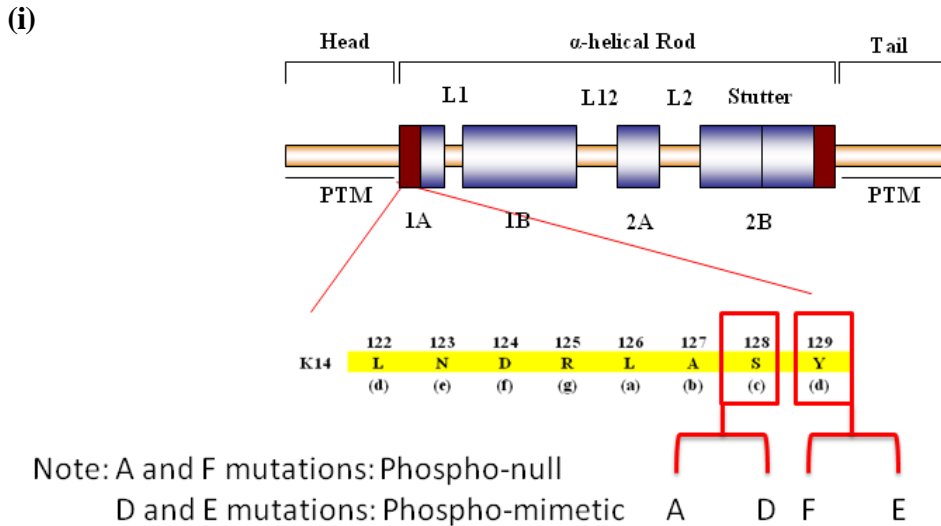
Figure 5.3 (i) Schematic diagrams showing the mutations of K14 S128 and K14 Y129 at helix initiation motif to generate phosphomimetics (ii) Spontaneous formation of keratin aggregates in K14 Y129 but not K14 S128 phosphomimetic cells. Keratin aggregates co-existed with filaments in phosphomimetic cells. (ii) Transient expression of (A) EGFP-K14 S128A, (B) EGFP-K14 S128D, (C) EGFP-K14 S128del, (D) EGFP-K14 Y129F, (E) EGFP-K14 Y129E and (F) EGFP-K5 S181del in NEB-1 keratinocytes. Scale bar, 30 μm.

Keratin 14   **Keratin 5**
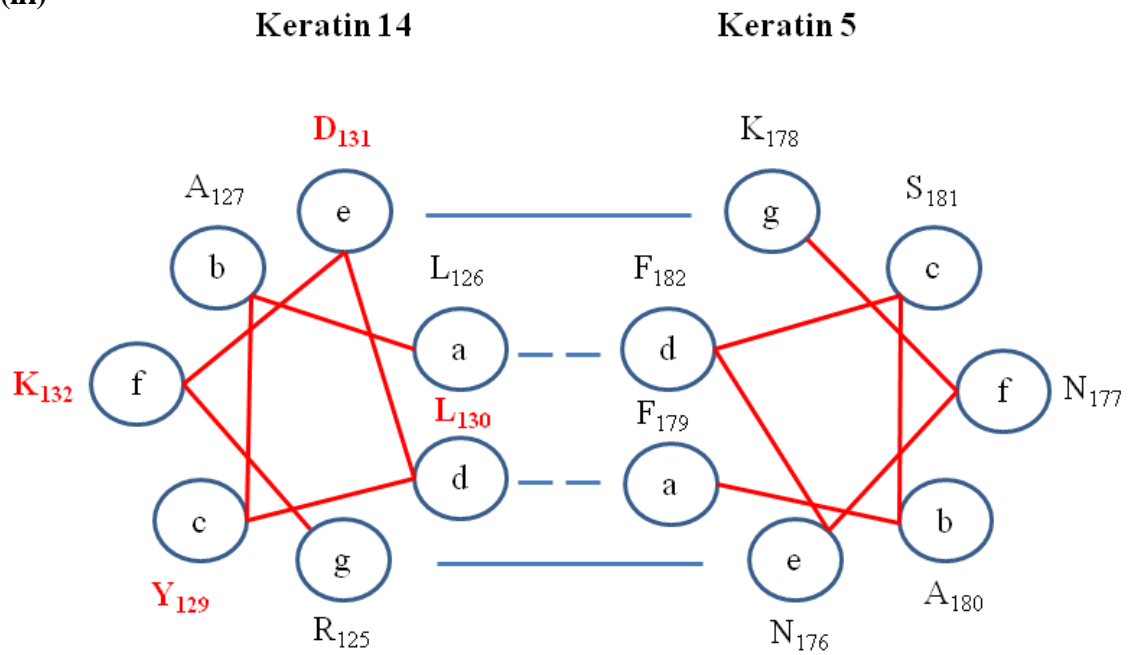
Figure 5.3 (iii) Schematic diagrams showing the shift of K14 Y129 from "d" to a "c" position after K14 S128 is deleted. Note that the interactions between the hydrophobic cores are restored by K14 L130 shifting to the "d" position and electrostatic interactions are also restored by K14 D131 shifting to the "e" position.

Keratin 14   **Keratin 5**
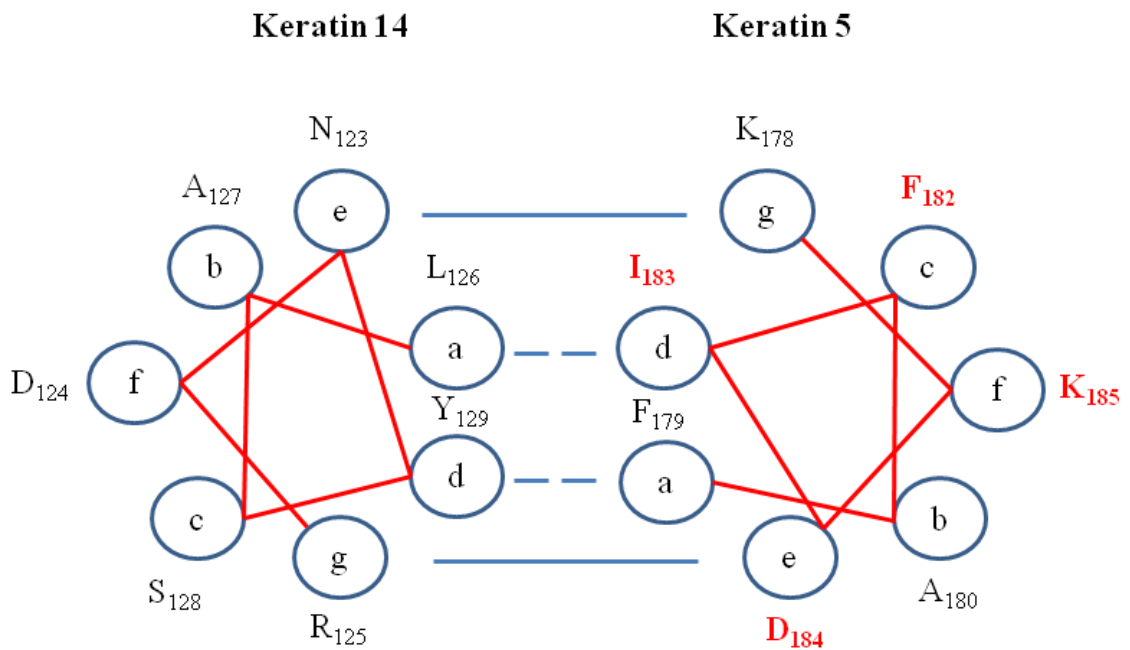
Figure 5.3 (iv) Schematic diagrams showing the shift of F182 from "d" to a "c" position after K5 S181 is deleted. Note that the interactions between the hydrophobic cores are restored by K5 I183 shifting to the "d" position and electrostatic interactions are also restored by K5 D184 shifting to the "e" position.

5.2.4 Similar keratin aggregates seen in K14 R125P and K14 Y129E cells

Stable cell lines expressing these phospho-mimetic constructs in N/TERT-1 cells were generated, and a similar phenotype of peripheral keratin aggregates was confirmed in both AcGFP-K14 R125P and AcGFP-K14 Y129E cells [Figure 5.5 (i)]. Ratios of exogenous (transfected) to endogenous K14 expression were compared in all the stable cell lines and found to be close to a 1:1 ratio [Figure 5.5 (ii)]. Hence, the peripheral keratin aggregates observed in the AcGFP-K14 Y129E cells were inherently due to K14 Y129E mutation and did not represent artefacts of over-expression resulting from the AcGFP-tag.

5.2.5 Sustained stress activation in phosphomimetic cells during osmotic stress

Since AcGFP-K14 Y129E cells showed the same phenotype as AcGFP-K14 R125P cells, it was of interest to find out whether they have similar stress response to osmotic stress as determined in the EGFP-K14 R125P cells in Chapter 3. It was observed that there was a higher level of p38 kinase activation after 240 min recovery from osmotic stress treatment in the phospho-mimetic keratinocytes, but not the phospho-null keratinocytes [Figure 5.5]. This suggested that the presence of keratin aggregates could predispose these mutant keratinocytes to sustained stress activation.

(i)

AcGFP-K14 WT   **AcGFP-K14 R125P**   **AcGFP-K14 S128del**

AcGFP-K14 Y129F   **AcGFP-K14 Y129E**

(ii)
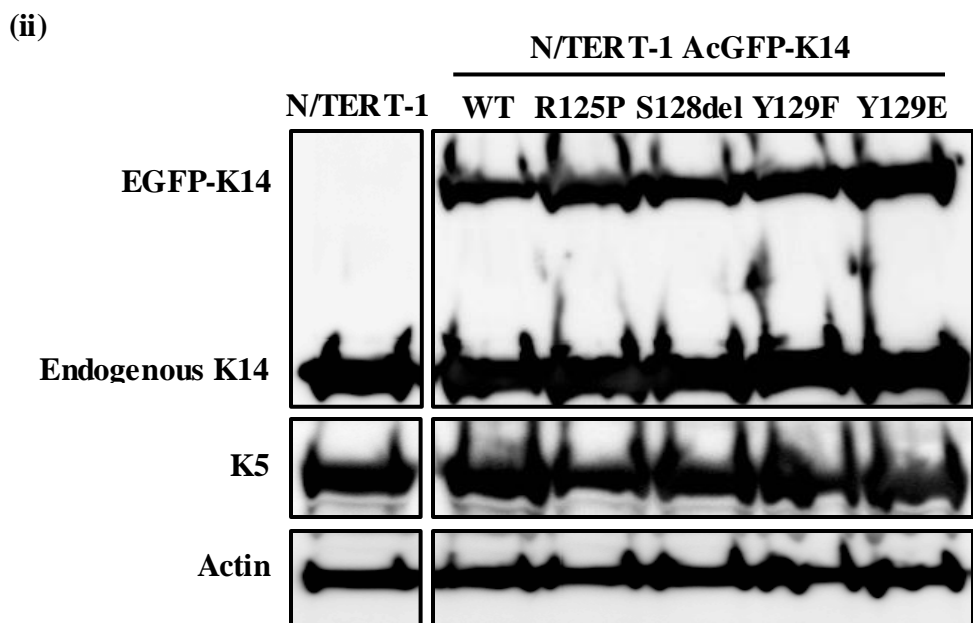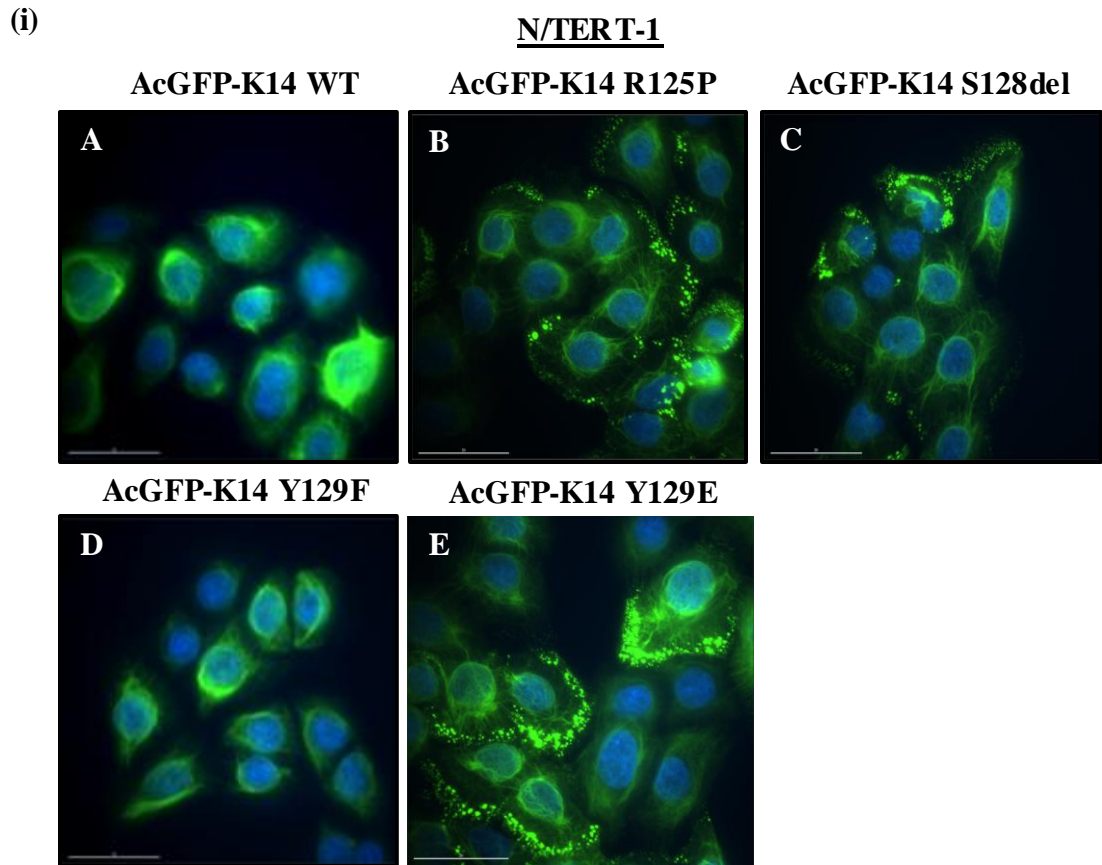
Figure 5.4 Similar keratin aggregates seen in AcGFP-K14 R125P and AcGFP-K14 Y129E cells. Phosphorylation of K14 Y129 may contribute to keratin aggregate formation. (i) Stable expression of (A) AcGFP-K14 WT, (B) AcGFP-K14 R125P, (C) AcGFP-K14 S128del, (D) AcGFP-K14 Y129F and (E) AcGFP-K14 Y129E in N/TERT-1 keratinocytes. Scale bar, 30 μm. (ii) Insoluble fractions of cell extracts were prepared from these cell lines at subconfluence. Immunoblot analysis of these cell lysates shown using antibodies to K14 (LL001) and K5 (XM-26). Actin used as loading control.

(i)
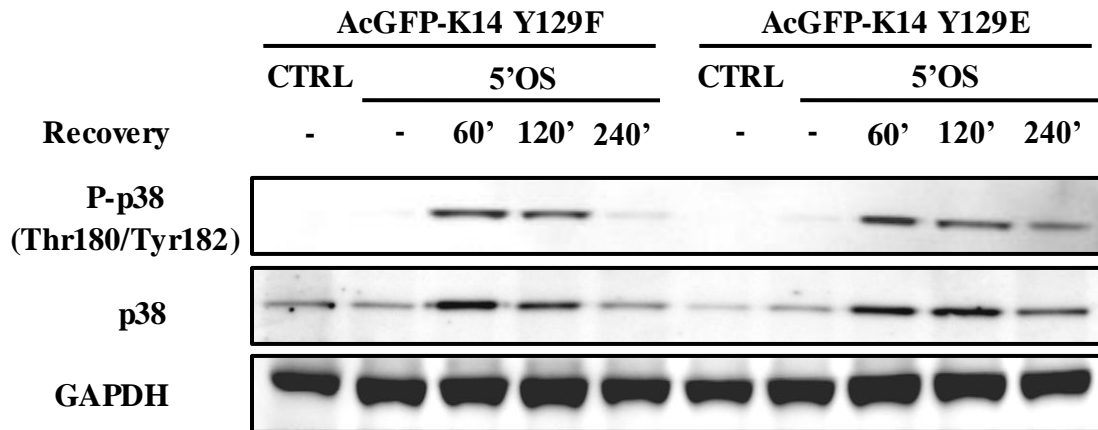
(ii)
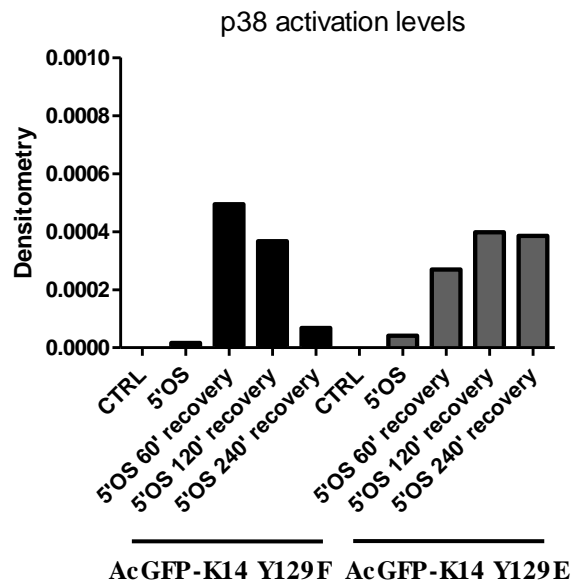
Figure 5.5 Sustained stress activation in phosphomimetic cells during osmotic stress. Phosphomimetic cells have sustained levels of stress-activated protein kinases (P-p38). (i) AcGFP-K14 Y129F and AcGFP-K14 Y129E cells were exposed to 5 min of 150 mM urea treatment, and left to recover for 60 min, 120 min and 240 min respectively. Soluble fractions of cell extracts were prepared from these cells. Immunoblot analysis of these cell lysates shown using antibodies to P-p38 (Thr180/Tyr182) and p38. GAPDH used as loading control. (ii) Densitometry values of P-p38 protein levels for the respective cell lines at different conditions, normalized to total p38 and GAPDH loading control.

5.2.6 Phospho-null cells close up wound slower than wild-type cells in scratch wound assays

To determine whether K14 Y129 phosphorylation state could play a role in cell migration, both the AcGFP-K14 WT and phospho-null AcGFP-K14 Y129F cells were subjected to scratch wound assays [Figure 5.6 (i)]. It was found that there was a significant decrease (* $p < 0.05$) in wound closure in these phospho-null AcGFP-K14 Y129F cells (0.78 ± 0.14) as compared to AcGFP-K14 WT cells (0.91 ± 0.13) [Figure 5.6 (ii)], thus suggesting that the phosphorylation state of K14 Y129 affects cell migration.

5.2.7 Double mutant AcGFP-K14 R125P_Y129F infected cells form less peripheral keratin aggregates than AcGFP-K14 R125P infected cells

Knowing that K14 Y129 phosphomimetic construct increased the stress response in AcGFP-K14 Y129E cells through the formation of keratin aggregates and that phospho-null AcGFP-K14 Y129 reduced cell migration, it was hypothesized that K14 R125P mutants may have an intrinsic effect through phosphorylation at K14 Y129. A AcGFP-K14 R125P_Y129F double mutant construct was therefore generated to introduce both K14 R125P (hypothetical phosphorylation facilitator) and K14 Y129F (phospho-null mimetic) into the same cell. Both lentiviral-packaged AcGFP-K14 R125P and AcGFP-K14 R125P_Y129F constructs were collected for transient infections of N/TERT-1 cells at different multiplicity of infections (M.O.Is = 0.5, 1.0 and 2.0) [Figure 5.7 (i-ii)]. The number of keratinocytes with peripheral aggregates were counted and compared at the same infection efficiency. It was observed that there was a significant decrease (** $p < 0.01$) in the number of cells with aggregates in the double mutant AcGFP-K14 R125P_Y129F cells (4.01 ± 1.05 %) as compared

to those with only the AcGFP-K14 R125P construct (9.11 ± 0.80 %) [Figure 5.7 (ii)]. This supports the hypothesis that phosphorylation of K14 Y129 is part of the mechanism generating aggregates in the K14 R125P mutant cells. This could be due to disruption of keratin heterodimer formation (by proline residue) increasing accessibility of tyrosine kinase to phosphorylate the K14 Y129 residue.

(i)

(ii)
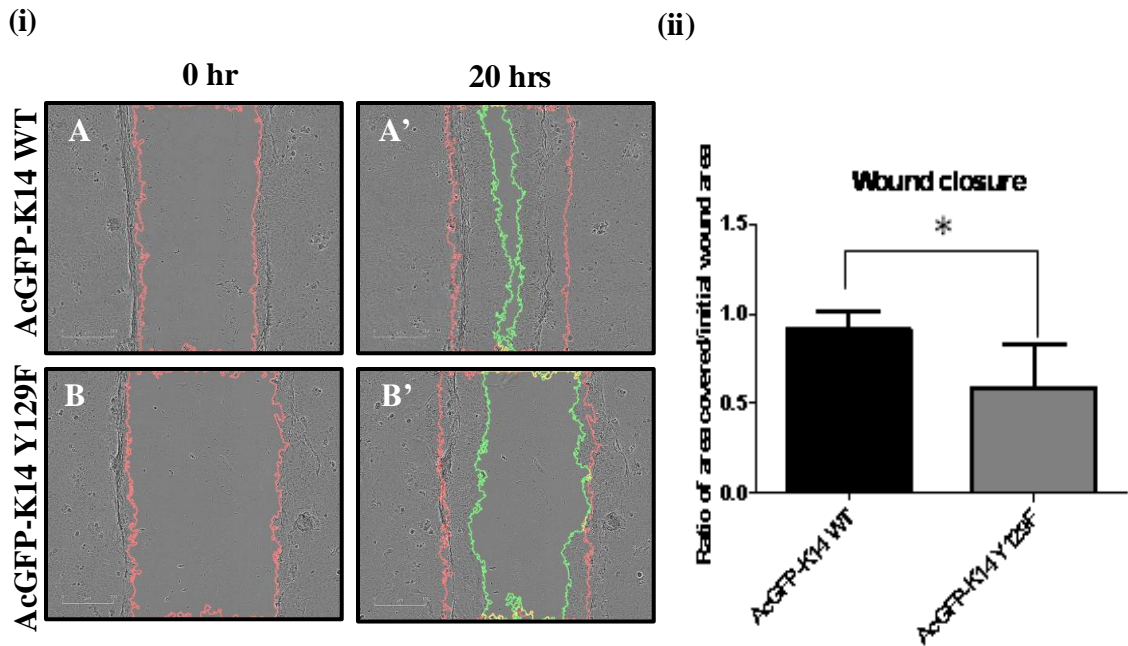
Figure 5.6 Phospho-null cells close up wound slower than wild-type cells in scratch wound assay. K14 Y129 phosphorylation affects cell migration. (i) AcGFP-K14 WT and AcGFP-K14 Y129F cells grown to confluence in an Essen ImageLock 96-well plate were subjected to wounding with a 96-well WoundMaker Tool. Images were acquired immediately and at 1 hr intervals for 20 hrs using the IncuCyte imaging system. Data were then processed by ImageJ software. Red line marks the denuded area from which cells were removed at the start of the wound (0 hr); green line marks the remaining uncovered area after 20 hrs wound closure time (20 hrs). (ii) Areas between red (or green) lines were derived from a macro written with ImageJ. Data presented as ratio of area covered/initial wound area and as mean ± S.D for n = 3 of each group. Statistical significance was assessed by unpaired t-test, * $p <$ 0.05 vs. AcGFP-K14 WT group.

(i)
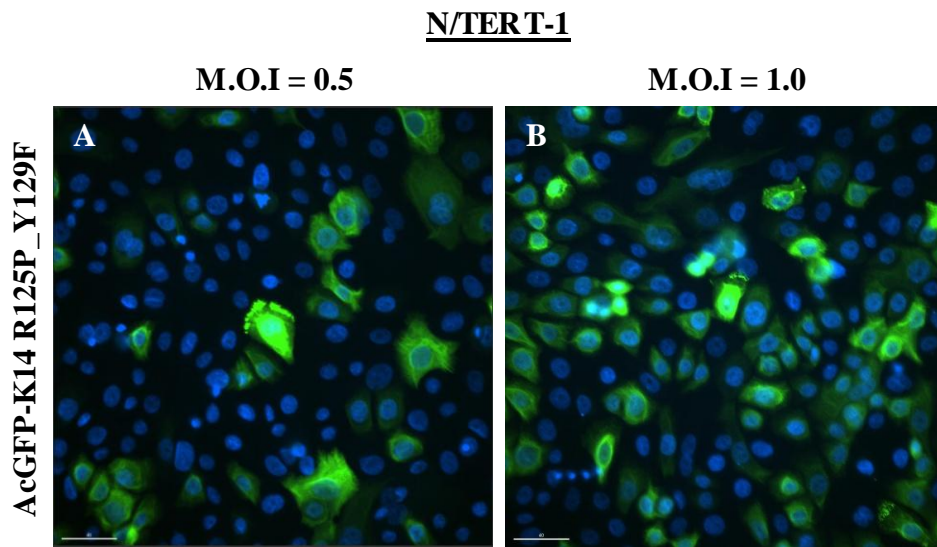
(ii)
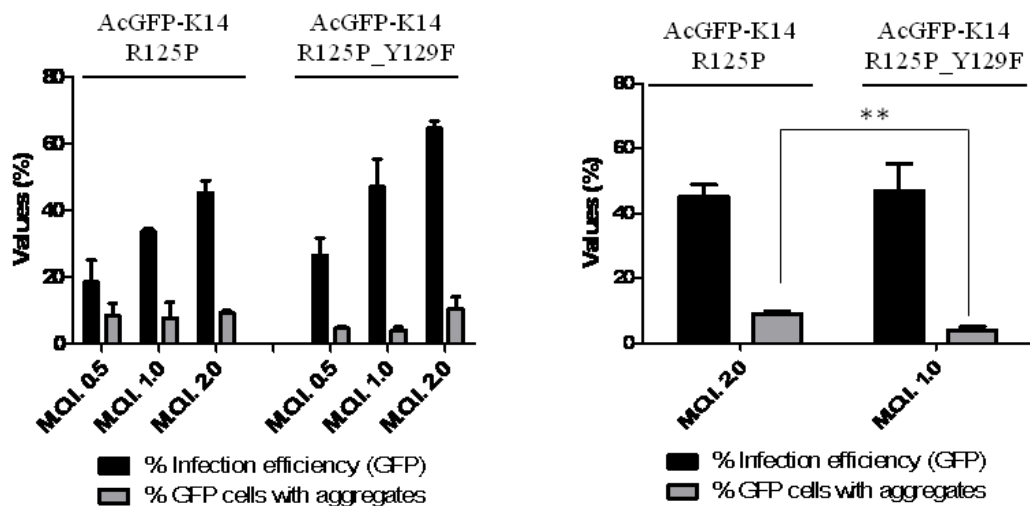
Figure 5.7 Double mutant AcGFP-K14 R125P_Y129F infected cells form less peripheral keratin aggregates than AcGFP-K14 R125P infected cells. A decrease in keratin aggregates of EBS-DM cells was associated with non-phosphorylatable K14 Y129. (i) N/TERT-1 cells were transiently infected with the viral-packaged AcGFP-K14 R125P_Y129F double mutant construct for 72 hrs before fixation. Immunofluorescence images showing the effects of viral-packaged double mutant AcGFP-K14 R125P_Y129F construct at increasing multiplicity of infection (M.O.I.) values from 0.5 to 1.0. Scale bar, 40 μm. (ii) Bar graphs showing the effects of viral-packaged AcGFP-K14 R125P and AcGFP-R125P_Y129F constructs at increasing M.O.I. values on keratin aggregate formation. Cells were counted in each of the viral infected group at each M.O.I. using ImageJ and quantified. Data presented as % infection efficiency (No. of GFP positive cells/total no. of cells x 100%) and % GFP cells with aggregates (No. of GFP cells with aggregates/ No. of GFP cells x 100%) and as mean ± S.D for n = 3 sets of 500-3000 cells counted. Statistical significance was assessed by unpaired t-test, ** $p < 0.01$ vs. AcGFP-K14 R125P group of M.O.I. = 2.0.

5.3   Discussion

The findings in this chapter raise several novel and important aspects of keratin modifications in the pathogenesis of EBS-DM. (1) These results revealed the first suggestion of phosphorylation in the helix initiation motif of K14 rod 1A domain, i.e. at the K14 tyrosine 129 residue, and suggest that this may be involved in EBS pathogenesis. (2) Evidence is presented suggesting that the Dowling-Meara mutation at K14 R125 is less likely to give rise to aggregates if the tyrosine residue K14 Y129 cannot be phosphorylated. (3) These data also suggest that phosphorylation of K14 Y129 might be an indication of a keratinocyte activated state due to increased keratin remodelling and cell migration.

Keratin intermediate filaments are organised into a dynamic scaffold that form the cytoskeleton of the cell. The keratin subunits are constantly undergoing a reversible process of assembly and disassembly during mitosis and in response to various stress stimuli (reviewed in Goldman et al., 2008). One of the more established mechanism through which keratin assembly is modulated is via keratin phosphorylation by protein Ser/Thr kinases as exemplified by K8, K18 and K19 (Chou and Omary, 1991; Zhou et al., 1999). However, tyrosine phosphorylation in keratins is not as well characterized as serine phosphorylation because there were barely detectable phospho-tyrosine levels in crude epidermal keratin preparations (Steinert et al., 1982) or low levels of phosphorylated tyrosine residue were seen in keratins upon exposure to EGF treatment (Aoyagi et al., 1985). Previous studies had also shown indirectly that the tyrosine residues in K8 and K19 could be phosphorylated by inhibition of tyrosine phosphatases using the potent and irreversible tyrosine phosphatase inhibitor pervanadate (Feng et al., 1999), and that tyrosine phosphorylation was involved in the rapid and reversible keratin network remodeling through the use of orthovanadate,

another tyrosine phosphatase inhibitor (Strnad et al., 2002). Although these studies showed that tyrosine phosphorylation could occur in keratins, they did not specify the identity of the tyrosine residue being phosphorylated until recently, a direct evidence that K19 could be phosphorylated on its tyrosine-391 residue located at the tail domain was demonstrated (Zhou et al., 2010).

The results in this chapter demonstrate that tyrosine phosphorylation is also possible in the rod 1A domain of K14, at the K14 Y129 residue residing in the helix initiation motif. This K14 Y129 residue is located at the "d" position of the heptad repeats necessary for driving coiled coil formation of the heterodimer, and is highly conserved in all the epidermal keratins and across its orthologs. Mutation in this tyrosine residue (ie. K14 Y129D) results in significant structural distortions of the α-helical backbone (Smith et al., 2004), which could explain why patients harboring this kind of mutation suffer from EBS-DM (a severe skin blistering disorder) (Chan et al., 1996). Interestingly, a variant of the K14 Y129 mutation (K14 Y129C) results in patients suffering from a milder phenotype of skin blistering disorder, intermediate between EBS-generalized and EBS-DM (Rugg et al., 2007), suggesting that replacing the highly conserved tyrosine residue did not contribute to the severity of blistering disorder per se but rather the charge of the mutated residue or the degree of structural distortion was the determinant factor. In this study, the possibility of tyrosine phosphorylation at this K14 Y129 residue was explored by generating phospho-mimetic (K14 Y129E) and phospho-null (K14 Y129F) constructs. It was demonstrated that the phospho-mimetic expression resulted in cells having peripheral keratin aggregates as opposed to the phospho-null construct. Since the formation of keratin granules or aggregates are largely thought to be mediated by phosphorylation due to their appearance in response to various phosphatase inhibitors (Kasahara et al.,

1993; Takuma et al., 1993; Yatsunami et al., 1993; Feng et al., 1999; Strnad et al., 2001), it was clear that K14 Y129 phosphorylation was contributing to keratin aggregate formation. The possibility that K14 S128 could be phosphorylated was not apparant because over-expression of K14 S128D did not result in cells having keratin aggregates.

In normal physiological conditions, apolar residues occupying the "a" and "d" positions of the heptad repeats are packed together in the interior of the helix bundle (hydrophobic core), whereas those hydrophilic residues occupying the "e" and "g" positions have opposing charges and form a salt bridge stabilized by electrostatic interactions that are in contact with the solvent-exposed surface, hence shielding the apolar residues from the aqueous environment (Pauling and Corey, 1953). It was of interest to find out whether by shifting the K14 Y129 residue out of the hydrophobic core to the exterior surfaces of the helix would it increase its probability of being phosphorylated. With this in mind, K14 S128del and K5 S181del constructs were generated and it was demonstrated that deleting these residues itself did not hinder the formation of keratin heterodimer as observed in K5 S181del over-expression (filamentous keratin network) and that the appearance of keratin aggregates in K14 S128del was largely due to the shifting of K14 Y129 residue to the "c" position of the heptad repeats that might increase its phosphorylation state as opposed to the shifting of a phospho-null K5 F182 to the "c" position of the heptad repeats in K5 S181 deletion.

Stable cell lines harbouring the phospho-mimetic and phospho-null expression constructs were generated and it was demonstrated that the phospho-mimetic AcGFP-K14 Y129E cell line has intrinsic and sustained stress kinase activation which was reminiscent to the EBS-DM cell lines (AcGFP-K14 R125P), thus strengthening the

role of keratin aggregates as an indicator for keratinocyte activation as described in Chapter 3. It was also shown that the phosphorylation state of K14 Y129 might play a role in cell migration since AcGFP-K14 Y129F cells closed up wound slower than AcGFP-K14 WT cells.

EBS-DM cells harbouring the K14 R125P mutation are known to exhibit faster cell migration and intrinsic stress response (as discussed in Chapter 3). A proline mutation in this position is likely to be disruptive to helical formation, since it was previously reported that a proline residue residing in the α-helical strand could result in a kink of the α-helix axis by about 26º (Barlow and Thornton, 1988). Because the K14 Y129 residue (d) resides beside the K14 R125 residue (g) in the helical structure, a K14 R125P mutation could distort the helical structure and expose K14 Y129 residue to the exterior and thus facilitate its phosphorylation. This notion was tested by simultaneously introducing mutations at both these residues in N/TERT-1 cells. It was demonstrated that there was a significant decrease in the number of keratinocytes with aggregates in the transiently infected AcGFP-K14 R125P_Y129F double mutant cells as compared to the AcGFP-K14 R125P transiently infected cells. In conclusion, these results support the hypothesis that Y129 phosphorylation could play a role in the pathogenesis of EBS-DM condition. A schematic diagram summarising the results of Chapter 5 is depicted in Figure 5.8.

It would be interesting to find out which tyrosine kinase may be involved in phosphorylating K14 Y129 residue, as this could be important in regulating the stress response in wound-induced situations. Potential tyrosine kinases could be FAK (Schaller et al., 1992) or Src (sarcoma) kinases (Oppermann et al., 1979) because these tyrosine kinases are known to play a role in cell migration and recent study has shown that FAK-Src complex could regulate adhesion turnover through paxillin, ERK

and myosin light-chain kinase at the leading edge (Webb et al., 2004), rendering them in close proximity to the keratin aggregates. Further work will be done to investigate this possibility.

In summary, the results in this chapter have opened up new avenues for strategies targeting post-translational modifications of keratins in view of the treatment of devastating skin blistering disorders ranging from epidermolysis bullosa simplex to epidermolytic hyperkeratosis. In this case, phospho-Y129 could be a useful biomarker of keratinocyte activation. More work is needed to validate this hypothesis.

Direction of cell migration

Lamellipodia protrusions

Keratin filaments

K14 Y129 - P

F-Actin

Focal contacts

MIGRATORY
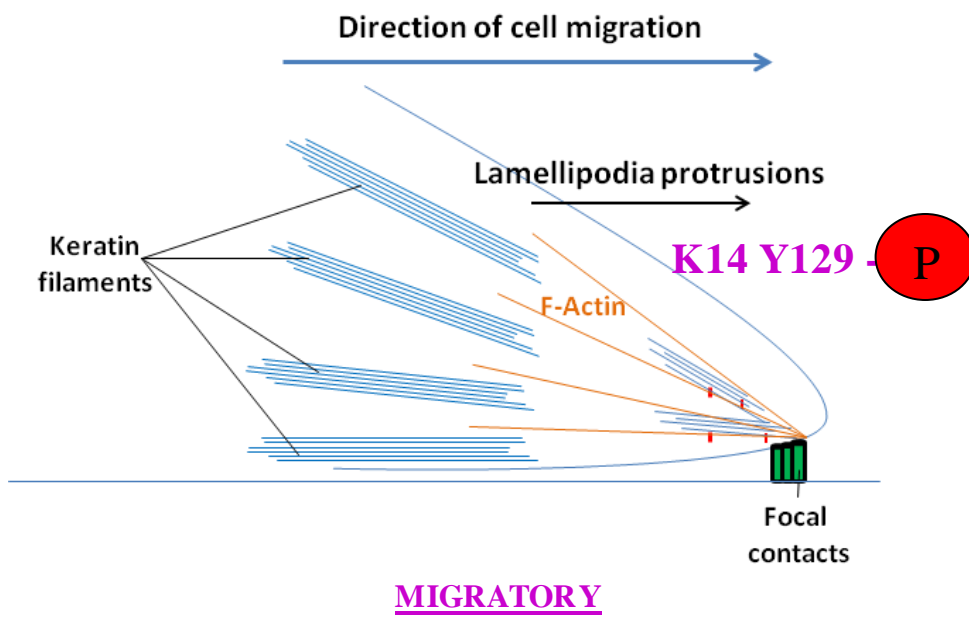
Figure 5.8 Schematic diagram summarising the results of Chapter 5.

CHAPTER 6

SIGNIFICANCE AND IMPLICATIONS OF

THESE STUDIES

6.1   Significance and implications of these studies

In the introduction to this thesis (Chapter 1), a literature review of epidermal tissue maintenance is presented, describing a process in which differential keratin expression in keratinocytes is regulated as the cells migrate upwards through the epidermal layers, paralleled by changes in expression of adhesion junctions. A defect in any of these cytoskeletal components (keratins or junctional proteins) can result in epidermal malfunction, mainly resulting in skin blistering disorders. Hence, these cytoskeletal components are important for providing mechanical resilience to the skin. In mechanical injury, the normal processes of keratinocyte differentiation are perturbed and keratinocytes initiate an activation cycle (Freedberg et al., 2001) that takes them through the wound healing process and back to a steady state after epidermal regeneration. Wound healing is a tightly regulated sequence of events wherein cell-matrix junctional proteins are altered (partial dissolving of hemidesmosomes), and the keratinocytes produce a different set of integrins for lateral migration and express matrix metalloproteinases for remodelling of the provisional matrix at the wound bed (reviewed in Santoro and Gaudino, 2005). An impaired wound healing process can lead to the formation of chronic (non-healing) wounds such as diabetic ulcers and pressure ulcers (Menke et al., 2007), where the epidermis is hyperpoliferative (indicated by mitotically active cells in the suprabasal layers), hyperkeratotic (indicated by thick cornified layer) and parakeratotic (indicated by presence of nuclei in the cornified layer). These histological observations suggest that the chronic wound keratinocytes do not sucessfully complete either the activation (keratinocytes are able to proliferate but do not migrate) or differentiation (incomplete differentiation due to presence of nuclei in cornified layer) stage of the keratinocyte activation cycle (Morasso and Tomic-Canic, 2005). Hence, chronic wounds failed to

proceed through an orderly and timely process of healing, resulting in poor anatomical and functional outcome (Lazarus et al., 1994).

Because knowing the mechanisms underlying keratinocyte activation cycle is crucial to understanding wound healing processes, it was of interest to explore and attempt to unravel the mechanisms underlying these processes in this thesis work. In Chapter 3 of this thesis, the EBS-DM keratinocytes (harbouring K14 R125P mutation) were shown to be a valid cell culture model of activated keratinocytes because of their intrinsic stress and upregulation of wound-response proteins, predisposing them to migrate faster in wound closure assays as reported in previous studies (D'Alessandro et al., 2002; Morley et al., 2003). Thus, EBS-DM keratinocytes may be a useful model for analysing early stages of epidermal wound activation. It is also suggested that the appearance of keratin aggregates (keratin remodelling at the leading edge) could be an indicator of the activated state because aggregates diminished or disappeared when monolayer keratinocytes approached the quiescent state of the keratinocyte activation cycle upon increasing confluence (mimicking wound closure).

Desmosomes are now known to be highly dynamic structures that are assembled during cell-cell contact. This desmosomal assembly is a coordinated process, with an initial phase of rapid desmoplakin accumulation at cell-cell borders, followed by the assembly and translocation of cytoplasmic particles containing both desmoplakin and plakophilin, mediated by both desmoplakin-intermediate filament interactions and actin microfilaments (Godsel et al., 2005). Moreover, a recent study has shown that desmoplakin assembly and dynamics in migrating epithelial cells is initially dependent on actin microfilaments prior to association with keratin intermediate filaments, thus revealing a role for desmosomal assembly during wound healing (Roberts et al., 2011). The EBS-DM keratinocytes used here reflect similar

desmoplakin changes, as a change in localization of desmoplakin was seen to occur upon transition from subconfluence to confluence, i.e. from cytoplasmic desmoplakin (subconfluent, activated state) to desmoplakin at cell-cell adhesion borders (confluent, approaching quiescent state).

Previous studies have proposed a role of K17 in the timely closure of embryonic skin wounds (Mazzalupo et al., 2003), and it has been reported that K17 induction can regulate cell growth via controlling protein synthesis during the wound healing process (Kim et al., 2006). In the present study, it was also demonstrated that during reversion from confluent to activated state in *in vitro* scratch wound assays, EBS-DM cells induced more soluble K17 proteins than wild-type cells, confirming their constitutively activated state.

The role of EGF in regulating wound closure and keratin remodelling was explored in Chapter 4. EGF stimulation induces keratinocyte migration, as shown by earlier studies (Barrandon and Green, 1987), and the same effect was observed here in the EBS-DM cells. EGF was shown to increase lamellipodial formation (Chinkers et al., 1979), and it is specifically in the lamellipodia that the EBS-DM keratin aggregates form [Figure 3.2]. Keratinocyte motility, stimulated by EGF signalling and blocked by EGF signalling inhibition, was observed to be tightly coupled to the degree of keratin aggregate formation. EGF-induced changes in desmoplakin localization were also observed in EBS-DM cells, suggesting a reduction of desmosome adhesions, which is coherent to a shift in migratory behaviour in the activation of keratinocytes.

Plectin is a major cytoskeleton linker protein, which is expressed as several different isoforms (plectin 1, 1a, 1b, 1c, 1d, 1e, 1f and 1g) due to differential splicing, with organelle-specific localization and show preferential binding to hemidesmosomes,

focal adhesions, mitochondria, microtubules or Z-disks (reviewed in Wiche and Winter, 2011). Previous studies have shown differences in wound closure speeds in different plectin knockout cell lines, depending on which plectin isoform the cells predominantly expressed. For instance, plectin isoform $1^{-/-}$ fibroblasts migrated slower in scratch wound assays (Abrahamsberg et al., 2005) whereas plectin$^{-/-}$ keratinocytes resulted in faster migration, which upon re-expression of plectin 1a could cause slower migration (Osmanagic-Myers et al., 2006). Hence, these results revealed the differential role played by plectin isoforms in regulating cell migration. It is not known which plectin isoforms are preferentially being expressed in the wild-type and the EBS-DM cells yet, and the expression of different plectin isoforms may be different in the two cell lines, which contribute to different migration speeds in wound closure assays. Further experiments will be needed to validate this idea.

It was also demonstrated that constitutive activation of ERK1/2 kinase in EBS-DM cells, downstream of EGF signaling, contributed to their activated state and this ERK1/2-dependent EGF effect could also modulate plectin levels. Overall, the results confirm a potential role of EGF in regulating the constitutively activated state of EBS-DM keratinocytes. Further experiments will be undertaken to see whether this can ultimately be manipulated for therapeutic applications.

In Chapter 5, a hypothesis is developed on the role of keratin phosphorylation in keratinocyte activation and keratin aggregate formation. Assembly and disassembly of intermediate filament proteins is known to be driven by phosphorylation cycles (Inagaki et al., 1989; Izawa and Inagaki, 2006), thought to occur predominantly in the head and tail domains (reviewed in Omary et al., 2006). The findings in the present study provide the first suggestion that phosphorylation can occur in the rod 1A domain of K14 and have identified a tyrosine residue in the helix initiation motif as a

potential target site. Past work aimed at defining the phosphorylation sites of keratin intermediate filament proteins have mostly focussed on serine/threonine residues located at the "head" and "tail" domains of K8/K18 (Ku and Omary, 1997; Ku et al., 1998a; Omary et al., 2009), and this has become a paradigm for post-translational modifications in keratins. Any changes in phosphorylation status of these serine/threonine residues could contribute to both physiological processes and pathological diseases (Omary et al., 2006). Hence, understanding their regulation could give some insights to keratin remodelling in stress.

Keratins can also be glycosylated (King and Hounsell, 1989; Ku et al., 2010) and ubiquitylated (Ku and Omary, 2000; Jaitovich et al., 2008), and recent studies have also demonstrated the possibility of sumoylation (Snider et al., 2011). The Snider study reported that sumoylation occurs on lysine residues in rod 2B domain of K8/K18/K19, thus indicating that the rod domain may be accessible for post-translational modifications (Snider et al., 2011), contrary to earlier views that this domain should be tightly packed in a coiled-coil with its type II partner (K5 in this case).

In the present study, it is demonstrated that engineering a phosphomimetic residue at K14 Y129 (AcGFP-K14 Y129E) can give rise to peripheral keratin aggregates and that such cells show constitutive stress kinase activation, reminiscent to that of EBS-DM cells (KEB-7 and EGFP-K14 R125P). The localization of keratin aggregates observed in EBS-DM cells are clearly different from the cytoplasmic granules that are generated during stress stimuli (heat or osmotic stress), phosphatase inhibitor (okadaic acid or orthovanadate) treatments or mitosis (Strnad et al., 2002; Toivola et al., 2002; Woll et al., 2007), as unlike the cytoplasmic granules, EBS-DM keratin aggregates are mainly confined to the lamellipodia. This may depend on either the types of kinases

(serine/threonine vs. tyrosine) phosphorylating the keratin or the site of keratin residues being phosphorylated ("head" or "tail" domains vs. rod domain). Further work will be needed to understand how these different kinases regulate keratin reorganisation and to identify their target residue in the keratin structure.

Previous studies suggest that the helix 1A region of keratins may not be as tightly folded as was originally thought to be (Parry et al., 2002; Smith et al., 2002; Strelkov et al., 2002), and this may possibly allow tyrosine kinase to gain access and phosphorylate the K14 Y129 residue. One can postulate that in times of stress, phosphorylation of K5 partner leads to unwinding of the α-helical strands of the two-stranded coiled-coil segment 1A or K5 may simply begin to interact with another keratin such as wound-induced K17, allowing K14 to be susceptible to tyrosine phosphorylation.

Using phospho-null variants, it was demonstrated that K14 Y129 phosphorylation status may also play a role in cell migration. It is predicted that the K14 R125P mutation seen in EBS-DM cells may lead to more phosphorylation at K14 Y129 by increasing the accessibility of this residue to potential tyrosine kinases such as FAK or Src, which are recruited and localized at focal contacts during lamellipodial formation (reviewed in McLean et al., 2005), the site where keratin aggregates are localized. Although there is no direct interaction between these tyrosine kinases and keratin aggregates [as quantitated using immunostaining by members of our group (unpublished data)], they may be associated in a parallel manner, wherein mutant keratin filament reorganisation at the leading edge may increase the probability of K14 Y129 being phosphorylated by these tyrosine kinases when these kinases are recruited to focal contacts to regulate adhesion turnover during lamellipodial formation. In support of this, a recent study has shown that vimentin disassembly by

phosphorylation at the cell periphery facilitates lamellipodial protrusions (Helfand et al., 2011).

Further breakthroughs are needed to better understand the mechanism of keratin intermediate filament assembly, and its spatial and temporal regulation in living cells. As more of the complexity of keratin function is understood, it is becoming very important to know how different keratin networks are generated, maintained and regulated in epithelial cells.

6.2   Conclusion

The work carried out in this thesis has been achieved mainly due to the availability of immortalised cell lines derived from EBS patients and also the generation of cell lines stably expressing EGFP-tagged K14 mutation. Taken into account all the findings in this thesis, it is proposed that constitutive stress activation arising from keratin mutation (K14 R125P) could be a possible mechanism to the pathogenesis of inherited skin blistering disorder such as EBS Dowling-Meara type. Much evidence points to the fact that EBS-DM keratinocytes are in a constitutively activated state, based on their higher SAPK activation, and they have faster stress and wound response than normal keratinocytes. It is shown that EGF-ERK1/2 signalling can modulate the activated state of EBS-DM keratinocytes and this can be seen by changes in keratin aggregates at the leading edge. Evidence is presented that phosphorylation of a tyrosine residue (K14 Y129) in the helical rod 1A domain is likely to contribute to keratin aggregate formation in EBS-DM keratinocytes and that increasing the phosphorylation state of this residue is associated with increased cell migration, possibly because both processes are likely to be mediated by a common

tyrosine kinase such as FAK or Src. It is proposed that the remodelling of keratin filaments, which occurs at the lamellipodia and is mediated by recruitment of tyrosine kinases at these sites, is increased in EBS-DM cells due to the greater probability of K14 Y129 phosphorylation that results from the K14 R125P mutation. This elevated phosphorylation may be responsible for the observed aggregate formation at the leading edge. Furthermore, if lamellipodial formation is induced by remodelling of intermediate filaments as proposed by (Helfand et al., 2011), then increased keratin remodelling (resulting from increased phosphorylation) could lead to increased keratinocyte migration, explaining the faster scratch wound closure observed in these cells.

It is also suggested that phospho-K14 Y129 could be a useful biomarker of keratinocyte activation. More work is needed to validate this hypothesis. Knowing these mechanisms will open up new avenues to alleviate wound injury and also offer new therapeutic options for the treatment of hereditary skin blistering disorder such as EBS.

6.3   Future perspectives

An exciting consequence of the research described in this thesis is that it may open up a new approach to therapy for a group of diseases that have so far been incurable, ie. epithelial fragility disorders caused by keratin mutations, such as epidermolysis bullosa simplex. Several gene correction strategies have been suggested for inherited skin disorders. To overcome the dominant negative effects of keratin mutations, translation of mutated keratins can be inhibited by siRNA (Hickerson et al., 2006; Leachman et al., 2008) or the mRNA exon segments encoding the mutant keratin can

be replaced using spliceosome-mediated RNA trans-splicing (SMaRT) (Wally et al., 2010). Another approach is to induce the expression of another gene with similar function, but which is not susceptible to the disruptive effect of the mutant gene. For instance, desmin, an intermediate filament protein normally expressed in muscle cells, can be used to reinforce the fragile keratin network in EBS-DM cells (Magin et al., 2000; D'Alessandro et al., 2004). Functional redundancy of the keratin protein family can also be exploited to improve EBS-DM conditions. For example, sulphoraphane, a component of broccoli, can upregulate K16 and K17 to compensate for the loss of K14 protein in K14 knockout mouse and reduce blister formation (Kerns et al., 2007). Despite many efforts, gene therapy has only entered the phase 1b of clinical trial in pachonychia congenita (Leachman et al., 2010).

The findings in this thesis further suggest another strategy to deal with the EBS-DM condition by targeting the EGF/SAPK signalling pathways, which contribute to the constitutive activation of EBS-DM keratinocytes. This therapeutic strategy could be designed to target any keratin mutation that results in sustained stress activation irrespective of their type of mutation. The identification of phospho-K14 Y129 could be a useful biomarker of keratinocyte activation and could be used for treatment efficacy. The next stages in this research will involve the use of these EBS-DM cell lines in larger scale to test and screen for compounds that can reduce their stress activation state, in a bid to alleviate EBS patient conditions and improve the patient's quality of life.

BIBLIOGRAPHY

Abrahamsberg, C., P. Fuchs, S. Osmanagic-Myers, I. Fischer, F. Propst, A. Elbe-Burger, and G. Wiche. 2005. Targeted ablation of plectin isoform 1 uncovers role of cytolinker proteins in leukocyte recruitment. *Proc Natl Acad Sci U S A*. 102:18449-18454.

Aebi, U., W.E. Fowler, P. Rew, and T.T. Sun. 1983. The fibrillar substructure of keratin filaments unraveled. *J Cell Biol*. 97:1131-1143.

Aho, S., and J. Uitto. 1998. Direct interaction between the intracellular domains of bullous pemphigoid antigen 2 (BP180) and beta 4 integrin, hemidesmosomal components of basal keratinocytes. *Biochem Biophys Res Commun*. 243:694-699.

Albers, K., and E. Fuchs. 1989. Expression of mutant keratin cDNAs in epithelial cells reveals possible mechanisms for initiation and assembly of intermediate filaments. *J Cell Biol*. 108:1477-1493.

Allen, E.M., G.J. Giudice, and L.A. Diaz. 1993. Subclass reactivity of pemphigus foliaceus autoantibodies with recombinant human desmoglein. *J Invest Dermatol*. 100:685-691.

Amagai, M., V. Klaus-Kovtun, and J.R. Stanley. 1991. Autoantibodies against a novel epithelial cadherin in pemphigus vulgaris, a disease of cell adhesion. *Cell*. 67:869-877.

Amagai, M. 1994. Autoantibodies against cell adhesion molecules in pemphigus. *J Dermatol*. 21:833-837.

Amagai, M., N. Matsuyoshi, Z.H. Wang, C. Andl, and J.R. Stanley. 2000. Toxin in bullous impetigo and staphylococcal scalded-skin syndrome targets desmoglein 1. *Nat Med*. 6:1275-1277.

Andra, K., H. Lassmann, R. Bittner, S. Shorny, R. Fassler, F. Propst, and G. Wiche. 1997. Targeted inactivation of plectin reveals essential function in maintaining the integrity of skin, muscle, and heart cytoarchitecture. *Genes Dev*. 11:3143-3156.

Andra, K., B. Nikolic, M. Stocher, D. Drenckhahn, and G. Wiche. 1998. Not just scaffolding: plectin regulates actin dynamics in cultured cells. *Genes Dev*. 12:3442-3451.

Angst, B.D., L.A. Nilles, and K.J. Green. 1990. Desmoplakin II expression is not restricted to stratified epithelia. *J Cell Sci*. 97 (Pt 2):247-257.

Anhalt, G.J., S.C. Kim, J.R. Stanley, N.J. Korman, D.A. Jabs, M. Kory, H. Izumi, H. Ratrie, 3rd, D. Mutasim, L. Ariss-Abdo, and et al. 1990. Paraneoplastic pemphigus. An autoimmune mucocutaneous disease associated with neoplasia. *N Engl J Med*. 323:1729-1735.

Anton-Lamprecht, I., and U.W. Schnyder. 1982. Epidermolysis bullosa herpetiformis Dowling-Meara. Report of a case and pathomorphogenesis. *Dermatologica*. 164:221-235.

Aoyagi, T., H. Suya, K. Umeda, N. Kato, O. Nemoto, H. Kobayashi, and Y. Miura. 1985. Epidermal growth factor stimulates tyrosine phosphorylation of pig epidermal fibrous keratin. *J Invest Dermatol*. 84:118-121.

Arin, M.J., M.A. Longley, I. Anton-Lamprecht, G. Kurze, M. Huber, D. Hohl, J.A. Rothnagel, and D.R. Roop. 1999. A novel substitution in keratin 10 in epidermolytic hyperkeratosis. *J Invest Dermatol*. 112:506-508.

Arin, M.J. 2009. The molecular basis of human keratin disorders. *Hum Genet*. 125:355-373.

Armstrong, D.K., K.E. McKenna, P.E. Purkis, K.J. Green, R.A. Eady, I.M. Leigh, and A.E. Hughes. 1999. Haploinsufficiency of desmoplakin causes a striate subtype of palmoplantar keratoderma. *Hum Mol Genet*. 8:143-148.

Arwert, E.N., E. Hoste, and F.M. Watt. 2012. Epithelial stem cells, wound healing and cancer. *Nat Rev Cancer*. 12:170-180.

Ashwell, J.D. 2006. The many paths to p38 mitogen-activated protein kinase activation in the immune system. *Nat Rev Immunol*. 6:532-540.

Ayub, M., S. Basit, M. Jelani, F. Ur Rehman, M. Iqbal, M. Yasinzai, and W. Ahmad. 2009. A homozygous nonsense mutation in the human desmocollin-3 (DSC3) gene underlies hereditary hypotrichosis and recurrent skin vesicles. *Am J Hum Genet*. 85:515-520.

Barlow, D.J., and J.M. Thornton. 1988. Helix geometry in proteins. *J Mol Biol*. 201:601-619.

Barrandon, Y., and H. Green. 1987. Cell migration is essential for sustained growth of keratinocyte colonies: the roles of transforming growth factor-alpha and epidermal growth factor. *Cell*. 50:1131-1137.

Batta, K., E.L. Rugg, N.J. Wilson, N. West, H. Goodyear, E.B. Lane, M. Gratian, P. Dopping-Hepenstal, C. Moss, and R.A. Eady. 2000. A keratin 14 'knockout' mutation in recessive epidermolysis bullosa simplex resulting in less severe disease. *Br J Dermatol*. 143:621-627.

Bazzoni, G., and E. Dejana. 2001. Pores in the sieve and channels in the wall: control of paracellular permeability by junctional proteins in endothelial cells. *Microcirculation*. 8:143-152.

Bergink, S., and S. Jentsch. 2009. Principles of ubiquitin and SUMO modifications in DNA repair. *Nature*. 458:461-467.

Beriault, D.R., O. Haddad, J.V. McCuaig, Z.J. Robinson, D. Russell, E.B. Lane, and D.S. Fudge. 2012. The mechanical behavior of mutant K14-R125P keratin bundles and networks in NEB-1 keratinocytes. *PLoS One*. 7:e31320.

Bernot, K.M., C.H. Lee, and P.A. Coulombe. 2005. A small surface hydrophobic stripe in the coiled-coil domain of type I keratins mediates tetramer stability. *J Cell Biol.* 168:965-974.

Bertrand, J.Y., A. Jalil, M. Klaine, S. Jung, A. Cumano, and I. Godin. 2005. Three pathways to mature macrophages in the early mouse yolk sac. *Blood.* 106:3004-3011.

Blanpain, C., W.E. Lowry, H.A. Pasolli, and E. Fuchs. 2006. Canonical notch signaling functions as a commitment switch in the epidermal lineage. *Genes Dev.* 20:3022-3035.

Blanpain, C., V. Horsley, and E. Fuchs. 2007. Epithelial stem cells: turning over new leaves. *Cell.* 128:445-458.

Bolling, M.C., H.H. Lemmink, G.H. Jansen, and M.F. Jonkman. 2011. Mutations in KRT5 and KRT14 cause epidermolysis bullosa simplex in 75% of the patients. *Br J Dermatol.* 164:637-644.

Bonifas, J.M., A.L. Rothman, and E.H. Epstein, Jr. 1991. Epidermolysis bullosa simplex: evidence in two families for keratin gene abnormalities. *Science.* 254:1202-1205.

Borradori, L., P.J. Koch, C.M. Niessen, S. Erkeland, M.R. van Leusden, and A. Sonnenberg. 1997. The localization of bullous pemphigoid antigen 180 (BP180) in hemidesmosomes is mediated by its cytoplasmic domain and seems to be regulated by the beta4 integrin subunit. *J Cell Biol.* 136:1333-1347.

Borradori, L., S. Chavanas, R.Q. Schaapveld, L. Gagnoux-Palacios, J. Calafat, G. Meneguzzi, and A. Sonnenberg. 1998. Role of the bullous pemphigoid antigen 180 (BP180) in the assembly of hemidesmosomes and cell adhesion--reexpression of BP180 in generalized atrophic benign epidermolysis bullosa keratinocytes. *Exp Cell Res.* 239:463-476.

Borradori, L., and A. Sonnenberg. 1999. Structure and function of hemidesmosomes: more than simple adhesion complexes. *J Invest Dermatol.* 112:411-418.

Bowden, P.E., J.L. Haley, A. Kansky, J.A. Rothnagel, D.O. Jones, and R.J. Turner. 1995. Mutation of a type II keratin gene (K6a) in pachyonychia congenita. *Nat Genet.* 10:363-365.

Brancho, D., N. Tanaka, A. Jaeschke, J.J. Ventura, N. Kelkar, Y. Tanaka, M. Kyuuma, T. Takeshita, R.A. Flavell, and R.J. Davis. 2003. Mechanism of p38 MAP kinase activation in vivo. *Genes Dev.* 17:1969-1978.

Brooke, M.A., D. Nitoiu, and D.P. Kelsell. 2012. Cell-cell connectivity: desmosomes and disease. *J Pathol.* 226:158-171.

Brown, A., G. Bernier, M. Mathieu, J. Rossant, and R. Kothary. 1995. The mouse dystonia musculorum gene is a neural isoform of bullous pemphigoid antigen 1. *Nat Genet.* 10:301-306.

Brown, M.D., and D.B. Sacks. 2009. Protein scaffolds in MAP kinase signalling. *Cell Signal.* 21:462-469.

Bubb, M.R., L. Govindasamy, E.G. Yarmola, S.M. Vorobiev, S.C. Almo, T. Somasundaram, M.S. Chapman, M. Agbandje-McKenna, and R. McKenna. 2002. Polylysine induces an antiparallel actin dimer that nucleates filament assembly: crystal structure at 3.5-A resolution. *J Biol Chem.* 277:20999-21006.

Buck, C.A., and A.F. Horwitz. 1987. Cell surface receptors for extracellular matrix molecules. *Annu Rev Cell Biol.* 3:179-205.

Burgeson, R.E., and A.M. Christiano. 1997. The dermal-epidermal junction. *Curr Opin Cell Biol.* 9:651-658.

Burridge, K., and J.R. Feramisco. 1980. Microinjection and localization of a 130K protein in living fibroblasts: a relationship to actin and fibronectin. *Cell.* 19:587-595.

Burridge, K., T. Kelly, and L. Connell. 1982. Proteins involved in the attachment of actin to the plasma membrane. *Philos Trans R Soc Lond B Biol Sci.* 299:291-299.

Busch, T., M. Armacki, T. Eiseler, G. Joodi, C. Temme, J. Jansen, G. von Wichert, M.B. Omary, J. Spatz, and T. Seufferlein. 2012. Keratin 8 phosphorylation regulates keratin reorganization and migration of epithelial tumor cells. *J Cell Sci.* 125:2148-2159.

Butz, S., J. Stappert, H. Weissig, and R. Kemler. 1992. Plakoglobin and beta-catenin: distinct but closely related. *Science.* 257:1142-1144.

Buxman, M.M., and K.D. Wuepper. 1978. Cellular localization of epidermal transglutaminase: a histochemical and immunochemical study. *J Histochem Cytochem.* 26:340-348.

Buxton, R.S., and A.I. Magee. 1992. Structure and interactions of desmosomal and other cadherins. *Semin Cell Biol.* 3:157-167.

Casar, B., A. Pinto, and P. Crespo. 2008. Essential role of ERK dimers in the activation of cytoplasmic but not nuclear substrates by ERK-scaffold complexes. *Mol Cell.* 31:708-721.

Caulin, C., G.S. Salvesen, and R.G. Oshima. 1997. Caspase cleavage of keratin 18 and reorganization of intermediate filaments during epithelial cell apoptosis. *J Cell Biol.* 138:1379-1394.

Caunt, C.J., S.P. Armstrong, C.A. Rivers, M.R. Norman, and C.A. McArdle. 2008a. Spatiotemporal regulation of ERK2 by dual specificity phosphatases. *J Biol Chem.* 283:26612-26623.

Caunt, C.J., C.A. Rivers, B.L. Conway-Campbell, M.R. Norman, and C.A. McArdle. 2008b. Epidermal growth factor receptor and protein kinase C signaling to

ERK2: spatiotemporal regulation of ERK2 by dual specificity phosphatases. *J Biol Chem*. 283:6241-6252.

Cavani, A., G. Zambruno, A. Marconi, V. Manca, M. Marchetti, and A. Giannetti. 1993. Distinctive integrin expression in the newly forming epidermis during wound healing in humans. *J Invest Dermatol*. 101:600-604.

Celis, J.E., P.M. Larsen, S.J. Fey, and A. Celis. 1983. Phosphorylation of keratin and vimentin polypeptides in normal and transformed mitotic human epithelial amnion cells: behavior of keratin and vimentin filaments during mitosis. *J Cell Biol*. 97:1429-1434.

Celis, J.E., S.J. Fey, P.M. Larsen, and A. Celis. 1985. Preferential phosphorylation of keratins and vimentin during mitosis in normal and transformed human amnion cells. *Ann N Y Acad Sci*. 455:268-281.

Champliaud, M.F., G.P. Lunstrum, P. Rousselle, T. Nishiyama, D.R. Keene, and R.E. Burgeson. 1996. Human amnion contains a novel laminin variant, laminin 7, which like laminin 6, covalently associates with laminin 5 to promote stable epithelial-stromal attachment. *J Cell Biol*. 132:1189-1198.

Chan, Y., I. Anton-Lamprecht, Q.C. Yu, A. Jackel, B. Zabel, J.P. Ernst, and E. Fuchs. 1994. A human keratin 14 "knockout": the absence of K14 leads to severe epidermolysis bullosa simplex and a function for an intermediate filament protein. *Genes Dev*. 8:2574-2587.

Chan, Y.M., J. Cheng, T. Gedde-Dahl, Jr., K.M. Niemi, and E. Fuchs. 1996. Genetic analysis of a severe case of Dowling-Meara epidermolysis bullosa simplex. *J Invest Dermatol*. 106:327-334.

Chang, L., and M. Karin. 2001. Mammalian MAP kinase signalling cascades. *Nature*. 410:37-40.

Chang, L., and R.D. Goldman. 2004. Intermediate filaments mediate cytoskeletal crosstalk. *Nat Rev Mol Cell Biol*. 5:601-613.

Chavanas, S., C. Bodemer, A. Rochat, D. Hamel-Teillac, M. Ali, A.D. Irvine, J.L. Bonafe, J. Wilkinson, A. Taieb, Y. Barrandon, J.I. Harper, Y. de Prost, and A. Hovnanian. 2000. Mutations in SPINK5, encoding a serine protease inhibitor, cause Netherton syndrome. *Nat Genet*. 25:141-142.

Cheng, J., A.J. Syder, Q.C. Yu, A. Letai, A.S. Paller, and E. Fuchs. 1992. The genetic basis of epidermolytic hyperkeratosis: a disorder of differentiation-specific epidermal keratin genes. *Cell*. 70:811-819.

Chidgey, M., C. Brakebusch, E. Gustafsson, A. Cruchley, C. Hail, S. Kirk, A. Merritt, A. North, C. Tselepis, J. Hewitt, C. Byrne, R. Fassler, and D. Garrod. 2001. Mice lacking desmocollin 1 show epidermal fragility accompanied by barrier defects and abnormal differentiation. *J Cell Biol*. 155:821-832.

Chinkers, M., J.A. McKanna, and S. Cohen. 1979. Rapid induction of morphological changes in human carcinoma cells A-431 by epidermal growth factors. *J Cell Biol*. 83:260-265.

Chipev, C.C., B.P. Korge, N. Markova, S.J. Bale, J.J. DiGiovanna, J.G. Compton, and P.M. Steinert. 1992. A leucine----proline mutation in the H1 subdomain of keratin 1 causes epidermolytic hyperkeratosis. *Cell*. 70:821-828.

Chipev, C.C., J.M. Yang, J.J. DiGiovanna, P.M. Steinert, L. Marekov, J.G. Compton, and S.J. Bale. 1994. Preferential sites in keratin 10 that are mutated in epidermolytic hyperkeratosis. *Am J Hum Genet*. 54:179-190.

Choi, H.J., S. Park-Snyder, L.T. Pascoe, K.J. Green, and W.I. Weis. 2002. Structures of two intermediate filament-binding fragments of desmoplakin reveal a unique repeat motif structure. *Nat Struct Biol*. 9:612-620.

Choi, H.J., and W.I. Weis. 2005. Structure of the armadillo repeat domain of plakophilin 1. *J Mol Biol*. 346:367-376.

Chou, C.F., and M.B. Omary. 1991. Phorbol acetate enhances the phosphorylation of cytokeratins 8 and 18 in human colonic epithelial cells. *FEBS Lett*. 282:200-204.

Chou, C.F., A.J. Smith, and M.B. Omary. 1992. Characterization and dynamics of O-linked glycosylation of human cytokeratin 8 and 18. *J Biol Chem*. 267:3901-3906.

Chou, C.F., and M.B. Omary. 1993. Mitotic arrest-associated enhancement of O-linked glycosylation and phosphorylation of human keratins 8 and 18. *J Biol Chem*. 268:4465-4472.

Christiano, A.M., D.S. Greenspan, G.G. Hoffman, X. Zhang, Y. Tamai, A.N. Lin, H.C. Dietz, A. Hovnanian, and J. Uitto. 1993. A missense mutation in type VII collagen in two affected siblings with recessive dystrophic epidermolysis bullosa. *Nat Genet*. 4:62-66.

Ciechanover, A., A. Orian, and A.L. Schwartz. 2000. The ubiquitin-mediated proteolytic pathway: mode of action and clinical implications. *J Cell Biochem Suppl*. 34:40-51.

Clark, R.A. 1990. Fibronectin matrix deposition and fibronectin receptor expression in healing and normal skin. *J Invest Dermatol*. 94:128S-134S.

Cockayne, E.A. 1947. Recurrent bullous eruption of the feet. *Br J Dermatol Syph*. 59:109-112.

Colakoglu, G., and A. Brown. 2009. Intermediate filaments exchange subunits along their length and elongate by end-to-end annealing. *J Cell Biol*. 185:769-777.

Collin, C., R. Moll, S. Kubicka, J.P. Ouhayoun, and W.W. Franke. 1992. Characterization of human cytokeratin 2, an epidermal cytoskeletal protein synthesized late during differentiation. *Exp Cell Res*. 202:132-141.

Collins, J.E., P.K. Legan, T.P. Kenny, J. MacGarvie, J.L. Holton, and D.R. Garrod. 1991. Cloning and sequence analysis of desmosomal glycoproteins 2 and 3 (desmocollins): cadherin-like desmosomal adhesion molecules with heterogeneous cytoplasmic domains. *J Cell Biol.* 113:381-391.

Corden, L.D., and W.H. McLean. 1996. Human keratin diseases: hereditary fragility of specific epithelial tissues. *Exp Dermatol.* 5:297-307.

Cotsarelis, G., T.T. Sun, and R.M. Lavker. 1990. Label-retaining cells reside in the bulge area of pilosebaceous unit: implications for follicular stem cells, hair cycle, and skin carcinogenesis. *Cell.* 61:1329-1337.

Coulombe, P.A., M.E. Hutton, A. Letai, A. Hebert, A.S. Paller, and E. Fuchs. 1991a. Point mutations in human keratin 14 genes of epidermolysis bullosa simplex patients: genetic and functional analyses. *Cell.* 66:1301-1311.

Coulombe, P.A., M.E. Hutton, R. Vassar, and E. Fuchs. 1991b. A function for keratins and a common thread among different types of epidermolysis bullosa simplex diseases. *J Cell Biol.* 115:1661-1674.

Coulombe, P.A. 1997. Towards a molecular definition of keratinocyte activation after acute injury to stratified epithelia. *Biochem Biophys Res Commun.* 236:231-238.

Coulombe, P.A., O. Bousquet, L. Ma, S. Yamada, and D. Wirtz. 2000. The 'ins' and 'outs' of intermediate filament organization. *Trends Cell Biol.* 10:420-428.

Coulombe, P.A., and M.B. Omary. 2002. 'Hard' and 'soft' principles defining the structure, function and regulation of keratin intermediate filaments. *Curr Opin Cell Biol.* 14:110-122.

Coulombe, P.A., M.L. Kerns, and E. Fuchs. 2009. Epidermolysis bullosa simplex: a paradigm for disorders of tissue fragility. *J Clin Invest.* 119:1784-1793.

Cowin, P., H.P. Kapprell, W.W. Franke, J. Tamkun, and R.O. Hynes. 1986. Plakoglobin: a protein common to different kinds of intercellular adhering junctions. *Cell.* 46:1063-1073.

Cummins, R.E., S. Klingberg, J. Wesley, M. Rogers, Y. Zhao, and D.F. Murrell. 2001. Keratin 14 point mutations at codon 119 of helix 1A resulting in different epidermolysis bullosa simplex phenotypes. *J Invest Dermatol.* 117:1103-1107.

D'Alessandro, M., D. Russell, S.M. Morley, A.M. Davies, and E.B. Lane. 2002. Keratin mutations of epidermolysis bullosa simplex alter the kinetics of stress response to osmotic shock. *J Cell Sci.* 115:4341-4351.

D'Alessandro, M., S.M. Morley, P.H. Ogden, M. Liovic, R.M. Porter, and E.B. Lane. 2004. Functional improvement of mutant keratin cells on addition of desmin: an alternative approach to gene therapy for dominant diseases. *Gene Ther.* 11:1290-1295.

Davis, E.C., S.A. Blattel, and R.P. Mecham. 1999. Remodeling of elastic fiber components in scleroderma skin. *Connect Tissue Res*. 40:113-121.

Davis, R.J. 2000. Signal transduction by the JNK group of MAP kinases. *Cell*. 103:239-252.

de Pereda, J.M., E. Ortega, N. Alonso-Garcia, M. Gomez-Hernandez, and A. Sonnenberg. 2009. Advances and perspectives of the architecture of hemidesmosomes: lessons from structural biology. *Cell Adh Migr*. 3:361-364.

Demarchez, M., D.J. Hartmann, M. Regnier, and D. Asselineau. 1992. The role of fibroblasts in dermal vascularization and remodeling of reconstructed human skin after transplantation onto the nude mouse. *Transplantation*. 54:317-326.

Deodhar, A.K., and R.E. Rana. 1997. Surgical physiology of wound healing: a review. *J Postgrad Med*. 43:52-56.

Derijard, B., M. Hibi, I.H. Wu, T. Barrett, B. Su, T. Deng, M. Karin, and R.J. Davis. 1994. JNK1: a protein kinase stimulated by UV light and Ha-Ras that binds and phosphorylates the c-Jun activation domain. *Cell*. 76:1025-1037.

Desiniotis, A., and N. Kyprianou. 2011. Significance of talin in cancer progression and metastasis. *Int Rev Cell Mol Biol*. 289:117-147.

Diaz, L.A., H. Ratrie, 3rd, W.S. Saunders, S. Futamura, H.L. Squiquera, G.J. Anhalt, and G.J. Giudice. 1990. Isolation of a human epidermal cDNA corresponding to the 180-kD autoantigen recognized by bullous pemphigoid and herpes gestationis sera. Immunolocalization of this protein to the hemidesmosome. *J Clin Invest*. 86:1088-1094.

Dickson, M.A., W.C. Hahn, Y. Ino, V. Ronfard, J.Y. Wu, R.A. Weinberg, D.N. Louis, F.P. Li, and J.G. Rheinwald. 2000. Human keratinocytes that express hTERT and also bypass a p16(INK4a)-enforced mechanism that limits life span become immortal yet retain normal growth and differentiation characteristics. *Mol Cell Biol*. 20:1436-1447.

DiGiovanna, J.J., and S.J. Bale. 1994. Clinical heterogeneity in epidermolytic hyperkeratosis. *Arch Dermatol*. 130:1026-1035.

Dogic, D., P. Rousselle, and M. Aumailley. 1998. Cell adhesion to laminin 1 or 5 induces isoform-specific clustering of integrins and other focal adhesion components. *J Cell Sci*. 111 (Pt 6):793-802.

Dowling, G.B., and R.H. Meara. 1954. Epidermolysis bullosa resembling juvenile dermatitis herpetiformis. *Br J Dermatol*. 66:139-143.

Duan, S., Z. Yao, Y. Zhu, G. Wang, D. Hou, L. Wen, and M. Wu. 2009. The Pirh2-keratin 8/18 interaction modulates the cellular distribution of mitochondria and UV-induced apoptosis. *Cell Death Differ*. 16:826-837.

Edwards, G., and C. Streuli. 1995. Signalling in extracellular-matrix-mediated control of epithelial cell phenotype. *Biochem Soc Trans*. 23:464-468.

Elion, E.A. 2001. The Ste5p scaffold. *J Cell Sci*. 114:3967-3978.

Elliott, C.E., B. Becker, S. Oehler, M.J. Castanon, R. Hauptmann, and G. Wiche. 1997. Plectin transcript diversity: identification and tissue distribution of variants with distinct first coding exons and rodless isoforms. *Genomics*. 42:115-125.

Erickson, A.C., and J.R. Couchman. 2000. Still more complexity in mammalian basement membranes. *J Histochem Cytochem*. 48:1291-1306.

Eriksson, J.E., D.L. Brautigan, R. Vallee, J. Olmsted, H. Fujiki, and R.D. Goldman. 1992. Cytoskeletal integrity in interphase cells requires protein phosphatase activity. *Proc Natl Acad Sci U S A*. 89:11093-11097.

Eriksson, J.E., T. Dechat, B. Grin, B. Helfand, M. Mendez, H.M. Pallari, and R.D. Goldman. 2009. Introducing intermediate filaments: from discovery to disease. *J Clin Invest*. 119:1763-1771.

Essenfelder, G.M., R. Bruzzone, J. Lamartine, A. Charollais, C. Blanchet-Bardon, M.T. Barbe, P. Meda, and G. Waksman. 2004. Connexin30 mutations responsible for hidrotic ectodermal dysplasia cause abnormal hemichannel activity. *Hum Mol Genet*. 13:1703-1714.

Favata, M.F., K.Y. Horiuchi, E.J. Manos, A.J. Daulerio, D.A. Stradley, W.S. Feeser, D.E. Van Dyk, W.J. Pitts, R.A. Earl, F. Hobbs, R.A. Copeland, R.L. Magolda, P.A. Scherle, and J.M. Trzaskos. 1998. Identification of a novel inhibitor of mitogen-activated protein kinase kinase. *J Biol Chem*. 273:18623-18632.

Feng, L., X. Zhou, J. Liao, and M.B. Omary. 1999. Pervanadate-mediated tyrosine phosphorylation of keratins 8 and 19 via a p38 mitogen-activated protein kinase-dependent pathway. *J Cell Sci*. 112 (Pt 13):2081-2090.

Fickert, P., M. Trauner, A. Fuchsbichler, C. Stumptner, K. Zatloukal, and H. Denk. 2003. Mallory body formation in primary biliary cirrhosis is associated with increased amounts and abnormal phosphorylation and ubiquitination of cytokeratins. *J Hepatol*. 38:387-394.

Fine, J.D., R.A. Eady, E.A. Bauer, J.W. Bauer, L. Bruckner-Tuderman, A. Heagerty, H. Hintner, A. Hovnanian, M.F. Jonkman, I. Leigh, J.A. McGrath, J.E. Mellerio, D.F. Murrell, H. Shimizu, J. Uitto, A. Vahlquist, D. Woodley, and G. Zambruno. 2008. The classification of inherited epidermolysis bullosa (EB): Report of the Third International Consensus Meeting on Diagnosis and Classification of EB. *J Am Acad Dermatol*. 58:931-950.

Fischer, T., and T. Gedde-Dahl, Jr. 1979. Epidermolysis bullosa simplex and mottled pigmentation: a new dominant syndrome. I. Clinical and histological features. *Clin Genet*. 15:228-238.

Frame, M., and J. Norman. 2008. A tal(in) of cell spreading. *Nat Cell Biol*. 10:1017-1019.

Freedberg, I.M., M. Tomic-Canic, M. Komine, and M. Blumenberg. 2001. Keratins and the keratinocyte activation cycle. *J Invest Dermatol*. 116:633-640.

Frelinger, J.G., L. Hood, S. Hill, and J.A. Frelinger. 1979. Mouse epidermal Ia molecules have a bone marrow origin. *Nature*. 282:321-323.

Fuchs, E., and H. Green. 1980. Changes in keratin gene expression during terminal differentiation of the keratinocyte. *Cell*. 19:1033-1042.

Fuchs, E. 1995. Keratins and the skin. *Annu Rev Cell Dev Biol*. 11:123-153.

Fuchs, E., and I. Karakesisoglou. 2001. Bridging cytoskeletal intersections. *Genes Dev*. 15:1-14.

Fuchs, E., and S. Raghavan. 2002. Getting under the skin of epidermal morphogenesis. *Nat Rev Genet*. 3:199-209.

Furuse, M., M. Hata, K. Furuse, Y. Yoshida, A. Haratake, Y. Sugitani, T. Noda, A. Kubo, and S. Tsukita. 2002. Claudin-based tight junctions are crucial for the mammalian epidermal barrier: a lesson from claudin-1-deficient mice. *J Cell Biol*. 156:1099-1111.

Gache, Y., S. Chavanas, J.P. Lacour, G. Wiche, K. Owaribe, G. Meneguzzi, and J.P. Ortonne. 1996. Defective expression of plectin/HD1 in epidermolysis bullosa simplex with muscular dystrophy. *J Clin Invest*. 97:2289-2298.

Galarneau, L., A. Loranger, S. Gilbert, and N. Marceau. 2007. Keratins modulate hepatic cell adhesion, size and G1/S transition. *Exp Cell Res*. 313:179-194.

Gallicano, G.I., P. Kouklis, C. Bauer, M. Yin, V. Vasioukhin, L. Degenstein, and E. Fuchs. 1998. Desmoplakin is required early in development for assembly of desmosomes and cytoskeletal linkage. *J Cell Biol*. 143:2009-2022.

Gallicano, G.I., C. Bauer, and E. Fuchs. 2001. Rescuing desmoplakin function in extra-embryonic ectoderm reveals the importance of this protein in embryonic heart, neuroepithelium, skin and vasculature. *Development*. 128:929-941.

Garlick, J.A., and L.B. Taichman. 1994. Fate of human keratinocytes during reepithelialization in an organotypic culture model. *Lab Invest*. 70:916-924.

Garrod, D., and M. Chidgey. 2008. Desmosome structure, composition and function. *Biochim Biophys Acta*. 1778:572-587.

Garrod, D.R., M.Y. Berika, W.F. Bardsley, D. Holmes, and L. Tabernero. 2005. Hyper-adhesion in desmosomes: its regulation in wound healing and possible relationship to cadherin crystal structure. *J Cell Sci*. 118:5743-5754.

Geiger, B. 1979. A 130K protein from chicken gizzard: its localization at the termini of microfilament bundles in cultured chicken cells. *Cell*. 18:193-205.

Geiss-Friedlander, R., and F. Melchior. 2007. Concepts in sumoylation: a decade on. *Nat Rev Mol Cell Biol*. 8:947-956.

Georges-Labouesse, E., N. Messaddeq, G. Yehia, L. Cadalbert, A. Dierich, and M. Le Meur. 1996. Absence of integrin alpha 6 leads to epidermolysis bullosa and neonatal death in mice. *Nat Genet*. 13:370-373.

Gerace, L., and G. Blobel. 1980. The nuclear envelope lamina is reversibly depolymerized during mitosis. *Cell*. 19:277-287.

Getsios, S., A.C. Huen, and K.J. Green. 2004. Working out the strength and flexibility of desmosomes. *Nat Rev Mol Cell Biol*. 5:271-281.

Gilmartin, M.E., V.B. Culbertson, and I.M. Freedberg. 1980. Phosphorylation of epidermal keratins. *J Invest Dermatol*. 75:211-216.

Ginhoux, F., and M. Merad. 2010. Ontogeny and homeostasis of Langerhans cells. *Immunol Cell Biol*. 88:387-392.

Giudice, G.J., D.J. Emery, and L.A. Diaz. 1992. Cloning and primary structural analysis of the bullous pemphigoid autoantigen BP180. *J Invest Dermatol*. 99:243-250.

Godsel, L.M., S.N. Hsieh, E.V. Amargo, A.E. Bass, L.T. Pascoe-McGillicuddy, A.C. Huen, M.E. Thorne, C.A. Gaudry, J.K. Park, K. Myung, R.D. Goldman, T.L. Chew, and K.J. Green. 2005. Desmoplakin assembly dynamics in four dimensions: multiple phases differentially regulated by intermediate filaments and actin. *J Cell Biol*. 171:1045-1059.

Godsel, L.M., R.P. Hobbs, and K.J. Green. 2008. Intermediate filament assembly: dynamics to disease. *Trends Cell Biol*. 18:28-37.

Goldman, R.D., B. Grin, M.G. Mendez, and E.R. Kuczmarski. 2008. Intermediate filaments: versatile building blocks of cell structure. *Curr Opin Cell Biol*. 20:28-34.

Goldsmith, L.A. 1990. My organ is bigger than your organ. *Arch Dermatol*. 126:301-302.

Green, K.J., R.D. Goldman, and R.L. Chisholm. 1988. Isolation of cDNAs encoding desmosomal plaque proteins: evidence that bovine desmoplakins I and II are derived from two mRNAs and a single gene. *Proc Natl Acad Sci U S A*. 85:2613-2617.

Green, K.J., D.A. Parry, P.M. Steinert, M.L. Virata, R.M. Wagner, B.D. Angst, and L.A. Nilles. 1990. Structure of the human desmoplakins. Implications for function in the desmosomal plaque. *J Biol Chem*. 265:2603-2612.

Green, K.J., M.L. Virata, G.W. Elgart, J.R. Stanley, and D.A. Parry. 1992. Comparative structural analysis of desmoplakin, bullous pemphigoid antigen and plectin: members of a new gene family involved in organization of intermediate filaments. *Int J Biol Macromol*. 14:145-153.

Green, K.J., and C.A. Gaudry. 2000. Are desmosomes more than tethers for intermediate filaments? *Nat Rev Mol Cell Biol*. 1:208-216.

Green, K.J., and C.L. Simpson. 2007. Desmosomes: new perspectives on a classic. *J Invest Dermatol*. 127:2499-2515.

Grinnell, F. 1990. The activated keratinocyte: up regulation of cell adhesion and migration during wound healing. *J Trauma*. 30:S144-149.

Grinnell, F. 1992. Wound repair, keratinocyte activation and integrin modulation. *J Cell Sci*. 101 (Pt 1):1-5.

Groves, R.W., L. Liu, P.J. Dopping-Hepenstal, H.S. Markus, P.A. Lovell, L. Ozoemena, J.E. Lai-Cheong, J. Gawler, K. Owaribe, T. Hashimoto, J.E. Mellerio, J.B. Mee, and J.A. McGrath. 2010. A homozygous nonsense mutation within the dystonin gene coding for the coiled-coil domain of the epithelial isoform of BPAG1 underlies a new subtype of autosomal recessive epidermolysis bullosa simplex. *J Invest Dermatol*. 130:1551-1557.

Gruber, R., N.J. Wilson, F.J. Smith, D. Grabher, L. Steinwender, P.O. Fritsch, and M. Schmuth. 2009. Increased pachyonychia congenita severity in patients with concurrent keratin and filaggrin mutations. *Br J Dermatol*. 161:1391-1395.

Gu, L.H., S.C. Kim, Y. Ichiki, J. Park, M. Nagai, and Y. Kitajima. 2003. A usual frameshift and delayed termination codon mutation in keratin 5 causes a novel type of epidermolysis bullosa simplex with migratory circinate erythema. *J Invest Dermatol*. 121:482-485.

Gumbiner, B.M. 1996. Cell adhesion: the molecular basis of tissue architecture and morphogenesis. *Cell*. 84:345-357.

Guo, L., L. Degenstein, J. Dowling, Q.C. Yu, R. Wollmann, B. Perman, and E. Fuchs. 1995. Gene targeting of BPAG1: abnormalities in mechanical strength and cell migration in stratified epithelia and neurologic degeneration. *Cell*. 81:233-243.

Gupta, S., D. Campbell, B. Derijard, and R.J. Davis. 1995. Transcription factor ATF2 regulation by the JNK signal transduction pathway. *Science*. 267:389-393.

Gurtner, G.C., S. Werner, Y. Barrandon, and M.T. Longaker. 2008. Wound repair and regeneration. *Nature*. 453:314-321.

Haapasalmi, K., K. Zhang, M. Tonnesen, J. Olerud, D. Sheppard, T. Salo, R. Kramer, R.A. Clark, V.J. Uitto, and H. Larjava. 1996. Keratinocytes in human wounds express alpha v beta 6 integrin. *J Invest Dermatol*. 106:42-48.

Hadj-Rabia, S., L. Baala, P. Vabres, D. Hamel-Teillac, E. Jacquemin, M. Fabre, S. Lyonnet, Y. De Prost, A. Munnich, M. Hadchouel, and A. Smahi. 2004. Claudin-1 gene mutations in neonatal sclerosing cholangitis associated with ichthyosis: a tight junction disease. *Gastroenterology*. 127:1386-1390.

Hamill, K.J., S.B. Hopkinson, P. DeBiase, and J.C. Jones. 2009. BPAG1e maintains keratinocyte polarity through beta4 integrin-mediated modulation of Rac1 and cofilin activities. *Mol Biol Cell*. 20:2954-2962.

Han, J., J.D. Lee, L. Bibbs, and R.J. Ulevitch. 1994. A MAP kinase targeted by endotoxin and hyperosmolarity in mammalian cells. *Science*. 265:808-811.

Harper, E.G., S.M. Alvares, and W.G. Carter. 2005. Wounding activates p38 map kinase and activation transcription factor 3 in leading keratinocytes. *J Cell Sci*. 118:3471-3485.

Hatzfeld, M., and W.W. Franke. 1985. Pair formation and promiscuity of cytokeratins: formation in vitro of heterotypic complexes and intermediate-sized filaments by homologous and heterologous recombinations of purified polypeptides. *J Cell Biol*. 101:1826-1841.

Hatzfeld, M., and K. Weber. 1990. The coiled coil of in vitro assembled keratin filaments is a heterodimer of type I and II keratins: use of site-specific mutagenesis and recombinant protein expression. *J Cell Biol*. 110:1199-1210.

Hatzfeld, M. 2007. Plakophilins: Multifunctional proteins or just regulators of desmosomal adhesion? *Biochim Biophys Acta*. 1773:69-77.

He, H., Q. Gu, M. Zheng, D. Normolle, and Y. Sun. 2008. SAG/ROC2/RBX2 E3 ligase promotes UVB-induced skin hyperplasia, but not skin tumors, by simultaneously targeting c-Jun/AP-1 and p27. *Carcinogenesis*. 29:858-865.

He, X.H., X.N. Zhang, W. Mao, H.P. Chen, L.R. Xu, H. Chen, X.L. He, and Y.P. Le. 2004. A novel mutation of keratin 9 in a large Chinese family with epidermolytic palmoplantar keratoderma. *Br J Dermatol*. 150:647-651.

Heid, H.W., A. Schmidt, R. Zimbelmann, S. Schafer, S. Winter-Simanowski, S. Stumpp, M. Keith, U. Figge, M. Schnolzer, and W.W. Franke. 1994. Cell type-specific desmosomal plaque proteins of the plakoglobin family: plakophilin 1 (band 6 protein). *Differentiation*. 58:113-131.

Helfand, B.T., M.G. Mendez, S.N. Murthy, D.K. Shumaker, B. Grin, S. Mahammad, U. Aebi, T. Wedig, Y.I. Wu, K.M. Hahn, M. Inagaki, H. Herrmann, and R.D. Goldman. 2011. Vimentin organization modulates the formation of lamellipodia. *Mol Biol Cell*. 22:1274-1289.

Henikoff, S., and J.G. Henikoff. 1992. Amino acid substitution matrices from protein blocks. *Proc Natl Acad Sci U S A*. 89:10915-10919.

Herrmann, H., M. Haner, M. Brettel, S.A. Muller, K.N. Goldie, B. Fedtke, A. Lustig, W.W. Franke, and U. Aebi. 1996. Structure and assembly properties of the intermediate filament protein vimentin: the role of its head, rod and tail domains. *J Mol Biol*. 264:933-953.

Herrmann, H., S.V. Strelkov, B. Feja, K.R. Rogers, M. Brettel, A. Lustig, M. Haner, D.A. Parry, P.M. Steinert, P. Burkhard, and U. Aebi. 2000. The intermediate filament protein consensus motif of helix 2B: its atomic structure and contribution to assembly. *J Mol Biol*. 298:817-832.

Herrmann, H., S.V. Strelkov, P. Burkhard, and U. Aebi. 2009. Intermediate filaments: primary determinants of cell architecture and plasticity. *J Clin Invest*. 119:1772-1783.

Hershko, A., and A. Ciechanover. 1998. The ubiquitin system. *Annu Rev Biochem*. 67:425-479.

Heuser, A., E.R. Plovie, P.T. Ellinor, K.S. Grossmann, J.T. Shin, T. Wichter, C.T. Basson, B.B. Lerman, S. Sasse-Klaassen, L. Thierfelder, C.A. MacRae, and B. Gerull. 2006. Mutant desmocollin-2 causes arrhythmogenic right ventricular cardiomyopathy. *Am J Hum Genet*. 79:1081-1088.

Hibi, M., A. Lin, T. Smeal, A. Minden, and M. Karin. 1993. Identification of an oncoprotein- and UV-responsive protein kinase that binds and potentiates the c-Jun activation domain. *Genes Dev*. 7:2135-2148.

Hickerson, R.P., F.J. Smith, W.H. McLean, M. Landthaler, R.E. Leube, and R.L. Kaspar. 2006. SiRNA-mediated selective inhibition of mutant keratin mRNAs responsible for the skin disorder pachyonychia congenita. *Ann N Y Acad Sci*. 1082:56-61.

Hill, C.S., and R. Treisman. 1995. Transcriptional regulation by extracellular signals: mechanisms and specificity. *Cell*. 80:199-211.

Hirako, Y., J. Usukura, Y. Nishizawa, and K. Owaribe. 1996. Demonstration of the molecular shape of BP180, a 180-kDa bullous pemphigoid antigen and its potential for trimer formation. *J Biol Chem*. 271:13739-13745.

Holbrook, K.A., R.A. Underwood, A.M. Vogel, A.M. Gown, and H. Kimball. 1989. The appearance, density and distribution of melanocytes in human embryonic and fetal skin revealed by the anti-melanoma monoclonal antibody, HMB-45. *Anat Embryol (Berl)*. 180:443-455.

Hopkinson, S.B., S.E. Baker, and J.C. Jones. 1995. Molecular genetic studies of a human epidermal autoantigen (the 180-kD bullous pemphigoid antigen/BP180): identification of functionally important sequences within the BP180 molecule and evidence for an interaction between BP180 and alpha 6 integrin. *J Cell Biol*. 130:117-125.

Hopkinson, S.B., K. Findlay, G.W. deHart, and J.C. Jones. 1998. Interaction of BP180 (type XVII collagen) and alpha6 integrin is necessary for stabilization of hemidesmosome structure. *J Invest Dermatol*. 111:1015-1022.

Hopkinson, S.B., and J.C. Jones. 2000. The N terminus of the transmembrane protein BP180 interacts with the N-terminal domain of BP230, thereby mediating keratin cytoskeleton anchorage to the cell surface at the site of the hemidesmosome. *Mol Biol Cell*. 11:277-286.

Horn, H.M., and M.J. Tidman. 2000. The clinical spectrum of epidermolysis bullosa simplex. *Br J Dermatol*. 142:468-472.

Hu, Z., J.M. Bonifas, J. Beech, G. Bench, T. Shigihara, H. Ogawa, S. Ikeda, T. Mauro, and E.H. Epstein, Jr. 2000. Mutations in ATP2C1, encoding a calcium pump, cause Hailey-Hailey disease. *Nat Genet*. 24:61-65.

Huber, M., I. Rettler, K. Bernasconi, E. Frenk, S.P. Lavrijsen, M. Ponec, A. Bon, S. Lautenschlager, D.F. Schorderet, and D. Hohl. 1995. Mutations of keratinocyte transglutaminase in lamellar ichthyosis. *Science*. 267:525-528.

Hudson, L.G., and L.J. McCawley. 1998. Contributions of the epidermal growth factor receptor to keratinocyte motility. *Microsc Res Tech*. 43:444-455.

Hunt, D.M., L. Rickman, N.V. Whittock, R.A. Eady, D. Simrak, P.J. Dopping-Hepenstal, H.P. Stevens, D.K. Armstrong, H.C. Hennies, W. Kuster, A.E. Hughes, J. Arnemann, I.M. Leigh, J.A. McGrath, D.P. Kelsell, and R.S. Buxton. 2001. Spectrum of dominant mutations in the desmosomal cadherin desmoglein 1, causing the skin disease striate palmoplantar keratoderma. *Eur J Hum Genet*. 9:197-203.

Ikai, K., and J.S. McGuire. 1983. Phosphorylation of keratin polypeptides. *Biochim Biophys Acta*. 760:371-376.

Inagaki, M., Y. Nishi, K. Nishizawa, M. Matsuyama, and C. Sato. 1987. Site-specific phosphorylation induces disassembly of vimentin filaments in vitro. *Nature*. 328:649-652.

Inagaki, M., Y. Gonda, S. Ando, S. Kitamura, Y. Nishi, and C. Sato. 1989. Regulation of assembly-disassembly of intermediate filaments in vitro. *Cell Struct Funct*. 14:279-286.

Ishida-Yamamoto, A., J.A. McGrath, S.J. Chapman, I.M. Leigh, E.B. Lane, and R.A. Eady. 1991. Epidermolysis bullosa simplex (Dowling-Meara type) is a genetic disease characterized by an abnormal keratin-filament network involving keratins K5 and K14. *J Invest Dermatol*. 97:959-968.

Ishida-Yamamoto, A., and M. Kishibe. 2011. Involvement of corneodesmosome degradation and lamellar granule transportation in the desquamation process. *Med Mol Morphol*. 44:1-6.

Ito, M., Y. Liu, Z. Yang, J. Nguyen, F. Liang, R.J. Morris, and G. Cotsarelis. 2005. Stem cells in the hair follicle bulge contribute to wound repair but not to homeostasis of the epidermis. *Nat Med*. 11:1351-1354.

Izawa, I., and M. Inagaki. 2006. Regulatory mechanisms and functions of intermediate filaments: a study using site- and phosphorylation state-specific antibodies. *Cancer Sci*. 97:167-174.

Jaitovich, A., S. Mehta, N. Na, A. Ciechanover, R.D. Goldman, and K.M. Ridge. 2008. Ubiquitin-proteasome-mediated degradation of keratin intermediate filaments in mechanically stimulated A549 cells. *J Biol Chem*. 283:25348-25355.

Jerabkova, B., J. Marek, H. Buckova, L. Kopeckova, K. Vesely, J. Valickova, J. Fajkus, and L. Fajkusova. 2010. Keratin mutations in patients with epidermolysis bullosa simplex: correlations between phenotype severity and disturbance of intermediate filament molecular structure. *Br J Dermatol.* 162:1004-1013.

Jiang, C.K., T. Magnaldo, M. Ohtsuki, I.M. Freedberg, F. Bernerd, and M. Blumenberg. 1993. Epidermal growth factor and transforming growth factor alpha specifically induce the activation- and hyperproliferation-associated keratins 6 and 16. *Proc Natl Acad Sci U S A.* 90:6786-6790.

Jobard, F., B. Bouadjar, F. Caux, S. Hadj-Rabia, C. Has, F. Matsuda, J. Weissenbach, M. Lathrop, J.F. Prud'homme, and J. Fischer. 2003. Identification of mutations in a new gene encoding a FERM family protein with a pleckstrin homology domain in Kindler syndrome. *Hum Mol Genet.* 12:925-935.

Jockusch, B.M., P. Bubeck, K. Giehl, M. Kroemker, J. Moschner, M. Rothkegel, M. Rudiger, K. Schluter, G. Stanke, and J. Winkler. 1995. The molecular architecture of focal adhesions. *Annu Rev Cell Dev Biol.* 11:379-416.

Johnson, G.L., and R. Lapadat. 2002. Mitogen-activated protein kinase pathways mediated by ERK, JNK, and p38 protein kinases. *Science.* 298:1911-1912.

Jones, J.C., S.B. Hopkinson, and L.E. Goldfinger. 1998. Structure and assembly of hemidesmosomes. *Bioessays.* 20:488-494.

Jones, P., and B.D. Simons. 2008. Epidermal homeostasis: do committed progenitors work while stem cells sleep? *Nat Rev Mol Cell Biol.* 9:82-88.

Jonkman, M.F., M.C. de Jong, K. Heeres, H.H. Pas, J.B. van der Meer, K. Owaribe, A.M. Martinez de Velasco, C.M. Niessen, and A. Sonnenberg. 1995. 180-kD bullous pemphigoid antigen (BP180) is deficient in generalized atrophic benign epidermolysis bullosa. *J Clin Invest.* 95:1345-1352.

Jonkman, M.F., K. Heeres, H.H. Pas, M.J. van Luyn, J.D. Elema, L.D. Corden, F.J. Smith, W.H. McLean, F.C. Ramaekers, M. Burton, and H. Scheffer. 1996. Effects of keratin 14 ablation on the clinical and cellular phenotype in a kindred with recessive epidermolysis bullosa simplex. *J Invest Dermatol.* 107:764-769.

Jonkman, M.F. 1999. Hereditary skin diseases of hemidesmosomes. *J Dermatol Sci.* 20:103-121.

Jonkman, M.F., A.M. Pasmooij, S.G. Pasmans, M.P. van den Berg, H.J. Ter Horst, A. Timmer, and H.H. Pas. 2005. Loss of desmoplakin tail causes lethal acantholytic epidermolysis bullosa. *Am J Hum Genet.* 77:653-660.

Kalluri, R., and R.A. Weinberg. 2009. The basics of epithelial-mesenchymal transition. *J Clin Invest.* 119:1420-1428.

Kapprell, H.P., P. Cowin, and W.W. Franke. 1987. Biochemical characterization of the soluble form of the junctional plaque protein, plakoglobin, from different cell types. *Eur J Biochem*. 166:505-517.

Kapprell, H.P., K. Owaribe, and W.W. Franke. 1988. Identification of a basic protein of Mr 75,000 as an accessory desmosomal plaque protein in stratified and complex epithelia. *J Cell Biol*. 106:1679-1691.

Kartasova, T., D.R. Roop, K.A. Holbrook, and S.H. Yuspa. 1993. Mouse differentiation-specific keratins 1 and 10 require a preexisting keratin scaffold to form a filament network. *J Cell Biol*. 120:1251-1261.

Kasahara, K., T. Kartasova, X.Q. Ren, T. Ikuta, K. Chida, and T. Kuroki. 1993. Hyperphosphorylation of keratins by treatment with okadaic acid of BALB/MK-2 mouse keratinocytes. *J Biol Chem*. 268:23531-23537.

Katz, S.I., K. Tamaki, and D.H. Sachs. 1979. Epidermal Langerhans cells are derived from cells originating in bone marrow. *Nature*. 282:324-326.

Keene, D.R., L.Y. Sakai, G.P. Lunstrum, N.P. Morris, and R.E. Burgeson. 1987. Type VII collagen forms an extended network of anchoring fibrils. *J Cell Biol*. 104:611-621.

Kelsell, D.P., J. Dunlop, H.P. Stevens, N.J. Lench, J.N. Liang, G. Parry, R.F. Mueller, and I.M. Leigh. 1997. Connexin 26 mutations in hereditary non-syndromic sensorineural deafness. *Nature*. 387:80-83.

Kelsell, D.P., W.L. Di, and M.J. Houseman. 2001. Connexin mutations in skin disease and hearing loss. *Am J Hum Genet*. 68:559-568.

Kelsell, D.P., E.E. Norgett, H. Unsworth, M.T. Teh, T. Cullup, C.A. Mein, P.J. Dopping-Hepenstal, B.A. Dale, G. Tadini, P. Fleckman, K.G. Stephens, V.P. Sybert, S.B. Mallory, B.V. North, D.R. Witt, E. Sprecher, A.E. Taylor, A. Ilchyshyn, C.T. Kennedy, H. Goodyear, C. Moss, D. Paige, J.I. Harper, B.D. Young, I.M. Leigh, R.A. Eady, and E.A. O'Toole. 2005. Mutations in ABCA12 underlie the severe congenital skin disease harlequin ichthyosis. *Am J Hum Genet*. 76:794-803.

Kerns, M.L., D. DePianto, A.T. Dinkova-Kostova, P. Talalay, and P.A. Coulombe. 2007. Reprogramming of keratin biosynthesis by sulforaphane restores skin integrity in epidermolysis bullosa simplex. *Proc Natl Acad Sci U S A*. 104:14460-14465.

Khapare, N., S.T. Kundu, L. Sehgal, M. Sawant, R. Priya, P. Gosavi, N. Gupta, H. Alam, M. Karkhanis, N. Naik, M.M. Vaidya, and S.N. Dalal. 2012. Plakophilin3 loss leads to an increase in PRL3 levels promoting K8 dephosphorylation, which is required for transformation and metastasis. *PLoS One*. 7:e38561.

Kim, S., P. Wong, and P.A. Coulombe. 2006. A keratin cytoskeletal protein regulates protein synthesis and epithelial cell growth. *Nature*. 441:362-365.

Kimura, T.E., A.J. Merritt, and D.R. Garrod. 2007. Calcium-independent desmosomes of keratinocytes are hyper-adhesive. *J Invest Dermatol*. 127:775-781.

Kinashi, T. 2012. Overview of integrin signaling in the immune system. *Methods Mol Biol*. 757:261-278.

King, I.A., and E.F. Hounsell. 1989. Cytokeratin 13 contains O-glycosidically linked N-acetylglucosamine residues. *J Biol Chem*. 264:14022-14028.

Kirfel, G., and V. Herzog. 2004. Migration of epidermal keratinocytes: mechanisms, regulation, and biological significance. *Protoplasma*. 223:67-78.

Kivirikko, S., J.A. McGrath, C. Baudoin, D. Aberdam, S. Ciatti, M.G. Dunnill, J.R. McMillan, R.A. Eady, J.P. Ortonne, G. Meneguzzi, and et al. 1995. A homozygous nonsense mutation in the alpha 3 chain gene of laminin 5 (LAMA3) in lethal (Herlitz) junctional epidermolysis bullosa. *Hum Mol Genet*. 4:959-962.

Kivirikko, S., J.A. McGrath, L. Pulkkinen, J. Uitto, and A.M. Christiano. 1996. Mutational hotspots in the LAMB3 gene in the lethal (Herlitz) type of junctional epidermolysis bullosa. *Hum Mol Genet*. 5:231-237.

Kjaer, K.W., L. Hansen, G.C. Schwabe, A.P. Marques-de-Faria, H. Eiberg, S. Mundlos, N. Tommerup, and T. Rosenberg. 2005. Distinct CDH3 mutations cause ectodermal dysplasia, ectrodactyly, macular dystrophy (EEM syndrome). *J Med Genet*. 42:292-298.

Klareskog, L., U. Tjernlund, U. Forsum, and P.A. Peterson. 1977. Epidermal Langerhans cells express Ia antigens. *Nature*. 268:248-250.

Klemke, R.L., S. Cai, A.L. Giannini, P.J. Gallagher, P. de Lanerolle, and D.A. Cheresh. 1997. Regulation of cell motility by mitogen-activated protein kinase. *J Cell Biol*. 137:481-492.

Kljuic, A., H. Bazzi, J.P. Sundberg, A. Martinez-Mir, R. O'Shaughnessy, M.G. Mahoney, M. Levy, X. Montagutelli, W. Ahmad, V.M. Aita, D. Gordon, J. Uitto, D. Whiting, J. Ott, S. Fischer, T.C. Gilliam, C.A. Jahoda, R.J. Morris, A.A. Panteleyev, V.T. Nguyen, and A.M. Christiano. 2003. Desmoglein 4 in hair follicle differentiation and epidermal adhesion: evidence from inherited hypotrichosis and acquired pemphigus vulgaris. *Cell*. 113:249-260.

Koch, P.J., M.J. Walsh, M. Schmelz, M.D. Goldschmidt, R. Zimbelmann, and W.W. Franke. 1990. Identification of desmoglein, a constitutive desmosomal glycoprotein, as a member of the cadherin family of cell adhesion molecules. *Eur J Cell Biol*. 53:1-12.

Koch, P.J., and W.W. Franke. 1994. Desmosomal cadherins: another growing multigene family of adhesion molecules. *Curr Opin Cell Biol*. 6:682-687.

Koch, P.J., M.G. Mahoney, H. Ishikawa, L. Pulkkinen, J. Uitto, L. Shultz, G.F. Murphy, D. Whitaker-Menezes, and J.R. Stanley. 1997. Targeted disruption of the pemphigus vulgaris antigen (desmoglein 3) gene in mice causes loss of

keratinocyte cell adhesion with a phenotype similar to pemphigus vulgaris. *J Cell Biol*. 137:1091-1102.

Koebner, H. 1886. Hereditare anlage zur blasendilbung (epidermolysis bullosa hereditaria) *Dtsch. Med. Wochenschr*. 12:21-22.

Kolev, V., A. Mandinova, J. Guinea-Viniegra, B. Hu, K. Lefort, C. Lambertini, V. Neel, R. Dummer, E.F. Wagner, and G.P. Dotto. 2008. EGFR signalling as a negative regulator of Notch1 gene transcription and function in proliferating keratinocytes and cancer. *Nat Cell Biol*. 10:902-911.

Kollias, N., R.M. Sayre, L. Zeise, and M.R. Chedekel. 1991. Photoprotection by melanin. *J Photochem Photobiol B*. 9:135-160.

Kolsch, A., R. Windoffer, and R.E. Leube. 2009. Actin-dependent dynamics of keratin filament precursors. *Cell Motil Cytoskeleton*. 66:976-985.

Kornfeld, K., D.B. Hom, and H.R. Horvitz. 1995. The ksr-1 gene encodes a novel protein kinase involved in Ras-mediated signaling in C. elegans. *Cell*. 83:903-913.

Koss-Harnes, D., B. Hoyheim, I. Anton-Lamprecht, A. Gjesti, R.S. Jorgensen, F.L. Jahnsen, B. Olaisen, G. Wiche, and T. Gedde-Dahl, Jr. 2002. A site-specific plectin mutation causes dominant epidermolysis bullosa simplex Ogna: two identical de novo mutations. *J Invest Dermatol*. 118:87-93.

Koster, J., D. Geerts, B. Favre, L. Borradori, and A. Sonnenberg. 2003. Analysis of the interactions between BP180, BP230, plectin and the integrin alpha6beta4 important for hemidesmosome assembly. *J Cell Sci*. 116:387-399.

Koster, M.I., and D.R. Roop. 2007. Mechanisms regulating epithelial stratification. *Annu Rev Cell Dev Biol*. 23:93-113.

Kouklis, P.D., E. Hutton, and E. Fuchs. 1994. Making a connection: direct binding between keratin intermediate filaments and desmosomal proteins. *J Cell Biol*. 127:1049-1060.

Koulu, L., A. Kusumi, M.S. Steinberg, V. Klaus-Kovtun, and J.R. Stanley. 1984. Human autoantibodies against a desmosomal core protein in pemphigus foliaceus. *J Exp Med*. 160:1509-1518.

Kowalczyk, A.P., E.A. Bornslaeger, J.E. Borgwardt, H.L. Palka, A.S. Dhaliwal, C.M. Corcoran, M.F. Denning, and K.J. Green. 1997. The amino-terminal domain of desmoplakin binds to plakoglobin and clusters desmosomal cadherin-plakoglobin complexes. *J Cell Biol*. 139:773-784.

Kowalczyk, A.P., E.A. Bornslaeger, S.M. Norvell, H.L. Palka, and K.J. Green. 1999. Desmosomes: intercellular adhesive junctions specialized for attachment of intermediate filaments. *Int Rev Cytol*. 185:237-302.

Ku, N.O., and M.B. Omary. 1995. Identification and mutational analysis of the glycosylation sites of human keratin 18. *J Biol Chem*. 270:11820-11827.

Ku, N.O., J. Liao, and M.B. Omary. 1997. Apoptosis generates stable fragments of human type I keratins. *J Biol Chem*. 272:33197-33203.

Ku, N.O., and M.B. Omary. 1997. Phosphorylation of human keratin 8 in vivo at conserved head domain serine 23 and at epidermal growth factor-stimulated tail domain serine 431. *J Biol Chem*. 272:7556-7564.

Ku, N.O., J. Liao, and M.B. Omary. 1998a. Phosphorylation of human keratin 18 serine 33 regulates binding to 14-3-3 proteins. *Embo J*. 17:1892-1906.

Ku, N.O., S.A. Michie, R.M. Soetikno, E.Z. Resurreccion, R.L. Broome, and M.B. Omary. 1998b. Mutation of a major keratin phosphorylation site predisposes to hepatotoxic injury in transgenic mice. *J Cell Biol*. 143:2023-2032.

Ku, N.O., and M.B. Omary. 2000. Keratins turn over by ubiquitination in a phosphorylation-modulated fashion. *J Cell Biol*. 149:547-552.

Ku, N.O., and M.B. Omary. 2001. Effect of mutation and phosphorylation of type I keratins on their caspase-mediated degradation. *J Biol Chem*. 276:26792-26798.

Ku, N.O., S. Michie, E.Z. Resurreccion, R.L. Broome, and M.B. Omary. 2002. Keratin binding to 14-3-3 proteins modulates keratin filaments and hepatocyte mitotic progression. *Proc Natl Acad Sci U S A*. 99:4373-4378.

Ku, N.O., J.M. Darling, S.M. Krams, C.O. Esquivel, E.B. Keeffe, R.K. Sibley, Y.M. Lee, T.L. Wright, and M.B. Omary. 2003. Keratin 8 and 18 mutations are risk factors for developing liver disease of multiple etiologies. *Proc Natl Acad Sci U S A*. 100:6063-6068.

Ku, N.O., and M.B. Omary. 2006. A disease- and phosphorylation-related nonmechanical function for keratin 8. *J Cell Biol*. 174:115-125.

Ku, N.O., D.M. Toivola, P. Strnad, and M.B. Omary. 2010. Cytoskeletal keratin glycosylation protects epithelial tissue from injury. *Nat Cell Biol*. 12:876-885.

Kurpakus, M.A., E.L. Stock, and J.C. Jones. 1990. Analysis of wound healing in an in vitro model: early appearance of laminin and a 125 x 10(3) Mr polypeptide during adhesion complex formation. *J Cell Sci*. 96 (Pt 4):651-660.

Lane, E.B., S.L. Goodman, and L.K. Trejdosiewicz. 1982. Disruption of the keratin filament network during epithelial cell division. *Embo J*. 1:1365-1372.

Lane, E.B., E.L. Rugg, H. Navsaria, I.M. Leigh, A.H. Heagerty, A. Ishida-Yamamoto, and R.A. Eady. 1992. A mutation in the conserved helix termination peptide of keratin 5 in hereditary skin blistering. *Nature*. 356:244-246.

Lane, E.B. 1994. Keratin diseases. *Curr Opin Genet Dev*. 4:412-418.

Lane, E.B., and W.H. McLean. 2004. Keratins and skin disorders. *J Pathol*. 204:355-366.

Langbein, L., M.A. Rogers, H. Winter, S. Praetzel, U. Beckhaus, H.R. Rackwitz, and J. Schweizer. 1999. The catalog of human hair keratins. I. Expression of the nine type I members in the hair follicle. *J Biol Chem*. 274:19874-19884.

Langbein, L., M.A. Rogers, H. Winter, S. Praetzel, and J. Schweizer. 2001. The catalog of human hair keratins. II. Expression of the six type II members in the hair follicle and the combined catalog of human type I and II keratins. *J Biol Chem*. 276:35123-35132.

Laplante, A.F., L. Germain, F.A. Auger, and V. Moulin. 2001. Mechanisms of wound reepithelialization: hints from a tissue-engineered reconstructed skin to long-standing questions. *Faseb J*. 15:2377-2389.

Lau, K., R. Paus, S. Tiede, P. Day, and A. Bayat. 2009. Exploring the role of stem cells in cutaneous wound healing. *Exp Dermatol*. 18:921-933.

Lauffenburger, D.A., and A.F. Horwitz. 1996. Cell migration: a physically integrated molecular process. *Cell*. 84:359-369.

Lazarides, E., and K. Burridge. 1975. Alpha-actinin: immunofluorescent localization of a muscle structural protein in nonmuscle cells. *Cell*. 6:289-298.

Lazarus, G.S., D.M. Cooper, D.R. Knighton, D.J. Margolis, R.E. Pecoraro, G. Rodeheaver, and M.C. Robson. 1994. Definitions and guidelines for assessment of wounds and evaluation of healing. *Arch Dermatol*. 130:489-493.

Leachman, S.A., R.P. Hickerson, P.R. Hull, F.J. Smith, L.M. Milstone, E.B. Lane, S.J. Bale, D.R. Roop, W.H. McLean, and R.L. Kaspar. 2008. Therapeutic siRNAs for dominant genetic skin disorders including pachyonychia congenita. *J Dermatol Sci*. 51:151-157.

Leachman, S.A., R.P. Hickerson, M.E. Schwartz, E.E. Bullough, S.L. Hutcherson, K.M. Boucher, C.D. Hansen, M.J. Eliason, G.S. Srivatsa, D.J. Kornbrust, F.J. Smith, W.I. McLean, L.M. Milstone, and R.L. Kaspar. 2010. First-in-human mutation-targeted siRNA phase Ib trial of an inherited skin disorder. *Mol Ther*. 18:442-446.

Lechler, T., and E. Fuchs. 2005. Asymmetric cell divisions promote stratification and differentiation of mammalian skin. *Nature*. 437:275-280.

Lee, C.H., M.S. Kim, B.M. Chung, D.J. Leahy, and P.A. Coulombe. 2012. Structural basis for heteromeric assembly and perinuclear organization of keratin filaments. *Nat Struct Mol Biol*. 19:707-715.

Lemmon, M.A., and J. Schlessinger. 2010. Cell signaling by receptor tyrosine kinases. *Cell*. 141:1117-1134.

Leopold, P.L., J. Vincent, and H. Wang. 2012. A comparison of epithelial-to-mesenchymal transition and re-epithelialization. *Semin Cancer Biol*. 22:471-483.

Letai, A., P.A. Coulombe, M.B. McCormick, Q.C. Yu, E. Hutton, and E. Fuchs. 1993. Disease severity correlates with position of keratin point mutations in patients with epidermolysis bullosa simplex. *Proc Natl Acad Sci U S A*. 90:3197-3201.

Leung, C.L., K.J. Green, and R.K. Liem. 2002. Plakins: a family of versatile cytolinker proteins. *Trends Cell Biol*. 12:37-45.

Levy-Nissenbaum, E., R.C. Betz, M. Frydman, M. Simon, H. Lahat, T. Bakhan, B. Goldman, A. Bygum, M. Pierick, A.M. Hillmer, N. Jonca, J. Toribio, R. Kruse, G. Dewald, S. Cichon, C. Kubisch, M. Guerrin, G. Serre, M.M. Nothen, and E. Pras. 2003. Hypotrichosis simplex of the scalp is associated with nonsense mutations in CDSN encoding corneodesmosin. *Nat Genet*. 34:151-153.

Liang, L., and J.R. Bickenbach. 2002. Somatic epidermal stem cells can produce multiple cell lineages during development. *Stem Cells*. 20:21-31.

Liao, J., N.O. Ku, and M.B. Omary. 1997. Stress, apoptosis, and mitosis induce phosphorylation of human keratin 8 at Ser-73 in tissues and cultured cells. *J Biol Chem*. 272:17565-17573.

Liovic, M., M.M. Mogensen, A.R. Prescott, and E.B. Lane. 2003. Observation of keratin particles showing fast bidirectional movement colocalized with microtubules. *J Cell Sci*. 116:1417-1427.

Liovic, M., B. Lee, M. Tomic-Canic, M. D'Alessandro, V.N. Bolshakov, and E.B. Lane. 2008. Dual-specificity phosphatases in the hypo-osmotic stress response of keratin-defective epithelial cell lines. *Exp Cell Res*. 314:2066-2075.

Liovic, M., M. D'Alessandro, M. Tomic-Canic, V.N. Bolshakov, S.E. Coats, and E.B. Lane. 2009. Severe keratin 5 and 14 mutations induce down-regulation of junction proteins in keratinocytes. *Exp Cell Res*. 315:2995-3003.

Lloyd, C., Q.C. Yu, J. Cheng, K. Turksen, L. Degenstein, E. Hutton, and E. Fuchs. 1995. The basal keratin network of stratified squamous epithelia: defining K15 function in the absence of K14. *J Cell Biol*. 129:1329-1344.

Lowe, J., A. Blanchard, K. Morrell, G. Lennox, L. Reynolds, M. Billett, M. Landon, and R.J. Mayer. 1988. Ubiquitin is a common factor in intermediate filament inclusion bodies of diverse type in man, including those of Parkinson's disease, Pick's disease, and Alzheimer's disease, as well as Rosenthal fibres in cerebellar astrocytomas, cytoplasmic bodies in muscle, and mallory bodies in alcoholic liver disease. *J Pathol*. 155:9-15.

Lu, C.P., L. Polak, A.S. Rocha, H.A. Pasolli, S.C. Chen, N. Sharma, C. Blanpain, and E. Fuchs. 2012. Identification of stem cell populations in sweat glands and ducts reveals roles in homeostasis and wound repair. *Cell*. 150:136-150.

Lu, H., M. Hesse, B. Peters, and T.M. Magin. 2005. Type II keratins precede type I keratins during early embryonic development. *Eur J Cell Biol*. 84:709-718.

Luttrell, L.M., S.S. Ferguson, Y. Daaka, W.E. Miller, S. Maudsley, G.J. Della Rocca, F. Lin, H. Kawakatsu, K. Owada, D.K. Luttrell, M.G. Caron, and R.J.

Lefkowitz. 1999. Beta-arrestin-dependent formation of beta2 adrenergic receptor-Src protein kinase complexes. *Science*. 283:655-661.

Lynley, A.M., and B.A. Dale. 1983. The characterization of human epidermal filaggrin. A histidine-rich, keratin filament-aggregating protein. *Biochim Biophys Acta*. 744:28-35.

Ma, S., L. Rao, I.M. Freedberg, and M. Blumenberg. 1997. Transcriptional control of K5, K6, K14, and K17 keratin genes by AP-1 and NF-kappaB family members. *Gene Expr*. 6:361-370.

Macari, F., M. Landau, P. Cousin, B. Mevorah, S. Brenner, R. Panizzon, D.F. Schorderet, D. Hohl, and M. Huber. 2000. Mutation in the gene for connexin 30.3 in a family with erythrokeratodermia variabilis. *Am J Hum Genet*. 67:1296-1301.

Mackenzie, J.C. 1969. Ordered structure of the stratum corneum of mammalian skin. *Nature*. 222:881-882.

Madara, J.L. 1998. Regulation of the movement of solutes across tight junctions. *Annu Rev Physiol*. 60:143-159.

Maestrini, E., A.P. Monaco, J.A. McGrath, A. Ishida-Yamamoto, C. Camisa, A. Hovnanian, D.E. Weeks, M. Lathrop, J. Uitto, and A.M. Christiano. 1996. A molecular defect in loricrin, the major component of the cornified cell envelope, underlies Vohwinkel's syndrome. *Nat Genet*. 13:70-77.

Maestrini, E., B.P. Korge, J. Ocana-Sierra, E. Calzolari, S. Cambiaghi, P.M. Scudder, A. Hovnanian, A.P. Monaco, and C.S. Munro. 1999. A missense mutation in connexin26, D66H, causes mutilating keratoderma with sensorineural deafness (Vohwinkel's syndrome) in three unrelated families. *Hum Mol Genet*. 8:1237-1243.

Magin, T.M., H.W. Kaiser, S. Leitgeb, C. Grund, I.M. Leigh, S.M. Morley, and E.B. Lane. 2000. Supplementation of a mutant keratin by stable expression of desmin in cultured human EBS keratinocytes. *J Cell Sci*. 113 Pt 23:4231-4239.

Magin, T.M., J. Reichelt, and M. Hatzfeld. 2004. Emerging functions: diseases and animal models reshape our view of the cytoskeleton. *Exp Cell Res*. 301:91-102.

Mainiero, F., A. Pepe, M. Yeon, Y. Ren, and F.G. Giancotti. 1996. The intracellular functions of alpha6beta4 integrin are regulated by EGF. *J Cell Biol*. 134:241-253.

Manser, E., H.Y. Huang, T.H. Loo, X.Q. Chen, J.M. Dong, T. Leung, and L. Lim. 1997. Expression of constitutively active alpha-PAK reveals effects of the kinase on actin and focal complexes. *Mol Cell Biol*. 17:1129-1143.

Marinkovich, M.P., G.P. Lunstrum, and R.E. Burgeson. 1992. The anchoring filament protein kalinin is synthesized and secreted as a high molecular weight precursor. *J Biol Chem*. 267:17900-17906.

Martin, P. 1997. Wound healing--aiming for perfect skin regeneration. *Science*. 276:75-81.

Masunaga, T., H. Shimizu, C. Yee, L. Borradori, Z. Lazarova, T. Nishikawa, and K.B. Yancey. 1997. The extracellular domain of BPAG2 localizes to anchoring filaments and its carboxyl terminus extends to the lamina densa of normal human epidermal basement membrane. *J Invest Dermatol*. 109:200-206.

Mathur, M., L. Goodwin, and P. Cowin. 1994. Interactions of the cytoplasmic domain of the desmosomal cadherin Dsg1 with plakoglobin. *J Biol Chem*. 269:14075-14080.

Matoltsy, A.G. 1955. In vitro wound repair of adult human skin. *Anat Rec*. 122:581-587.

Mazzalupo, S., P. Wong, P. Martin, and P.A. Coulombe. 2003. Role for keratins 6 and 17 during wound closure in embryonic mouse skin. *Dev Dyn*. 226:356-365.

McCrea, P.D., C.W. Turck, and B. Gumbiner. 1991. A homolog of the armadillo protein in Drosophila (plakoglobin) associated with E-cadherin. *Science*. 254:1359-1361.

McGrath, J.A., B. Gatalica, A.M. Christiano, K. Li, K. Owaribe, J.R. McMillan, R.A. Eady, and J. Uitto. 1995. Mutations in the 180-kD bullous pemphigoid antigen (BPAG2), a hemidesmosomal transmembrane collagen (COL17A1), in generalized atrophic benign epidermolysis bullosa. *Nat Genet*. 11:83-86.

McGrath, J.A., J.R. McMillan, C.S. Shemanko, S.K. Runswick, I.M. Leigh, E.B. Lane, D.R. Garrod, and R.A. Eady. 1997. Mutations in the plakophilin 1 gene result in ectodermal dysplasia/skin fragility syndrome. *Nat Genet*. 17:240-244.

McGrath, J.A., R.A.J. Eady, and F.M. Pope. 2004. Anatomy and Organization of Human Skin. In: *Rook's Textbook of Dermatology, Seventh Edition* (T. Burns, S. Breathnach, N. Cox, and C. Griffiths. eds., ed): Blackwell Publishing. doi: 10.1002/9780470750520.ch3.

McKoy, G., N. Protonotarios, A. Crosby, A. Tsatsopoulou, A. Anastasakis, A. Coonar, M. Norman, C. Baboonian, S. Jeffery, and W.J. McKenna. 2000. Identification of a deletion in plakoglobin in arrhythmogenic right ventricular cardiomyopathy with palmoplantar keratoderma and woolly hair (Naxos disease). *Lancet*. 355:2119-2124.

McLean, G.W., N.O. Carragher, E. Avizienyte, J. Evans, V.G. Brunton, and M.C. Frame. 2005. The role of focal-adhesion kinase in cancer - a new therapeutic opportunity. *Nat Rev Cancer*. 5:505-515.

McLean, W.H., and E.B. Lane. 1995. Intermediate filaments in disease. *Curr Opin Cell Biol*. 7:118-125.

McLean, W.H., E.L. Rugg, D.P. Lunny, S.M. Morley, E.B. Lane, O. Swensson, P.J. Dopping-Hepenstal, W.A. Griffiths, R.A. Eady, C. Higgins, and et al. 1995.

Keratin 16 and keratin 17 mutations cause pachyonychia congenita. *Nat Genet.* 9:273-278.

McLean, W.H., L. Pulkkinen, F.J. Smith, E.L. Rugg, E.B. Lane, F. Bullrich, R.E. Burgeson, S. Amano, D.L. Hudson, K. Owaribe, J.A. McGrath, J.R. McMillan, R.A. Eady, I.M. Leigh, A.M. Christiano, and J. Uitto. 1996. Loss of plectin causes epidermolysis bullosa with muscular dystrophy: cDNA cloning and genomic organization. *Genes Dev.* 10:1724-1735.

Menke, N.B., K.R. Ward, T.M. Witten, D.G. Bonchev, and R.F. Diegelmann. 2007. Impaired wound healing. *Clin Dermatol.* 25:19-25.

Menon, G.K. 2002. New insights into skin structure: scratching the surface. *Adv Drug Deliv Rev.* 54 Suppl 1:S3-17.

Menon, M.B., J. Schwermann, A.K. Singh, M. Franz-Wachtel, O. Pabst, U. Seidler, M.B. Omary, A. Kotlyarov, and M. Gaestel. 2010. p38 MAP kinase and MAPKAP kinases MK2/3 cooperatively phosphorylate epithelial keratins. *J Biol Chem.* 285:33242-33251.

Mese, G., G. Richard, and T.W. White. 2007. Gap junctions: basic structure and function. *J Invest Dermatol.* 127:2516-2524.

Messent, A.J., M.J. Blissett, G.L. Smith, A.J. North, A. Magee, D. Foreman, D.R. Garrod, and M. Boulton. 2000. Expression of a single pair of desmosomal glycoproteins renders the corneal epithelium unique amongst stratified epithelia. *Invest Ophthalmol Vis Sci.* 41:8-15.

Meyer, R.K., and U. Aebi. 1990. Bundling of actin filaments by alpha-actinin depends on its molecular length. *J Cell Biol.* 110:2013-2024.

Midwood, K.S., L.V. Williams, and J.E. Schwarzbauer. 2004. Tissue repair and the dynamics of the extracellular matrix. *Int J Biochem Cell Biol.* 36:1031-1037.

Mikhailov, A., and G.G. Gundersen. 1998. Relationship between microtubule dynamics and lamellipodium formation revealed by direct imaging of microtubules in cells treated with nocodazole or taxol. *Cell Motil Cytoskeleton.* 41:325-340.

Mitchison, T.J., and L.P. Cramer. 1996. Actin-based cell motility and cell locomotion. *Cell.* 84:371-379.

Miyamoto, S., H. Teramoto, O.A. Coso, J.S. Gutkind, P.D. Burbelo, S.K. Akiyama, and K.M. Yamada. 1995. Integrin function: molecular hierarchies of cytoskeletal and signaling molecules. *J Cell Biol.* 131:791-805.

Mizuuchi, E., S. Semba, Y. Kodama, and H. Yokozaki. 2009. Down-modulation of keratin 8 phosphorylation levels by PRL-3 contributes to colorectal carcinoma progression. *Int J Cancer.* 124:1802-1810.

Moll, R., W.W. Franke, B. Volc-Platzer, and R. Krepler. 1982. Different keratin polypeptides in epidermis and other epithelia of human skin: a specific

cytokeratin of molecular weight 46,000 in epithelia of the pilosebaceous tract and basal cell epitheliomas. *J Cell Biol*. 95:285-295.

Morasso, M.I., and M. Tomic-Canic. 2005. Epidermal stem cells: the cradle of epidermal determination, differentiation and wound healing. *Biol Cell*. 97:173-183.

Morley, S.M., M. D'Alessandro, C. Sexton, E.L. Rugg, H. Navsaria, C.S. Shemanko, M. Huber, D. Hohl, A.I. Heagerty, I.M. Leigh, and E.B. Lane. 2003. Generation and characterization of epidermolysis bullosa simplex cell lines: scratch assays show faster migration with disruptive keratin mutations. *Br J Dermatol*. 149:46-58.

Morrison, L.H., R.S. Labib, J.J. Zone, L.A. Diaz, and G.J. Anhalt. 1988. Herpes gestationis autoantibodies recognize a 180-kD human epidermal antigen. *J Clin Invest*. 81:2023-2026.

Muller, F.B., W. Kuster, K. Wodecki, H. Almeida, Jr., L. Bruckner-Tuderman, T. Krieg, B.P. Korge, and M.J. Arin. 2006. Novel and recurrent mutations in keratin KRT5 and KRT14 genes in epidermolysis bullosa simplex: implications for disease phenotype and keratin filament assembly. *Hum Mutat*. 27:719-720.

Murrell, D.F., N. Trisnowati, S. Miyakis, and A.S. Paller. 2011. The yin and the yang of keratin amino acid substitutions and epidermolysis bullosa simplex. *J Invest Dermatol*. 131:1787-1790.

Myers, S.R., I.M. Leigh, and H. Navsaria. 2007. Epidermal repair results from activation of follicular and epidermal progenitor keratinocytes mediated by a growth factor cascade. *Wound Repair Regen*. 15:693-701.

Nakamura, H., D. Sawamura, M. Goto, J.R. McMillan, S. Park, S. Kono, S. Hasegawa, S. Paku, T. Nakamura, Y. Ogiso, and H. Shimizu. 2005. Epidermolysis bullosa simplex associated with pyloric atresia is a novel clinical subtype caused by mutations in the plectin gene (PLEC1). *J Mol Diagn*. 7:28-35.

Nan, L., J. Dedes, B.A. French, F. Bardag-Gorce, J. Li, Y. Wu, and S.W. French. 2006. Mallory body (cytokeratin aggresomes) formation is prevented in vitro by p38 inhibitor. *Exp Mol Pathol*. 80:228-240.

Natsuga, K., W. Nishie, B.J. Smith, S. Shinkuma, T.A. Smith, D.A. Parry, N. Oiso, A. Kawada, K. Yoneda, M. Akiyama, and H. Shimizu. 2011. Consequences of two different amino-acid substitutions at the same codon in KRT14 indicate definitive roles of structural distortion in epidermolysis bullosa simplex pathogenesis. *J Invest Dermatol*. 131:1869-1876.

Nelson, W.G., and T.T. Sun. 1983. The 50- and 58-kdalton keratin classes as molecular markers for stratified squamous epithelia: cell culture studies. *J Cell Biol*. 97:244-251.

Nguyen, B.C., K. Lefort, A. Mandinova, D. Antonini, V. Devgan, G. Della Gatta, M.I. Koster, Z. Zhang, J. Wang, A. Tommasi di Vignano, J. Kitajewski, G.

Chiorino, D.R. Roop, C. Missero, and G.P. Dotto. 2006. Cross-regulation between Notch and p63 in keratinocyte commitment to differentiation. *Genes Dev*. 20:1028-1042.

Nickoloff, B.J., R.S. Mitra, B.L. Riser, V.M. Dixit, and J. Varani. 1988. Modulation of keratinocyte motility. Correlation with production of extracellular matrix molecules in response to growth promoting and antiproliferative factors. *Am J Pathol*. 132:543-551.

Niessen, C.M., F. Hogervorst, L.H. Jaspars, A.A. de Melker, G.O. Delwel, E.H. Hulsman, I. Kuikman, and A. Sonnenberg. 1994. The alpha 6 beta 4 integrin is a receptor for both laminin and kalinin. *Exp Cell Res*. 211:360-367.

Niessen, C.M., E.H. Hulsman, L.C. Oomen, I. Kuikman, and A. Sonnenberg. 1997. A minimal region on the integrin beta4 subunit that is critical to its localization in hemidesmosomes regulates the distribution of HD1/plectin in COS-7 cells. *J Cell Sci*. 110 (Pt 15):1705-1716.

Niessen, C.M. 2007. Tight junctions/adherens junctions: basic structure and function. *J Invest Dermatol*. 127:2525-2532.

Nievers, M.G., R.Q. Schaapveld, and A. Sonnenberg. 1999. Biology and function of hemidesmosomes. *Matrix Biol*. 18:5-17.

Nikolic, B., E. Mac Nulty, B. Mir, and G. Wiche. 1996. Basic amino acid residue cluster within nuclear targeting sequence motif is essential for cytoplasmic plectin-vimentin network junctions. *J Cell Biol*. 134:1455-1467.

Nobes, C.D., and A. Hall. 1995. Rho, rac, and cdc42 GTPases regulate the assembly of multimolecular focal complexes associated with actin stress fibers, lamellipodia, and filopodia. *Cell*. 81:53-62.

Nogales, E., S.G. Wolf, and K.H. Downing. 1998. Structure of the alpha beta tubulin dimer by electron crystallography. *Nature*. 391:199-203.

Norgett, E.E., S.J. Hatsell, L. Carvajal-Huerta, J.C. Cabezas, J. Common, P.E. Purkis, N. Whittock, I.M. Leigh, H.P. Stevens, and D.P. Kelsell. 2000. Recessive mutation in desmoplakin disrupts desmoplakin-intermediate filament interactions and causes dilated cardiomyopathy, woolly hair and keratoderma. *Hum Mol Genet*. 9:2761-2766.

Norlen, L., and A. Al-Amoudi. 2004. Stratum corneum keratin structure, function, and formation: the cubic rod-packing and membrane templating model. *J Invest Dermatol*. 123:715-732.

North, A.C., P.M. Steinert, and D.A. Parry. 1994. Coiled-coil stutter and link segments in keratin and other intermediate filament molecules: a computer modeling study. *Proteins*. 20:174-184.

North, A.J., W.G. Bardsley, J. Hyam, E.A. Bornslaeger, H.C. Cordingley, B. Trinnaman, M. Hatzfeld, K.J. Green, A.I. Magee, and D.R. Garrod. 1999. Molecular map of the desmosomal plaque. *J Cell Sci*. 112 (Pt 23):4325-4336.

Noselli, S., and N. Perrimon. 2000. Signal transduction. Are there close encounters between signaling pathways? *Science*. 290:68-69.

Nuber, U.A., S. Schafer, A. Schmidt, P.J. Koch, and W.W. Franke. 1995. The widespread human desmocollin Dsc2 and tissue-specific patterns of synthesis of various desmocollin subtypes. *Eur J Cell Biol*. 66:69-74.

O'Keefe, E.J., R.E. Payne, Jr., N. Russell, and D.T. Woodley. 1985. Spreading and enhanced motility of human keratinocytes on fibronectin. *J Invest Dermatol*. 85:125-130.

O'Keefe, E.J., H.P. Erickson, and V. Bennett. 1989. Desmoplakin I and desmoplakin II. Purification and characterization. *J Biol Chem*. 264:8310-8318.

Obata, T., G.E. Brown, and M.B. Yaffe. 2000. MAP kinase pathways activated by stress: the p38 MAPK pathway. *Crit Care Med*. 28:N67-77.

Oji, V., K.M. Eckl, K. Aufenvenne, M. Natebus, T. Tarinski, K. Ackermann, N. Seller, D. Metze, G. Nurnberg, R. Folster-Holst, M. Schafer-Korting, I. Hausser, H. Traupe, and H.C. Hennies. 2010. Loss of corneodesmosin leads to severe skin barrier defect, pruritus, and atopy: unraveling the peeling skin disease. *Am J Hum Genet*. 87:274-281.

Olaisen, B., and T. Gedde-Dahl, Jr. 1973. GPT--epidermolysis bullosa simplex (EBS Ogna) linkage in man. *Hum Hered*. 23:189-196.

Omary, M.B., N.O. Ku, G.Z. Tao, D.M. Toivola, and J. Liao. 2006. "Heads and tails" of intermediate filament phosphorylation: multiple sites and functional insights. *Trends Biochem Sci*. 31:383-394.

Omary, M.B., N.O. Ku, P. Strnad, and S. Hanada. 2009. Toward unraveling the complexity of simple epithelial keratins in human disease. *J Clin Invest*. 119:1794-1805.

Oppermann, H., A.D. Levinson, H.E. Varmus, L. Levintow, and J.M. Bishop. 1979. Uninfected vertebrate cells contain a protein that is closely related to the product of the avian sarcoma virus transforming gene (src). *Proc Natl Acad Sci U S A*. 76:1804-1808.

Ortonne, J.P., T. Loning, D. Schmitt, and J. Thivolet. 1981. Immunomorphological and ultrastructural aspects of keratinocyte migration in epidermal wound healing. *Virchows Arch A Pathol Anat Histol*. 392:217-230.

Osmanagic-Myers, S., M. Gregor, G. Walko, G. Burgstaller, S. Reipert, and G. Wiche. 2006. Plectin-controlled keratin cytoarchitecture affects MAP kinases involved in cellular stress response and migration. *J Cell Biol*. 174:557-568.

Otey, C.A., F.M. Pavalko, and K. Burridge. 1990. An interaction between alpha-actinin and the beta 1 integrin subunit in vitro. *J Cell Biol*. 111:721-729.

Ouyang, P., and S.P. Sugrue. 1996. Characterization of pinin, a novel protein associated with the desmosome-intermediate filament complex. *J Cell Biol*. 135:1027-1042.

Owens, D.W., and E.B. Lane. 2003. The quest for the function of simple epithelial keratins. *Bioessays*. 25:748-758.

Paladini, R.D., K. Takahashi, N.S. Bravo, and P.A. Coulombe. 1996. Onset of re-epithelialization after skin injury correlates with a reorganization of keratin filaments in wound edge keratinocytes: defining a potential role for keratin 16. *J Cell Biol*. 132:381-397.

Palmer, C.N., A.D. Irvine, A. Terron-Kwiatkowski, Y. Zhao, H. Liao, S.P. Lee, D.R. Goudie, A. Sandilands, L.E. Campbell, F.J. Smith, G.M. O'Regan, R.M. Watson, J.E. Cecil, S.J. Bale, J.G. Compton, J.J. DiGiovanna, P. Fleckman, S. Lewis-Jones, G. Arseculeratne, A. Sergeant, C.S. Munro, B. El Houate, K. McElreavey, L.B. Halkjaer, H. Bisgaard, S. Mukhopadhyay, and W.H. McLean. 2006. Common loss-of-function variants of the epidermal barrier protein filaggrin are a major predisposing factor for atopic dermatitis. *Nat Genet*. 38:441-446.

Paramio, J.M., and J.L. Jorcano. 1994. Assembly dynamics of epidermal keratins K1 and K10 in transfected cells. *Exp Cell Res*. 215:319-331.

Paramio, J.M. 1999. A role for phosphorylation in the dynamics of keratin intermediate filaments. *Eur J Cell Biol*. 78:33-43.

Parker, A.E., G.N. Wheeler, J. Arnemann, S.C. Pidsley, P. Ataliotis, C.L. Thomas, D.A. Rees, A.I. Magee, and R.S. Buxton. 1991. Desmosomal glycoproteins II and III. Cadherin-like junctional molecules generated by alternative splicing. *J Biol Chem*. 266:10438-10445.

Parry, D.A., A.C. Steven, and P.M. Steinert. 1985. The coiled-coil molecules of intermediate filaments consist of two parallel chains in exact axial register. *Biochem Biophys Res Commun*. 127:1012-1018.

Parry, D.A., L.N. Marekov, P.M. Steinert, and T.A. Smith. 2002. A role for the 1A and L1 rod domain segments in head domain organization and function of intermediate filaments: structural analysis of trichocyte keratin. *J Struct Biol*. 137:97-108.

Pauling, L., and R.B. Corey. 1953. Compound helical configurations of polypeptide chains: structure of proteins of the alpha-keratin type. *Nature*. 171:59-61.

Pawson, T. 2004. Specificity in signal transduction: from phosphotyrosine-SH2 domain interactions to complex cellular systems. *Cell*. 116:191-203.

Pearson, R.W. 1962. Studies on the pathogenesis of epidermolysis bullosa. *J Invest Dermatol*. 39:551-575.

Peifer, M., and E. Wieschaus. 1990. The segment polarity gene armadillo encodes a functionally modular protein that is the Drosophila homolog of human plakoglobin. *Cell*. 63:1167-1176.

Peifer, M., P.D. McCrea, K.J. Green, E. Wieschaus, and B.M. Gumbiner. 1992. The vertebrate adhesive junction proteins beta-catenin and plakoglobin and the Drosophila segment polarity gene armadillo form a multigene family with similar properties. *J Cell Biol*. 118:681-691.

Pekny, M., and E.B. Lane. 2007. Intermediate filaments and stress. *Exp Cell Res*. 313:2244-2254.

Peters, B., J. Kirfel, H. Bussow, M. Vidal, and T.M. Magin. 2001. Complete cytolysis and neonatal lethality in keratin 5 knockout mice reveal its fundamental role in skin integrity and in epidermolysis bullosa simplex. *Mol Biol Cell*. 12:1775-1789.

Pigors, M., D. Kiritsi, S. Krumpelmann, N. Wagner, Y. He, M. Podda, J. Kohlhase, I. Hausser, L. Bruckner-Tuderman, and C. Has. 2011. Lack of plakoglobin leads to lethal congenital epidermolysis bullosa: a novel clinico-genetic entity. *Hum Mol Genet*. 20:1811-1819.

Poulson, N.D., and T. Lechler. 2010. Robust control of mitotic spindle orientation in the developing epidermis. *J Cell Biol*. 191:915-922.

Proksch, E., J.M. Brandner, and J.M. Jensen. 2008. The skin: an indispensable barrier. *Exp Dermatol*. 17:1063-1072.

Pulkkinen, L., A.M. Christiano, T. Airenne, H. Haakana, K. Tryggvason, and J. Uitto. 1994a. Mutations in the gamma 2 chain gene (LAMC2) of kalinin/laminin 5 in the junctional forms of epidermolysis bullosa. *Nat Genet*. 6:293-297.

Pulkkinen, L., A.M. Christiano, D. Gerecke, D.W. Wagman, R.E. Burgeson, M.R. Pittelkow, and J. Uitto. 1994b. A homozygous nonsense mutation in the beta 3 chain gene of laminin 5 (LAMB3) in Herlitz junctional epidermolysis bullosa. *Genomics*. 24:357-360.

Purkis, P.E., J.B. Steel, I.C. Mackenzie, W.B. Nathrath, I.M. Leigh, and E.B. Lane. 1990. Antibody markers of basal cells in complex epithelia. *J Cell Sci*. 97 (Pt 1):39-50.

Raja, K. Sivamani, M.S. Garcia, and R.R. Isseroff. 2007. Wound re-epithelialization: modulating keratinocyte migration in wound healing. *Front Biosci*. 12:2849-2868.

Ray, S., and T. Lechler. 2011. Regulation of asymmetric cell division in the epidermis. *Cell Div*. 6:12.

Reddy, M.B., R.H. Guy, and A.L. Bunge. 2000. Does epidermal turnover reduce percutaneous penetration? *Pharm Res*. 17:1414-1419.

Reis, A., H.C. Hennies, L. Langbein, M. Digweed, D. Mischke, M. Drechsler, E. Schrock, B. Royer-Pokora, W.W. Franke, K. Sperling, and et al. 1994. Keratin 9 gene mutations in epidermolytic palmoplantar keratoderma (EPPK). *Nat Genet*. 6:174-179.

Rezniczek, G.A., J.M. de Pereda, S. Reipert, and G. Wiche. 1998. Linking integrin alpha6beta4-based cell adhesion to the intermediate filament cytoskeleton: direct interaction between the beta4 subunit and plectin at multiple molecular sites. *J Cell Biol*. 141:209-225.

Rheinwald, J.G., and H. Green. 1975. Serial cultivation of strains of human epidermal keratinocytes: the formation of keratinizing colonies from single cells. *Cell*. 6:331-343.

Rheinwald, J.G., and H. Green. 1977. Epidermal growth factor and the multiplication of cultured human epidermal keratinocytes. *Nature*. 265:421-424.

Rice, R.H., and H. Green. 1977. The cornified envelope of terminally differentiated human epidermal keratinocytes consists of cross-linked protein. *Cell*. 11:417-422.

Richard, G., V. De Laurenzi, B. Didona, S.J. Bale, and J.G. Compton. 1995. Keratin 13 point mutation underlies the hereditary mucosal epithelial disorder white sponge nevus. *Nat Genet*. 11:453-455.

Richard, G., L.E. Smith, R.A. Bailey, P. Itin, D. Hohl, E.H. Epstein, Jr., J.J. DiGiovanna, J.G. Compton, and S.J. Bale. 1998. Mutations in the human connexin gene GJB3 cause erythrokeratodermia variabilis. *Nat Genet*. 20:366-369.

Richard, G., F. Rouan, C.E. Willoughby, N. Brown, P. Chung, M. Ryynanen, E.W. Jabs, S.J. Bale, J.J. DiGiovanna, J. Uitto, and L. Russell. 2002. Missense mutations in GJB2 encoding connexin-26 cause the ectodermal dysplasia keratitis-ichthyosis-deafness syndrome. *Am J Hum Genet*. 70:1341-1348.

Richard, G., N. Brown, A. Ishida-Yamamoto, and A. Krol. 2004. Expanding the phenotypic spectrum of Cx26 disorders: Bart-Pumphrey syndrome is caused by a novel missense mutation in GJB2. *J Invest Dermatol*. 123:856-863.

Rickman, L., D. Simrak, H.P. Stevens, D.M. Hunt, I.A. King, S.P. Bryant, R.A. Eady, I.M. Leigh, J. Arnemann, A.I. Magee, D.P. Kelsell, and R.S. Buxton. 1999. N-terminal deletion in a desmosomal cadherin causes the autosomal dominant skin disease striate palmoplantar keratoderma. *Hum Mol Genet*. 8:971-976.

Ridge, K.M., L. Linz, F.W. Flitney, E.R. Kuczmarski, Y.H. Chou, M.B. Omary, J.I. Sznajder, and R.D. Goldman. 2005. Keratin 8 phosphorylation by protein kinase C delta regulates shear stress-mediated disassembly of keratin intermediate filaments in alveolar epithelial cells. *J Biol Chem*. 280:30400-30405.

Riggleman, B., E. Wieschaus, and P. Schedl. 1989. Molecular analysis of the armadillo locus: uniformly distributed transcripts and a protein with novel

internal repeats are associated with a Drosophila segment polarity gene. *Genes Dev*. 3:96-113.

Rimm, D.L., E.R. Koslov, P. Kebriaei, C.D. Cianci, and J.S. Morrow. 1995. Alpha 1(E)-catenin is an actin-binding and -bundling protein mediating the attachment of F-actin to the membrane adhesion complex. *Proc Natl Acad Sci U S A*. 92:8813-8817.

Roberts, B.J., A. Pashaj, K.R. Johnson, and J.K. Wahl, 3rd. 2011. Desmosome dynamics in migrating epithelial cells requires the actin cytoskeleton. *Exp Cell Res*. 317:2814-2822.

Rothnagel, J.A., H. Traupe, S. Wojcik, M. Huber, D. Hohl, M.R. Pittelkow, H. Saeki, Y. Ishibashi, and D.R. Roop. 1994. Mutations in the rod domain of keratin 2e in patients with ichthyosis bullosa of Siemens. *Nat Genet*. 7:485-490.

Rousselle, P., G.P. Lunstrum, D.R. Keene, and R.E. Burgeson. 1991. Kalinin: an epithelium-specific basement membrane adhesion molecule that is a component of anchoring filaments. *J Cell Biol*. 114:567-576.

Rousselle, P., R. Golbik, M. van der Rest, and M. Aumailley. 1995. Structural requirement for cell adhesion to kalinin (laminin-5). *J Biol Chem*. 270:13766-13770.

Rousselle, P., D.R. Keene, F. Ruggiero, M.F. Champliaud, M. Rest, and R.E. Burgeson. 1997. Laminin 5 binds the NC-1 domain of type VII collagen. *J Cell Biol*. 138:719-728.

Rudnicka, L., J. Varga, A.M. Christiano, R.V. Iozzo, S.A. Jimenez, and J. Uitto. 1994. Elevated expression of type VII collagen in the skin of patients with systemic sclerosis. Regulation by transforming growth factor-beta. *J Clin Invest*. 93:1709-1715.

Rugg, E.L., W.H. McLean, E.B. Lane, R. Pitera, J.R. McMillan, P.J. Dopping-Hepenstal, H.A. Navsaria, I.M. Leigh, and R.A. Eady. 1994. A functional "knockout" of human keratin 14. *Genes Dev*. 8:2563-2573.

Rugg, E.L., W.H. McLean, W.E. Allison, D.P. Lunny, R.I. Macleod, D.H. Felix, E.B. Lane, and C.S. Munro. 1995. A mutation in the mucosal keratin K4 is associated with oral white sponge nevus. *Nat Genet*. 11:450-452.

Rugg, E.L., H.M. Horn, F.J. Smith, N.J. Wilson, A.J. Hill, G.J. Magee, C.S. Shemanko, D.U. Baty, M.J. Tidman, and E.B. Lane. 2007. Epidermolysis bullosa simplex in Scotland caused by a spectrum of keratin mutations. *J Invest Dermatol*. 127:574-580.

Ruhrberg, C., M.A. Hajibagheri, D.A. Parry, and F.M. Watt. 1997. Periplakin, a novel component of cornified envelopes and desmosomes that belongs to the plakin family and forms complexes with envoplakin. *J Cell Biol*. 139:1835-1849.

Ruhrberg, C., and F.M. Watt. 1997. The plakin family: versatile organizers of cytoskeletal architecture. *Curr Opin Genet Dev*. 7:392-397.

Russell, D., P.D. Andrews, J. James, and E.B. Lane. 2004. Mechanical stress induces profound remodelling of keratin filaments and cell junctions in epidermolysis bullosa simplex keratinocytes. *J Cell Sci.* 117:5233-5243.

Russell, D., H. Ross, and E.B. Lane. 2010. ERK involvement in resistance to apoptosis in keratinocytes with mutant keratin. *J Invest Dermatol.* 130:671-681.

Ryan, M.C., K. Lee, Y. Miyashita, and W.G. Carter. 1999. Targeted disruption of the LAMA3 gene in mice reveals abnormalities in survival and late stage differentiation of epithelial cells. *J Cell Biol.* 145:1309-1323.

Sakuntabhai, A., S. Burge, S. Monk, and A. Hovnanian. 1999a. Spectrum of novel ATP2A2 mutations in patients with Darier's disease. *Hum Mol Genet.* 8:1611-1619.

Sakuntabhai, A., V. Ruiz-Perez, S. Carter, N. Jacobsen, S. Burge, S. Monk, M. Smith, C.S. Munro, M. O'Donovan, N. Craddock, R. Kucherlapati, J.L. Rees, M. Owen, G.M. Lathrop, A.P. Monaco, T. Strachan, and A. Hovnanian. 1999b. Mutations in ATP2A2, encoding a Ca2+ pump, cause Darier disease. *Nat Genet.* 21:271-277.

Salo, T., M. Makela, M. Kylmaniemi, H. Autio-Harmainen, and H. Larjava. 1994. Expression of matrix metalloproteinase-2 and -9 during early human wound healing. *Lab Invest.* 70:176-182.

Santoro, M.M., and G. Gaudino. 2005. Cellular and molecular facets of keratinocyte reepithelization during wound healing. *Exp Cell Res.* 304:274-286.

Sawamura, D., K. Li, M.L. Chu, and J. Uitto. 1991. Human bullous pemphigoid antigen (BPAG1). Amino acid sequences deduced from cloned cDNAs predict biologically important peptide segments and protein domains. *J Biol Chem.* 266:17784-17790.

Schaeffer, H.J., A.D. Catling, S.T. Eblen, L.S. Collier, A. Krauss, and M.J. Weber. 1998. MP1: a MEK binding partner that enhances enzymatic activation of the MAP kinase cascade. *Science.* 281:1668-1671.

Schafer, S., P.J. Koch, and W.W. Franke. 1994. Identification of the ubiquitous human desmoglein, Dsg2, and the expression catalogue of the desmoglein subfamily of desmosomal cadherins. *Exp Cell Res.* 211:391-399.

Schaller, M.D., C.A. Borgman, B.S. Cobb, R.R. Vines, A.B. Reynolds, and J.T. Parsons. 1992. pp125FAK a structurally distinctive protein-tyrosine kinase associated with focal adhesions. *Proc Natl Acad Sci U S A.* 89:5192-5196.

Schlessinger, J., and M.A. Lemmon. 2003. SH2 and PTB domains in tyrosine kinase signaling. *Sci STKE.* 2003:RE12.

Schmelz, M. 2011. Neuronal sensitivity of the skin. *Eur J Dermatol.* 21 Suppl 2:43-47.

Schweizer, J., P.E. Bowden, P.A. Coulombe, L. Langbein, E.B. Lane, T.M. Magin, L. Maltais, M.B. Omary, D.A. Parry, M.A. Rogers, and M.W. Wright. 2006. New consensus nomenclature for mammalian keratins. *J Cell Biol*. 174:169-174.

Sehgal, B.U., P.J. DeBiase, S. Matzno, T.L. Chew, J.N. Claiborne, S.B. Hopkinson, A. Russell, M.P. Marinkovich, and J.C. Jones. 2006. Integrin beta4 regulates migratory behavior of keratinocytes by determining laminin-332 organization. *J Biol Chem*. 281:35487-35498.

Shelley, W.B., and L. Juhlin. 1976. Langerhans cells form a reticuloepithelial trap for external contact antigens. *Nature*. 261:46-47.

Shimizu, H., K. Suzumori, N. Hatta, and T. Nishikawa. 1996. Absence of detectable alpha 6 integrin in pyloric atresia-junctional epidermolysis bullosa syndrome. Application for prenatal diagnosis in a family at risk for recurrence. *Arch Dermatol*. 132:919-925.

Shinkuma, S., J.R. McMillan, and H. Shimizu. 2011. Ultrastructure and molecular pathogenesis of epidermolysis bullosa. *Clin Dermatol*. 29:412-419.

Siegel, D.H., G.H. Ashton, H.G. Penagos, J.V. Lee, H.S. Feiler, K.C. Wilhelmsen, A.P. South, F.J. Smith, A.R. Prescott, V. Wessagowit, N. Oyama, M. Akiyama, D. Al Aboud, K. Al Aboud, A. Al Githami, K. Al Hawsawi, A. Al Ismaily, R. Al-Suwaid, D.J. Atherton, R. Caputo, J.D. Fine, I.J. Frieden, E. Fuchs, R.M. Haber, T. Harada, Y. Kitajima, S.B. Mallory, H. Ogawa, S. Sahin, H. Shimizu, Y. Suga, G. Tadini, K. Tsuchiya, C.B. Wiebe, F. Wojnarowska, A.B. Zaghloul, T. Hamada, R. Mallipeddi, R.A. Eady, W.H. McLean, J.A. McGrath, and E.H. Epstein. 2003. Loss of kindlin-1, a human homolog of the Caenorhabditis elegans actin-extracellular-matrix linker protein UNC-112, causes Kindler syndrome. *Am J Hum Genet*. 73:174-187.

Silver, F.H., J.W. Freeman, and D. DeVore. 2001. Viscoelastic properties of human skin and processed dermis. *Skin Res Technol*. 7:18-23.

Simpson, C.L., D.M. Patel, and K.J. Green. 2011. Deconstructing the skin: cytoarchitectural determinants of epidermal morphogenesis. *Nat Rev Mol Cell Biol*. 12:565-580.

Simpson, M.A., S. Mansour, D. Ahnood, K. Kalidas, M.A. Patton, W.J. McKenna, E.R. Behr, and A.H. Crosby. 2009. Homozygous mutation of desmocollin-2 in arrhythmogenic right ventricular cardiomyopathy with mild palmoplantar keratoderma and woolly hair. *Cardiology*. 113:28-34.

Singer, A.J., and R.A. Clark. 1999. Cutaneous wound healing. *N Engl J Med*. 341:738-746.

Sinha, S., L. Degenstein, C. Copenhaver, and E. Fuchs. 2000. Defining the regulatory factors required for epidermal gene expression. *Mol Cell Biol*. 20:2543-2555.

Skalli, O., J.C. Jones, R. Gagescu, and R.D. Goldman. 1994. IFAP 300 is common to desmosomes and hemidesmosomes and is a possible linker of intermediate filaments to these junctions. *J Cell Biol*. 125:159-170.

Smart, I.H. 1970. Variation in the plane of cell cleavage during the process of stratification in the mouse epidermis. *Br J Dermatol*. 82:276-282.

Smith, F.J., R.A. Eady, I.M. Leigh, J.R. McMillan, E.L. Rugg, D.P. Kelsell, S.P. Bryant, N.K. Spurr, J.F. Geddes, G. Kirtschig, G. Milana, A.G. de Bono, K. Owaribe, G. Wiche, L. Pulkkinen, J. Uitto, W.H. McLean, and E.B. Lane. 1996. Plectin deficiency results in muscular dystrophy with epidermolysis bullosa. *Nat Genet*. 13:450-457.

Smith, F.J., L.D. Corden, E.L. Rugg, R. Ratnavel, I.M. Leigh, C. Moss, M.J. Tidman, D. Hohl, M. Huber, L. Kunkeler, C.S. Munro, E.B. Lane, and W.H. McLean. 1997. Missense mutations in keratin 17 cause either pachyonychia congenita type 2 or a phenotype resembling steatocystoma multiplex. *J Invest Dermatol*. 108:220-223.

Smith, F.J., V.A. McKusick, K. Nielsen, E. Pfendner, J. Uitto, and W.H. McLean. 1999. Cloning of multiple keratin 16 genes facilitates prenatal diagnosis of pachyonychia congenita type 1. *Prenat Diagn*. 19:941-946.

Smith, F.J., A.D. Irvine, A. Terron-Kwiatkowski, A. Sandilands, L.E. Campbell, Y. Zhao, H. Liao, A.T. Evans, D.R. Goudie, S. Lewis-Jones, G. Arseculeratne, C.S. Munro, A. Sergeant, G. O'Regan, S.J. Bale, J.G. Compton, J.J. DiGiovanna, R.B. Presland, P. Fleckman, and W.H. McLean. 2006. Loss-of-function mutations in the gene encoding filaggrin cause ichthyosis vulgaris. *Nat Genet*. 38:337-342.

Smith, T.A., S.V. Strelkov, P. Burkhard, U. Aebi, and D.A. Parry. 2002. Sequence comparisons of intermediate filament chains: evidence of a unique functional/structural role for coiled-coil segment 1A and linker L1. *J Struct Biol*. 137:128-145.

Smith, T.A., P.M. Steinert, and D.A. Parry. 2004. Modeling effects of mutations in coiled-coil structures: case study using epidermolysis bullosa simplex mutations in segment 1a of K5/K14 intermediate filaments. *Proteins*. 55:1043-1052.

Snider, N.T., S.V. Weerasinghe, J.A. Iniguez-Lluhi, H. Herrmann, and M.B. Omary. 2011. Keratin hypersumoylation alters filament dynamics and is a marker for human liver disease and keratin mutation. *J Biol Chem*. 286:2273-2284.

Soellner, P., R.A. Quinlan, and W.W. Franke. 1985. Identification of a distinct soluble subunit of an intermediate filament protein: tetrameric vimentin from living cells. *Proc Natl Acad Sci U S A*. 82:7929-7933.

Sondermann, H., D. Dogic, M. Pesch, and M. Aumailley. 1999. Targeting of cytoskeletal linker proteins to focal adhesion complexes is reduced in

fibroblasts adhering to laminin-1 when compared to fibronectin. *Cell Adhes Commun.* 7:43-56.

Spinardi, L., Y.L. Ren, R. Sanders, and F.G. Giancotti. 1993. The beta 4 subunit cytoplasmic domain mediates the interaction of alpha 6 beta 4 integrin with the cytoskeleton of hemidesmosomes. *Mol Biol Cell.* 4:871-884.

Sprecher, E., R. Bergman, G. Richard, R. Lurie, S. Shalev, D. Petronius, A. Shalata, Y. Anbinder, R. Leibu, I. Perlman, N. Cohen, and R. Szargel. 2001. Hypotrichosis with juvenile macular dystrophy is caused by a mutation in CDH3, encoding P-cadherin. *Nat Genet.* 29:134-136.

Stanley, J.R., P. Hawley-Nelson, S.H. Yuspa, E.M. Shevach, and S.I. Katz. 1981. Characterization of bullous pemphigoid antigen: a unique basement membrane protein of stratified squamous epithelia. *Cell.* 24:897-903.

Stanley, J.R., T. Tanaka, S. Mueller, V. Klaus-Kovtun, and D. Roop. 1988. Isolation of complementary DNA for bullous pemphigoid antigen by use of patients' autoantibodies. *J Clin Invest.* 82:1864-1870.

Steinbock, F.A., and G. Wiche. 1999. Plectin: a cytolinker by design. *Biol Chem.* 380:151-158.

Steinert, P.M., M.L. Wantz, and W.W. Idler. 1982. O-phosphoserine content of intermediate filament subunits. *Biochemistry.* 21:177-183.

Steinert, P.M., R.H. Rice, D.R. Roop, B.L. Trus, and A.C. Steven. 1983. Complete amino acid sequence of a mouse epidermal keratin subunit and implications for the structure of intermediate filaments. *Nature.* 302:794-800.

Steinert, P.M., D.A. Parry, W.W. Idler, L.D. Johnson, A.C. Steven, and D.R. Roop. 1985. Amino acid sequences of mouse and human epidermal type II keratins of Mr 67,000 provide a systematic basis for the structural and functional diversity of the end domains of keratin intermediate filament subunits. *J Biol Chem.* 260:7142-7149.

Steinert, P.M. 1990. The two-chain coiled-coil molecule of native epidermal keratin intermediate filaments is a type I-type II heterodimer. *J Biol Chem.* 265:8766-8774.

Steinert, P.M., L.N. Marekov, R.D. Fraser, and D.A. Parry. 1993. Keratin intermediate filament structure. Crosslinking studies yield quantitative information on molecular dimensions and mechanism of assembly. *J Mol Biol.* 230:436-452.

Steinert, P.M., A.C. North, and D.A. Parry. 1994. Structural features of keratin intermediate filaments. *J Invest Dermatol.* 103:19S-24S.

Steven, A.C., M.E. Bisher, D.R. Roop, and P.M. Steinert. 1990. Biosynthetic pathways of filaggrin and loricrin--two major proteins expressed by terminally differentiated epidermal keratinocytes. *J Struct Biol.* 104:150-162.

Strelkov, S.V., H. Herrmann, N. Geisler, A. Lustig, S. Ivaninskii, R. Zimbelmann, P. Burkhard, and U. Aebi. 2001. Divide-and-conquer crystallographic approach towards an atomic structure of intermediate filaments. *J Mol Biol*. 306:773-781.

Strelkov, S.V., H. Herrmann, N. Geisler, T. Wedig, R. Zimbelmann, U. Aebi, and P. Burkhard. 2002. Conserved segments 1A and 2B of the intermediate filament dimer: their atomic structures and role in filament assembly. *Embo J*. 21:1255-1266.

Strelkov, S.V., J. Schumacher, P. Burkhard, U. Aebi, and H. Herrmann. 2004. Crystal structure of the human lamin A coil 2B dimer: implications for the head-to-tail association of nuclear lamins. *J Mol Biol*. 343:1067-1080.

Strnad, P., R. Windoffer, and R.E. Leube. 2001. In vivo detection of cytokeratin filament network breakdown in cells treated with the phosphatase inhibitor okadaic acid. *Cell Tissue Res*. 306:277-293.

Strnad, P., R. Windoffer, and R.E. Leube. 2002. Induction of rapid and reversible cytokeratin filament network remodeling by inhibition of tyrosine phosphatases. *J Cell Sci*. 115:4133-4148.

Szeder, V., M. Grim, Z. Halata, and M. Sieber-Blum. 2003. Neural crest origin of mammalian Merkel cells. *Dev Biol*. 253:258-263.

Szeverenyi, I., A.J. Cassidy, C.W. Chung, B.T. Lee, J.E. Common, S.C. Ogg, H. Chen, S.Y. Sim, W.L. Goh, K.W. Ng, J.A. Simpson, L.L. Chee, G.H. Eng, B. Li, D.P. Lunny, D. Chuon, A. Venkatesh, K.H. Khoo, W.H. McLean, Y.P. Lim, and E.B. Lane. 2008. The Human Intermediate Filament Database: comprehensive information on a gene family involved in many human diseases. *Hum Mutat*. 29:351-360.

Takuma, T., T. Ichida, K. Okumura, and M. Kanazawa. 1993. Protein phosphatase inhibitor calyculin A induces hyperphosphorylation of cytokeratins and inhibits amylase exocytosis in the rat parotid acini. *FEBS Lett*. 323:145-150.

Tamura, R.N., C. Rozzo, L. Starr, J. Chambers, L.F. Reichardt, H.M. Cooper, and V. Quaranta. 1990. Epithelial integrin alpha 6 beta 4: complete primary structure of alpha 6 and variant forms of beta 4. *J Cell Biol*. 111:1593-1604.

Tanaka, T., D.A. Parry, V. Klaus-Kovtun, P.M. Steinert, and J.R. Stanley. 1991. Comparison of molecularly cloned bullous pemphigoid antigen to desmoplakin I confirms that they define a new family of cell adhesion junction plaque proteins. *J Biol Chem*. 266:12555-12559.

Tao, G.Z., C. Kirby, S.A. Whelan, F. Rossi, X. Bi, M. MacLaren, E. Gentalen, R.A. O'Neill, G.W. Hart, and M.B. Omary. 2006a. Reciprocal keratin 18 Ser48 O-GlcNAcylation and Ser52 phosphorylation using peptide analysis. *Biochem Biophys Res Commun*. 351:708-712.

Tao, G.Z., D.M. Toivola, Q. Zhou, P. Strnad, B. Xu, S.A. Michie, and M.B. Omary. 2006b. Protein phosphatase-2A associates with and dephosphorylates keratin 8

after hyposmotic stress in a site- and cell-specific manner. *J Cell Sci.* 119:1425-1432.

Taylor, G., M.S. Lehrer, P.J. Jensen, T.T. Sun, and R.M. Lavker. 2000. Involvement of follicular stem cells in forming not only the follicle but also the epidermis. *Cell.* 102:451-461.

Taylor, N.A. 1986. Eccrine sweat glands. Adaptations to physical training and heat acclimation. *Sports Med.* 3:387-397.

Terrinoni, A., F.J. Smith, B. Didona, F. Canzona, M. Paradisi, M. Huber, D. Hohl, A. David, A. Verloes, I.M. Leigh, C.S. Munro, G. Melino, and W.H. McLean. 2001. Novel and recurrent mutations in the genes encoding keratins K6a, K16 and K17 in 13 cases of pachyonychia congenita. *J Invest Dermatol.* 117:1391-1396.

Timpl, R. 1996. Macromolecular organization of basement membranes. *Curr Opin Cell Biol.* 8:618-624.

Tinkle, C.L., T. Lechler, H.A. Pasolli, and E. Fuchs. 2004. Conditional targeting of E-cadherin in skin: insights into hyperproliferative and degenerative responses. *Proc Natl Acad Sci U S A.* 101:552-557.

Tinkle, C.L., H.A. Pasolli, N. Stokes, and E. Fuchs. 2008. New insights into cadherin function in epidermal sheet formation and maintenance of tissue integrity. *Proc Natl Acad Sci U S A.* 105:15405-15410.

Toivola, D.M., Q. Zhou, L.S. English, and M.B. Omary. 2002. Type II keratins are phosphorylated on a unique motif during stress and mitosis in tissues and cultured cells. *Mol Biol Cell.* 13:1857-1870.

Tomic-Canic, M., M. Komine, I.M. Freedberg, and M. Blumenberg. 1998. Epidermal signal transduction and transcription factor activation in activated keratinocytes. *J Dermatol Sci.* 17:167-181.

Troyanovsky, S.M., V.I. Guelstein, T.A. Tchipysheva, V.A. Krutovskikh, and G.A. Bannikov. 1989. Patterns of expression of keratin 17 in human epithelia: dependency on cell position. *J Cell Sci.* 93 (Pt 3):419-426.

Troyanovsky, S.M., R.B. Troyanovsky, L.G. Eshkind, R.E. Leube, and W.W. Franke. 1994. Identification of amino acid sequence motifs in desmocollin, a desmosomal glycoprotein, that are required for plakoglobin binding and plaque formation. *Proc Natl Acad Sci U S A.* 91:10790-10794.

Tsukita, S. 1985. Desmocalmin: a calmodulin-binding high molecular weight protein isolated from desmosomes. *J Cell Biol.* 101:2070-2080.

Tunggal, J.A., I. Helfrich, A. Schmitz, H. Schwarz, D. Gunzel, M. Fromm, R. Kemler, T. Krieg, and C.M. Niessen. 2005. E-cadherin is essential for in vivo epidermal barrier function by regulating tight junctions. *Embo J.* 24:1146-1156.

Turner, C.E., and J.T. Miller. 1994. Primary sequence of paxillin contains putative SH2 and SH3 domain binding motifs and multiple LIM domains: identification of a vinculin and pp125Fak-binding region. *J Cell Sci.* 107 (Pt 6):1583-1591.

Uematsu, J., Y. Nishizawa, A. Sonnenberg, and K. Owaribe. 1994. Demonstration of type II hemidesmosomes in a mammary gland epithelial cell line, BMGE-H. *J Biochem.* 115:469-476.

Ullrich, A., and J. Schlessinger. 1990. Signal transduction by receptors with tyrosine kinase activity. *Cell.* 61:203-212.

van der Neut, R., P. Krimpenfort, J. Calafat, C.M. Niessen, and A. Sonnenberg. 1996. Epithelial detachment due to absence of hemidesmosomes in integrin beta 4 null mice. *Nat Genet.* 13:366-369.

Vasioukhin, V., E. Bowers, C. Bauer, L. Degenstein, and E. Fuchs. 2001. Desmoplakin is essential in epidermal sheet formation. *Nat Cell Biol.* 3:1076-1085.

Vasioukhin, V., and E. Fuchs. 2001. Actin dynamics and cell-cell adhesion in epithelia. *Curr Opin Cell Biol.* 13:76-84.

Vial, E., E. Sahai, and C.J. Marshall. 2003. ERK-MAPK signaling coordinately regulates activity of Rac1 and RhoA for tumor cell motility. *Cancer Cell.* 4:67-79.

Vidal, F., D. Aberdam, C. Miquel, A.M. Christiano, L. Pulkkinen, J. Uitto, J.P. Ortonne, and G. Meneguzzi. 1995. Integrin beta 4 mutations associated with junctional epidermolysis bullosa with pyloric atresia. *Nat Genet.* 10:229-234.

Vijayaraj, P., C. Kroger, U. Reuter, R. Windoffer, R.E. Leube, and T.M. Magin. 2009. Keratins regulate protein biosynthesis through localization of GLUT1 and -3 upstream of AMP kinase and Raptor. *J Cell Biol.* 187:175-184.

Wallis, S., S. Lloyd, I. Wise, G. Ireland, T.P. Fleming, and D. Garrod. 2000. The alpha isoform of protein kinase C is involved in signaling the response of desmosomes to wounding in cultured epithelial cells. *Mol Biol Cell.* 11:1077-1092.

Wally, V., M. Brunner, T. Lettner, M. Wagner, U. Koller, A. Trost, E.M. Murauer, S. Hainzl, H. Hintner, and J.W. Bauer. 2010. K14 mRNA reprogramming for dominant epidermolysis bullosa simplex. *Hum Mol Genet.* 19:4715-4725.

Wang, Y.N., Y.J. Chen, and W.C. Chang. 2006. Activation of extracellular signal-regulated kinase signaling by epidermal growth factor mediates c-Jun activation and p300 recruitment in keratin 16 gene expression. *Mol Pharmacol.* 69:85-98.

Waseem, A., A.C. Gough, N.K. Spurr, and E.B. Lane. 1990. Localization of the gene for human simple epithelial keratin 18 to chromosome 12 using polymerase chain reaction. *Genomics.* 7:188-194.

Waterman-Storer, C.M., and E. Salmon. 1999. Positive feedback interactions between microtubule and actin dynamics during cell motility. *Curr Opin Cell Biol.* 11:61-67.

Watt, F.M. 2002. Role of integrins in regulating epidermal adhesion, growth and differentiation. *Embo J.* 21:3919-3926.

Webb, D.J., K. Donais, L.A. Whitmore, S.M. Thomas, C.E. Turner, J.T. Parsons, and A.F. Horwitz. 2004. FAK-Src signalling through paxillin, ERK and MLCK regulates adhesion disassembly. *Nat Cell Biol.* 6:154-161.

Weber, F.P. 1926. Recurrent Bullous Eruption on the Feet in a Child. *Proc R Soc Med.* 19:72.

Weber, K., and N. Geisler. 1985. Intermediate filaments: structural conservation and divergence. *Ann N Y Acad Sci.* 455:126-143.

Weber, K., U. Plessmann, H. Dodemont, and K. Kossmagk-Stephan. 1988. Amino acid sequences and homopolymer-forming ability of the intermediate filament proteins from an invertebrate epithelium. *Embo J.* 7:2995-3001.

Weiss, L.W., and A.S. Zelickson. 1975. Embryology of the epidermis: ultrastructural aspects. 1. Formation and early development in the mouse with mammalian comparisons. *Acta Derm Venereol.* 55:161-168.

Weiss, R.A., R. Eichner, and T.T. Sun. 1984. Monoclonal antibody analysis of keratin expression in epidermal diseases: a 48- and 56-kdalton keratin as molecular markers for hyperproliferative keratinocytes. *J Cell Biol.* 98:1397-1406.

Welch, M.D., A. Mallavarapu, J. Rosenblatt, and T.J. Mitchison. 1997. Actin dynamics in vivo. *Curr Opin Cell Biol.* 9:54-61.

Werner, N.S., R. Windoffer, P. Strnad, C. Grund, R.E. Leube, and T.M. Magin. 2004. Epidermolysis bullosa simplex-type mutations alter the dynamics of the keratin cytoskeleton and reveal a contribution of actin to the transport of keratin subunits. *Mol Biol Cell.* 15:990-1002.

Weston, C.R., and R.J. Davis. 2007. The JNK signal transduction pathway. *Curr Opin Cell Biol.* 19:142-149.

Whittock, N.V., G.H. Ashton, P.J. Dopping-Hepenstal, M.J. Gratian, F.M. Keane, R.A. Eady, and J.A. McGrath. 1999. Striate palmoplantar keratoderma resulting from desmoplakin haploinsufficiency. *J Invest Dermatol.* 113:940-946.

Wiche, G., B. Becker, K. Luber, G. Weitzer, M.J. Castanon, R. Hauptmann, C. Stratowa, and M. Stewart. 1991. Cloning and sequencing of rat plectin indicates a 466-kD polypeptide chain with a three-domain structure based on a central alpha-helical coiled coil. *J Cell Biol.* 114:83-99.

Wiche, G. 1998. Role of plectin in cytoskeleton organization and dynamics. *J Cell Sci.* 111 (Pt 17):2477-2486.

Wiche, G., and L. Winter. 2011. Plectin isoforms as organizers of intermediate filament cytoarchitecture. *Bioarchitecture*. 1:14-20.

Williams, S.E., S. Beronja, H.A. Pasolli, and E. Fuchs. 2011. Asymmetric cell divisions promote Notch-dependent epidermal differentiation. *Nature*. 470:353-358.

Wilson, N.J., S.A. Leachman, C.D. Hansen, A.C. McMullan, L.M. Milstone, M.E. Schwartz, W.H. McLean, P.R. Hull, and F.J. Smith. 2011. A large mutational study in pachyonychia congenita. *J Invest Dermatol*. 131:1018-1024.

Windoffer, R., and R.E. Leube. 1999. Detection of cytokeratin dynamics by time-lapse fluorescence microscopy in living cells. *J Cell Sci*. 112 (Pt 24):4521-4534.

Windoffer, R., S. Woll, P. Strnad, and R.E. Leube. 2004. Identification of novel principles of keratin filament network turnover in living cells. *Mol Biol Cell*. 15:2436-2448.

Windoffer, R., A. Kolsch, S. Woll, and R.E. Leube. 2006. Focal adhesions are hotspots for keratin filament precursor formation. *J Cell Biol*. 173:341-348.

Windoffer, R., M. Beil, T.M. Magin, and R.E. Leube. 2011. Cytoskeleton in motion: the dynamics of keratin intermediate filaments in epithelia. *J Cell Biol*. 194:669-678.

Winter, G.D. 1962. Formation of the scab and the rate of epithelization of superficial wounds in the skin of the young domestic pig. *Nature*. 193:293-294.

Wojcik, S.M., D.S. Bundman, and D.R. Roop. 2000. Delayed wound healing in keratin 6a knockout mice. *Mol Cell Biol*. 20:5248-5255.

Woll, S., R. Windoffer, and R.E. Leube. 2005. Dissection of keratin dynamics: different contributions of the actin and microtubule systems. *Eur J Cell Biol*. 84:311-328.

Woll, S., R. Windoffer, and R.E. Leube. 2007. p38 MAPK-dependent shaping of the keratin cytoskeleton in cultured cells. *J Cell Biol*. 177:795-807.

Wood, P., D.U. Baty, E.B. Lane, and W.H. McLean. 2003. Long-range polymerase chain reaction for specific full-length amplification of the human keratin 14 gene and novel keratin 14 mutations in epidermolysis bullosa simplex patients. *J Invest Dermatol*. 120:495-497.

Wu, Y., L. Nan, F. Bardag-Gorce, J. Li, B.A. French, L.T. Wilson, J. Dedes, and S.W. French. 2005. The role of laminin-integrin signaling in triggering MB formation. An in vivo and in vitro study. *Exp Mol Pathol*. 79:1-8.

Wysocki, A.B., and F. Grinnell. 1990. Fibronectin profiles in normal and chronic wound fluid. *Lab Invest*. 63:825-831.

Yatsunami, J., A. Komori, T. Ohta, M. Suganuma, S.H. Yuspa, and H. Fujiki. 1993. Hyperphosphorylation of cytokeratins by okadaic acid class tumor promoters in primary human keratinocytes. *Cancer Res*. 53:992-996.

Yin, T., S. Getsios, R. Caldelari, L.M. Godsel, A.P. Kowalczyk, E.J. Muller, and K.J. Green. 2005. Mechanisms of plakoglobin-dependent adhesion: desmosome-specific functions in assembly and regulation by epidermal growth factor receptor. *J Biol Chem*. 280:40355-40363.

Yoneda, N., Y. Sato, A. Kitao, H. Ikeda, S. Sawada-Kitamura, M. Miyakoshi, K. Harada, M. Sasaki, O. Matsui, and Y. Nakanuma. 2011. Epidermal growth factor induces cytokeratin 19 expression accompanied by increased growth abilities in human hepatocellular carcinoma. *Lab Invest*. 91:262-272.

Yoon, K.H., M. Yoon, R.D. Moir, S. Khuon, F.W. Flitney, and R.D. Goldman. 2001. Insights into the dynamic properties of keratin intermediate filaments in living epithelial cells. *J Cell Biol*. 153:503-516.

Young, P., O. Boussadia, H. Halfter, R. Grose, P. Berger, D.P. Leone, H. Robenek, P. Charnay, R. Kemler, and U. Suter. 2003. E-cadherin controls adherens junctions in the epidermis and the renewal of hair follicles. *Embo J*. 22:5723-5733.

Yurchenco, P.D., and J.J. O'Rear. 1994. Basal lamina assembly. *Curr Opin Cell Biol*. 6:674-681.

Zackroff, R.V., and R.D. Goldman. 1979. In vitro assembly of intermediate filaments from baby hamster kidney (BHK-21) cells. *Proc Natl Acad Sci U S A*. 76:6226-6230.

Zamir, E., and B. Geiger. 2001. Components of cell-matrix adhesions. *J Cell Sci*. 114:3577-3579.

Zhou, Q., M. Cadrin, H. Herrmann, C.H. Chen, R.J. Chalkley, A.L. Burlingame, and M.B. Omary. 2006. Keratin 20 serine 13 phosphorylation is a stress and intestinal goblet cell marker. *J Biol Chem*. 281:16453-16461.

Zhou, Q., N.T. Snider, J. Liao, D.H. Li, A. Hong, N.O. Ku, C.A. Cartwright, and M.B. Omary. 2010. Characterization of in vivo keratin 19 phosphorylation on tyrosine-391. *PLoS One*. 5:e13538.

Zhou, X., J. Liao, L. Hu, L. Feng, and M.B. Omary. 1999. Characterization of the major physiologic phosphorylation site of human keratin 19 and its role in filament organization. *J Biol Chem*. 274:12861-12866.
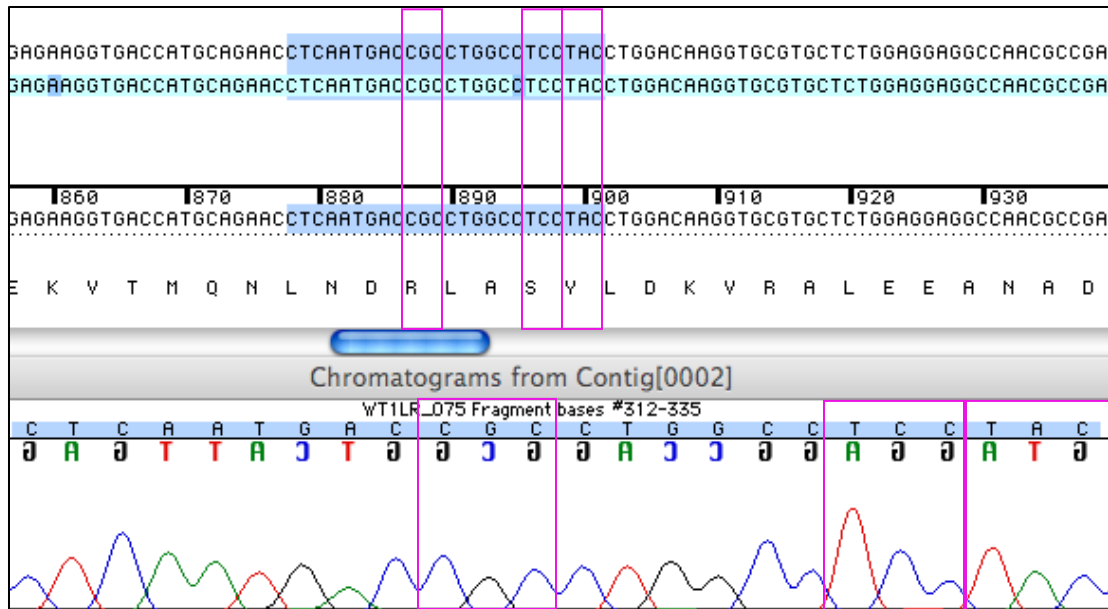
APPENDICES

Appendix 1

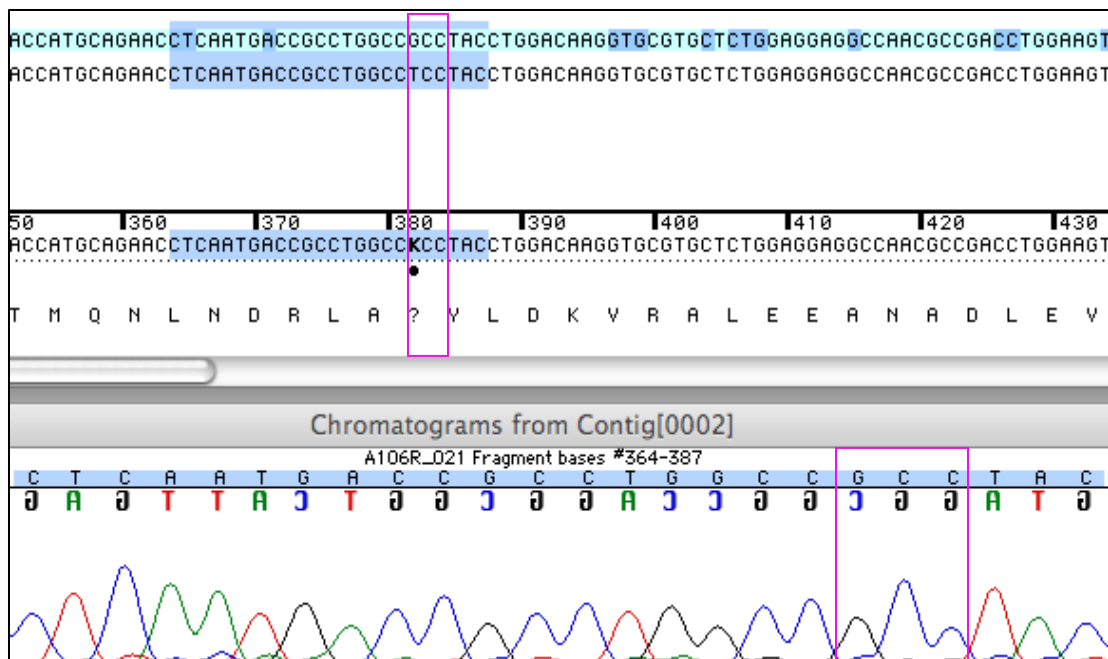**Generation of EGFP-K14 phospho-mimetic constructs and their verification**

(i)

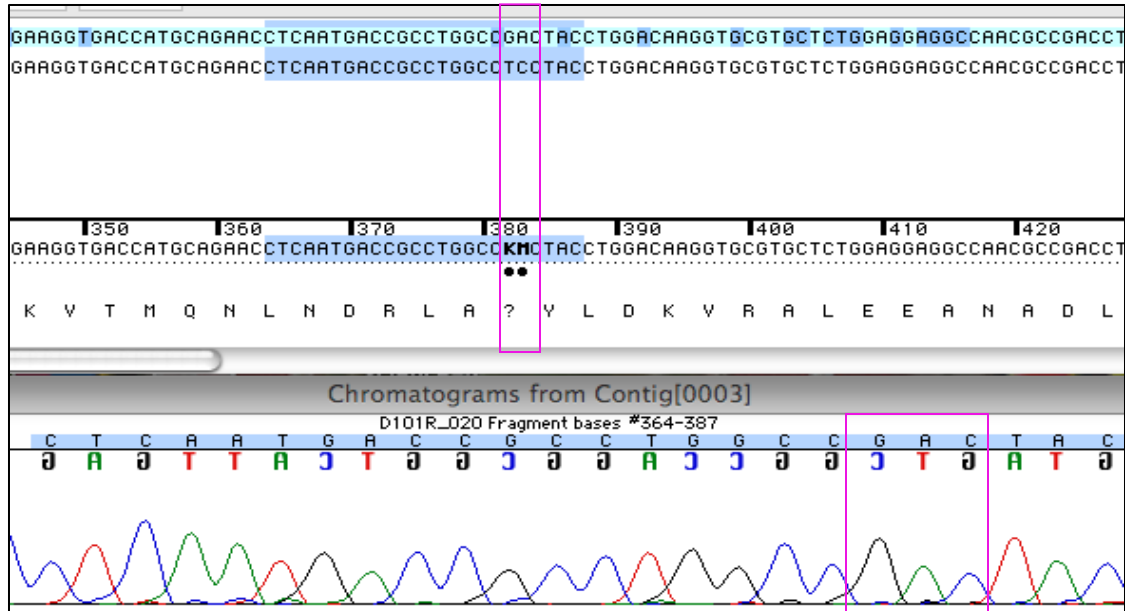<p style="text-align:center">EGFP-K14 WT</p>

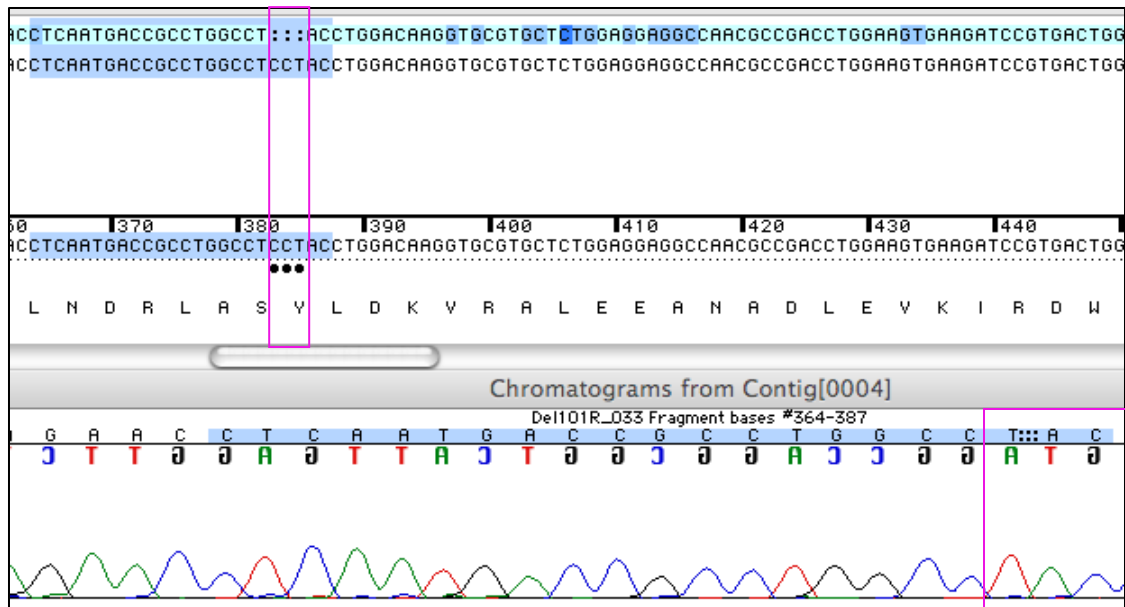**(ii)**

<p style="text-align:center">EGFP-K14 S128A (TCC to GCC)</p>
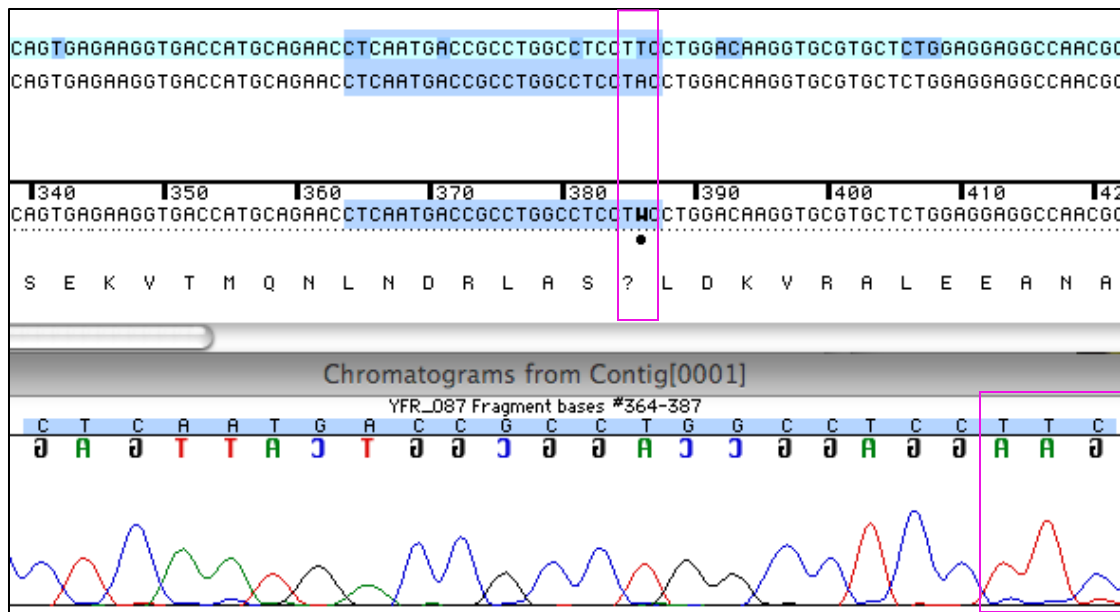
(iii)

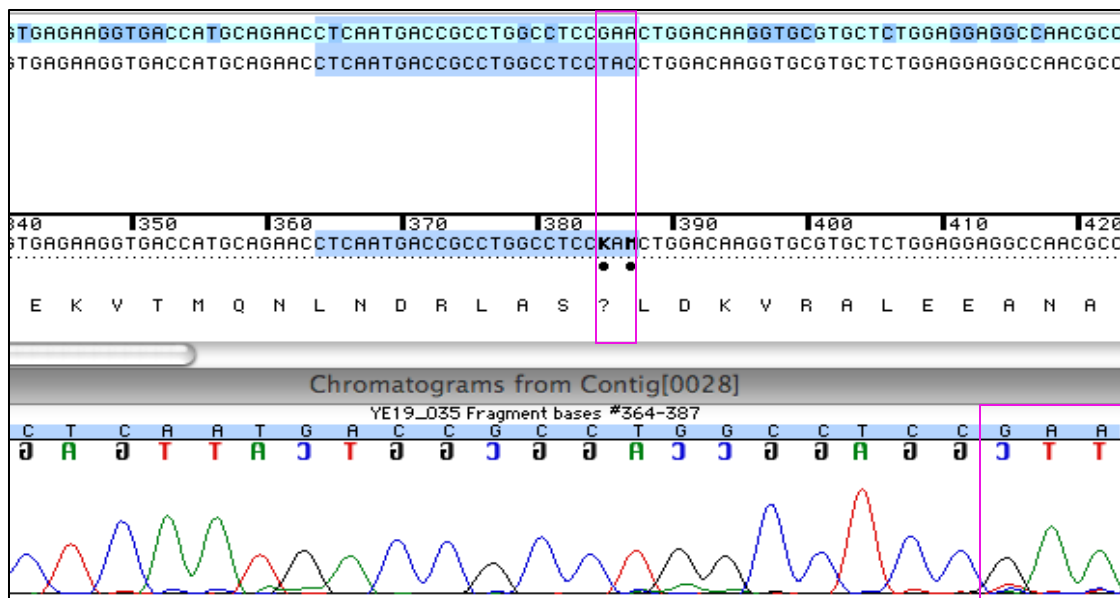## EGFP-K14 S128D (TCC to GAC)

(iv)

EGFP-K14 S128 del (CCT del)

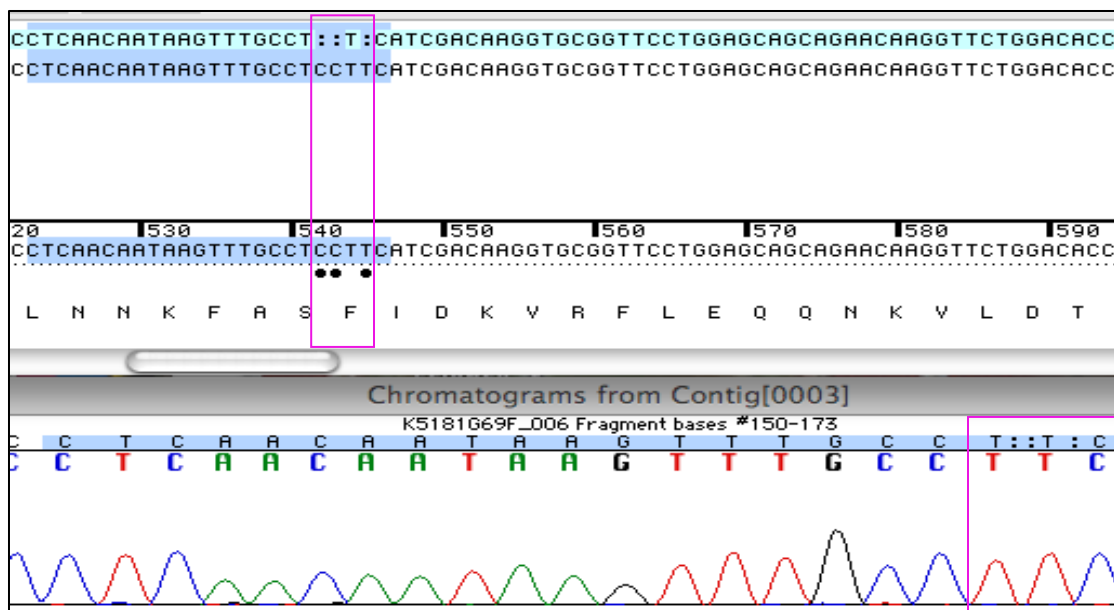**(v)**

EGFP-K14 Y129F (TAC to T**T**C)

(vi)

EGFP-K14 Y129E (TAC to **GAA**)

Appendix 2

Generation of EGFP-K5 mutant construct and its verification
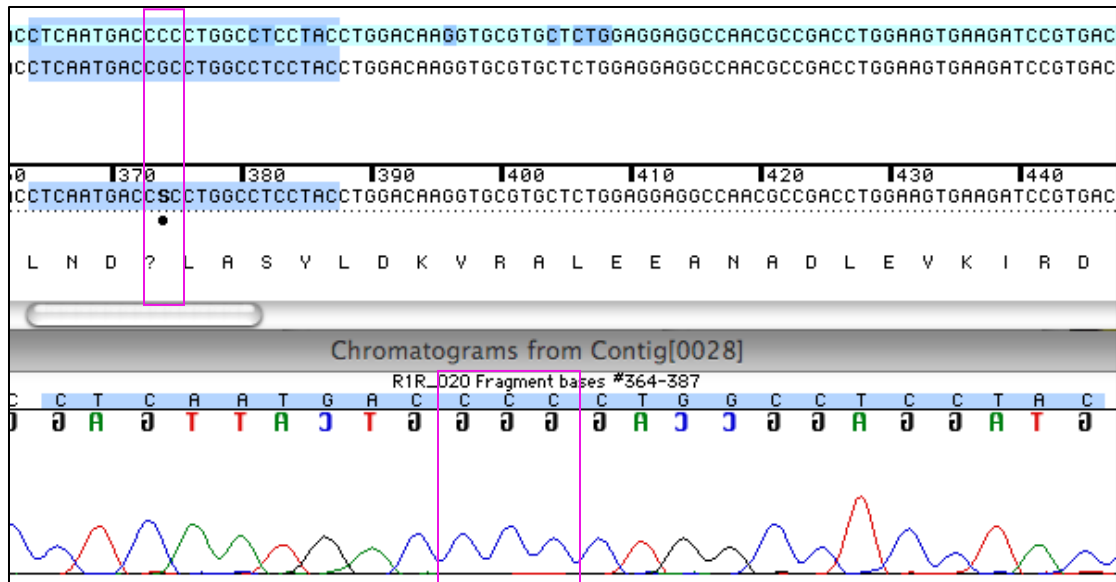
EGFP-K5 S181 del (TCC del)

Appendix 3

Generation of EGFP-K14 R125P_Y129F double mutant construct and its verification

(i)

EGFP-K14 R125P (CGC to CCC)

(ii)

EGFP-K14 R125P_Y129F (CGC to CCC; TAC to TTC)